THE MINOR PLANET BULLETIN

BULLETIN OF THE MINOR PLANETS SECTION OF THE ASSOCIATION OF LUNAR AND PLANETARY OBSERVERS

VOLUME 50, NUMBER 1, A.D. 2023 JANUARY-MARCH 1.

EDITORIAL: THE MINOR PLANET BULLETIN AT 50

With this issue, the *Minor Planet Bulletin* and the Minor Planets Section of the Association of Lunar and Planetary Observers commemorate their 50th year. (Official founding was in mid-1973.) At this milestone for our field, we are extremely fortunate to receive a continuing retrospective from the Founder, Professor Richard G. Hodgson. Commensurate with this milestone, Professor Frederick Pilcher, Minor Planets Section Coordinator since 1982 (formerly titled as "Recorder") shares in this issue his recollections "A Lifetime with the Asteroids." Professor Pilcher's essay is a treasure trove of thoughts that are most gratefully received.

As an *MPB* subscriber since Volume 1 (and Editor since Volume 10), I simply note the personal and professional pleasure of interacting closely with these individuals over an entire half-century. But the greatest pleasure and satisfaction comes from connecting with and encouraging new and seasoned observers worldwide. It is simply "giving back" for the encouragement I received as a student entering the field. The enterprise of the *Minor Planet Bulletin* would not be possible without the dedicated volunteer service of Associate Editor Brian Warner, Assistant Editor David Polishook, and the diligence of our Producer Pedro Valdés Sada. Gratitude also to Melissa Hayes-Gehrke as the Distributor, with a hearty nod to past Producer Bob Werner (35 years of service) and to the late Derald Nye, Distributor and benefactor for 37 years.

Above and beyond the names above, the true credit for success of our endeavor goes to the observers who fill these pages with their observations that fuel the science of understanding these small worlds. May the passion and curiosity of their study never end.

Richard P. Binzel, Editor

THE EARLY YEARS OF THE *MINOR PLANET BULLETIN*

Richard G. Hodgson
Professor Emeritus of Astronomy and Planetary Science
Dordt College, Sioux Center, Iowa
Founding Recorder [Coordinator] of the
A.L.P.O. Minor Planets Section, 1973-1983
Founding Editor of the *Minor Planet Bulletin, 1973-1982*
dnhodgson2888@gmail.com

(Received: 2022 June 27)

The founding of the Minor Planets Section and The Minor Planet Bulletin are recollected, including their earliest sense of purpose and aspirations.

Early in 1973 the Association of Lunar and Planetary Observers (ALPO) under the leadership of its Director Walter Haas decided to establish an Asteroid or Minor Planets Section. In the year or two prior I (and I suspect several others) had been urging formation of such a section. I was delighted to receive Walter's invitation to head it up as Recorder – the position now titled as Coordinator. (I had previously been Mercury Recorder.) In those days the then-known smaller, non-comet, non-satellite Solar System objects were called "asteroids" and "minor planets" interchangeably in English. Americans tended to use "asteroids" more frequently; Eurasians inclined more to "minor planets." Thinking more globally, and influenced by the publication *Minor Planet Circulars*, I chose the name "Minor Planet Section." Under the old astronomical definition of the time (prior to the 2006 IAU revision) anything that orbited the Sun and was not a comet could be properly called a planet – size did not matter. You will note this steady usage of "planet" in Section papers.

Shortly after becoming Recorder, I decided if we were to stimulate member interest, we needed to make reports not only in the *Strolling Astronomer (Journal of the A.L.P.O.),* but also rapidly and frequently in a separately subscribed section journal. In the latter, appeals for observations of individual minor planets, and resulting observations of seldom-observed, or long lost, or newly-found objects could be rapidly reported and discussed. By 1973 May 30, a letter offering subscriptions to ALPO members was circulated. I chose to call the new section journal the *Minor Planet Bulletin ("MPB"* for short). The name and initials would not conflict with any existing astronomical institution or journal. Volume 1, Number 1 of MPB appeared as a quarterly in 1973 July. The rest was exciting history!

Copies of the new journal were circulated not only to ALPO members, but to *Sky & Telescope*, J.U. Gunter's *Tonight's Asteroids*, where its existence was reported to a much wider circle of readers. From the very beginning free copies were always supplied to the Astronomishes Rechen-Institut in Heidelberg, West Germany, so that the articles could be entered into *Astronomy and Astrophysics Abstracts* for consultation by readers around the world. In like manner, we freely supplied copies to Brian G. Marsden, Director at the IAU Minor Planet Center (MPC). I was determined from the start that we do serious, high-quality work, and that we take ourselves seriously. (If you don't, no one else will either!).

Reactions to the first issue were warm and generous. Dr. Joseph Ashbrook, *Sky & Telescope* editor, praised the project, but took exception to my suggestion that asteroids should be checked for possible satellites when at highly favorable oppositions. To him such a search was a waste of time since their gravity fields would be far too weak to retain them. I remained firmly in the "let's look" camp. (From my childhood, I had a fantasy that minor moons might be possible. Of course, 243 Ida's moon Dactyl would not be discovered for another decade, and their discovery was always very helpful as a means to determine the mass of the system. Subsequent discovery from Earth today requires far larger telescopes than I then imagined. Brian Marsden, then MPC Director, was always very helpful supplying ephemerides and other news for the *MPB*. On occasion we met in Cambridge. About 40 subscriptions rolled in, mostly from individuals but also including some universities and colleges. But from that point, we were underway!

[EDITOR'S NOTE: Interested readers in the history of the Minor Planet Section and *Minor Planet Bulletin* will find longer recollections in Hodgson (2013; *Minor Planet Bulletin* **40**, 1-4) and Hodgson (2013; *The Strolling Astronomer* **55**, No. 2, 36-40). Portions of the text printed here are drawn by the author from his previous published recollections.]

A LIFETIME WITH ASTEROIDS

Frederick Pilcher
Minor Planets Section Coordinator
4438 Organ Mesa Loop
Las Cruces, NM 88011 USA
fpilcher35@gmail.com

Asteroids have been a part of my life for seven decades, moving forward from being an aspiring amateur astronomer, to observatory builder, to methodical observer, and dedicated collaborator seeking to advance lightcurve studies. I have been part of the Minor Planets Section for all of its 50 years, with the honor to serve as Coordinator (originally titled "Recorder") for the past 40 years, and continuing.

In my later years I have realized that, no matter where I grew up, or who the important people in my life may have been, I would have been drawn to asteroid studies. Something very fundamental in my character matches me with the asteroids. I was born, to use a phrase coined recently by Alan W. Harris, an "asteroid nerd."

As a small child I was fascinated just by looking at the moon and stars, and knew about the planets and how they moved around the Sun. At the age of ten one of my teachers gave me her college level astronomy textbook, Robert H. Baker's "Astronomy." This book contained tables of the sizes, distances from their primaries, and periods of revolution for the nine planets and 28 satellites then recognized. Within a few weeks I had memorized, and still remember, all of the numerical values in these tables. In the next two years I read several other books on astronomy, and by the age of twelve knew the basics of all the major classes of astronomical objects known at the time.

My parents gave me a subscription to *Sky and Telescope* magazine starting with the November, 1949, issue. Baker's book taught me the names and numbers of the first four asteroids. The January, 1950, issue of *Sky and Telescope* published the first of their continuing series of ephemerides of bright asteroids coming to opposition. I made no effort to look for them in the sky, but still remember learning the names and numbers of the asteroids in that first list, 1 Ceres, 3 Juno, 516 Amherstia, and 532 Herculina. In the next several years I had memorized the names and numbers of all of the several tens of asteroids published in their lists. I didn't know anything else about any of them, and didn't try to look for any of them in the sky.

At the age of about fifteen, my uncle took me to visit the Perkins Observatory, then still located in Delaware, Ohio, a short distance north of Columbus. In the library there was a pre-war edition of the *Astronomische Nachrichten* that contained a list of more than 1000 asteroids and their orbital elements. A treasure trove had opened. I copied down their names, numbers, absolute magnitudes that provided approximate sizes, and semimajor axes, but not the other orbital elements whose meanings baffled me. Each asteroid became more than a name and a number.

Later, having decided to major in physics and be only an amateur in astronomy, I went on to college and graduate school. In 1962 I was offered an assistant professorship in physics at Illinois College, Jacksonville, a four-year liberal arts college at that year having an enrollment of about 550 students. When the next year the department was enlarged from one to two faculty, I was able to add a liberal arts level course in astronomy to the curriculum, reenter

the field, and expand my astronomical knowledge. With the aid of a *Sky and Telescope* ephemeris, I actually saw my first asteroid, tracking Vesta across the sky in the summer of 1966 with small binoculars.

In the fall of 1966, I was called out of my astronomy class, of all places, to visit the President of Illinois College, L. Vernon Caine. He told me that an alumnus and longtime supporter of the college, Walter H. Balcke, had offered to give the college a new ten-inch Celestron. Would it be useful to the curriculum? Of course! The telescope was mounted in a small shed on rails on the flat roof of the science building, where, starting in the fall of 1967, my astronomy students enjoyed improved views of planets, double stars, and some of the brighter deep sky objects.

During the following few months, I obtained Hans Vehrenberg's photographic *Atlas Falkau* showing stars to the thirteen magnitude. Joseph Ashbrook of *Sky and Telescope* kindly sent the ordering address of the Leningrad Institute of Theoretical Astronomy (ITA) for the 1968 *Ephemerides of Minor Planets.*

The prevailing wisdom at the time was that to find an asteroid in the telescope, one had to endure considerable time and effort to draw a map of many stars near the predicted position and wait at least several hours or until the next night to see which one moved. I was about to remove that obstacle forever. I may or may not have been the first person to devise the new and much simpler method of finding and tracking asteroids enabled by the *Atlas Falkau*, but I claim originality. With the coordinate grid superimposed upon the star field, the positions at ten-day intervals in the *Ephemerides of Minor Planets* were plotted for each asteroid to be observed. At the telescope I star hopped to the predicted position, and there it was, standing out like the proverbial sore thumb from its absence on the *Atlas Falkau.* That first night, 1968 Apr. 13, and for the three following nights, I tracked 3 Juno and 13 Egeria as they moved along their predicted paths. The next month, with the same procedure, asteroids 7 Iris and 85 Io were found and tracked. I wrote a letter to *Sky and Telescope* describing my method of identifying asteroids in the star field and watching them move. A few months later *Sky and Telescope* printed the letter. Some people who would become significant in both my life and progress in asteroid studies read it.

Actually, X marks were not written on the atlas itself at the ten-day predicted positions, nor were dots to show where they were observed. On a blank sheet of paper lines were drawn marking the coordinates of the chart center and superimposed with a clipboard upon the chart and the coordinate grid. Each ten-day position was marked with X on the paper. At the telescope I removed the coordinate grid, aligned the coordinate centers of the star chart and the paper with the penciled predicted positions, shined a flashlight through both, and placed a dot at the observed position of the asteroid. That method served me well for more than thirty years during which I tracked visually more than 1800 different asteroids. But my own personal observing, though time-consuming, is only a small part of my story.

Many other people also tracked asteroids beginning about 1970. Three people who tracked a number of asteroids even larger than my 1800 merit special commendation. Ben Hudgens, with more than 2000; Andrew Salthouse, with more than 3000 and who also prepared a comprehensive statistical study of his limits of observation; and Roger Harvey whose more than 8000 asteroids observed visually with a 0.8-meter telescope will probably never again be approached in all the years and centuries to come.

Dave Williams, who was launching an independent semimonthly magazine, *The Review of Popular Astronomy*, read my *Sky and Telescope* article, and invited me to write a short column about observing asteroids in each issue. I followed the format of *Sky and Telescope* of the early 1950's, providing ephemerides copied out of the *Ephemerides of Minor Planets*, which until the Soviet Union started collapsing in the late 1980's was available each year without charge from the ITA. Dave called me "Mr. Asteroid" on one occasion. I don't know whether I'm glad or sad that moniker vanished as completely as Biela's Comet.

As a one-man operation by a person hardly out of college, *The Review of Popular Astronomy* folded after about a year. One man who read my asteroid column was Dr. J.U. Gunter, soon to retire as Chief Pathologist at Duke University, Durham, North Carolina. He used my technique to start observing asteroids on his own.

Gunter was the man who popularized asteroid observing among amateur astronomers. It was my pleasure and privilege to have been his technical adviser. As a retirement activity, Dr. Gunter started preparing, printing, and mailing free of charge *Tonight's Asteroids.* Each monthly issue contained finder charts photocopied from the *Atlas Falkau* of asteroid plotted paths for about five or six asteroids, as well as fascinating relevant historical and personal anecdotes. Many people subscribed to *Tonight's Asteroids*. Dr. Gunter continued distributing *Tonight's Asteroids* to include charts for the 1985-86 apparition of Halley's Comet, after which at the age of 75 he retired completely.

Dr. Caine was scheduled to retire from the presidency of Illinois College in 1973. In the meantime, Celestron had made a much larger 14-inch scope that would give me the opportunity to observe many hundreds of asteroids too faint for the 10-inch. Hans Vehrenberg had also published his *Atlas Stellarum* that showed stars much fainter than on the *Atlas Falkau* and with which these faint asteroids could be identified. The 10-inch telescope had inspired me to the considerable achievements described in the preceding paragraphs. I would write a letter to Walter Balcke, tell him how much his gift had contributed to my personal development, and ask for $4500 to buy for Illinois College a 14-inch Celestron. But Dr. Caine was a real tightwad, and might decline the gift. Walter Balcke was about 90 years old and might not live until Dr. Caine retired. I decided to wait until July, 1973, hope that Walter Balcke was still alive and would accept my proposal when I wrote a letter to him. Then I could spring it on incoming president Donald Mundinger and have him approve before he really understood how the college worked... It was a miracle! I succeeded. Walter Balcke died about a year later, but my career has expanded steadily for five following decades.

Also in 1973, and finally completed in early 1974, I privately published, in collaboration with Jean Meeus in Belgium, *Tables of Minor Planets*, a compendium of numerical information about the 1813 asteroids numbered at the time. With advertising in *Sky and Telescope,* within a few years I had sold a printing of 1000 copies and actually made a small profit. The field has expanded exponentially since that time and *Tables of Minor Planets* has become hopelessly out of date. But it set a precedent. Now there are many online tabulations of numerical data for nearly one million known asteroids. How many people my book may have attracted to participate in the field I will never know.

In 1973 Dick Hodgson founded the Minor Planets Section as a new section of the Association of Lunar and Planetary Observers (ALPO), and invited me to become a charter member. Until 1982, he operated a one-man show, collecting author reports, editing,

printing, and distributing the *Minor Planet Bulletin* on a quarterly schedule. I contributed many articles.

Starting in 1975, I prepared for the *Bulletin* annual lists of asteroids that were favored for observation by being much brighter than usual by being near the perihelia of their high eccentricity orbits. The roots for creating this highlight list reached back to the age of ten when I had been fascinated by some oppositions of Mars being much brighter and therefore more favorable than others. For quite a few years my annual list in the *Minor Planet Bulletin* was done on a sort of ad hoc basis, but readers, including myself, found them useful. A method to refine and formalize the time-consuming process for generating this list was still many years into the future.

It was about 1976 that Rick Binzel sent his first letter to me, starting what would become decades of fruitful communication. As a high school student, he was attending a summer astronomy camp in California. He and camp organizer and director James Patterson together used a simple photoelectric photometer to plot a lightcurve for 18 Melpomene. They corrected the value published by one of the leading professional astronomers of the time who specialized in asteroid studies, Tom Gehrels of the University of Arizona Lunar and Planetary Laboratory. Years later Rick commented that without that summer camp, he would have become a professional astronomer in any case, but would not have made physical studies of asteroids his lifelong research field.

With the 14-inch telescope I was observing many new asteroids every year, communicating with amateurs interested in the field, and publishing a steady stream of articles in *The Minor Planet Bulletin.* The year 1982 became one of big change. Dick Hodgson was suddenly unable to continue in any of his duties connected with *The Bulletin.* The *Bulletin* might have folded, and the entire Minor Planets Section of the ALPO might have ceased. Rick Binzel, then only a starting graduate student, came to the rescue.

He volunteered to become Editor of *The Minor Planet Bulletin.* He invited Bob Werner to become Producer, Derald D. Nye to become Distributor, and me to become Coordinator of the Minor Planets Section. We all accepted the invitations. In the several decades that followed both *The Minor Planet Bulletin* and the Minor Planets Section of the ALPO have flourished under their capable and distributed leadership.

In the early 1990's an unexpected letter from Dr. John Reed arrived. He had written a program to find asteroid ephemerides that was nearly as accurate as the JPL programs. In the following months I acted as a beta tester and at my recommendation he inserted many features that made it more versatile and easier to use. I have used his program ever since without having to rely on JPL.

At long last I was able to do for thousands of asteroids what the textbooks did for Mars. My son, Timothy, who is a skilled programmer, adapted John Reed's program to mass produce opposition data for each asteroid for all years between 1950 and 2060. For any specific numbered asteroid, I could look up the list of oppositions and identify those for which it would be brighter than usual and easier to observe. My publications continue in *The Minor Planet Bulletin* of annual lists of asteroids passing through opposition in the coming year and much brighter than their average magnitudes. From the 1990's and continuing through the present, these lists enable me to find when an asteroid I wish to observe will be within the range of my equipment to schedule my own observing program.

In the 1990's *The Minor Planet Bulletin* began publishing photoelectric lightcurves and derived rotation periods of asteroids in addition to the results of visual observations. Near the start of the 21st century two events revolutionized amateur activities in asteroid observing and the content emphasis of the *Bulletin.*

The CCD and powerful controlling software were making asteroid lightcurve data acquisition and rotation period determination much cheaper, easier, and more productive than was possible with a photoelectric photometer. GoTo software replaced the cumbersome use of setting circles and star hopping, enabling the user to slew in a very short time to any object or location in the sky. Brian D. Warner's two programs, *MPO Connections* to control the telescope and CCD, and *MPO Canopus* to measure the images, draw lightcurves, and find rotation periods, made these technological advances accessible to amateur observers. Brian also provides continuing advice and help to all amateur observers who ask for it. Many enthusiastic amateur observers entered the field, and between 2000 and 2015 *The Minor Planet Bulletin* grew from an average of 20 pages per quarterly issue to about 100. Nearly all of the articles from 2000 to the present have dealt with asteroid lightcurves and rotation periods.

In the year 2005 my 43-year career in teaching physics and astronomy at Illinois College came to an end. The asteroid lightcurves and rotation periods published in *The Minor Planet Bulletin* had inspired me to make a mid-life career change from physics teaching to astronomy research in the field of asteroid CCD photometry and lightcurve analysis.

Four people deserve special thanks for giving me a great deal of help near this time: the late Don Jardine, Brian Warner, David Dixon, and the late Dan Klinglesmith. Between them they taught me everything necessary to succeed in my chosen field. To facilitate my observing, I moved from the rain and clouds of Illinois to the clear sky and warm weather of southern New Mexico, to build a house a few miles outside Las Cruces.

Planning exactly what equipment would be most productive for asteroid lightcurve studies required long and careful thought. A Meade 14-inch LX200 GPS Schmidt-Cassegrain telescope should be adequate to sample thousands of asteroids to magnitude 15 and fainter. A fork mount is less sturdy than the German Equatorial, but does not require a meridian flip in the middle of an all-night photometric session. A sliding roof would remove the extra complexity of having the slit in the dome follow the telescope as the target moves across the sky. Of all the CCDs then sold by SBIG, the STL-1001E has a large field to provide a greater choice of comparison stars without the optical complexity of adding a focal reducer to the telescope. The guides on photometry recommended not taking measurements below 30 degrees altitude, but the sliding roof was designed to permit viewing in all directions to 25 degrees altitude. The additional time afforded to each session should more than compensate for the slightly reduced photometric accuracy at lower altitudes. Finally, by building the observatory only ten meters from the house, the routine opening and closing procedures could all be performed manually, with no need to travel to a remote observatory site in event of equipment failure. Made in advance of my first actual observing experience, these decisions turned out to be all the right ones for equipping an observatory dedicated to asteroid CCD photometry and lightcurve analysis.

As first light for the telescope and CCD approached in the year 2007, the time had come to plan my most effective observing strategy. To obtain the greatest possible rotation period accuracy and reliability for each observed target, I deemed that each session

and each resulting lightcurve segment should have as many hours as possible. It should start 45 minutes after sunset, or when the target rises to 25 degrees altitude, whichever comes last, and end 45 minutes before sunrise, or when the target sinks below 25 degrees altitude, whichever comes first. Near opposition sessions of eight hours for targets at the celestial equator, and nearly 10 hours at declination +20 degrees, are achieved. For one target at +45 degrees declination, 71 Niobe, and one week after winter solstice, sessions of 12 hours each on three successive nights covered a complete lightcurve with a period near 36 hours.

In addition to extending each session for as many hours as possible each night, the campaign on each asteroid is extended for at least several weeks, with campaigns in progress on several different asteroids at the same time. The longer interval of observation covers more rotational cycles and reduces the error in the published period. After the first few sessions on a particular asteroid are completed, a preliminary period can usually be found. The specific night can be predicted for which a gap still remaining in the lightcurve can be filled. Of course, this asteroid is chosen as my target for the night. Sometimes there is only one such night and, if lost because of clouds or otherwise, there will not be another opportunity for many nights. I have coined a personal term, "critical night," as one in which it is very important to get a lightcurve of a specific asteroid. Thanks to the high proportion of clear nights in southern New Mexico, the "critical night" lightcurve needed to fill the gap can usually be obtained.

Photometric all-night lightcurves are not needed every night for asteroids. At any one time I have several different targets under observation, and must choose before nightfall which target should be observed that particular night to obtain the most useful information.

Many years of experience taught me the most successful observing strategies for asteroids with a wide variety of rotation periods from about 2.4 hours up to several hundred hours. I recommend these procedures to all observers: If there is a gap of many rotational cycles between successive sessions, one cannot accurately count the number of intervening cycles. There is an ambiguity in the period. For asteroids with short periods that can be completely sampled in a single night, several hour sessions on successive nights can establish a unique period, but one which is not highly accurate. Sessions many nights apart will have a gap of many rotational cycles and the number of intervening rotational cycles cannot be accurately counted. If three or more sessions are separated by different and incommensurable numbers of days, the rotational ambiguity is removed. With many rotational cycles, both the accuracy and reliability of the derived period are very good.

These same principles apply to asteroids with intermediate periods up to 2 or 3 days, except that one should also cover both halves of the double period so that a split halves plot can resolve any ambiguity between one allowed period and twice that period.

For asteroids whose periods are nearly commensurate with Earth's 24 hour rotation, collaboration from observers in longitudes widely distributed around the world is necessary to fill gaps in a lightcurve that are unavoidable for observations at a single observatory. Many people at widely separated longitudes graciously accepted my invitations to collaborate from time to time as suitable targets approach opposition. My thanks are especially extended to several highly competent observers who have worked with me for many years: Vladimir Benishek, Lorenzo Franco, Julian Oey, Caroline Odden and her students, and the late Dan Klinglesmith.

For long period asteroids, especially periods of 200 hours or longer, zero points of individual sessions cannot be adjusted to fit. Calibration star magnitudes consistent within ± a few × 0.01 across the entire sky are mandatory. I thank Lorenzo Franco for introducing me in the year 2013 to the Carlsberg Meridian Circle (CMC14) catalog, soon to be supplanted by the CMC15. The recently published GAIA2 and ATLAS catalogs have an ever better internal consistency. I conceived an observing scheme to obtain accurate and reliable periods for very slow rotators.

My first target with this scheme was 288 Glauke, which had been found many years earlier to have a rotation period in the range between 1150 hours and 1200 hours with a fairly large amplitude. The list of asteroid oppositions assembled by my son using the John Reed's ephemeris program showed that between 2013 November and 2014 July it would be magnitude 15.0 or brighter and 60 degrees or farther from the Sun. A short session of 15 to 20 minutes every clear night, except when the target was close to the Moon, for this entire eight month interval, would provide full lightcurve coverage. Well before opposition this could be done at the end of the regular session, and well after opposition before the start of the regular session. At other times the GoTo procedure slewed the telescope from the regular target to 288 Glauke for about 15 minutes, then back to the regular target, with only a small gap in the lightcurve of the regular target. The calibrated magnitudes for the many sessions would have the internal consistency of a few × 0.01 magnitudes of the CMC14 and CMC15 catalogs with no zero point adjustments. I proposed my scheme to Alan Harris, who endorsed it. I thank Petr Pravec for analyzing my data with his custom software for tumbling asteroids to improve the principal period to 1170 hours and find a second tumbling period of 737 hours. In subsequent years this procedure has been used to find accurate and reliable rotation periods for several other very slow rotators. In each case Petr Pravec has generously analyzed my several months of data to find the principal period and attempt to find the second tumbling period.

An article about Giovanni Domenico Cassini in *Sky and Telescope,* 2021 May, p. 63, states "Cassini's greatest contribution to science was introducing three elements of modernity: a distinction between astronomers and telescope builders; a carefully organized observing method; and conceiving science as the collaboration among groups of scientists in order to achieve goals inaccessible to a single individual." I independently adopted all of these schemes years ahead of publication of the *Sky and Telescope* article and quotation. As strictly an astronomer, with no skill whatsoever in building or servicing telescopes and other astronomical equipment, I observe every clear night except when traveling away from home. This was also Cassini's practice when many other 17th century observers did not. I observe each target for a longer time interval than many other *Minor Planet Bulletin* authors, and on nights carefully chosen to optimize information without excessive redundancy. I pioneered intercontinental collaboration for targets with Earth commensurate rotation and whose sessions were essential to obtain full lightcurve coverage. From my vantage of many years' experience, these procedures are recommended to all active asteroid lightcurve observers.

At this writing, more than seven decades have passed since asteroids first crept into my life. It has been my great privilege to communicate with many of the leaders in asteroid research and be respected by them. My thanks are extended to the community of asteroid observers for providing my opportunity to participate in pioneering research. Some year in the not-too-distant future, I expect to retire from asteroid lightcurve observing. But not yet!

LIGHTCURVE OF KORONIS FAMILY MEMBER (993) MOULTONA

Eva Mae Crowley, Francis P. Wilkin
Union College
Department of Physics and Astronomy
807 Union St.
Schenectady, NY 12308
crowleye@union.edu

(Received: 2022 October 14)

Using three telescopes, a lightcurve was made for the asteroid (993) Moultona. There is no previously published lightcurve for this Koronis Family member. Based upon our lightcurve, the period is 5.2702 ± 0.0004 h, with amplitude 0.80 ± 0.06 mag.

Based on the observable Koronis family members during Summer 2022, our target (993) Moultona was chosen by using the Koronisfamily.com web tool (Slivan, 2003). It also appears prominently in a list of the first 1000 numbered asteroids lacking reliable periods (Álvarez, 2015).

Observations were conducted with three telescopes on three continents: The Union College Observatory (UCO) in Schenectady, NY, and remote facilities through iTelescope.net (T17) in Coonabarabran, Australia, and Telescope.Live (CHI-1) in Rio Hurtado, Chile. Exposure times were 300 s and binning 2×2. Filters used are given in Table I. In total, there were 15 observing sessions.

Images were processed for bias, dark, and flat field corrections. *AstroImageJ* was used to perform the photometry. Corrections for light travel time were applied using ephemerides from the NASA Horizons web application. Individual lightcurves were shifted in brightness to form a consistent composite lightcurve. The observed amplitude 0.80 ± 0.06 mag (trough to peak) is large enough to indicate that Moultona is sufficiently elongated to reject a singly-periodic lightcurve. Our doubly-periodic lightcurve yields a best-fit period of 5.2702 ± 0.0004 h.

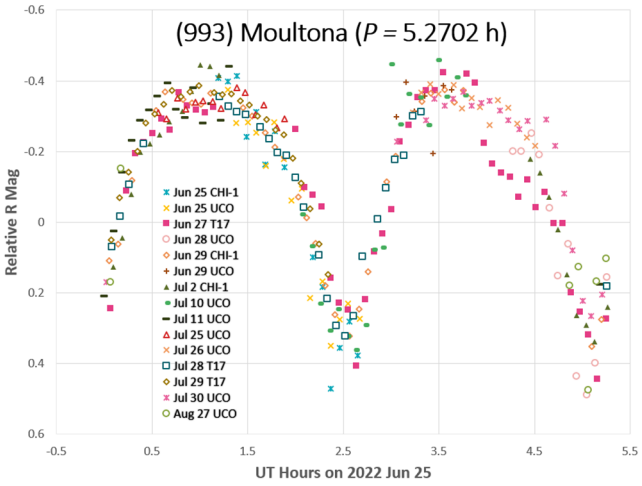

Acknowledgements

EMC thanks R. Koopmann and the NASA New York Space Grant for funding. FPW received financial support from the Union College Faculty Research Grant. We thank S. Slivan for encouragement and advice.

References

Álvarez, E.M. (2015). "Voids and Question Marks in the Present-Day Data Concerning the Rotation Period of the First 1000 Numbered Asteroids." *Minor Planet Bull.* **42**, 127-129.

NASA Horizons. *https://ssd.jpl.nasa.gov/horizons/app.html#/*

Slivan, S.M. (2003). "A Web-based tool to calculate observability of Koronis program asteroids." *Minor Planet Bull.* **30**, 71-72.

Name	Site	Telescope	Camera	Array	Filter	FOV(')	Scale ("/pix)
UCO	Schenectady, NY	0.50-m RC f/8.1	SBIG STXL-11002	2004×1336x9µm	R	30×20	0.93
T17	Coonabarabran, Aus	0.43-m CDK f/6.8	FLI-PL E2V	3072×2048x13µm	r2′	15.5×15.5	1.84
CHI-1	Rio Hurtado, Chile	0.61-m RC f/6.8	FLI-PL9000	3056×3056x12µm	r′	31.8×31.8	1.22

Table I. Telescopes and Cameras. RC=Ritchey-Chrétien; CDK = Planewave with f/4.5 focal reducer. UCO = Union College Observatory Filters: R, Cousins R; r', Sloan r'; r2', Astrodon Sloan Gen 2 r', 562-695 nm.

Number	Name	yyyy mm/dd	Phase	L_{PAB}	B_{PAB}	Period(h)	P.E.	Amp	A.E.	Grp
993	Moultona	2022 06/25-08/27	*12.2,11.4	305	2	5.2702	0.0004	0.80	0.06	Kor

Table II. Observing circumstances and results. The phase angle is given for the first and last date. If preceded by an asterisk, the phase angle reached an extremum during the period. L_{PAB} and B_{PAB} are the approximate phase angle bisector longitude/latitude at mid-date range.

LIGHTCURVE FOR KORONIS FAMILY MEMBER (1389) ONNIE

Francis P. Wilkin, Finlay MacDonald
Union College
Department of Physics and Astronomy
807 Union St.,
Schenectady, NY 12308
wilkinf@union.edu

Stephen M. Slivan
Massachusetts Institute of Technology,
Cambridge, MA 02139

(Received: 2022 October 15)

We have used east and west stationary point observations of (1389) Onnie to determine a definitive period of 23.044+/-0.001 h.

Koronis family member (1389) Onnie was observed by Binzel in 1983 as reported in Binzel (1987), which appears to contain the only published lightcurves. Although a complete lightcurve and unambiguous period could not be derived, the presence of two local maxima separated by 22.5 h provides a significant constraint. More recently, Hanuš et al. (2011; 2013) have reported sidereal periods and spin vectors. These analyses, as well as that of (Erasmus et al., 2020) use "survey sparse data" and are based on the adoption of the 22.5 h period value.

Given Binzel's 1983 dataset, and assuming an integer number of half-rotations during the 22.5 h interval between observed maxima, there are three candidate periods that produce self-consistent, folded composite lightcurves that are doubly-periodic: 45.0 h, 22.5 h, 15.0 h. The goal of our new observations is to resolve the period ambiguity and to obtain a complete lightcurve for the 2021 apparition (see also Slivan et al. (2023; this issue)).

All new observations in this work were conducted at the 0.61-m Ritchey-Chrétien Chi-1 in the Rio Hurtado Valley, Chile, operated by Telescope.Live. Observation planning used the Koronisfamily.com tool (Slivan, 2003). Exposures of 240 s in Sloan r' were binned 2×2, with image scale (0.62"/pix) and field of view 32'×32'. The observing campaign in April 2021 while Onnie was near its eastern stationary point, comprised 10 nights. We subsequently obtained observations on two consecutive nights in June, and 5 consecutive nights in July, when the asteroid was near the western stationary point.

Images were processed for bias, dark, and flat field corrections. We used *AstroImageJ* software (Collins et al., 2017) to perform photometry. Corrections for light travel time, unit distance and solar phase angle were made using ephemerides from NASA Horizons. A single pointing center allowed the use of the same on-chip comparison stars for all nights in April, for which only ~ half of a full rotational phase coverage was obtained. For July, the target was now near the west stationary point, again permitting a single field pointing center and the use of the same on-chip comparison stars for our 5 nights. The two nights in June were consecutive, again permitting the same on-chip comparison stars. Thus, in making a composite lightcurve of all of the April, June, and July observations, only two constant shifts in magnitude were required to put all observations onto a consistent relative scale.

As seen in our lightcurve, the rotational phase coverage of the two stationary point observations largely overlapped, and the majority of the remaining gap in coverage was filled by the two nights in June. Our observations were able to reject the candidate periods near 15.0 h and 45.0 h because they did not produce self-consistent composites. This conclusion was not sensitive to the assumed value of G. We obtained a best fit synodic period 23.044 +/- 0.001 h, which agrees with Binzel's inferred value 22.5+/-0.3 h within 2σ. The inferred amplitude (from trough to peak) is 0.70 +/- 0.03 mag.

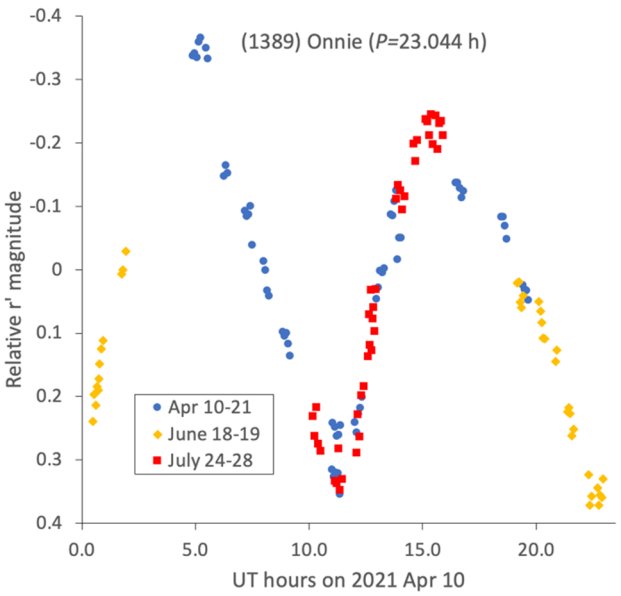

Number	Name	yyyy mm/dd	Phase	L_{PAB}	B_{PAB}	Period(h)	P.E.	Amp	A.E.	Grp
1389	Onnie	2021 04/15-07/22	*17.8,16.9	256	3	23.044	0.001	0.70	0.03	MB-Kor

Table I. Observing circumstances and results. The phase angle is given for the first and last date. If preceded by an asterisk, the phase angle reached an extremum during the period. L_{PAB} and B_{PAB} are the approximate phase angle bisector longitude/latitude at mid-date range.

Acknowledgements

FPW is grateful to the Faculty Research Grant for funding used to purchase telescope time. FM was supported by the NASA NY Space Grant.

References

Binzel, R.P. (1987). "A photoelectric survey of 130 asteroids." *Icarus* **72**, 135-208.

Collins, K.A.; Kielkopf, J.F.; Stassun, K.G.; Hessman, F.V. (2017). "AstroImageJ: Image Processing and Photmetric Extraction for Ultra-precise Astronomical Light Curves." *Astron. J.* **153**, 77-89.

Erasmus, N.; Navarro-Meza, S.; McNeill, A.; Trilling, D.E.; Sickafoose, A.A.; Denneau, L.; Flewelling, H.; Heinze, A.; Tonry, J.L. (2020). "Investigating Taxonomic Diversity within Asteroid Families through ATLAS Dual-band Photometry." *Astrophysical Journal Supplement Series* **247**, 13.

Hanuš, J.; Ďurech, J.; Brož, M.; Warner, B.D.; Pilcher, F.; Stephens, R.; Oey, J.; Bernasconi, L.; Casulli, S.; Behrend, R.; Polishook, D.; Henych, T.; Lehký, M.; Yoshida, F.; Ito, T. (2011). "A study of asteroid pole-latitude distribution based on an extended set of shape models derived by the lightcurve inversion method." *Astron. Astrophys.* **530**, A134.

Hanuš, J.; Ďurech, J.; Brož, M.; Marciniak, A.; Warner, B.D.; Pilcher, F.; Stephens, R.; Behrend, R.; Carry, B.; Čapek, D.; Antonini, P.; Audejean, M.; Augustesen, K.; Barbotin, E.; Baudouin, P.; and 105 authors (2013). "Asteroids' physical models from combined dense and sparse photometry and scaling of the YORP effect by the observed obliquity distribution." *Astron. Astrophys.* **551**, A67.

NASA Horizons. *https://ssd.jpl.nasa.gov/horizons/app.html#/*

Slivan, S.M. (2003). "A Web-based tool to calculate observability of Koronis program asteroids." *Minor Planet Bull.* **30**, 71-72.

Slivan, S.M.; Colclasure, A.M.; Larsen, S.S.; McLellan-Cassivi, C.J.; Neto, O.S.; Noto, M.I.; Redden, M.S.; Wilkin, F.P. (2023). "Synodic and Sidereal Rotation Periods of Koronis Family Member (1389) Onnie." *Minor Planet Bull.* **50**, 8-10.

SYNODIC AND SIDEREAL ROTATION PERIODS OF KORONIS FAMILY MEMBER (1389) ONNIE

Stephen M. Slivan, Abigail M. Colclasure, Skylar S. Larsen, Claire J. McLellan-Cassivi, Orisvaldo S. Neto, Maurielle I. Noto, Maya S. Redden
Massachusetts Institute of Technology,
Dept. of Earth, Atmospheric, and Planetary Sciences,
77 Mass. Ave. Rm. 54-424, Cambridge, MA 02139
slivan@mit.edu

Francis P. Wilkin
Union College Dept. of Physics and Astronomy
Schenectady, NY

(Received: 2022 October 15 Revised: 2022 October 17)

Lightcurve observations of (1389) Onnie during its 2022 apparition yield a secure determination of its synodic rotation period 23.038 ± 0.005 h, and an unambiguous count of sidereal rotations back to 2017 constrains the sidereal rotation period.

Asteroid (1389) Onnie appears to be the lowest-numbered Koronis family member lacking a secure determination of its rotation period having full lightcurve coverage and no ambiguity. Binzel (1987) recorded partial lightcurves of Onnie on three consecutive nights in 1983, each spanning about 4 to 5 hours. By assuming that either 0.5, 1.0, or 1.5 rotations elapse during the 22.5 h interval between the observed maxima, there are three candidate periods whose folded composite lightcurves are consistent with being doubly-periodic. 1.0 rotation for a 22.5 ± 0.3 h period was chosen as favored but the others could not be ruled out. Erasmus et al. (2020) refined the favored period based on ATLAS survey data "sparsely sampled" in time, but those observations share the same ~24-h cadence of the 1983 data and thus do not resolve the period ambiguity. Hanuš et al. (2011; 2013) have reported analyses of earlier sparsely-sampled data for sidereal periods and spin vectors. The new observations reported here were made with two specific objectives: to resolve the ambiguity in the rotation period (also see Wilkin et al. (2023; this issue)), and to obtain complete rotation coverage at its 2022 viewing aspect which is similar to that incompletely observed in 1983.

We observed Onnie mainly near its eastern stationary point in 2022 July to permit using the same on-chip field comparison stars over a series of nights. Nightly observing information is summarized in Table I, and instrumentation is detailed in Table II. Observations from June through August were made using telescopes at the MIT Wallace Astrophysical Observatory (WAO) in Westford, MA. Observations in September were made remotely using the CHI-2 telescope of Telescope Live in Rio Hurtado, Chile, for which the coverage was timed specifically to fill an unattractive straggler gap in rotation phase. Processing and measurement of the images were as described by Slivan et al. (2008), except that for the observations made using the smaller telescopes WAO-3 and WAO-4 the choices of synthetic aperture sizes for the on-chip relative photometry were guided by the experience of Howell (1989).

We reduced our observations for light-time and to unit distances, and for changing solar phase angle using $G = 0.23$ (Lagerkvist and Magnusson, 1990) as the slope parameter of the Lumme-Bowell model (Bowell et al., 1989). Composite lightcurves folded at the best-fitting periods corresponding to all three possible periods identified by Binzel (1987) confirm that the earlier favored solution is correct (Fig. 1) and rules out the two alias solutions (Fig. 2),

noting that the alias resolution was confirmed to be insensitive to the exact choice of *G* used in the reduction. The derived synodic period 23.038 ± 0.005 h is consistent with both the less-precise result of Erasmus et al. (2020), as well as with the more-precise result of Wilkin et al. (2023; this issue) which is based on observations made in 2021.

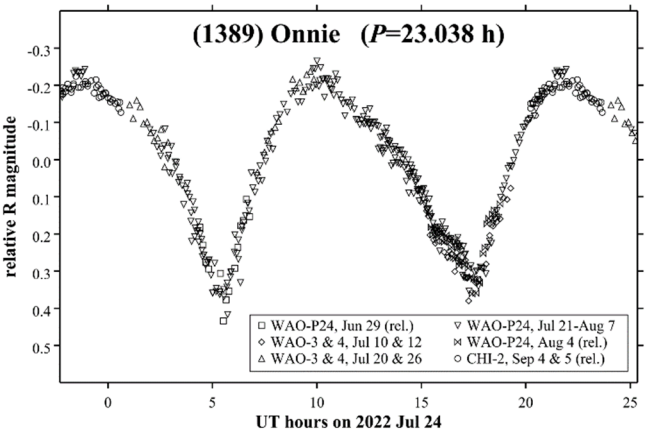

Figure 1. Folded composite lightcurve of (1389) Onnie during its 2022 apparition, light-time corrected, showing one rotation period plus the earliest and latest 10% repeated. Telescopes in the legend are identified in Table II. Lightcurves labeled "rel." were not calibrated to the same brightness zero-point as the stationary point observations; instead, they have been shifted in brightness to form a self-consistent composite.

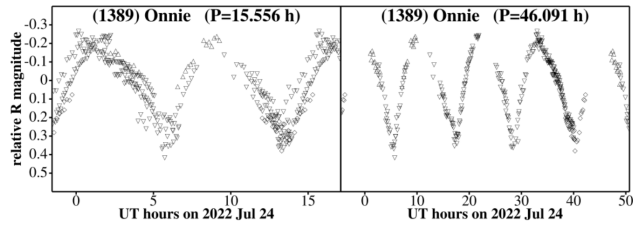

Figure 2. Similar to Fig. 1 but excluding the uncalibrated relative lightcurves, and folded at both alias periods to confirm that neither yields a self-consistent doubly-periodic composite.

In addition to the densely-sampled lightcurves from 2022 and from 2021, sparse-in-time observations made during three apparitions from 2017 to 2020 by the ATLAS astrometric survey (Tonry et al., 2018) are suitable for folded composite lightcurves and are publicly available online from the MPC astrometry Web site. The "sieve algorithm" of Slivan (2013) is used here to test whether sidereal rotations can be unambiguously counted across the combined lightcurve data set; the epochs measured for all five apparitions are given in Table III. The algorithm results (Fig. 3) confirm an unambiguous solution that corresponds to 1820.5 sidereal rotations during the maximum epoch interval, but the five apparitions from 2017 through 2022 are not sufficient to also distinguish the direction of spin, nor to unambiguously count rotations across the 27-apparition gap back to the original 1983 data. The derived sidereal period based on the epochs in Table III is constrained to be either 23.0448 ± 0.0006 h retrograde, or 23.0440 ± 0.0006 h prograde. Hanuš et al. (2011; 2013) both reported sparse-data sidereal periods of 23.0447 h with error "on the order of the last decimal place" and retrograde spin; our retrograde period agrees with theirs to within 0.0001 h.

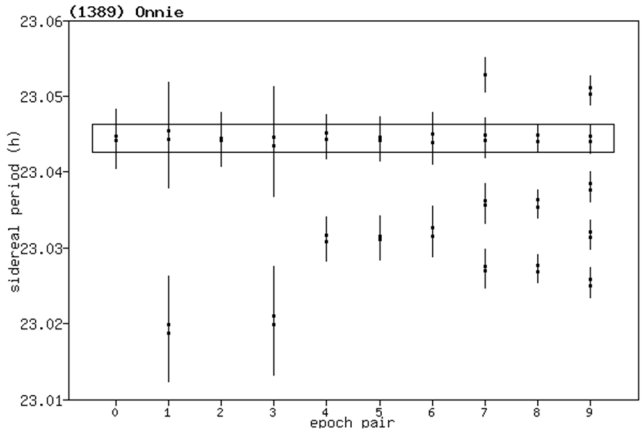

Figure 3: Single range of possible sidereal rotation periods allowed by the epochs in Table III as described in the text. The epoch measurement adopted errors are 1.5× the maximum observed asymmetry of the timing of the maxima in the corresponding composite lightcurves. Each horizontal coordinate index marks the time interval between a pair of epochs, with longer intervals to the right. Points and vertical bars represent sidereal periods and period ranges, respectively, calculated from every possible number of rotations that could elapse during the interval. The thin horizontal rectangle identifies the single range of periods that is allowed by all ten time intervals.

UT date 2022	α (°)	Tel. ID	Filter	Integration time (s)
Jun 29.3	19.8	WAO-PW	*R*	480
Jul 10.3	18.6	WAO-4	*R*	300
Jul 12.3	18.3	WAO-3	*R*	600
Jul 20.3	17.0	WAO-3	*R*	600
Jul 21.3	16.8	WAO-PW	*R*	600
Jul 22.3	16.6	WAO-PW	*R*	600
Jul 23.3	16.4	WAO-PW	*R*	600
Jul 24.3	16.1	WAO-PW	*R*	600
Jul 26.3	15.7	WAO-4	*R*	600
Jul 27.2	15.5	WAO-PW	*R*	600
Jul 31.2	14.5	WAO-PW	*R*	300
Aug 02.3	13.9	WAO-PW	*R*	300
Aug 03.2	13.7	WAO-PW	*R*	300
Aug 04.3	13.4	WAO-PW	*R*	300
Aug 07.3	12.5	WAO-PW	*R*	300
Sep 04.2	2.3	CHI-2	red	300
Sep 05.2	1.9	CHI-2	red	300

Table I: Nightly observing information, with rows grouped by lunation. Columns are: UT date at lightcurve mid-time, solar phase angle *α*, telescope ID (see Table II), filter (*R*, Cousins *R*; red, Astrodon Gen2 color separation red), and image integration time.

Number	Name	yyyy mm/dd	Phase	L_{PAB}	B_{PAB}	Period(h)	P.E.	Amp	A.E.
1389	Onnie	2022 06/29-09/05	19.8,1.9	346	1	23.038	0.005	0.58	0.04

Table IV. Observing circumstances and results. Solar phase angle is given for the first and last dates. L_{PAB} and B_{PAB} are the approximate phase angle bisector longitude/latitude at mid-date range.

Tel. ID	Dia. (m)	CCD camera	FOV (′)	Bin	Scale (″/pix)
WAO-3	0.36	FLI ML1001	20×20	1×1	1.18
WAO-4	0.36	SBIG STL-1001	21×21	1×1	1.25
WAO-PW	0.61	FLI PL16803	32×32	1×1	0.46
CHI-2	0.50	FLI PL16803	66×66	1×1	0.96

Table II: Telescopes and cameras information. Columns are: telescope ID (WAO-3, shed pier #3 Celestron C14; WAO-4, shed pier #4 Celestron C14; WAO-PW, Elliot PlaneWave 24-in CDK; CHI-2, ASA 500N), telescope diameter, CCD camera, detector field of view, image binning used, and binned image scale.

UT date	PAB λ (°)	Epoch (UT h)	Data ref.
2017 Oct 10	334.2	10.56 ± 1.50	a,b
2019 Jan 21	68.5	6.74 ± 1.74	a,b
2020 Mar 28	162.6	3.19 ± 1.13	a,b
2021 Apr 20	254.2	6.90 ± 0.35	c
2022 Jul 24	345.3	10.88 ± 1.31	d

Table III: Summary of lightcurve epochs, in each case locating a maximum from the second harmonic of a Fourier series model fit to the lightcurves. PAB *λ* is the J2000 ecliptic longitude of the phase angle bisector. Data references are a, ATLAS-MLO *o*-band; b, ATLAS-HKO *o*-band; c, Wilkin et al. (2023; this issue); d, this work. Photometry from the ATLAS survey (Tonry et al., 2018) was retrieved from the MPC Orbits/Observations Database.

Acknowledgements

We thank Dr. Michael Person and Timothy Brothers for allocation of telescope time at Wallace Observatory, and for observer instruction and support. The student observers were supported by a grant from MIT's Undergraduate Research Opportunities Program. F. Wilkin received funding from the Faculty Research Grant at Union College. This work also has made use of data and services provided by the International Astronomical Union's Minor Planet Center; specifically, the brightnesses accompanying astrometry from the Asteroid Terrestrial-impact Last Alert System (ATLAS) survey observing program.

References

Binzel, R.P. (1987). "A Photoelectric Survey of 130 Asteroids." *Icarus* **72**, 135-208.

Bowell, E.; Hapke, B.; Domingue, D.; Lumme, K.; Peltoniemi, J.; Harris, A.W. (1989). "Application of Photometric Models to Asteroids." In *Asteroids II* (R.P. Binzel; T. Gehrels; M.S. Matthews, eds.) pp. 524-556. Appendix: The IAU Two-Parameter Magnitude System for Asteroids. U. of Arizona Press, Tucson, AZ.

Erasmus, N.; Navarro-Meza, S.; McNeill, A.; Trilling, D.E.; Sickafoose, A.A.; Denneau, L.; Flewelling, H.; Heinze, A.; Tonry, J.L. (2020). "Investigating Taxonomic Diversity within Asteroid Families through ATLAS Dual-band Photometry." *Astrophys. J. Suppl. Ser*. **247**, A13.

Hanuš, J.; Ďurech, J.; Brož, M.; Warner, B.D.; Pilcher, F.; Stephens, R.; Oey, J.; Bernasconi, L.; Casulli, S.; Behrend, R.; Polishook, D.; Henych, T.; Lehký, M.; Yoshida, F.; Ito, T. (2011). "A study of asteroid pole-latitude distribution based on an extended set of shape models derived by the lightcurve inversion Method." *A&A* **530**, A134.

Hanuš, J.; Ďurech, J.; Brož, M.; Marciniak, A.; Warner, B.D.; Pilcher, F.; Stephens, R.; Behrend, R.; Carry, B.; Čapek, D.; Antonini, P.; Audejean, M.; Augustesen, K.; Barbotin, P.; Baudouin, P.; and 105 colleagues (2013). "Asteroids' physical models from combined dense and sparse photometry and scaling of the YORP effect by the observed obliquity distribution." *A&A* **551**, A67.

Howell, S.B. (1989). "Two-dimensional Aperture Photometry: Signal-to-noise Ratio of Point-source Observations and Optimal Data-extraction Techniques." *PASP* **101**, 616-622.

Lagerkvist, C.-I.; Magnusson, P. (1990). "Analysis of asteroid lightcurves. II - Phase curves in a generalized HG-system." *A&AS* **86**, 119-165.

Slivan, S.M.; Binzel, R.P.; Boroumand, S.C.; Pan, M.W.; Simpson, C.M.; Tanabe, J.T.; Villastrigo, R.M.; Yen, L.L.; Ditteon, R.P.; Pray, D.P.; Stephens, R.D. (2008). "Rotation Rates in the Koronis Family, Complete to $H \approx 11.2$." *Icarus* **195**, 226-276.

Slivan, S.M. (2013). "Epoch data in sidereal period determination. II. Combining epochs from different apparitions." *Minor Planet Bull.* **40**, 45-48.

Tonry, J.L.; Denneau, L.; Heinze, A.N.; Stalder, B.; Smith, K.W.; Smartt, S.J.; Stubbs, C.W.; Weiland, H.J.; Rest, A. (2018). "ATLAS: A High-cadence All-sky Survey System." *PASP* **130**, 064505.

Wilkin, F.P.; MacDonald, F.; Slivan, S.M. (2023). "Lightcurve for Koronis family member (1389) Onnie." *Minor Planet Bull.* **50**, 7-8.

LIGHTCURVE ANALYSIS OF ASTEROID 2685 MASURSKY

Melissa Hayes-Gehrke, Raiden Khan, Shijia Liao, Tucker Siegel,
Jorin Vincent, Stephen DeBoy, Evan Guenterberg,
Drew Hamilton, Brain Hopkins, Ilan Katz, Robert Sargent,
Cameron Storey, Gary Zhang
PSC 1113, BLDG 415
College Park, MD 20742, USA
mhayesge@umd.edu

Stephen M. Brincat
Flarestar Observatory
San Gwann, MALTA

Martin Mifsud
Manikata Observatory
Manikata, MALTA

(Received: 2022 August 22)

Photometric observations of the main-belt asteroid 2685 Masursky were conducted to determine the asteroid's synodic rotation period. Three telescopes based in Malta and Australia were used. The authors found a synodic rotation period of P = 59.531 ± 0.052 h with an amplitude of A = 1.26 mag.

2685 Masursky, a main-belt asteroid, was discovered by E. Bowell at Flagstaff (AZ) on 1981 May 3. It has a semimajor axis of 2.569 AU, an inclination of 12.124°, an eccentricity of 0.111, an absolute magnitude of 12.20, and an orbital period of 1504 days (JPL Small-Body Database Lookup, 2022). There are no prior recorded rotation periods for 2685 Masursky in The Asteroid Lightcurve Database (Warner et. al, 2009).

Observations of the asteroid 2685 Masursky were conducted at multiple locations with different telescopes. The first instrument used was Telescope 17 based in Siding Spring, Australia. It has a focal length of 2912 mm and a diameter of 0.43 m (iTelescope Support, 2021). Please refer to Table I for additional information. This telescope was used for observations on 2022 Apr 4. Observations on 2022 Apr 10, 19, 22, and 23 were conducted at Flarestar Observatory and Manikata Observatory in Malta with two other instruments (see Table I for further information). A luminance filter was used for all observations.

MPO Canopus (Warner, 2018) was used to analyze the images received from observations made throughout April 2022. The authors found a synodic rotation period of P = 59.531 ± 0.052 h with an amplitude of A = 1.26 mag (see Table II for more information). This rotation period is very atypical as few asteroids have a rotation period greater than 24 h. The found amplitude is also larger than expected. The final lightcurve can be seen in the figure. The shape of this lightcurve is slightly atypical; there are two maxima and two minima with a third local maximum around the data points corresponding to 2022 Apr 22. This suggests that Masursky might have an unusual shape or large craters; it might also indicate the existence of a secondary period. Given the long rotation period, we suggest future observations be planned over a longer range of time and specifically investigate the possibility of the binarity of the asteroid.

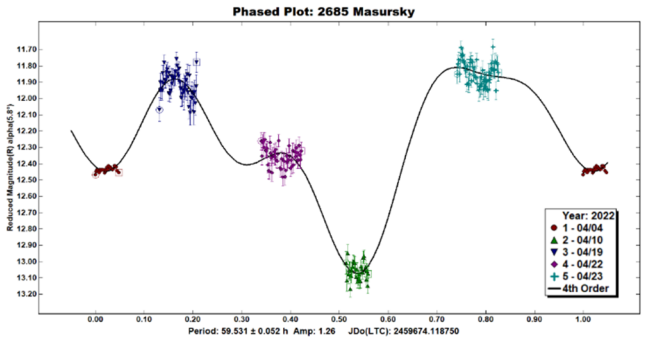

References

Harris, A.W.; Young, J.W.; Scaltriti, F.; Zappala, V. (1984). "Lightcurves and phase relations of the asteroids 82 Alkmene and 444 Gyptis." *Icarus* **57**, 251-258.

iTelescope Support (2021). Telescope 17. *https://support.itelescope.net/support/solutions/articles/231915-telescope-17*

JPL Small-Body Database Lookup (2022). *https://ssd.jpl.nasa.gov/tools/sbdb_lookup.html#/?sstr=2685*

Warner, B.D. (2018). MPO Canopus software version 10.7.12.9., *http://www.bdwpublishing.com*

Warner, B.D.; Harris, A.W.; Pravec, P. (2009). "The Asteroid Lightcurve Database." *Icarus* **202**, 134-146. Updated 2016 Sep. *https://www.minorplanet.info/php/lcdb.php*

Obs	MPC	Scope	Cam	FOV (arcmin)	Resolution (arcsec/pix)	Latitude	Longitude	Elevation (m)
SSO	Q62	0.43-m CDK	FLI Proline PL4710	15.5×15.5	0.92	31°16′52″ S	149°03′52″ E	1122
FO	171	0.25-m SCT	Moravian G2-1600	25.5×17	0.99	35°54′37″ N	14°28′12″ E	126
MO	——	0.20-m SCT	SBIG ST-9	——	—	35°55′52″ N	14°55′52″ E	35

Table I. Equipment used for observations. Obs column; SSO: Siding Spring Observatory, FO: Flarestar Observatory, MO: Manikata Observatory. Scope column; CDK: Corrected Dall-Kirkham, SCT: Schmidt-Cassegrain Telescope.

Number	Name	yyyy mm/dd	Phase	L_{PAB}	B_{PAB}	Period(h)	P.E.	Amp	A.E.	Grp
2685	Masursky	2022 04/04-04/23	6.0,4.0	205	-3	59.531	0.052	1.26	—	MB

Table II. Observing circumstances and results. The phase angle is given for the first and last date. If preceded by an asterisk, the phase angle reached an extrema during the period. L_{PAB} and B_{PAB} are the approximate phase angle bisector longitude/latitude at mid-date range (see Harris et al., 1984). Grp is the asteroid family/group (Warner et al., 2009).

LIGHTCURVE, ROTATION PERIOD AND SPIN-SHAPE MODEL FOR 2764 MOELLER

Michael Fauerbach
Florida Gulf Coast University
and SARA Observatories
10501 FGCU Blvd.
Ft. Myers, FL33965-6565
mfauerba@fgcu.edu

Vladimir Benishek
Belgrade Astronomical Observatory
Volgina 7, 11060 Belgrade 38, SERBIA

Brian D. Warner
Center for Solar System Studies (CS3)
446 Sycamore Ave.
Eaton, CO 80615 USA

(Received: 2022 August 3 Revised: 2022 December 1)

We present a new lightcurve measurement and a shape and spin axis model for main-belt asteroid 2764 Moeller. The model was achieved with the lightcurve inversion process, using combined dense photometric data acquired from two apparitions, between 2018 and 2022 and sparse data from Catalina Sky Survey (693, 703, G97) and Asteroid Terrestrial-impact Last Alert System (ATLAS, T05-T08). Analysis of the resulting data found a sidereal period P = 5.953424 ± 0.000001 h and two mirrored pole solutions at (λ = 310°, β = 41°) and (λ = 133°, β = 39°) with an uncertainty of ± 20 degrees.

We report on photometric observations obtained with the 0.6m telescope of the Southeastern Association for Research in Astronomy (SARA) consortium at Cerro Tololo Inter-American Observatory. The telescope is coupled with an Andor iKon-L series CCD. A detailed description of the instrumentation and setup can be found in the paper by Keel et al. (2017). The data was calibrated using *MaximDL* and photometric analysis was performed using *MPO Canopus* (Warner, 2021a). Fauerbach observed 2764 Moeller on the nights of 2022 May 05 and 2022 May 09. The derived rotational period of 5.953 ± 0.001 h with an amplitude of 0.61 mag is in excellent agreement with the prior results by Waszczak et al. (2015, 5.954 h), Pravec et al. (2018, 5.953 h), Benishek (2018, 5.954 h), Ditteon (2019, 5.95 h) and Fauerbach and Nelson (2019, 5.952 h).

Dense lightcurves for 2764 Moeller were obtained during two apparitions (2018, 2022). The observational details of the dense data used are reported in Table I. Unfortunately, the dense lightcurves do not cover enough variation in viewing geometry to derive a reliable pole solution. Furthermore, as the dense lightcurves were all taken close to opposition, the phase angle coverage of the observations is very small. In order to cover several apparition geometries and a wider range of phase angles, we used sparse data from the Catalina Sky Survey (693, 703, G97, V-band only) and Asteroid Terrestrial-impact Last Alert System (ATLAS, T05-T08), downloaded from the Asteroids Dynamic Site (AstDyS-2, 2022). Figure 2 shows the PAB longitude/latitude, as well as the phase angle distribution for sparse data used in the lightcurve inversion process. For clarity purposes, we also plot the dates during which the sparse data was observed. The ATLAS data covers fewer apparitions but is overall denser than the data from the Catalina Sky Survey.

Lightcurve inversion was performed using *MPO LCInvert* v.11.8.4.1 (Warner, 2021b). For a description of the modeling process see the *LCInvert Operating Instructions Manual* (Warner, 2009) and references therein.

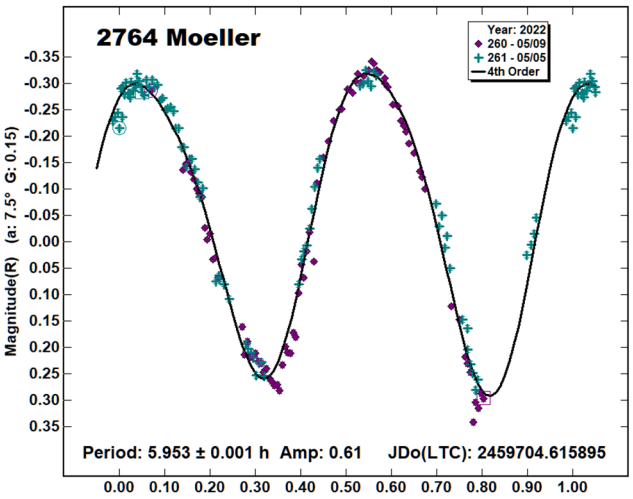

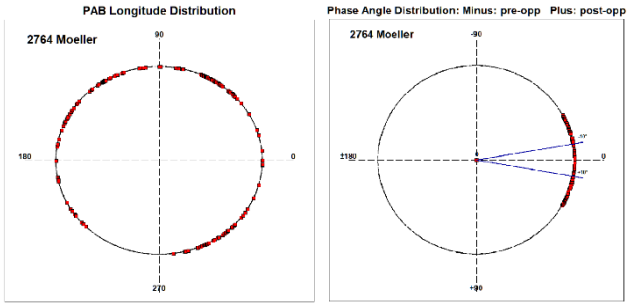

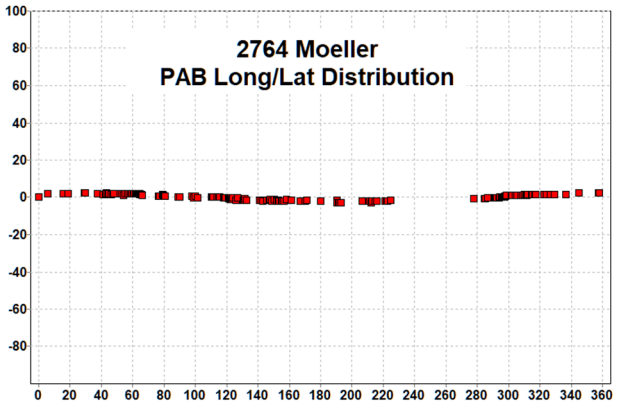

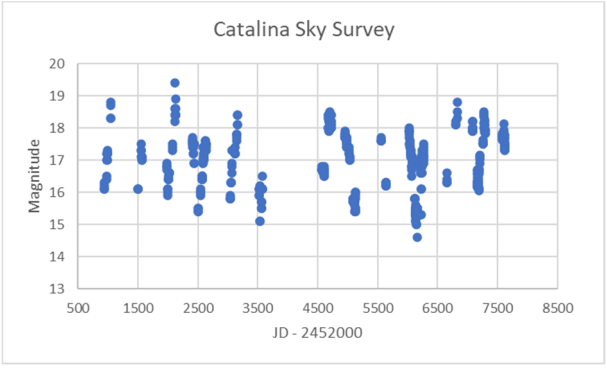

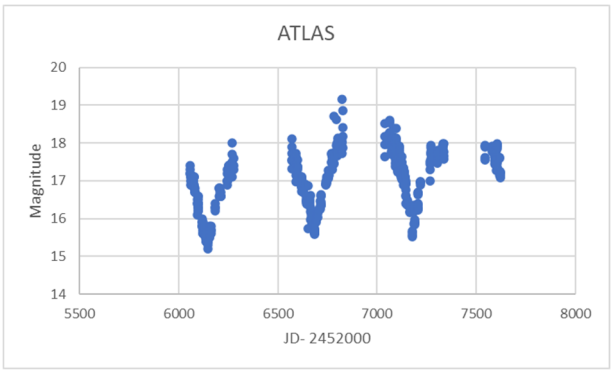

For the data analysis the weighting factor was set to 1.0 for dense and 0.3 for sparse data from Catalina and 0.5 for the sparse data from the ATLAS survey.

The sidereal period search was started with a wide margin on either side of the average of the synodic periods found in the asteroid lightcurve database (LCDB; Warner et al., 2009). In subsequent calculations the search area was narrowed down, and the step width decreased to get a finer measure. We found two almost identical sidereal periods with χ^2 values within 10% of the lowest values (Figure 3). The two best solutions were 5.95342351 h and 5.95342540 h respectively. The 5.95342351 h provided not only a slightly smaller χ^2 value, but also a significantly smaller dark area and therefore was used as starting value for the subsequent calculations.

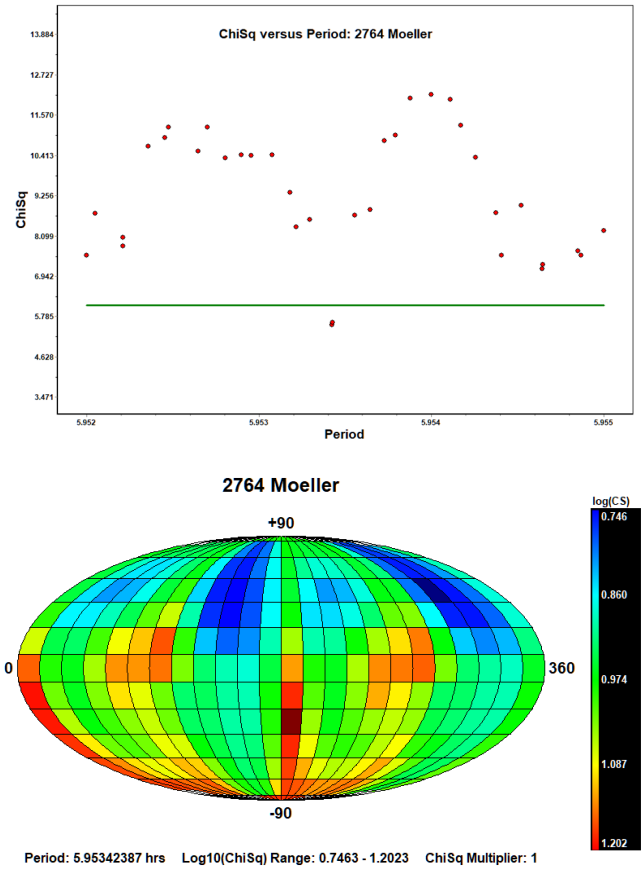

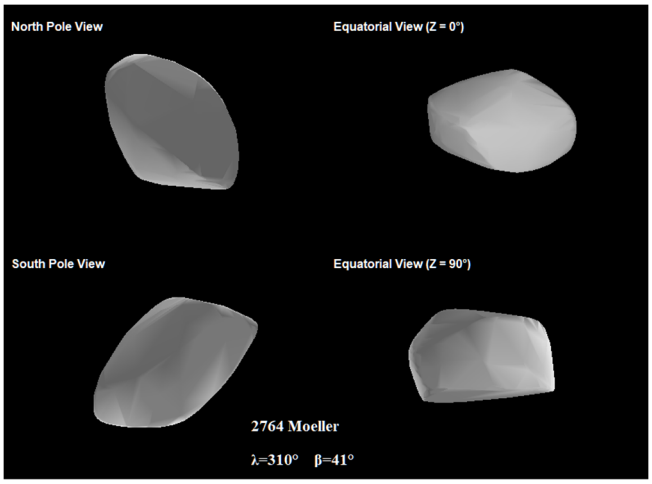

The pole search was started using the "medium" search option (312 fixed pole position with 15° longitude-latitude steps) and the sidereal period with the lowest χ^2 value set to "float". From this step we found two roughly mirrored lowest χ^2 solutions (Figure 4) separated by about 180° in longitude at ecliptic longitude-latitude pairs (300°, 45°) and (135°, 45°).

These two solutions were then used as inputs for fine pole searches. The final results -the two best solutions (lowest χ^2)- are reported in Table II. The sidereal period of 5.953424 ± 0.000001 h was obtained by averaging the two solutions found in the pole search process. Typical errors in the pole solution are ± 20°. Figure 5 shows the shape model (first solution with a lower χ^2) while Figure 6 shows the fit between the model (black line) and some observed lightcurves (red points). The overall agreement between the observed and calculated lightcurves is excellent.

The analysis did not identify a unique solution but two mirrored solutions with almost identical χ^2values. The good reproduction of the observed lightcurves by the modeled data is encouraging, but as is so often the case the call for "more data" is needed in order to increase the confidence in the results.

λ°	β°	Sidereal Period (hours)		RMS	Dark Area
310	41	5.953424 0.000001	±	0.0686	0.1254903
133	39			0.0687	0.0827130

Observer	yyyy	mm/dd	Phase	L_{PAB}	B_{PAB}	Period(h)	P.E.	Amp	A.E.
Fauerbach	2018	01/19,01/21	2.2,1.1	122	-1	5.952	0.003	0.25	0.04
Benishek	2018	01/24,01/26	1.4,2.1	122	-1	5.954	0.005	0.26	0.02
Fauerbach	2022	05/05,05/09	9.7,7.6	240	-2	5.953	0.001	0.61	0.04

Table I. Observing circumstances and results for the dense data used in the lightcurve inversion process for 2764 Moeller. The phase angle is given for the first and last date. If preceded by an asterisk, the phase angle reached an extrema during the period. L_{PAB} and B_{PAB} are the approximate phase angle bisector longitude/latitude at mid-date range (see Harris et al., 1984).

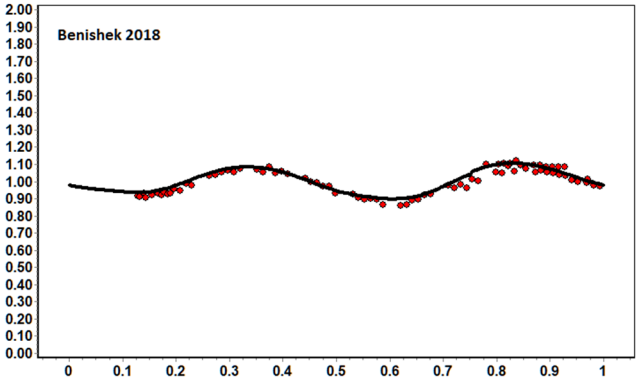

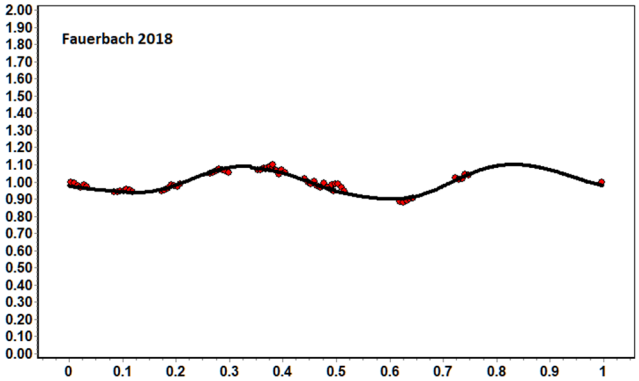

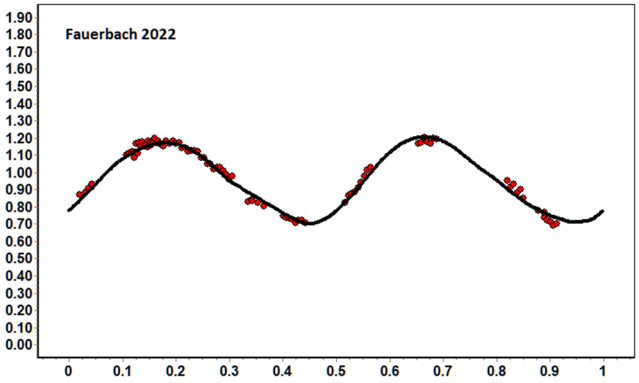

References

AstDyS-2 (2022), Asteroids - Dynamic Site. *https://newton.spacedys.com/astdys/*

Benishek, V. (2018). "Lightcurve and Rotation Period Determinations for Seven Asteroids." *Minor Planet Bulletin* **45**, 386-389.

Ditteon, R. (2019). "Lightcurve Analysis of Minor Planets Observed at the Oakley Southern Sky Observatory: 2018 January-March." *Minor Planet Bulletin* **46**, 127-129.

Fauerbach, M.; Nelson, K.M. (2019). "Photometric Observations of 1007 Pawlowia, 1774 Kulikov, 2764 Moeller, 5110 Belgirate, (8505) 1990 YK, and (34459) 2000 SC91." *Minor Planet Bulletin* **46**, 21-23.

Harris, A.W.; Young, J.W.; Scaltriti, F.; Zappala, V. (1984). "Lightcurves and phase relations of the asteroids 82 Alkmene and 444 Gyptis." *Icarus* **57**, 251-258.

Keel, W.C.; Oswalt, T.; Mack, P.; Henson, G.; Hillwig, T.; Batcheldor, D.; Berrington, R.; De Pree, C.; Hartmann, D.; Leake, M.; Licandro, J.; Murphy, B.; Webb, J.; Wood, M.A. (2017). "The Remote Observatories of the Southeastern Association for Research in Astronomy (SARA)." *Publications of the Astronomical Society of the Pacific* **129:015002** (12pp). *http://iopscience.iop.org/article/10.1088/1538-3873/129/971/015002/pdf*

Pravec, P.; Wolf, M.; Sarounova, L. (2018). *http://www.asu.cas.cz/~ppravec/neo.htm*

Warner, B.D. (2009). *LCInvert Operating Instructions Manual http://www.bdwpublishing.com/Manuals/LCInvert.pdf*

Warner, B.D.; Harris, A.W.; Pravec, P. (2009). "The asteroid lightcurve database." *Icarus* **202**, 134-146. Updated 2021 Dec. *http://www.minorplanet.info/lightcurvedatabase.html*

Warner, B.D. (2021a). *MPO Canopus* software version 10.8.5.0. *http://www.bdwpublishing.com*

Warner, B.D. (2021b). *MPO LCInvert* software version 11.8.4.1. *http://www.bdwpublishing.com*

Waszczak, A.; Chang, C.-K.; Ofek, E.O.; Laher, R.; Masci, F.; Levitan, D.; Surace, J.; Cheng, Y.-C.; Ip, W.-H.; Kinoshita, D.; Helou, G.; Prince, T.A.; Kulkarni, S. (2015). "Asteroid Light Curves from the Palomar Transient Factory Survey: Rotation Periods and Phase Functions from Sparse Photometry." *Astron. J.* **150**, article id. 75.

LIGHTCURVE ANALYSIS AND ROTATION PERIOD FOR ASTEROID 5147 MARUYAMA

Melissa Hayes-Gehrke, Caleb Arcilesi, Jacqueline Batres, William Byrne, Joshua Devan, Victor Eichenwald, Natalie Goodwin, Brian Huang, Sidharsh Joshi, Charles Karafotias, Nicole Maxwell, Nathan Pereyra
University of Maryland
College Park, MD, USA, 20742
mhayesge@umd.edu

Stephen M. Brincat
Flarestar Observatory (MPC 171)
San Gwann, MALTA

Charles Galdies
Znith Observatory
Naxxar, MALTA

(Received: 2022 July 26)

Photometric lightcurve analysis was applied to asteroid 5147 Maruyama based on observations taken in 2022 April. Observations were made from Australia and Malta to determine the rotation period of 5147 Maruyama. We used *MPO Canopus* to analyze the lightcurve of our asteroid in order to determine its rotation period to be P = 50.9 ± 0.1 h.

5147 Maruyama is a main-belt asteroid that was discovered on 1992 Jan 22 by Hiroshi Kaneda and Seiji Ueda. The Asteroid Lightcurve Database (Warner et al., 2009) does not have any previous rotation period data for Maruyama. 5147 Maruyama has a semi-major axis of 2.618 AU, an orbital period of 1547.536 days, and a diameter of 7.655 km. The absolute magnitude of the asteroid is 12.56 (JPL).

Photometric observations were taken of Maruyama in 2022 April at Siding Spring Observatory in Australia (MQ62) and at the Flarestar Observatory in San Gwann, Malta (MPC 171). The telescope used in Australia was a Planewave 17" CDK 0.43-m f/6.8 reflector equipped with a FLI ProLine E2V CCD47-10-1-109 CCD. The telescope used in Malta was a Meade SSC-10 Schmidt-Cassegrain f/6.3 equipped with a Morovian G2-1600 CCD. In both cases, a 300-second exposure time through a luminance filter was used for the capture of the images. Data analysis was performed using *MPO Canopus.*

In total, 219 images were used for photometric lightcurve analysis. Multiple Fourier models were tested and two potential rotation periods were found. The first potential rotation period was P = 101.12 ± 1.12 h. The second potential rotation period was P = 50.9 ± 0.1 h. The first appears to be twice the period of the second, which fits somewhat better with the data. Moreover, the error in the second plot was much lower at only 0.1h. The 101.1-hour fit was decided to be overfit to the data. The unusually low minima of the lightcurve may indicate that 5147 Maruyama has unusual qualities (one half of its surface possessing a much lower albedo, for example). This period should be considered provisional. More data are necessary during future apparitions in order to confirm this provisional period.

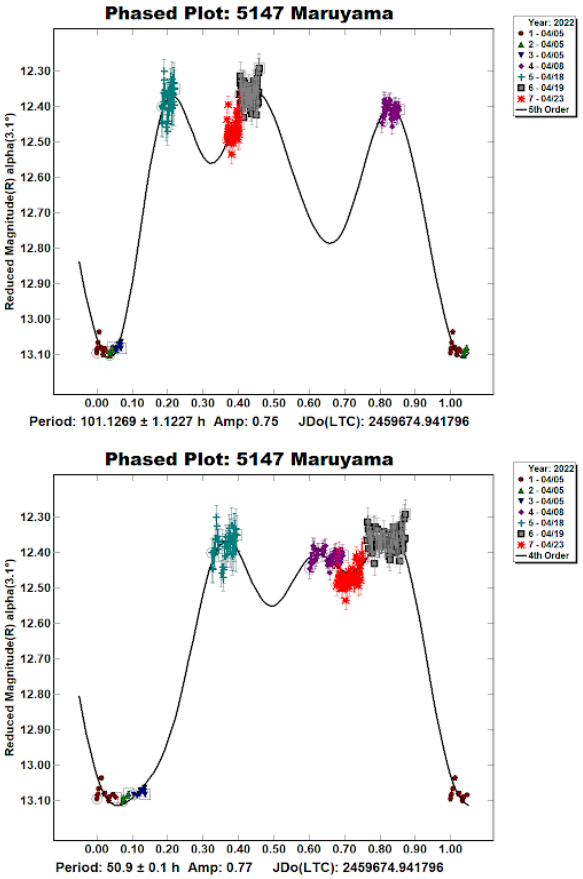

Acknowledgments

We would like to give thanks to the Department of Astronomy at University of Maryland, College Park and observing using the T17 Telescope at iTelescope.

References

Harris, A.W.; Young, J.W.; Scaltriti, F.; Zappala, V. (1984). "Lightcurves and phase relations of the asteroids 82 Alkmene and 444 Gyptis." *Icarus* **57**, 251-258.

JPL (2020). Small Body Database Browser. *https://ssd.jpl.nasa.gov*

Warner, B.D.; Harris, A.W.; Pravec, P. (2009). "The Asteroid Lightcurve Database." *Icarus* **202**, 134-146. Updated 2016 Sep. *http://www.minorplanet.info/lightcurvedatabase.html*

Warner, B.D. (2019). MPO Software, MPO Canopus v10.8.1.1. Bdw Publishing. *http://minorplanetobserver.com*

Number	Name	yyyy mm/dd	Phase	L_{PAB}	B_{PAB}	Period(h)	P.E.	Amp	A.E.	Grp
5147	Maruyama	2022 04/05-04/27	3.0,11.6	195.7	-6.1	50.9	0.1	0.77		MBA

Table I. Observing circumstances and results. The phase angle is given for the first and last date. If preceded by an asterisk, the phase angle reached an extrema during the period. L_{PAB} and B_{PAB} are the approximate phase angle bisector longitude/latitude at mid-date range (see Harris et al., 1984). Grp is the asteroid family/group (Warner et al., 2009).

ROTATION PERIOD DETERMINATION FOR (7335) 1989 JA

Ryan Lambert, Franck Marchis
SETI Institute, Carl Sagan Center, 189 Bernardo Avenue,
Suite 200, Mountain View CA, 94043, USA
rlambert@seti.org

Josef Hanuš
Charles University, Faculty of Mathematics and Physics,
Institute of Astronomy, V Holešovickách 2
18000 Prague 8, CZECH REPUBLIC

John Archer, Mario Billiani, John K. Bradley, Phil Breeze-Lamb, Michael Camilleri, Martin Davy, John Deitz, Stephen Donnelly, Mark Fairfax, Keiichi Fukui, Ryan Gamurot, Tateki Goto, Bruno Guillet, Scott Kardel, Rachel Knight, William Hedegaard Langvad, Margaret A. Loose, Nicola Meneghelli, Mike Mitchell, Pavel Nikiforov, Bruce Parker, John W. Pickering, Michael Primm, Justus Randolph, Felipe Braga Ribas, Fabien Richardot, Darren A. Rivett, Masao Shimizu, Georges Simard, Martin Smallen, Ethan Teng, Marcos A. van Dam, Aad Verveen, Joe Widi
Unistellar Citizen Astronomers

(Received: 2022 September 30)

We present the results of an observational study of the near-Earth asteroid (7335) 1989 JA conducted during its May 2022 close approach. Using data collected from participating Unistellar citizen astronomers, we report a best-fitting synodic rotation period of 2.592 ± 0.006 hours with a corresponding amplitude of 0.09 ± 0.01 magnitudes for (7335) 1989 JA.

Beginning on 2022 May 5, the Unistellar citizen science network (Marchis et al., 2020) began a campaign to observe the near-Earth asteroid, (7335) 1989 JA during its close approach on 2022 May 27. The campaign ran from 2022 May 5 to Jun 2 and resulted in 75 observations from 35 different citizen astronomers. Observations were taken using Unistellar digital telescopes, named eVscope, eQuinox, and eVscope 2. These telescopes are 114mm *f*/4 reflectors and use a Sony Exmor IMX224 (eVscope, eQuinox) and Sony Exmor IMX347 CMOS (eVscope 2) detector. Before 2022 May 22, observations were performed as a series of consecutive, unfiltered 4-second exposures with a gain of 25dB. Exposures were taken for 40 minutes before the eVscope was realigned onto the target. On 2022 May 22, the proper motion of 1989 JA was great enough that the observation procedures were updated to realign every 20 minutes to avoid the asteroid leaving the field of view. Observations were then uploaded to the Unistellar server where the images were dark subtracted, plate-solved, and stacked according to the proper motion of (7335) 1989 JA at the time of observation.

(7335) 1989 JA was discovered in 1989 May by Eleanor Helin at the Palomar observatory. It is a potentially hazardous near-Earth asteroid with a semi-major axis of 1.772 au, eccentricity of 0.485, inclination of 15.17°, and orbital period of 2.36 years. The diameter has been estimated to be 0.932 ± 0.153 km from the NEOWISE survey (Mainzer et al.; 2019) using an absolute magnitude H = 17. Radar observations taken by Mahapatra et al. (2002) constrained the synodic rotation period to <12 hours but no further attempts to constrain the rotation period appear on the asteroid lightcurve database (LCDB; Warner et al., 2009).

To determine the synodic rotation period, a subsample of 13 observations that occurred between 2022 May 24-25 were selected. Since (7335) 1989 JA was in the midst of a close approach, this two-day window was chosen to minimize the change in magnitude that would occur across observations due to the changing distance and phase angle. Analysis of the periodogram created from the lightcurves of these 13 observations reveals a best fitting synodic rotation period of 2.592 hours with other high-probability signals occurring at the integer aliases of this rotation period. We assumed an uncertainty corresponding to a 10% rotation phase offset, resulting in a synodic rotation period of 2.592 ± 0.006 hours. In the second figure, we present a rotation phase plot of our 13-observation subsample. Each observation has been labeled by the 6-character serial number of the eVscope that took the observation along with the date the observation was taken. To more easily identify features in the lightcurve, a black line has been added to the plot that is the rolling weighted average magnitude of 200 subsequent magnitude measurements. We estimate the amplitude as half of the difference between the highest and lowest magnitude across the weighted rolling average. Using this method, we find an amplitude of A = 0.09 ± 0.01 mag.

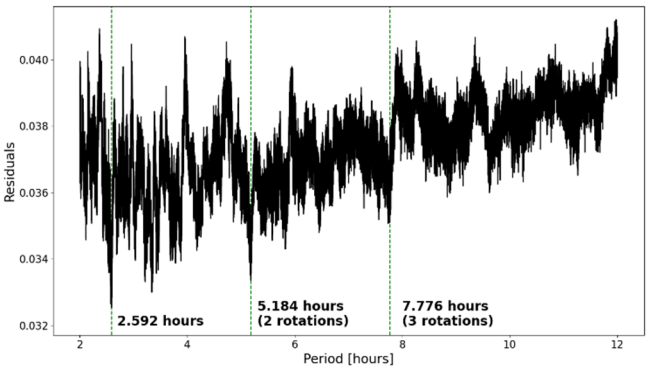

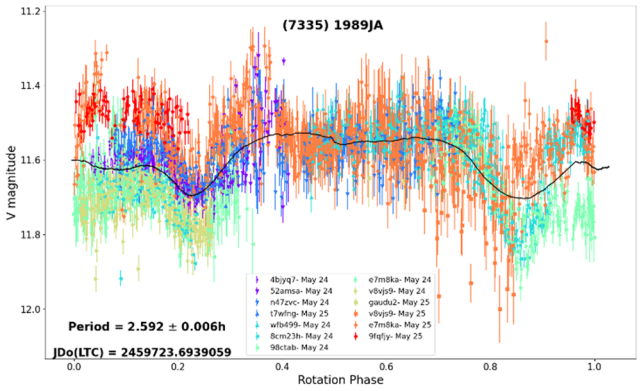

Number	Name	20yy mm/dd	Phase	L_{PAB}	B_{PAB}	Period(h)	P.E.	Amp	A.E.	Exp	Grp
7335	1989JA	22 05/24-05/25	30.7,35.5	226	-1	2.592	0.006	0.09	0.01	4200	PHA

Table I. Observing circumstances and results. The phase angle is given for the first and last date. L_{PAB} and B_{PAB} are the approximate phase angle bisector longitude and latitude at mid-date range (see Harris et al., 1984). Exp is the exposure (sec) or average if a range of exposures was used. Grp is the asteroid family/group (Warner et al., 2009).

Acknowledgements

The authors thank all the citizen astronomers that participated in this observation campaign and contributed their valuable data. This research was supported with a generous donation by the Gordon and Betty Moore Foundation. The scientific data presented herein were obtained using the Unistellar Network, which is managed jointly by Unistellar and the SETI Institute. The work of Josef Hanuš has been supported by the Czech Science Foundation through grant 22-17783S.

References

Harris, A.W.; Young, J.W.; Scaltriti, F.; Zappala, V. (1984). "Lightcurves and phase relations of the asteroids 82 Alkmene and 444 Gyptis." *Icarus* **57**, 251-258.

Mahapatra, P.R.; Benner, L.A.M.; Ostro, S.J.; Jurgens, R.F.; Giorgini, J.D.; Yeomans, D.K.; Chandler, J.F.; Shapiro, I.I. (2002). "Radar observations of asteroid 7335 (1989 JA)." *Planetary and Space Science* **50**, 257-260.

Mainzer, A.; Bauer, J.; Cutri, R.; Grav, T.; Kramer, E.; Masiero, J.; Sonnett, S.; Wright, E., Eds. (2019). *NEOWISE Diameters and Albedos V2.0*, NASA Planetary Data System.

Marchis F.; Malvache, A.; Marfisi, L.; Borot, A.; Arbouch, E. (2020). "Unistellar eVscopes: Smart, portable, and easy-to-use telescopes for exploration, interactive learning, and citizen astronomy." *Acta Astronautica* **166**, 23-28.

Warner, B.D.; Harris, A.W.; Pravec, P. (2009). "The Asteroid Lightcurve Database." *Icarus* **202**, 134-146. Updated 2021 Dec. *http://www.minorplanet.info/php/lcdb.php*

ROTATION PERIOD DETERMINATION FOR ASTEROID 12919 TOMJOHNSON

Alessandro Marchini, Riccardo Papini
Astronomical Observatory, DSFTA - University of Siena (K54)
Via Roma 56, 53100 - Siena, ITALY
marchini@unisi.it

(Received: 2022 October 14)

Photometric observations of the main-belt asteroid 12919 Tomjohnson were conducted in order to determine its synodic rotation period. We found $P = 8.147 \pm 0.001$ h, $A = 0.51 \pm 0.03$ mag.

CCD photometric observations of the main-belt asteroid 12919 Tomjohnson were carried out in July 2022 at the Astronomical Observatory of the University of Siena (K54), a facility inside the Department of Physical Sciences, Earth and Environment (DSFTA, 2022). We used a 0.30-m *f*/5.6 Maksutov-Cassegrain telescope, SBIG STL-6303E NABG CCD camera, and clear filter; the pixel scale was 2.30 arcsec when binned at 2×2 pixels and all exposures were 300 seconds.

Data processing and analysis were done with *MPO Canopus* (Warner, 2018). All images were calibrated with dark and flat-field frames and the instrumental magnitudes converted to R magnitudes using solar-colored field stars from a version of the CMC-15 catalogue distributed with *MPO Canopus*. Table I shows the observing circumstances and results.

A search through the asteroid lightcurve database (LCDB; Warner et al., 2009) indicates that our result may be the first reported lightcurve observations and results for this asteroid.

12919 Tomjohnson (1998 VB6) was discovered on 1998 November 11 at Catalina by the Catalina Sky Survey and named in honor of Thomas J. Johnson who developed a technique for creating Schmidt telescope correctors that allowed the mass production of Schmidt-Cassegrain telescopes. It is an inner main-belt asteroid with a semi-major axis of 2.274 AU, eccentricity 0.218, inclination 6.368°, and an orbital period of 3.43 years. Its absolute magnitude is $H = 14.02$ (JPL, 2022). The WISE/NEOWISE satellite infrared radiometry survey (Masiero et al., 2011) found a diameter $D = 4.882 \pm 0.468$ km using an absolute magnitude $H = 13.7$.

Observations were conducted over four nights and collected 191 data points. The period analysis shows a bimodal solution for the rotational period of $P = 8.147 \pm 0.001$ h with an amplitude $A = 0.51 \pm 0.03$ mag. This target was observed within the Photometric Survey for Asynchronous Binary Asteroids under the leadership of Petr Pravec from Ondřejov Observatory, Czech Republic (Pravec et al., 2006; Pravec, 2022web) and their independent analysis confirmed our results.

Number	Name	2022/mm/dd	Phase	L_{PAB}	B_{PAB}	Period(h)	P.E.	Amp	A.E.	Grp
12919	Tomjohson	07/18-07/26	9.2,6.7	306	7	8.147	0.001	0.51	0.03	MBI

Table I. Observing circumstances and results. The phase angle is given for the first and last date. If preceded by an asterisk, the phase angle reached an extrema during the period. L_{PAB} and B_{PAB} are the approximate phase angle bisector longitude/latitude at mid-date range (see Harris et al., 1984). Grp is the asteroid family/group (Warner et al., 2009).

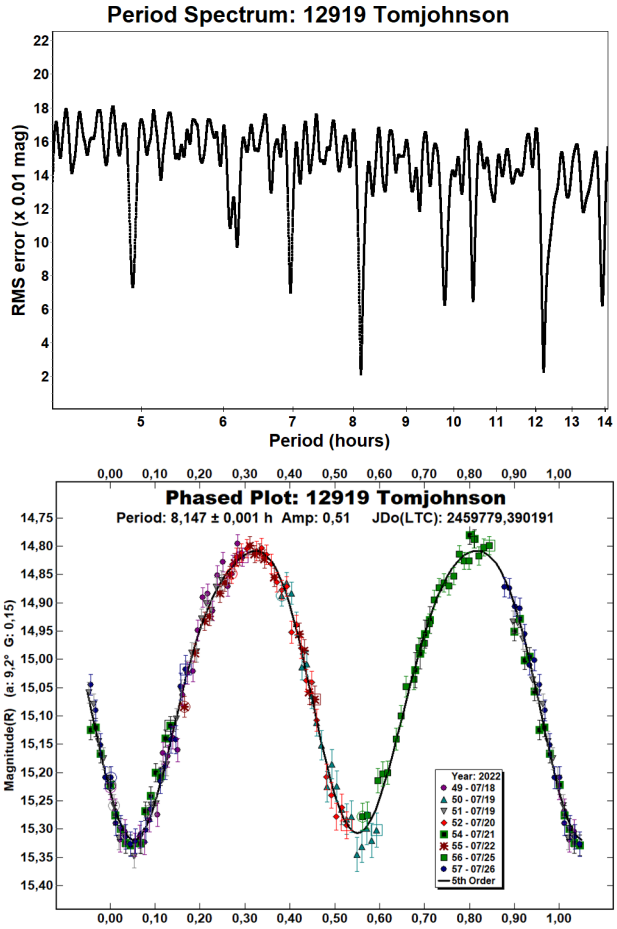

References

DSFTA (2022). Dipartimento di Scienze Fisiche, della Terra e dell'Ambiente – Astronomical Observatory. *https://www.dsfta.unisi.it/en/research/labs/astronomical-observatory*

Harris, A.W.; Young, J.W.; Scaltriti, F.; Zappala, V. (1984). "Lightcurves and phase relations of the asteroids 82 Alkmene and 444 Gyptis." *Icarus* **57**, 251-258.

JPL (2022). Small Body Database Search Engine. *https://ssd.jpl.nasa.gov*

Masiero, J.R.; Mainzer, A.K.; Grav, T.; Bauer, J.M.; Cutri, R.M.; Dailey, J.; Eisenhardt, P.R.M.; McMillan, R.S.; Spahr, T.B.; Skrutskie, M.F.; Tholen, D.; Walker, R.G.; Wright, E.L.; DeBaun, E.; Elsbury, D.; Gautier IV, T.; Gomillion, S.; Wilkins, A. (2011). "Main Belt Asteroids with WISE/NEOWISE. I. Preliminary Albedos and Diameters." *Astrophys. J.* **741**, A68.

Pravec, P.; Scheirich, P.; Kušnirák, P.; Šarounová, L.; Mottola, S.; Hahn, G.; Brown, P.; Esquerdo, G.; Kaiser, N.; Krzeminski, Z.; Pray, D.P.; Warner, B.D.; Harris, A.W.; Nolan, M.C.; Howell, E.S.; Benner, L.A.M.; Margot, J.-L.; Galád, A.; Holliday, W.; Hicks, M.D. Krugly, Yu.N.; Tholen, D.; Whiteley, R.; Marchis, F.; DeGraff, D.R.; Grauer, A.; Larson, S.; Velichko, F.P.; Cooney, W.R.; Stephens, R.; Zhu, J.; Kirsch, K.; Dyvig, R.; Snyder, L.; Reddy, V.; Moore, S.; Gajdoš, Š.; Világi, J.; Masi, G.; Higgins, D.; Funkhouser, G.; Knight, B.; Slivan, S.; Behrend, R.; Grenon, M.; Burki, G.; Roy, R.; Demeautis, C.; Matter, D.; Waelchli, N.; Revaz, Y.; Klotz, A.; Rieugné, M.; Thierry, P.; Cotrez, V.; Brunetto, L.; Kober, G. (2006). "Photometric survey of binary near-Earth asteroids." *Icarus* **181**, 63-93.

Pravec, P. (2022web). Photometric Survey for Asynchronous Binary Asteroids web site. *http://www.asu.cas.cz/~asteroid/binastphotsurvey.htm*

Warner, B.D.; Harris, A.W.; Pravec, P. (2009). "The Asteroid Lightcurve Database." *Icarus* **202**, 134-146. Updated 2021 Dec. *https://minplanobs.org/mpinfo/php/lcdb.php*

Warner, B.D. (2018). MPO Software, MPO Canopus v10.7.7.0. Bdw Publishing. *http://bdwpublishing.com/*

PHOTOMETRY OF NEA (285263) 1998 QE2 DURING ITS 2013 CLOSE APPROACH

Apostolos Christou
Armagh Observatory and Planetarium, College Hill,
Armagh BT61 9DG, United Kingdom
apostolos.christou@armagh.ac.uk

Kosmas Gazeas
Department of Astrophysics, Astronomy and Mechanics
University of Athens, University Campus
15784 Zografos, Athens, Greece
kgaze@phys.uoa.gr

(Received: 2022 October 14)

We present a new rotational lightcurve and period/amplitude determination for NEA (285263) 1998 QE2 from photometric data obtained during four consecutive nights in June 2013, when the asteroid was between 0.04 and 0.05 au from Earth. The results are: P = 4.7589 ± 0.0119 h and A = 0.21 ± 0.03.

Near-Earth asteroid (285263) 1998 QE2 was discovered in August 1998 by the LINEAR facility at Socorro, NM (Williams, 1998). In early June 2013 the asteroid made its closest approach to the Earth (0.039 au) until 2221. At that time, it became as bright as V = 11 mag and was subjected to intense observational scrutiny. Radar observations (Springmann et al., 2014) showed the asteroid to be ~3 km in diameter and thus one of the largest Potentially Hazardous Asteroids known to-date. The radar data also indicated the presence of a satellite ~800 m in diameter with an orbital period of 31.3 ± 0.1 h (Pravec, 2013).

Reflectance spectroscopy (Hicks et al., 2013; Lin et al., 2018; Binzel et al., 2019; Fieber-Beyer et al., 2020) shows a taxonomically primitive surface, consistent with an albedo of ~0.04 obtained from measurements of the asteroid's thermal emission (Trilling et al., 2010; Fieber-Beyer et al., 2020).

An examination of the Asteroid Lightcurve Database (LCDB) (Warner et al., 2009; retrieved 2022 Aug 18) yielded four previous rotational period determinations for this asteroid, based on data obtained during the 2013 close approach. Those by Pravec (2013; P = 4.749 ± 0.001 h, A = 0.19 ± 0.02 mag) and by Hills (2014; P = 4.751 ± 0.002 h, A = 0.20 ± 0.03 mag) are mutually consistent, the remaining two are by Hicks et al. (2013; P = 5.39 ± 0.02 h) and by Oey (2014; P = 2.726 ± 0.001 h, A = 0.11 ± 0.01 mag).

Here we present a photometric analysis of observations obtained with the 0.4-m f/8 Cassegrain reflector equipped with an SBIG ST-10 CCD and Johnson V filter at the University of Athens Observatory (UOAO) within the Department for Astrophysics, Astronomy and Mechanics at the National and Kapodistrian University of Athens (Gazeas, 2016) on 4 consecutive nights during the period 2013 June 2-5. Series of 30-s exposures were obtained every 35 s on the first two nights, switching to a 45 s cadence and 40-s exposure time for the remainder of the observing period as the asteroid faded from V = 11.4 mag to V = 12.1 mag. All CCD frames were acquired with 2×2 on-the-fly binning and an effective image scale of 1.4 arcsec/pix.

For data analysis, the raw FITS frames were dark-subtracted and flat-fielded using subroutines from the *IDL Astronomy User's Library* (*astrolib*; Landsman, 1993).

Differential photometry was carried out with *MPO Canopus v10.7.6.4* (Warner, 2016) using solar analog comparison stars from the *MPOSC3* catalog. Due to the asteroid's rapid sky motion (20 arcsec/min on the 2nd June, slowing to 13 arcsec/min on the 5th) which necessitated shifting the imaging field several times on every night, the dataset was split into groups of several tens of frames each prior to photometric reduction. Lightcurve analysis was done with the Fourier algorithm by Harris and Lupishko (1989).

The period spectrum from 19 measurement groups spanning all four nights (Fig. 1) shows the most significant RMS minima in the range [0.2-10.5] h, used as a guide to perform a high-resolution period search in the interval [4.5-5.0] h with a period step of 0.001 h. Figure 2 shows a 6th order Fourier series (black curve) fitted to those data. Our best-fit estimate of the primary rotation period from the fit is P = 4.7589 ± 0.0119 h with a corresponding estimate of A=0.21 ± 0.03 mag for the lightcurve amplitude. These are within 1-sigma of the Pravec and of the Hills et al. estimates, increasing confidence in a primary rotational period and lightcurve amplitude solution of P ≃ 4.75 h and A ≃ 0.20 for this asteroid. No attempt was made to search for secondary periods in the data.

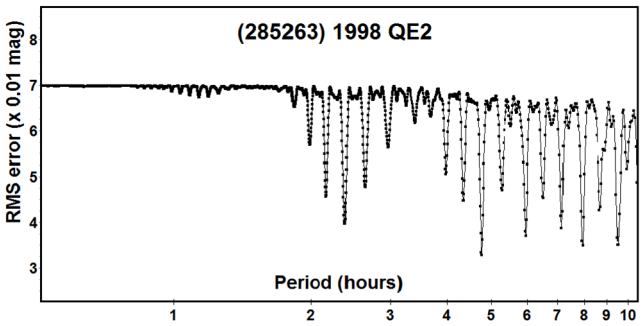

Figure 1: Period spectrum of (285263) 1998 QE2.

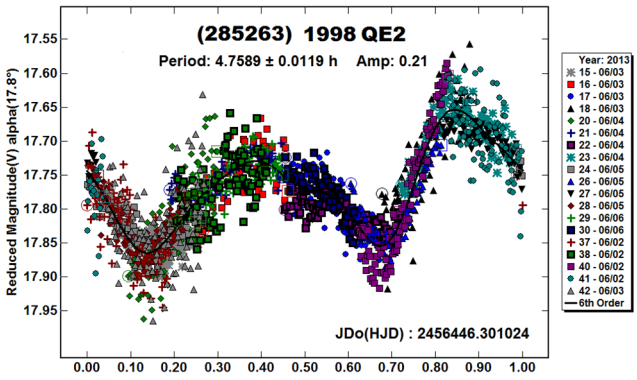

Figure 2: Phased lightcurve for (285263) 1998 QE2.

Number	Name	yyyy mm/dd	Phase	L_{PAB}	B_{PAB}	Period(h)	P.E.	Amp	A.E.	Grp
285263	1998 QE2	2013 06/02-06/06	17.4,23.8	248	8	4.7589	0.0119	0.21	0.03	NEA

Table I. Observing circumstances and results. The phase angle is given for the first and last date. If preceded by an asterisk, the phase angle reached an extrema during the period. L_{PAB} and B_{PAB} are the approximate phase angle bisector longitude/latitude at mid-date range (see Harris et al., 1984). Grp is the asteroid family/group (Warner et al., 2009).

Acknowledgments

MPOSC3 makes use of data products from the Two Micron All Sky Survey, which is a joint project of the University of Massachusetts and the Infrared Processing and Analysis Center/California Institute of Technology, funded by the National Aeronautics and Space Administration and the National Science Foundation. Astronomical research at the Armagh Observatory and Planetarium is funded by grant-in-aid from the Northern Ireland Department for Communities.

References

Binzel, R.P.; DeMeo, F.; Turtelboom, E.V.; Bus, S.J. and 16 co-authors (2019). "Compositional distributions and evolutionary processes for the near-Earth object population: Results from the MIT-Hawaii Near-Earth Object Spectroscopic Survey (MITHNEOS)." *Icarus* **324**, 41-76.

Fieber-Beyer, S.K.; Kareta, T.; Reddy, V.; Gaffey, M.J. (2020). "Near-earth asteroid: (285263) 1998 QE2." *Icarus* **347**, article id. 113807.

Gazeas, K. (2016). "The robotic and remotely controlled telescope at the University of Athens Observatory." *Rev. Mex. Astron. Astroph. Ser. Conf.* **48**, 22-23.

Harris, A.W.; Young, J.W.; Scaltriti, F.; Zappala, V. (1984). "Lightcurves and phase relations of the asteroids 82 Alkmene and 444 Gyptis." *Icarus* **57**, 251-258.

Harris, A.W., Lupishko, D.F. (1989). "Photometric lightcurve observations and reduction techniques." In: Asteroids II; Proceedings of the Conference, ed. R.P. Binzel, T. Gehrels, and M.S. Matthews, University of Arizona Press, p. 39-53.

Hicks, M.; Lawrence, K.; Chesley, S.; Chesley, J.; Rhoades, H.; Elberhar, S.; Carcione, A.; Borlase, R. (2013). "Palomar spectroscopy of near-earth asteroids 137199 (1999 KX4), 152756 (1999 JV3), 163249 (2002 GT), 163364 (2002 OD20), and (285263) 1998 QE2." *The Astronomer's Telegram* **5132** (1).

Hills, K. (2014). "Asteroid Lightcurve Analysis at Riverland Dingo Observatory (RDO): 2013 Results." *The Minor Planet Bulletin* **41**, 2-3.

Landsman, W.B. (1993). *In: Astronomical Data Analysis Software and Systems II, A.S.P. Conference Series,* **52**, ed. R.J. Hanisch, R.J.V. Brissenden, and Jeannette Barnes, p.246. Available at *https://idlastro.gsfc.nasa.gov/*

Lin, C.-S.; Ip, W.-H.; Lin, Z.-Y.; Cheng, Y.-C.; Lin, H.-W.; Chang, C.-K. (2018). "Photometric survey and taxonomic identifications of 92 near-Earth asteroids." *Planetary and Space Science* **152**, 116-135.

Oey, J. (2014). "Lightcurve Analysis of Asteroids from Blue Mountains Observatory in 2013." *The Minor Planet Bulletin* **41**, 276-281.

Pravec, P. (2013). Information retrieved on September 2022 by querying the Asteroid Lightcurve Photometry Database (ALCDEF: *https://alcdef.org*) for all available data on this asteroid.

Springmann, A.; Taylor, P.A.; Howell, E.S.; Nolan, M.C.; Benner, L.A.M.; Brozovic, M.; Giorgini, J.D.; Margot, J.L. (2014). "Radar shape model of binary near-earth asteroid (285263) (285263) 1998 QE2". *In: Proc. Lunar Sci. Conf.* **45**, 1777, p. 1313.

Trilling, D.E.; Mueller, M.; Hora, J.L.; Harris, A.W.; Bhattacharya, B.; Bottke, W.F.; Chesley, S.; Delbo, M.; Emery, J.P.; Fazio, G.; Mainzer, A.; Penprase, B.; Smith, H.A.; Spahr, T.B.; Stansberry, J.A.; Thomas, C.A. (2010). "ExploreNEOs I: description and first results from the warm Spitzer near-earth object survey." *Astron. J.* **140** (3), 770–784.

Warner, B.D. (2016). MPO Software, MPO Canopus v10.7.6.4. BDW Publishing. *http://bdwpublishing.com/mposoftware.aspx*

Warner, B.D.; Harris, A.W.; Pravec, P. (2009). "The Asteroid Lightcurve Database." *Icarus* **202**, 134-146. Updated 2021 Dec. *http://www.minorplanet.info/lightcurvedatabase.html*

Williams, G.V. (1998). "MPEC 1998-Q19: 1998 QE2." IAU Minor Planet Center. Issued 1998 August 22.

NEAR-EARTH ASTEROID LIGHTCURVE ANALYSIS AT THE CENTER FOR SOLAR SYSTEM STUDIES: 2022 JUNE-OCTOBER

Brian D. Warner
Center for Solar System Studies (CS3)
446 Sycamore Ave.
Eaton, CO 80615 USA
brian@MinorPlanetObserver.com

Robert D. Stephens
Center for Solar System Studies (CS3)
Rancho Cucamonga, CA

(Received: 2022 October 7)

CCD photometric observations of six near-Earth asteroids (NEA) were made at the Center for Solar System Studies from 2022 June to October. (54789) 2002 MZ7 appears to be in non-principal axis rotation ("tumbling"), which was reliably established by Pravec et al. (2005). Our analysis found an additional, unexpected short period, low amplitude lightcurve. 398188 Agni also appears to be tumbling. It was not possible to establish the true periods of rotation and precession for either asteroid.

CCD photometric observations of six near-Earth asteroids (NEAs) were made at the Center for Solar System Studies (CS3) in 2022 June to October. Two of the seven, (54789) 2002 MZ7 and 398188 Agni, are in a state of non-principal axis rotation, i.e., "tumbling." Given the limitations of the software used to analyze the data and insufficient data, the true periods of rotation and precession could not be determined.

Table I lists the telescopes and CCD cameras that were available to make observations. All the cameras use a KAF-1001E blue-enhanced CCD and so have essentially the same response. The pixel scales ranged from 1.24-1.60 arcsec/pixel.

Telescopes	Cameras
0.30-m *f*/10 Schmidt-Cass	FLI Microline 1001E
0.35-m *f*/9.1 Schmidt-Cass	FLI Proline 1001E
0.40-m *f*/10 Schmidt-Cass	SBIG STL-1001E
0.40-m *f*/10 Schmidt-Cass	
0.50-m *f*/8.1 Ritchey-Chrétien	

Table I. List of telescopes and CCD cameras at CS3 used for this paper. The exact combination for each telescope/camera pair is chosen to meet specific needs.

All lightcurve observations were unfiltered or with a clear filter, even though the latter can cause a 0.1-0.3 mag loss. The exposure duration varied depending on the asteroid's brightness and sky motion. Not all images were guided. Regardless, sometimes the asteroid was trailed on the image. In those cases, elliptical apertures were used to increase the target's SNR during measuring.

Measurements were made using *MPO Canopus*. The Comp Star Selector utility in *MPO Canopus* found up to five comparison stars of near solar-color for differential photometry. To reduce the number of times and amounts of adjusting nightly zero points, we use the ATLAS catalog r´ (SR) magnitudes (Tonry et al., 2018). Those adjustments are usually $|\Delta mag| \leq 0.03$. The rare larger corrections may have been due in part to using unfiltered observations, poor centroiding of the target and stars, not correcting for second-order extinction, and/or selecting what appears to be a single star but is actually an unresolved pair.

The Y-axis values are ATLAS SR "sky" (catalog) magnitudes. The values in the parentheses give the phase angle(s) (*a*) and the value of *G* used to normalize the data to the comparison stars used in the earliest session. This, in effect, corrects all the observations so that seem to have been made at a single fixed date/time and phase angle, presumably leaving any variations due only to the asteroid's rotation and/or albedo changes.

There can be up to three phase angles given. If two, the values are for the first and last night observations. If three, the middle value is the extrema (maximum or minimum) reached between the first and last observing runs. The X-axis shows rotational phase from -0.05 to 1.05. If the plot includes the amplitude, e.g., "Amp: 0.65," this is the amplitude of the Fourier model curve and *not necessarily the adopted amplitude for the lightcurve*.

"LCDB" substitutes for "Warner et al. (2009)" from here on.

2100 Ra-Shalom. Ostro et al. (1984) observed this NEA with radar and optical photometry to find a rotation period of 19.79 h, a period that has often been reproduced to within 0.01 h over the years, e.g., Pravec et al. (2003web; 2016web) and Warner (2017). Our results from the 2022 campaign are consistent with the established period.

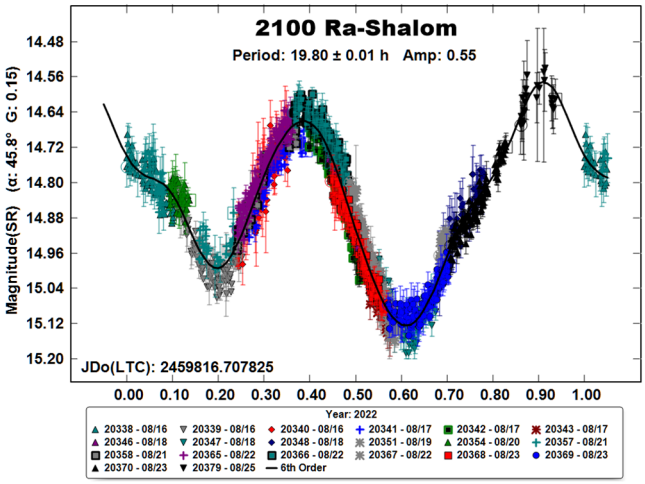

(17511) 1992 QN. Pravec et al. (1998) found a period of 5.9902 h. We observed the asteroid twice before: Warner (2014; 5.985h) and Warner (2018; 5.990 h). The 2022 data led to similar results.

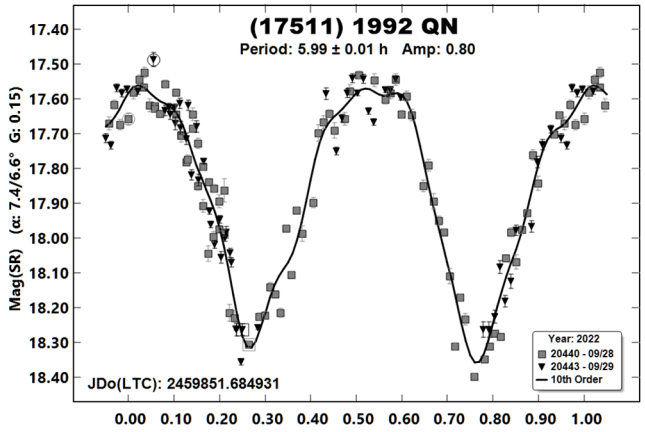

Number	Name	2022 mm/dd	Phase	L_{PAB}	B_{PAB}	Period(h)	P.E.	Amp	A.E.
2100	Ra-Shalom	08/16-08/23	45.6,33.5	347	19	19.80	0.01	0.55	0.03
17511	1992 QN	09/28-09/29	7.3,6.5	12	4	5.99	0.01	0.80	0.03
54789	2002 MZ7	06/30-07/07	26.1,26.8	252	27	T38.11	0.02	1.17	0.03
						7.330	0.003	0.16	0.02
398188	Agni	07/09-07/20	*51.9,51.7	279	29	T22.115	0.003	0.92	0.03
						32.5	0.1	0.68	0.03
						9.48	0.02	0.23	0.03
	2011 TG2	09/28-09/29	53.8,48.0	34	-9	2.562	0.002	0.60	0.05
	2012 PG6	08/24-08/28	41.1,50.5	350	19	10.58	0.02	1.27	0.06

Table II. Observing circumstances. The first line gives the sole period or, if preceded with T, the dominant period of a tumbler. Any additional lines give the secondary period(s). The phase angle (α) is given at the start and end of each date range. If preceded with an asterisk, the phase angle reaches a minimum or maximum between the first and last date. L_{PAB} and B_{PAB} are, respectively the average phase angle bisector longitude and latitude (see Harris et al.,1984).

(54789) 2002 MZ7. Pravec et al. (2005; see Pravec et al., 2014) established that the asteroid was tumbling and reported periods of 37.57 h and 52.79 h. The solution, however, was not unique, meaning that combinations of four possible periods provided a nearly equal fit. Despite the ambiguities, it was rated PAR = –3, i.e., reliable.

Our data were far too sparse for a definitive solution even with the proper software. Regardless, we found a dominant period (38.11 h; "P1") that is in good agreement with one of the periods found by Pravec et al. (2005). Not expected was, after subtracting the dominant period, finding a short period, low amplitude (7.330 h, 0.16 mag) lightcurve ("P2") with a very good fit that is reminiscent of a "typical" single body in single axis rotation. Likewise, subtracting this secondary period dramatically improved the fit of the data to the dominant period, but the result lightcurve shape is still somewhat unusual.

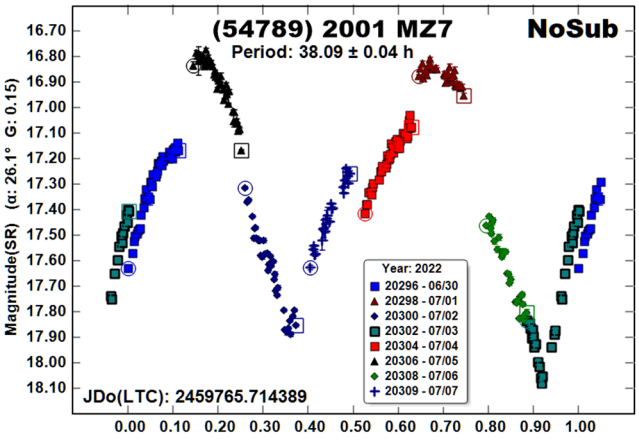

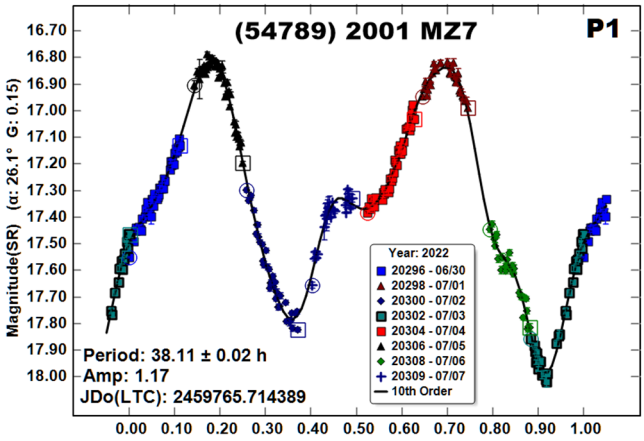

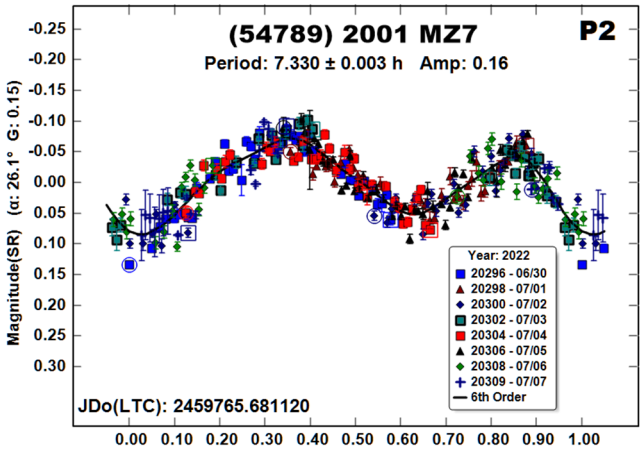

398188 Agni. We observed this asteroid in 2014 (Warner, 2015), finding dominant periods of 22.1 h and 32.6 h for what we believed to be a tumbling asteroid. Neither solution led to even a close fit of the data. We had better luck with the 2022 data.

The most dominant period was 22.115 h, in agreement with our previous result. A seemingly good fit at 11.059 h was, essentially, a monomodal lightcurve. The split-halves plot at the doubled period (22.115 h) showed the two halves were identical. However, given the large amplitude, a monomodal solution was considered unlikely (see Harris et al., 2014). More so, the inability of *MPO Canopus* to deal with tumbling asteroids, means both periods are somewhat suspect.

Our search for a secondary period to improve the fit of the primary led to an unusually-shaped bimodal lightcurve with a period of 32.5 h, in good agreement with our result from the 2014 data.

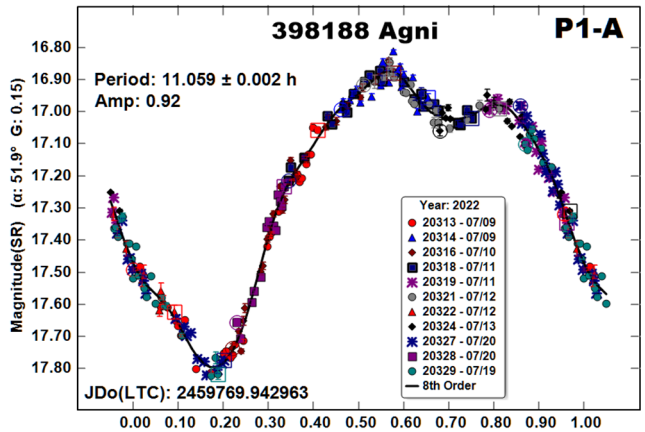

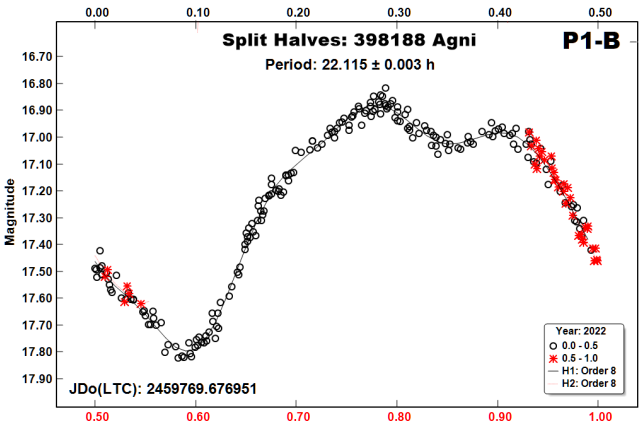

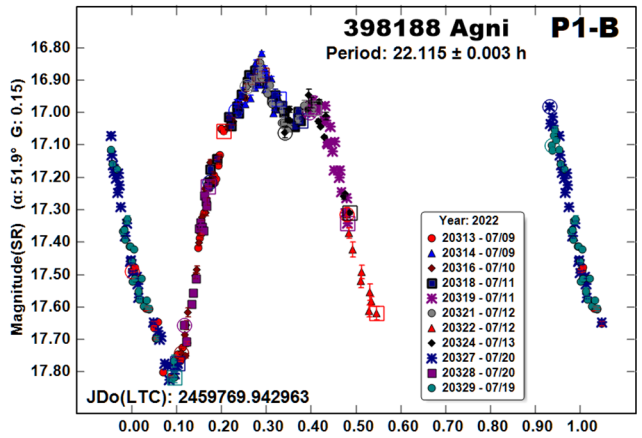

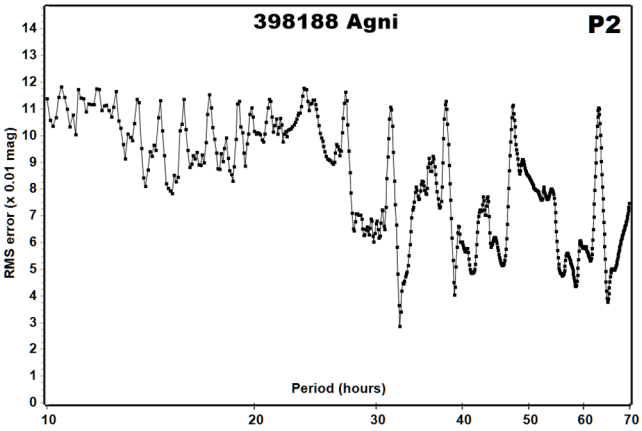

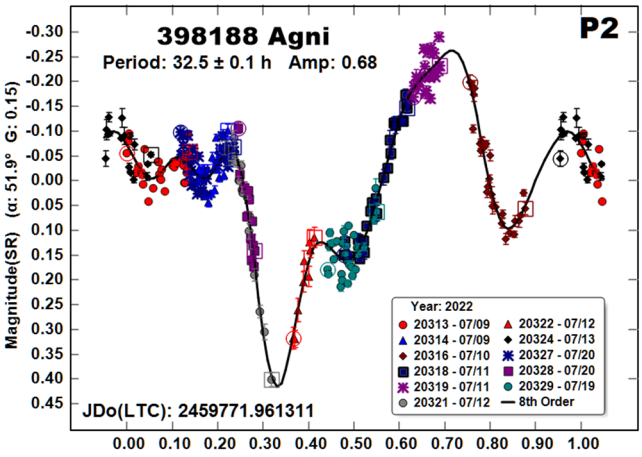

Sometimes, we can find a third period that does not have direct physical origin, i.e., is likely an analysis "artifact," but greatly improves the fit of the two main periods. This was the case with our 2022 data set.

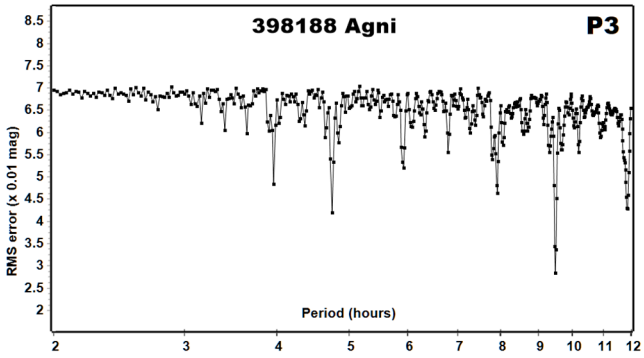

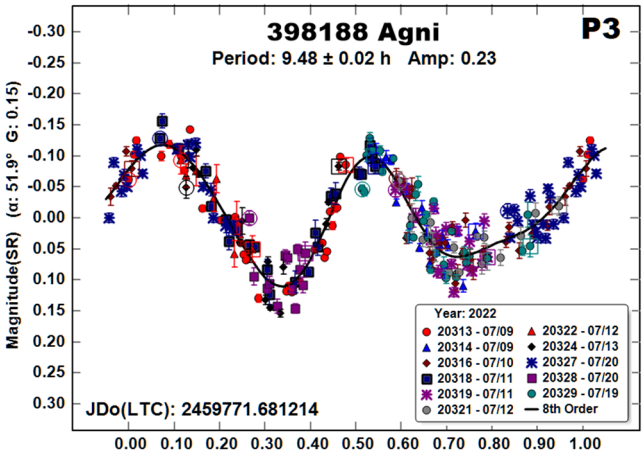

The fit for the third lightcurve to a period of 9.48 h is remarkably "clean" and, on its own, would be a typical for a "normal" asteroid. The lightcurves for P_1 and P_2 are the result of subtracting one from the other *and* this third period. Without the third period, the two other lightcurves have much poorer fits to their adopted periods.

2011 TG2. The estimated size of 2011 TG2 is about 250 m. There were no entries in the LCDB for the asteroid, but the current version of the LCDB is about a year old as of this writing. We observed on 2022 September 28 and 29. Combining the data from the two nights leads to a period of 2.562 h, but the fit of the data is not very good.

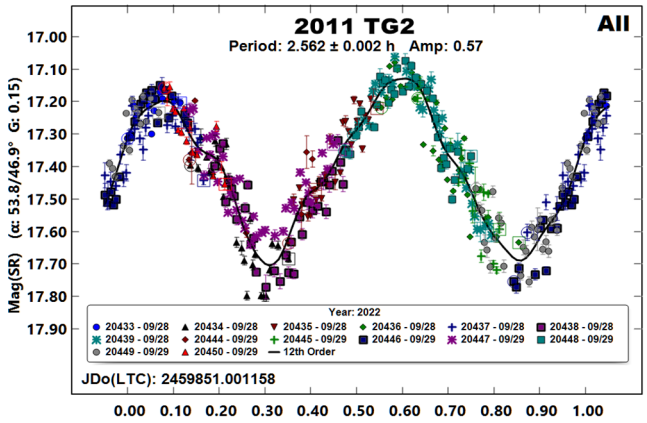

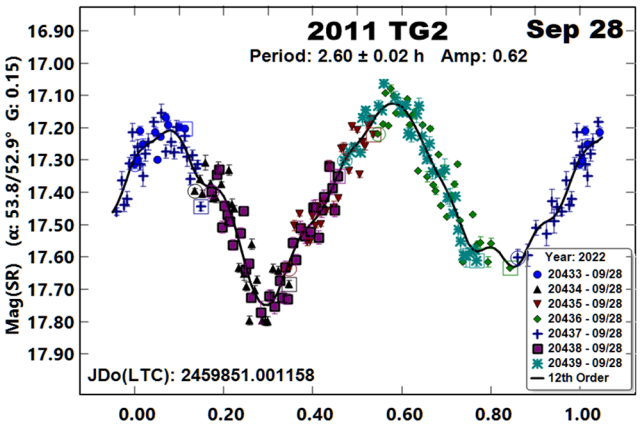

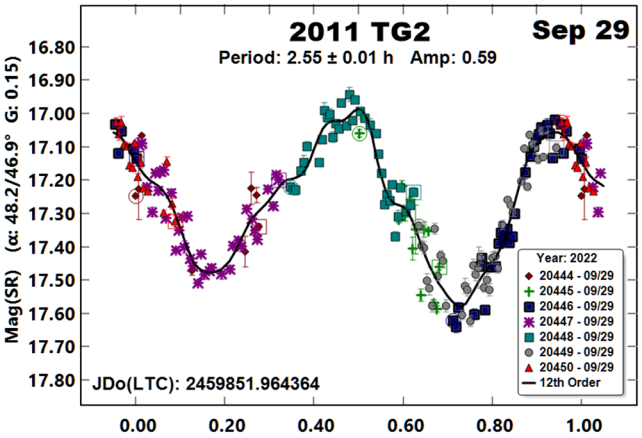

Since the phase angle was significantly different on the two nights, we suspected that the poor fit was due to the changing viewing aspect and not tumbling. This seemed confirmed after finding an independent solution for each night and comparing the lightcurve shapes and amplitude.

2012 PG6. We observed this asteroid on three nights, 2022 August 24, 26, and 28. As seen in the lightcurves, the combined data set has a good fit until the second half. This is due to the evolution of the lightcurve over four nights of observations. Three combinations of two nights of observing runs produced tight fits to the derived period for that combination. The resulting lightcurves show how the shape and, more so, the amplitude evolved.

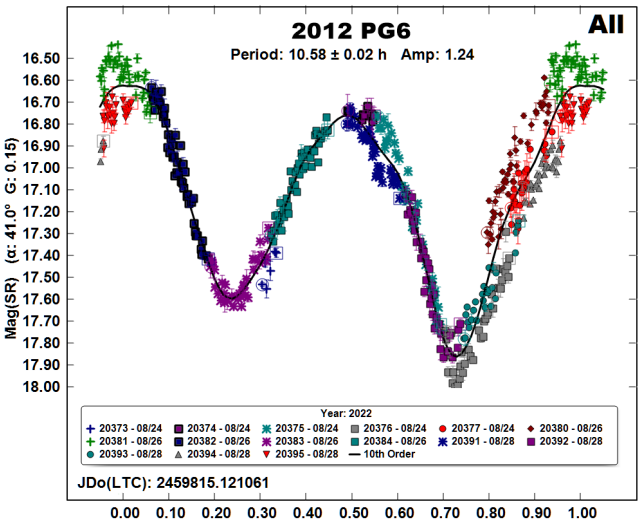

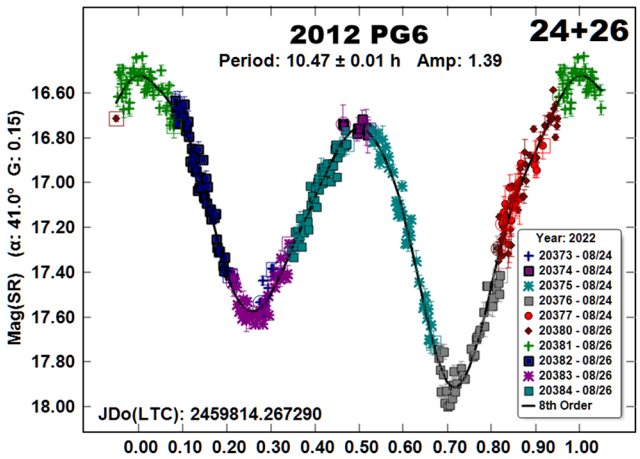

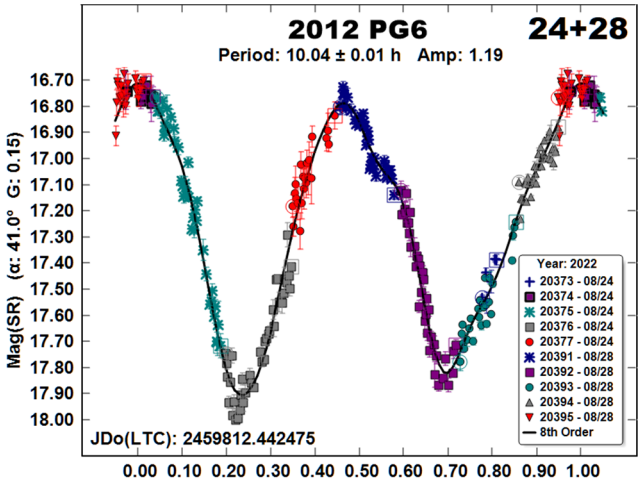

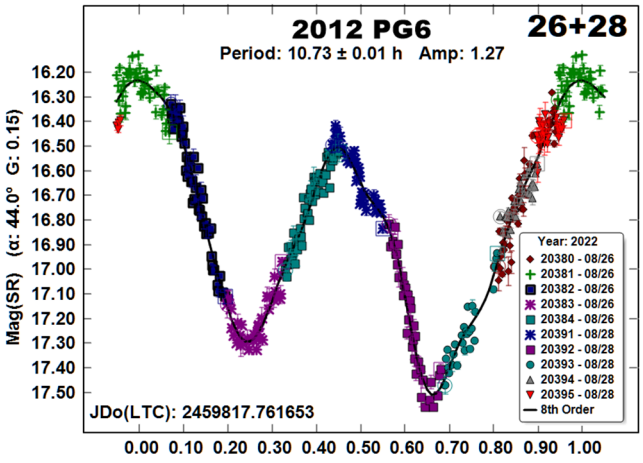

Acknowledgements

The authors gratefully acknowledge Shoemaker NEO Grants from the Planetary Society (2007, 2013). These were used to purchase some of the telescopes and CCD cameras used in this research. This work includes data from the Asteroid Terrestrial-impact Last Alert System (ATLAS) project. ATLAS is primarily funded to search for near earth asteroids through NASA grants NN12AR55G, 80NSSC18K0284, and 80NSSC18K1575; byproducts of the NEO search include images and catalogs from the survey area. The ATLAS science products have been made possible through the contributions of the University of Hawaii Institute for Astronomy, the Queen's University Belfast, the Space Telescope Science Institute, and the South African Astronomical Observatory. This paper made use of the services provided by the SAO/NASA Astrophysics Data System, which is operated by the Smithsonian Astrophysical Observatory under NASA Cooperative Agreement 80NSSC211M0056.

References

References from web sites should be considered transitory, unless from an agency with a long lifetime expectancy. Sites run by private individuals, even if on an institutional web site, do not necessarily fall into this category.

Harris, A.W.; Young, J.W.; Scaltriti, F.; Zappala, V. (1984). "Lightcurves and phase relations of the asteroids 82 Alkmene and 444 Gyptis." *Icarus* **57**, 251-258.

Harris, A.W.; Pravec, P.; Galad, A.; Skiff, B.A.; Warner, B.D.; Vilagi, J.; Gajdos, S.; Carbognani, A.; Hornoch, K.; Kusnirak, P.; Cooney, W.R.; Gross, J.; Terrell, D.; Higgins, D.; Bowell, E.; Koehn, B.W. (2014). "On the maximum amplitude of harmonics on an asteroid lightcurve." *Icarus* **235**, 55-59.

Ostro, S.J.; Harris, A.W.; Campbell, D.B.; Shapiro, I.I.; Young, J. (1984). "Radar and photoelectric observations of 2100 Ra-Shalom." *Icarus* **60**, 391-403.

Pravec, P.; Wolf, M.; Sarounova, L. (1998). "Lightcurves of 26 Near-EarthAsteroids." *Icarus* **136**, 124-153.

Pravec, P.; Wolf, M.; Sarounova, L. (2003web; 2016web). *http://www.asu.cas.cz/~ppravec/neo.htm.*

Pravec, P.; Harris, A.W.; Scheirich, P.; Kušnirák, P.; Šarounová, L.; Hergenrother, C.W.; Mottola, S.; Hicks, M.D.; Masi, G.; Krugly, Yu.N.; Shevchenko, V.G.; Nolan, M.C.; Howell, E.S.; Kaasalainen, M.; Galád, A.; Brown, P.; Degraff, D.R.; Lambert, J.V.; Cooney, W.R.; Foglia, S. (2005). "Tumbling asteroids." *Icarus* **173**, 108-131.

Pravec, P.; Scheirich, P.; Durech, J.; Pollock, J.; Kusnirak, P.; Hornoch, K.; Galad, A.; Vokrouhlicky, D.; Harris, A.W.; Jehin, E.; Manfroid, J.; Opitom, C.; Gillon, M.; Colas, F.; Oey, J.; Vrastil, J.; Reichart, D.; Ivarsen, K.; Haislip, J.; LaCluyze, A. (2014). "The tumbling state of (99942) Apophis." *Icarus* **233**, 48-60.

Tonry, J.L.; Denneau, L.; Flewelling, H.; Heinze, A.N.; Onken, C.A.; Smartt, S.J.; Stalder, B.; Weiland, H.J.; Wolf, C. (2018). "The ATLAS All-Sky Stellar Reference Catalog." *Ap. J.* **867**, A105.

Warner, B.D. (2014). "Near-Earth Asteroid Lightcurve Analysis at CS3-Palmer Divide Station: 2013 September-December." *Minor Planet Bull*. **41**, 113-124.

Warner, B.D. (2015). "Near-Earth Asteroid Lightcurve Analysis at CS3-Palmer Divide Station: 2014 June-October." *Minor Planet Bull*. **42**, 41-53.

Warner, B.D. (2017). "Near-Earth Asteroid Lightcurve Analysis at CS3-Palmer Divide Station: 2016 July-September." *Minor Planet Bull*. **44**, 22-36.

Warner, B.D. (2018). "Near-Earth Asteroid Lightcurve Analysis at CS3-Palmer Divide Station: 2017 October-December." *Minor Planet Bull*. **45**, 138-147.

Warner, B.D.; Harris, A.W.; Pravec, P. (2009). "The Asteroid Lightcurve Database." *Icarus* **202**, 134-146. Updated 2021 Dec. *http://www.minorplanet.info/lightcurvedatabase.html*

LIGHTCURVE ANALYSIS FOR EIGHT NEAR-EARTH ASTEROIDS

Peter Birtwhistle
Great Shefford Observatory
Phlox Cottage, Wantage Road
Great Shefford, Berkshire, RG17 7DA
United Kingdom
peter@birtwhistle.org.uk

(Received: 2022 October 12)

Lightcurves and amplitudes for eight near-Earth asteroids observed from Great Shefford Observatory during close approaches between 2022 July and September are reported. All are superfast rotators, with periods < 12 minutes and three are identified as tumblers, i.e., showing non-principal axis rotation.

Photometric observations of near-Earth asteroids during close approaches to Earth between 2022 July and September were made at Great Shefford Observatory using a 0.40-m Schmidt-Cassegrain and Apogee Alta U47+ CCD camera. All observations were made unfiltered and with the telescope operating with a focal reducer at *f*/6. The 1K×1K, 13-micron CCD was binned 2×2, resulting in an image scale of 2.16 arc seconds/pixel. All the images were calibrated with dark and flat frames and *Astrometrica* (Raab, 2018) was used to measure photometry using APASS Johnson V band data from the UCAC4 catalogue (Zacharias et al., 2013). *MPO Canopus* (Warner, 2022), incorporating the Fourier algorithm developed by Harris (Harris et al., 1989), was used for lightcurve analysis.

No previously reported results for any of the objects reported here have been found in the Asteroid Lightcurve Database (LCDB) (Warner et al., 2009), from searches via the Astrophysics Data System (ADS, 2022), or from wider searches unless otherwise noted. All size estimates are calculated using *H* values from the Small-Body Database Lookup (JPL 2022), using an assumed albedo for NEAs of 0.2 (LCDB readme.pdf file) and are therefore uncertain and offered for relative comparison only.

2022 NE. This small Apollo, with $H = 28.7$ implying a diameter of ~ 6 m was discovered by the Pan-STARRS2 team on 2022 July 4 at 20th mag, 51 hours before passing Earth at 0.4 Lunar Distances (LD) (Evans et al., 2022). It was observed for 45 minutes starting at 2022 July 5.98 UTC when it was at magnitude 17 and at a range of 1.1 LD. With an apparent speed of 80 - 90 arcsec/min. exposures were limited to 4.5 - 5 sec to keep trailing of the target within the measurement annulus used in *Astrometrica*. An initial analysis in *MPO Canopus* indicated a fast rotation period of 55.8 sec, but with a larger than expected scatter in the lightcurve, with the RMS being 0.31 mags. The lightcurve is given here labelled PAR, i.e., Principal Axis Rotation assumed. However, multiple potential solutions are apparent in the period spectrum, which is plotted on a linear scale for periods between 18 - 155 s. It is noted there are three apparent sets of four equally spaced minima, the strongest signal from multiples of 27.9 s, the next strongest from multiples of 36.1 s and the weakest from multiples of 21.9 s.

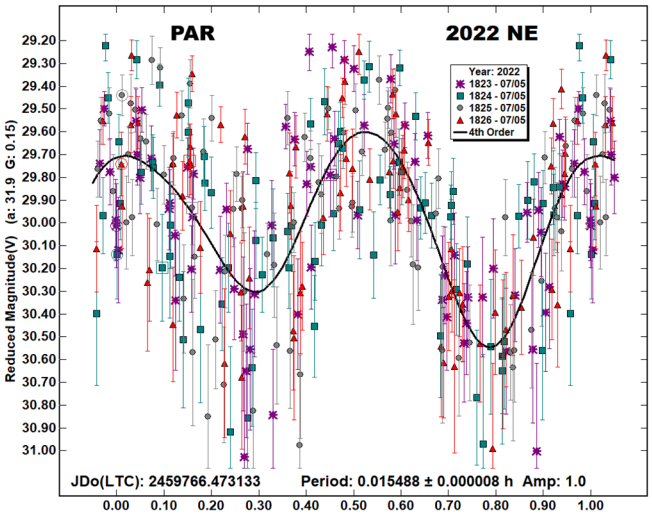

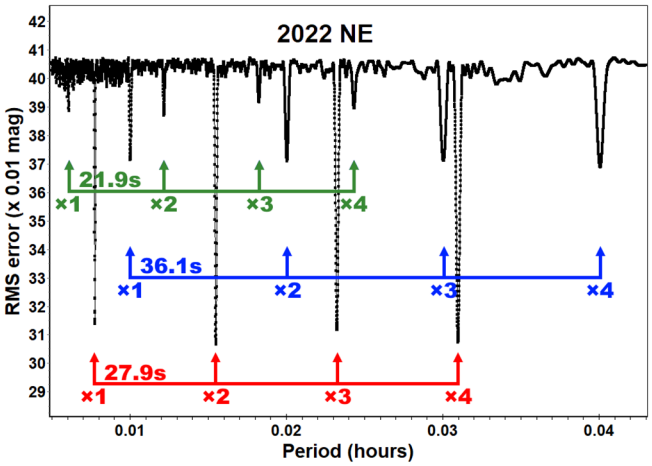

It was suspected that non-principal axis (NPA) rotation, or tumbling may be present and so the Dual-Period search function in *MPO Canopus* was used to try and identify the possible values for rotation and precession. This resolved two periods, $P_1 = 0.015488 \pm 0.000004$ h and $P_2 = 0.02005 \pm 0.00001$ h as providing the best fit to the observations, reducing the overall RMS to 0.25 mag. However, solutions were also possible using either the P_1 or P_2 value as a starting point in the dual period search, both searches isolating a period $P_3 \sim 0.01217$ h, with slightly poorer RMS values, the three pairs of solutions summarised here:

$P_1 = 0.015488 \pm 0.000004$ h and $P_2 = 0.02005 \pm 0.00001$ h, RMS = 0.25
$P_1 = 0.015487 \pm 0.000005$ h and $P_3 = 0.01217 \pm 0.00001$ h, RMS = 0.28
$P_2 = 0.02004 \pm 0.00002$ h and $P_3 = 0.01216 \pm 0.00001$ h, RMS = 0.35

Periods P_1, P_2 and P_3 match minima in the period spectrum marked as ×2 multiples, i.e., 55.8, 72.2 and 43.8 s respectively and all produce bimodal lightcurves. It is noted that the frequencies are related to each other, where $1/P_1 \approx 2/P_3 - 2/P_2$. The real periods of rotation and precession cannot be resolved from this analysis; one of the three periods will be an alias but it is not clear which one. It is expected that 2022 NE may be rated with a PAR code of -3 on the scale of Pravec et al. (2005), i.e., *NPA rotation reliably detected with the two periods resolved. An ambiguity of the periods solution may be tolerated provided the resulting spectrum of frequencies with significant signal is the same for the different solutions.* Lightcurves from the best fit solution for periods P_1 and P_2 are given and a lightcurve for period P_3 from the P_1 and P_3 solution is also given.

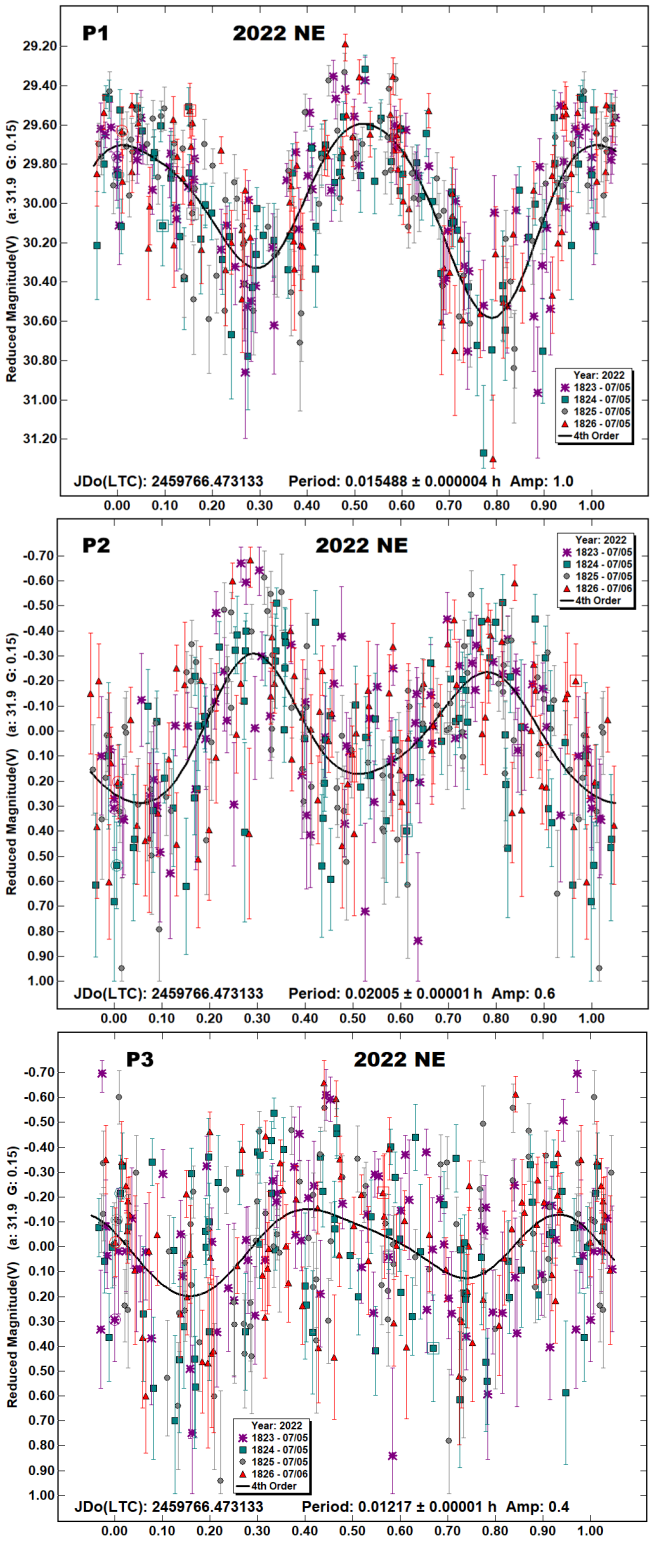

2022 NR. The Catalina Sky Survey's 0.68-m Schmidt picked this Apollo up at 18th mag on 2022 July 6.3 UTC, some four days before it passed Earth at 1 LD (Fazekas et al., 2022). With H = 25.8, its size is estimated at ~20 m. It was observed on 2022 July 7.9 UTC for 15 minutes to measure astrometry when it was still mag +18 and then for 2.5 h the next night when it had brightened to mag +17. By then its apparent speed was 40 arcsec/min and exposures were varied between 4 and 13 s to investigate if any fast rotation period was obvious and initial measurements indicated a period of ~4 minutes. It was then observed on 2022 July 9.91 UTC for 19 minutes when it had approached to 1.3 LD, had brightened to 15th mag, and was moving at 170 arcsec/min, but at an altitude of 26° or less and in twilight. Exposures were kept to 1 s duration to limit trailing. Over the three nights, 1002 individual images were obtained with exposures ranging from 1 - 13.1 s, but considering the initial determination of the period P at ~4 min and with the optimal exposure Δt for recording a strong signal without excessive smoothing of the resulting lightcurve being 0.185P (Pravec et al., 2005), these were then stacked in *Astrometrica* in groups so that the elapsed time from start of the first exposure to end of the last exposure in each stack was 30 s or less, so $\Delta t/P \sim 0.125$. This resulted in 191 stacked measurements being used in the final analysis. The period spectrum shows the best fit solution is indeed close to the initial estimate of P and the resulting asymmetric, bimodal lightcurve indicating P = 0.068406 h = 4.1 min.

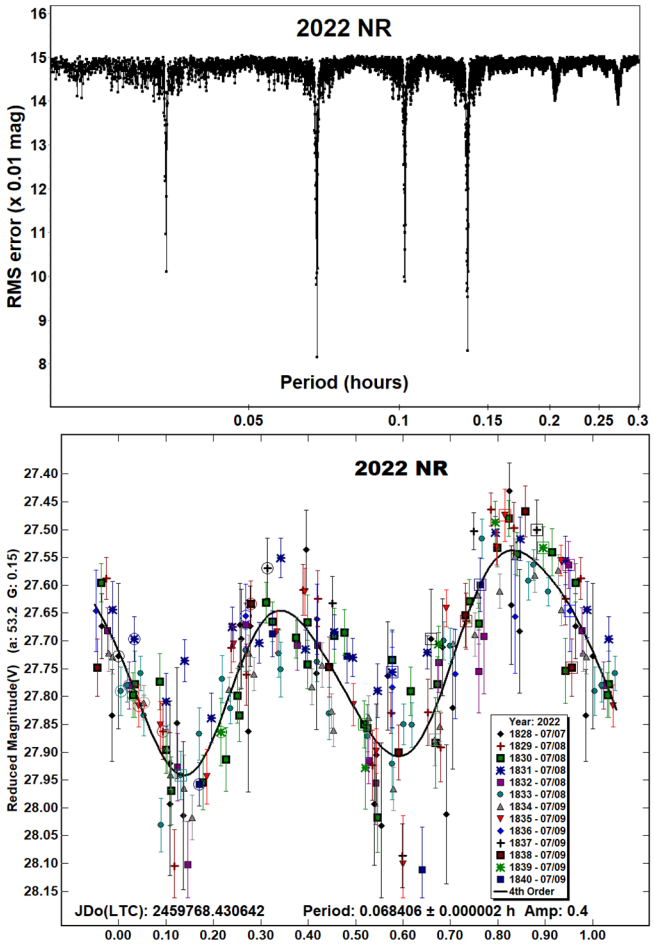

The period indicates that observations on the first night covered 3.7 revolutions, 37 on the second night, and 4.6 on the third night. 2022 NR was also observed by radar from Goldstone and an echo power spectrum is available from observations made on 2022 July 8 (Benner, 2022).

2022 QC. This Apollo was discovered by Pan-STARRS 2 on 2022 Aug 17.49 UTC and subsequently pre-discovery positions were reported by the same team from 11 days earlier (Dupouy et al., 2022). 2022 QC passed Earth at 2.6 LD on 2022 Aug 20.24 UTC and was observed for 7 minutes starting at 2022 Aug 19.92 UTC, then 1.75 h later for a further 25 minutes. A period spectrum shows a strong signal at 0.0337 h and the resulting lightcurve indicates this is a trimodal solution.

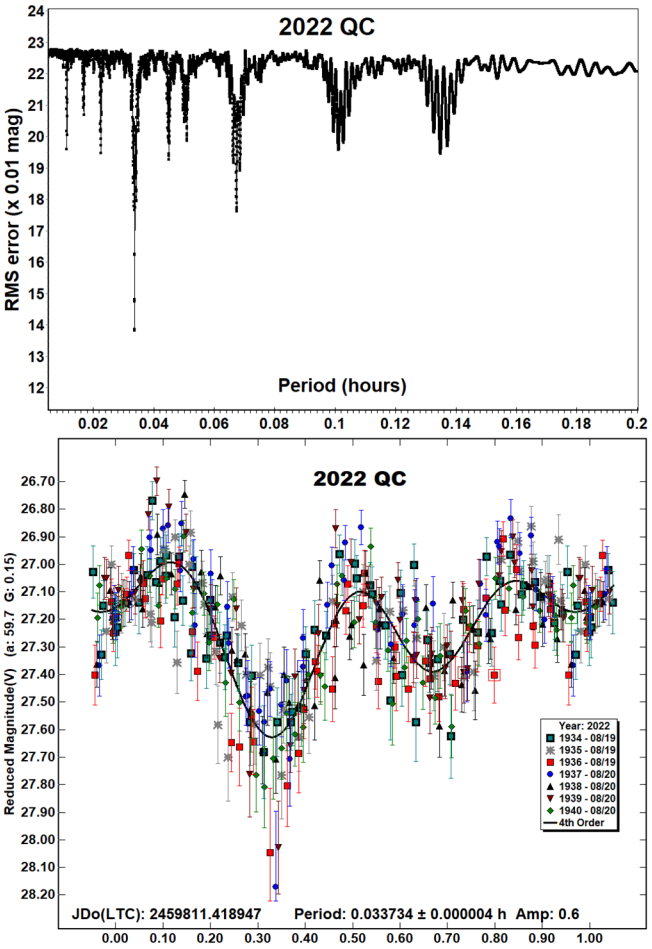

The SBDB listed value of H = 25.29 implies a diameter of approximately 26 m. The rotation period of 121 seconds indicate that 3.6 rotations were observed during the first set of observations and 12 revolutions during the second set.

2022 QV. This was observed for 20 minutes starting on 2022 Aug 21.98 UTC when at a distance of just under 3 LD and moving at 180 arcsec/min. About nine hours later, it passed Earth at 2.2 LD. It had been discovered 2.5 days before by the Pan-STARRS 2 team (Buzzi et al., 2022) and is an Apollo with an approximate diameter of 19 m (H = 26.0). Due to its apparent speed, exposures were limited to 2.8 seconds throughout.

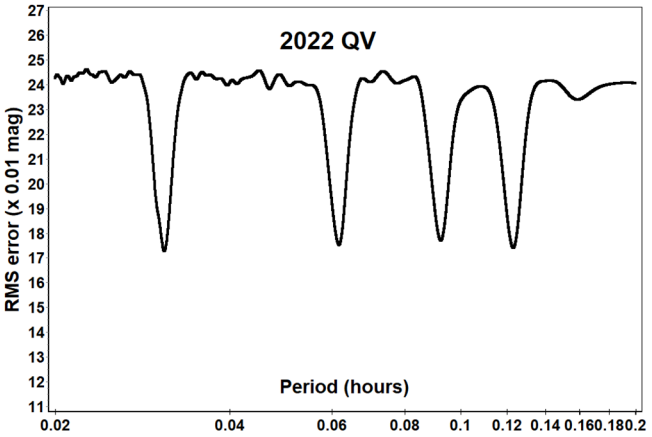

Analysis reveals a bimodal lightcurve with a rotation period of 3.7 minutes, meaning 5.4 revolutions occurred during the observation period.

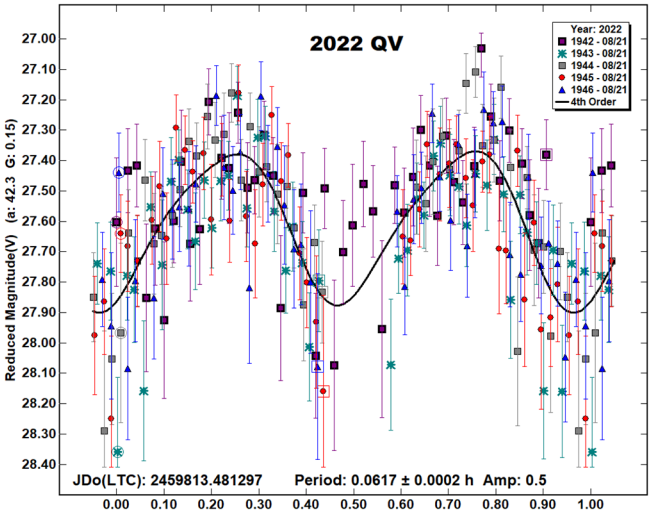

2022 QX4. Discovered by the ATLAS telescope in Chile on 2022 Aug 24 (Melnikov et al., 2022a), this Aten was the subject of some attention in the days after discovery due to an apparent very close approach to Earth in 1977, raising speculation that it might be an artificial object possibly associated with a launch around that time. Pre-discovery images from 2013 Aug were then reported on 2022 Sep 11 (Deen et al., 2022), showing that the effects of solar radiation pressure are negligible and that 2022 QX4 is most likely a natural object. Including the pre-discovery positions, the SBDB now lists 18 approaches to Earth within 10 LD, with an approach on 1977 Sep 5 being the closest, at 0.33 ± 0.01 LD. It was observed for 1.4 h starting 2022 Aug 28.04 UTC at an altitude of only 37° and again for 1.1 h starting 2022 Aug 29.89 UTC at an even lower altitude of 21°. Although the individual sessions were relatively consistent on each night, there was a difference in zero pointing between the two nights of 0.18 magnitudes probably due to the poor observing circumstances and this has been adjusted for in the lightcurve, reducing the overall RMS of the fit from 0.17 to 0.09 mag. A relatively low 0.3 mag amplitude, bimodal lightcurve of period 0.0888 h (5.3 minutes) was determined using *MPO Canopus*. The period spectrum shows the four strongest signals are associated with the 5.3-minute period (monomodal to quadrimodal solutions) but there are several other lesser minima suggesting some tumbling motion may be present, but attempts to resolve a second period using the *MPO Canopus* Dual-Period Search function were unsuccessful.

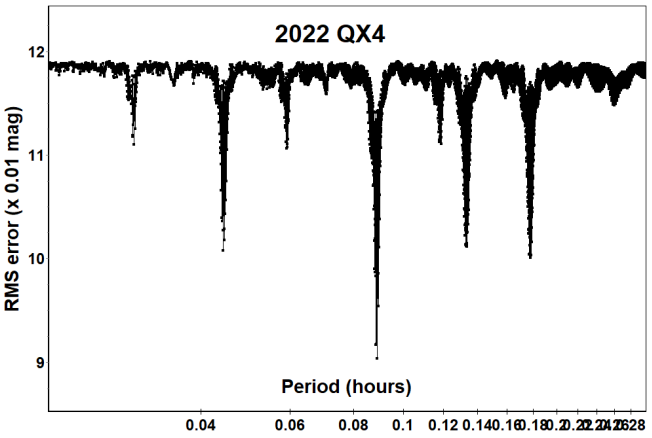

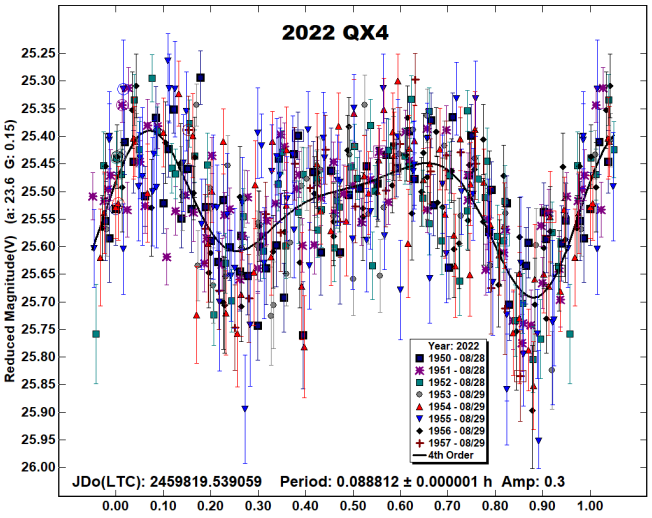

The period indicates that 15 revolutions were observed on the first night of observation and 12 on the second. The low amplitude lightcurve is consistent with 2022 QX4 being a natural object, other distant artificial objects observed from Great Shefford have typically had much larger amplitudes. Assuming it is a natural object, the SBDB value of H = 24.69 suggests a diameter of about 34 m.

2022 QT7. Discovered by Pan-STARRS 2 on 2022 Aug 29.5 UTC, this small Aten (H = 28.6, dia. ~ 6 m) passed Earth at 1.2 LD on 2022 Sep 1.4 UTC (Melnikov et al., 2022b). It was observed for 2.8 h starting on 2022 Aug 31.93 UTC at a distance of 1.5 LD and with its apparent speed increasing to 160 arcsec/minute exposure lengths were kept within the range 3.6 - 5.3 seconds. The average gap between images was 1.5 seconds. Large magnitude variations between consecutive images were evident during capture, with the asteroid sometimes appearing at approximately maximum brightness in one image, then being completely invisible in the next. This can cause problems for lightcurve analysis where a minimum may be poorly recorded, so exceptionally, in an attempt to get at least some definition of deep minima, measurements where the asteroid was visible but with SNr down to 2 were included, allowing 417 data points to be used for the analysis.

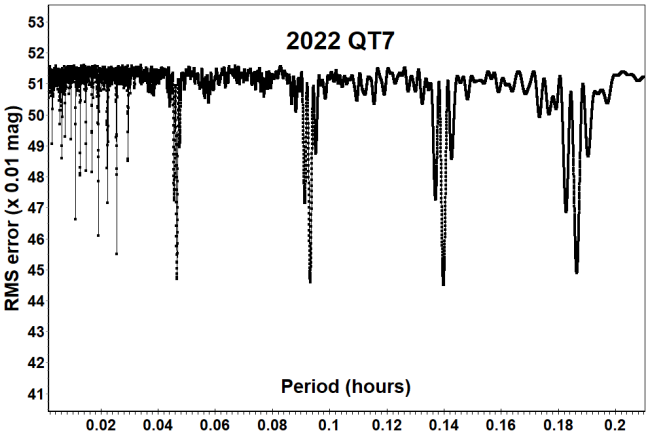

An initial search for rotation periods in the range 0.001 - 0.26 h resulted in the best fit being a bimodal solution with period 0.09327 h, this lightcurve is labelled PAR. Only slightly inferior fits at 0.047, 0.14 and 0.19 h shown on the linearly-scaled period spectrum relate to monomodal, trimodal and quadrimodal versions of the bimodal solution. However, there are obvious problems with the lightcurve, with large scatter even on the measurements with high SNr. It is also apparent that there appear to be a number of RMS minima in the period spectrum below 0.04 h.

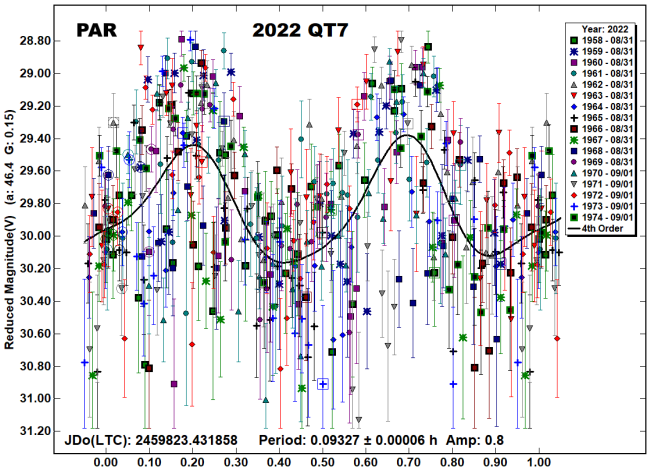

The *MPO Canopus* Dual-Period Search function was then used to search for possible tumbling rotation using 0.09327 h as the initial estimate for the main period. This resulted in improving the fit of the main lightcurve and finding a secondary period of 0.0063789 ± 0.0000003 h (23.0 seconds) and these lightcurves are given, labelled P1 and P2.

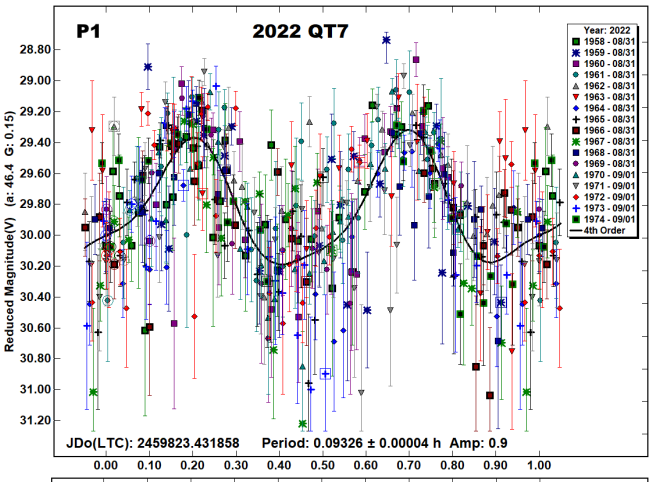

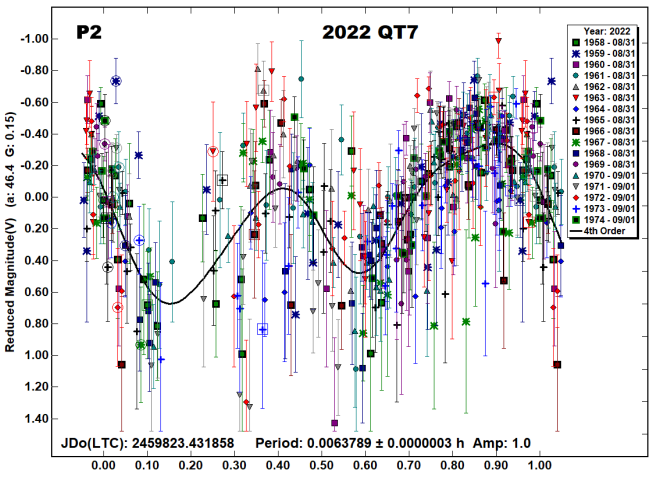

The many RMS minima in the period spectrum below 0.04 h were then examined using the Dual-Period Search to see whether or not the two periods of tumbling motion could be described entirely from those shorter rotation periods. The strongest signal initially located was a close match for the earlier P_2 period and given here labelled as P3. Subtracting the effect of the P_3 lightcurve using the Dual-Period Search produced a period spectrum showing two sets of RMS minima, being multiples of 0.0056096 and 0.0073888 h, (20.2 and 26.6 seconds respectively), with plausible solutions at double these values.

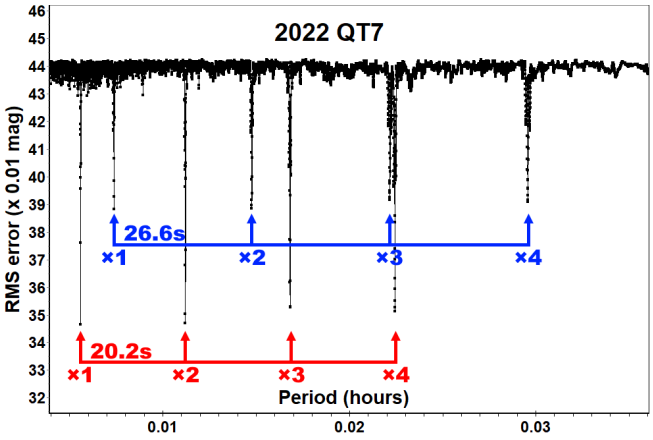

A lightcurve for the best fit solution, at 0.0112204 h is given, labelled P4 and the lesser fit at 0.0147778 h labelled P5.

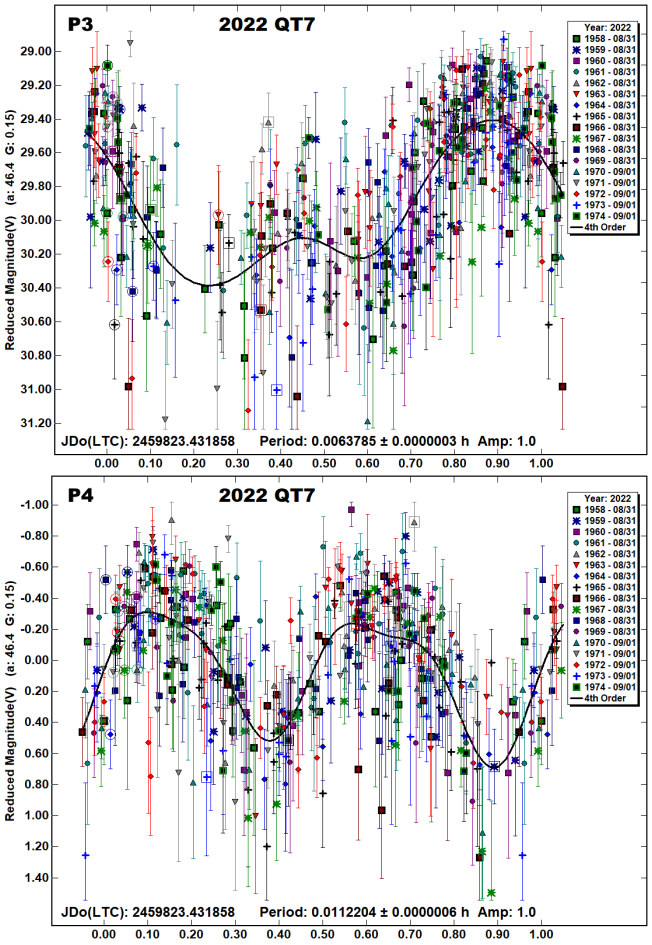

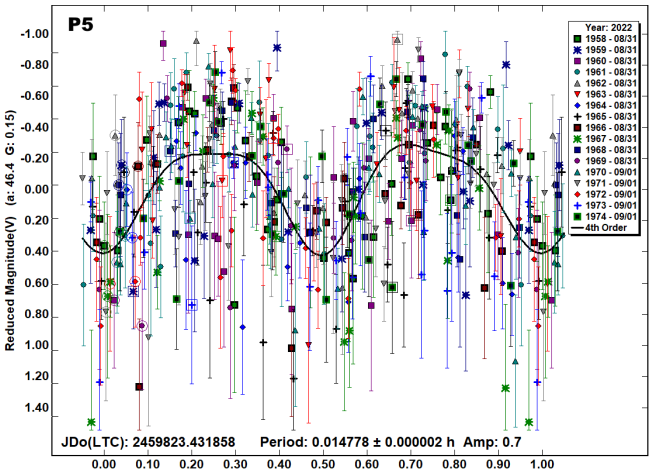

It is noted that the three short periods:

$P_3 = 0.0063785 \pm 0.0000003$ h
$P_4 = 0.0112204 \pm 0.0000006$ h
$P_5 = 0.014778 \pm 0.000002$ h

are related to each other by: $1/P_3 \approx 1/P_4 + 1/P_5$ and that the initially apparent dominant period P_1 of 0.09326 ± 0.00004 h is also related to the shorter periods, e.g.: $2/P_1 \approx 2/P_4 - 1/P_3$.

The P_1 period is expected to be a beat between the two real frequencies of the tumbling motion, the main period is likely to be P_4, but which one of the other periods may be real is not clear. It is expected that the rotation may be rated with a PAR code of -2, tending to -3 on the scale of Pravec et al. (2005) (Petr Pravec, personal communication).

The real amplitude of each of the lightcurves presented is likely to be larger than indicated, due to the asteroid being too faint to record at minimum light. Lightcurve smoothing also needs to be considered for the fastest period P_3 = 22.96 s and longest exposure = 5.3 s. The longest exposure as a fraction of period P_3 is 5.3/22.96 = 0.231P_3 and this would be expected to cause some appreciable smoothing, with the strength of the second harmonic being reduced to 68% of its true value. However, these exposures only account for 18 of the 417 data points (4.3%), with the remaining exposures being 0.192P or less, close to the optimum value of 0.185P for a strong detection of the normally dominant second harmonic (Pravec et al., 2000) and so smoothing is not expected to affect the shape of the lightcurves significantly.

2022 SG3. A discovery by Pan-STARRS 2 on 2022 Sep 20.4 UTC, with pre-discovery positions from the day before being reported from the ATLAS Chile site (Bacci et al., 2022a), 2022 SG3 made an approach to 1.7 LD on 2022 Sep 22.3 UTC. It was observed for 2.5 h starting on 2022 Sep 22.02 UTC when it was 16th mag and moving at up to 180 arcsec/minute; exposures were limited to 3.3 seconds or shorter throughout. An initial analysis produced a period spectrum showing a set of solutions in the range of 0.08 - 0.36 h.

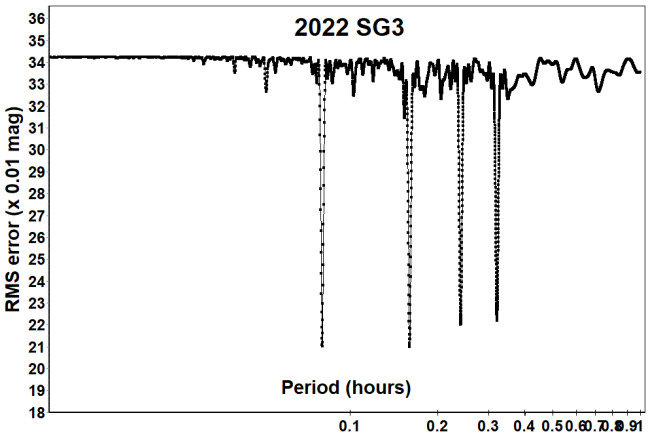

A bimodal lightcurve of period ~0.16 h gave the best fit and is here labelled PAR. The amount of scatter in the brighter parts of the curve was larger than expected and again a dual-period solution was attempted using *MPO Canopus* in case the object is tumbling. When the dominant period of 0.16034 h, amplitude 0.8 was located and subtracted by the Dual-Period Search function it revealed a well-defined secondary period of 0.10306 ± 0.00006 h with amplitude 0.3 mag. These lightcurves are labelled P1 and P2.

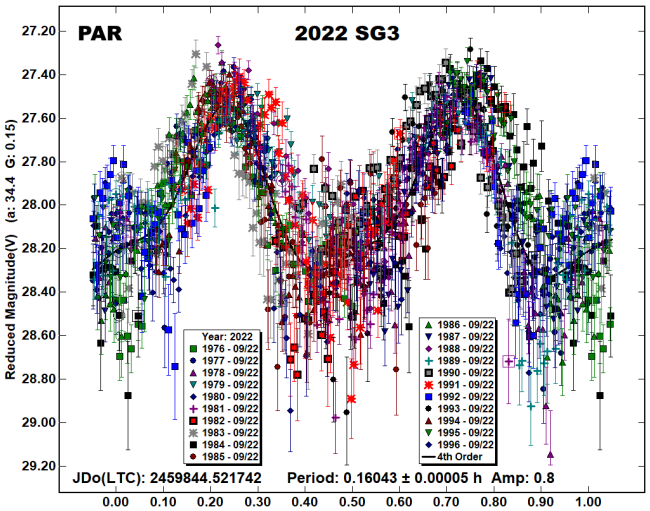

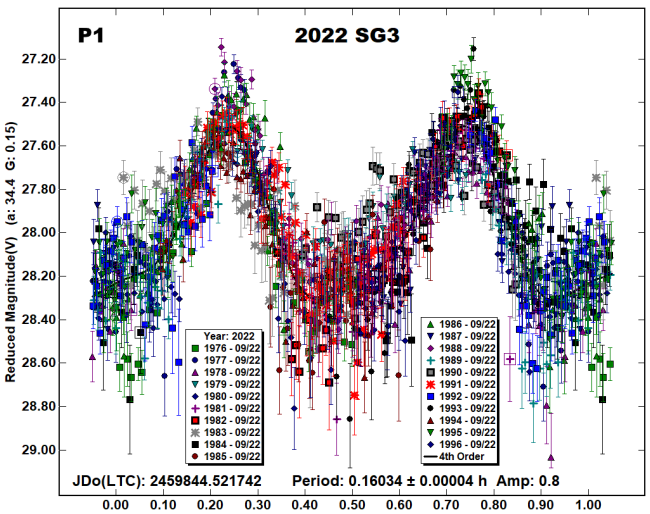

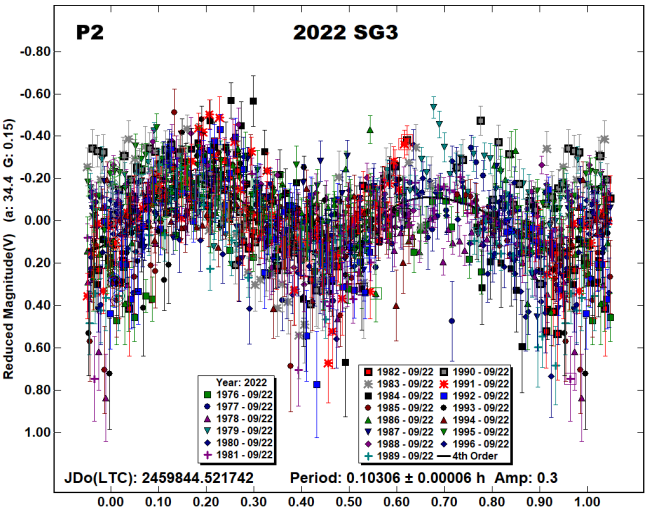

This non-principal axis (NPA) rotation solution is expected to be rated with a PAR code of -3 on the scale of Pravec et al. (2005)., i.e., *NPA rotation reliably detected with the two periods resolved. There may be some ambiguities in one or both periods...*

2022 SW3. This was an amateur discovery from the PASTIS Observatory, Banon, France, on 2022 Sep 20.14 UTC (Bacci et al., 2022b). The SBDB lists this Aten with H = 24.84, suggesting an approximate diameter of 32 m. It passed closest to Earth on 2022 Sep 23.2 UTC at 7 LD and was observed over three separate sessions, starting 2022 Sep 23.89, Sep 24.09 and Sep 25.09 UTC for 97, 75 and 102 minutes respectively. Large variations in magnitude were evident over several minutes during each session and an analysis shows a large amplitude bimodal lightcurve. It is noted that with an orbital period of 0.6699 years 2022 SW3 completes almost exactly three revolutions of the Sun every two Earth years and will approach to a similar distance of 7 LD from Earth on 2024 Sep 19, though not as well placed as in 2022, but then will not approach any closer until 2077.

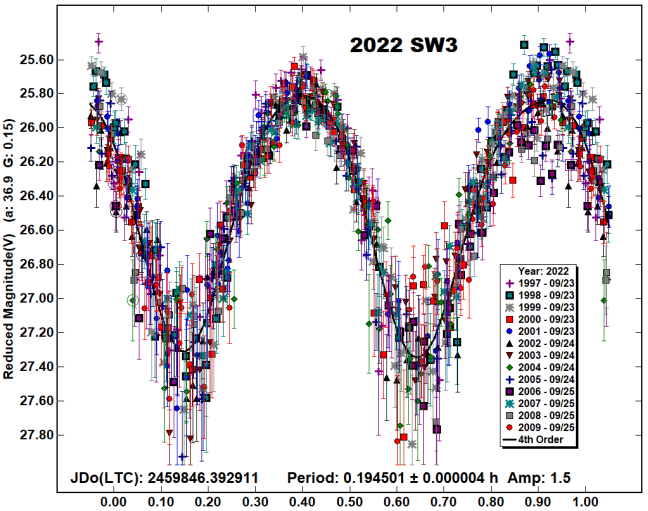

Name	2022 mm/ dd	Phase	L_{PAB}	B_{PAB}	Period(h)	P.E.	Amp	A.E	PAR	H
2022 NE	07/05-07/06	31.8-31.7	269	6	0.015488	0.000004	1.0	0.3	-3	28.65
					0.02005	0.00001	0.6	0.3		
					0.01217	0.00001	0.4	0.4		
2022 NR	07/07-07/09	53.1-65.3	262	14	0.068406	0.000002	0.4	0.1		25.87
2022 QC	08/19-08/20	59.6-66.6	351	22	0.033734	0.000004	0.6	0.2		25.30
2022 QV	08/21-08/21	42.3-42.9	350	2	0.0617	0.0002	0.5	0.2		25.95
2022 QX4	08/28-08/29	23.6-19.5	336	0	0.088812	0.000001	0.3	0.1		24.69
2022 QT7	08/31-09/01	46.4-51.1	358	15	0.0112204	0.0000006	1.0	0.5	-2/-3	28.59
					0.0063785	0.0000003	1.0	0.5		
					0.0147778	0.0000015	0.7	0.5		
2022 SG3	09/22-09/22	34.2-41.4	16	8	0.16034	0.00004	0.8	0.3	-3	27.05
					0.10306	0.00006	0.3	0.3		
2022 SW3	09/23-09/25	36.9-34.8	11	15	0.194501	0.000004	1.5	0.3		24.84

Table I. Observing circumstances and results. The phase angle is given for the first and last date. If preceded by an asterisk, the phase angle reached an extrema during the period. LPAB and BPAB are the approximate phase angle bisector longitude/latitude at mid-date range (see Harris et al., 1984). Amplitude error (A.E.) is calculated as √2 * (lightcurve RMS residual). PAR is the expected Principal Axis Rotation quality detection code (Pravec et al., 2005) and H is the absolute magnitude at 1 au from Sun and Earth taken from the Small-Body Database Lookup (JPL, 2022).

Acknowledgements

The author is indebted to Petr Pravec for help and encouragement in the analysis of the tumblers 2022 NE, 2022 QT7 and 2022 SG3. Also gratefully acknowledged is a Gene Shoemaker NEO Grant from the Planetary Society (2005) and a Ridley Grant from the British Astronomical Association (2005), both of which facilitated upgrades to observatory equipment used in this study.

References

ADS (2022). Astrophysics Data System. *https://ui.adsabs.harvard.edu/*

Bacci, P.; Maestripieri, M.; Tesi, L.; Fagioli, G.; Foglia, S.; Galli, G.; Buzzi, L.; Pettarin, E.; Dupouy, P.; de Vanssay, J.B.; Camarasa, J.; Duszanowicz, G.; Bulger, J.; Lowe, T.; Schultz, A. and 38 colleagues (2022a). "2022 SG3." *MPEC 2022-S101.* *https://minorplanetcenter.net/mpec/K22/K22SA1.html*

Bacci, P.; Maestripieri, M.; Tesi, L.; Fagioli, G.; Dupouy, P.; de Vanssay, J.B.; Camarasa, J.; Duszanowicz, G.; Holmes, R.; Linder, T.; Horn, L.; Losse, F.; Demeautis, C.; Attard, G.; Maury, A. and 2 colleagues (2022b). "2022 SW3." *MPEC 2022-S116.* *https://minorplanetcenter.net/mpec/K22/K22SB6.html*

Name	Integration times	intg/Pd	Max a/b	Min Pts	Flds
2022 NE	5	0.114	2.1	310	4
2022 NR	30^{Σ}	0.122	1.1*	191	13
2022 QC	2.7	0.022	1.2*	375	7
2022 QV	2.8	0.013	1.2*	228	5
2022 QX4	11.1	0.035	1.2	450	8
2022 QT7	5.3	0.231	1.9*	417	17
2022 SG3	3.3	0.009	1.6*	1266	21
2022 SW3	16.4	0.023	2.0	775	13

Table II. Ancillary information, listing the integration times used (seconds), the fraction of the period represented by the longest integration time (Pravec et al., 2000), the calculated minimum elongation of the asteroid (Zappala et al., 1990), the number of data points used in the analysis and the number of times the telescope was repositioned to different fields. Note: Σ = Longest elapsed integration time for stacked images (start of first to end of last exposure used), * = Value uncertain, based on phase angles > 40°.

Benner, L.A.M. (2022). "Goldstone Radar Observations Planning: 1994 AW1, 2022 NR, Tukmit, and 2006 YT13." *https://echo.jpl.nasa.gov/asteroids/1994AW1/1994AW1.2022.goldstone.planning.html*

Buzzi, L.; Linder, T.; Holmes, R.; Horn, L.; Bulger, J.; Chambers, K.; Lowe, T.; Schultz, A.; Smith, I.; Chastel, S.; Fairlamb, J.; Huber, M.; Ramanjooloo, Y.; Wainscoat, R.; Weryk, R. and 14 colleagues (2022). "2022 QV." *MPEC 2022-Q42.* *https://minorplanetcenter.net/mpec/K22/K22Q42.html*

Deen, S.; Sanchez, S.; Nomen, J.; Hurtado, M.; Jaume, J.A.; Yeung, W.K.Y.; Serra, F.; Valls, T.; Hurtado, J.; Micheli, M. (2022). "2022 QX4." *MPEC 2022-R148.* *https://minorplanetcenter.net/mpec/K22/K22RE8.html*

Dupouy, P.; Bulger, J.; Chambers, K.; Dukes, T.; Lowe, T.; Schultz, A.; Smith, I.; Chastel, S.; Fairlamb, J.; Huber, M.; Ramanjooloo, Y.; Wainscoat, R.; Weryk, R.; de Boer, T.; Gao, H. and 4 colleagues (2022). "2022 QC." *MPEC 2022-Q16.* *https://minorplanetcenter.net/mpec/K22/K22Q16.html*

Evans, N.; Choi, P.; Saini, N.; Zhai, C.; Trahan, R.; Shao, M.; Linder, T.; Holmes, R.; Horn, L.; Bulger, J.; Lowe, T.; Schultz, A.; Smith, I.; Chambers, K.; Dukes, T. and 11 colleagues (2022). "2022 NE." *MPEC 2022-N29.* *https://minorplanetcenter.net/mpec/K22/K22N29.html*

Fazekas, J.B.; Christensen, E.J.; Fay, D.; Fuls, D.C.; Gibbs, A.R.; Grauer, A.D.; Groeller, H.; Hogan, J.K.; Kowalski, R.A.; Larson, S.M.; Leonard, G.J.; Rankin, D.; Seaman, R.L.; Serrano, A.; Shelly, F.C. and 27 colleagues (2022). "2022 NR." *MPEC 2022-N43.* *https://minorplanetcenter.net/mpec/K22/K22N43.html*

Harris, A.W.; Young, J.W.; Scaltriti, F.; Zappala, V. (1984). "Lightcurves and phase relations of the asteroids 82 Alkmene and 444 Gyptis." *Icarus* **57**, 251-258.

Harris, A.W.; Young, J.W.; Bowell, E.; Martin, L.J.; Millis, R.L.; Poutanen, M.; Scaltriti, F.; Zappala, V.; Schober, H.J.; Debehogne, H.; Zeigler, K. (1989). "Photoelectric Observations of Asteroids 3, 24, 60, 261, and 863." *Icarus* **77**, 171-186.

JPL (2022). Small-Body Database Lookup. *https://ssd.jpl.nasa.gov/tools/sbdb_lookup.html*

Melnikov, S.; Hoegner, C.; Laux, U.; Ludwig, F.; Stecklum, B.; Holmes, R.; Linder, T.; Horn, L.; Hug, G.; Korlevic, K.; Dusevic, P.; Markovic, M.; Paleka, I.; Perovic, I.; Pettarin, E. and 14 colleagues (2022a). "2022 QX4." *MPEC 2022-Q123*. *https://minorplanetcenter.net/mpec/K22/K22QC3.html*

Melnikov, S.; Hoegner, C.; Laux, U.; Ludwig, F.; Stecklum, B.; Bulger, J.; Lowe, T.; Schultz, A.; Smith, I.; Chambers, K.; Dukes, T.; Chastel, S.; de Boer, T.; Fairlamb, J.; Gao, H., and 22 colleagues (2022b). "2022 QT7." *MPEC 2022-Q189*. *https://minorplanetcenter.net/mpec/K22/K22QI9.html*

Pravec, P.; Hergenrother, C.; Whiteley, R.; Sarounova, L.; Kusnirak, P.; Wolf, M. (2000). "Fast Rotating Asteroids 1999 TY2, 1999 SF10, and 1998 WB2." *Icarus* **147**, 477-486.

Pravec, P.; Harris, A.W.; Scheirich, P.; Kušnirák, P.; Šarounová, L.; Hergenrother, C.W.; Mottola, S.; Hicks, M.D.; Masi, G.; Krugly, Yu.N.; Shevchenko, V.G.; Nolan, M C.; Howell, E.S.; Kaasalainen, M.; Galád, A., and 5 colleagues. (2005). "Tumbling Asteroids." *Icarus* **173**, 108-131.

Raab, H. (2018). Astrometrica software, version 4.12.0.448. *http://www.astrometrica.at/*

Warner, B.D.; Harris, A.W.; Pravec, P. (2009). "The Asteroid Lightcurve Database." *Icarus* **202**, 134-146. Updated 2021 Dec. *https://minplanobs.org/mpinfo/php/lcdb.php*

Warner, B.D. (2022). MPO Software, Canopus version 10.8.6.9. Bdw Publishing, Eaton, CO. *http://minorplanetobserver.com*

Zacharias, N.; Finch, C.T.; Girard, T.M.; Henden, A.; Bartlett, J.L.; Monet, D.G.; Zacharias, M.I. (2013). "The Fourth US Naval Observatory CCD Astrograph Catalog (UCAC4)." *Astronomical Journal* **145**, 44-57.

Zappala, V.; Cellini, A.; Barucci, A.M.; Fulchignoni, M.; Lupishko, D.E. (1990). "An analysis of the amplitude-phase relationship among asteroids." *Astron. Astrophys.* **231**, 548-560.

LIGHTCURVE ANALYSIS OF HILDA ASTEROIDS AT THE CENTER FOR SOLAR SYSTEM STUDIES: 2022 JULY-OCTOBER

Brian D. Warner
Center for Solar System Studies (CS3)
446 Sycamore Ave.
Eaton, CO 80615 USA
brian@MinorPlanetObserver.com

Robert D. Stephens
Center for Solar System Studies (CS3)
Rancho Cucamonga, CA

(Received: 2022 October 7)

CCD photometric observations of eight Hilda asteroids were made at the Center for Solar System Studies between 2022 July and October.

CCD photometric observations of eight Hilda asteroids were carried out at the Center for Solar System Studies (CS3) from 2022 July-October as part of an ongoing study of the family/group that is located between the outer main-belt and Jupiter Trojans in a 3:2 orbital resonance with Jupiter. The goal is to determine the spin rate statistics of the Hildas and to find pole and shape models when possible. We also look to examine the degree of influence that the YORP (Yarkovsky-O'Keefe-Radzievskii-Paddack) effect (Rubincam, 2000) has on distant objects and to compare the spin rate distribution against the Jupiter Trojans, which can provide evidence that the Hildas are more "comet-like" than main-belt asteroids.

Telescopes	Cameras
0.30-m *f*/6.3 Schmidt-Cass	FLI Microline 1001E
0.35-m *f*/9.1 Schmidt-Cass	FLI Proline 1001E
0.35-m *f*/11 Schmidt-Cass	SBIG STL-1001E
0.40-m f/10 Schmidt-Cass	
0.50-m *f*/8.1 Ritchey-Chrétien	

Table I. List of available telescopes and CCD cameras at CS3. The exact combination for each telescope/camera pair can vary due to maintenance or specific needs.

Table I lists the telescopes and CCD cameras that are available to make observations. All the cameras use CCD chips from the KAF 1001 blue-enhanced family and so have essentially the same response. The pixel scales ranged from 1.24-1.60 arcsec/pixel. All lightcurve observations were unfiltered or with a clear filter, even though the latter can result in a 0.1-0.3 magnitude loss. The exposures varied depending on the asteroid's brightness.

To reduce the number of times and amounts of adjusting nightly zero-points, the ATLAS catalog r´ (SR) magnitudes (Tonry et al., 2018) are used. Those adjustments are usually ≤ ±0.03 mag. The rare greater corrections may have been related in part to using unfiltered observations, poor centroiding of the reference stars, and not correcting for second-order extinction. Another cause may be selecting what appears to be a single star but is actually an unresolved pair.

The Y-axis values are ATLAS SR "sky" (catalog) magnitudes. The values in the parentheses give the phase angle(s), *a*, and the value of *G* used to normalize the data to the comparison stars used in the earliest session. This, in effect, corrects all the observations so that seem to have been made at a single fixed date/time and phase angle,

presumably leaving any variations due only to the asteroid's rotation and/or albedo changes.

There can be up to three phase angles given. If two, the values are for the first and last night observations. If three, the middle value is the extrema (maximum or minimum) reached between the first and last observing runs. The X-axis shows rotational phase from -0.05 to 1.05. If the plot includes the amplitude, e.g., "Amp: 0.65," this is the amplitude of the Fourier model curve and *not necessarily the adopted amplitude for the lightcurve.*

For brevity, only some of the previous results are referenced. A more complete listing is in the asteroid lightcurve database (Warner et al., 2009; "LCDB" from here on).

1180 Rita. Dahlegren et al. (1998) determined a period of 14.902 h for this 78 km Hilda. We had observed it on three previous occasions. In 2017, we found a period of 13.090 h (Warner and Stephens, 2017). After observations in 2018 that led to a period of 14.849 h (Warner and Stephens, 2018), we re-examined the 2017 data and found a period of 14.928 h. In 2021 (Warner and Stephens, 2022) we found a similar period of 14.894 h. As with the 2017 observations, the lightcurve for our most recent data (2022 September and October) has a very low amplitude.

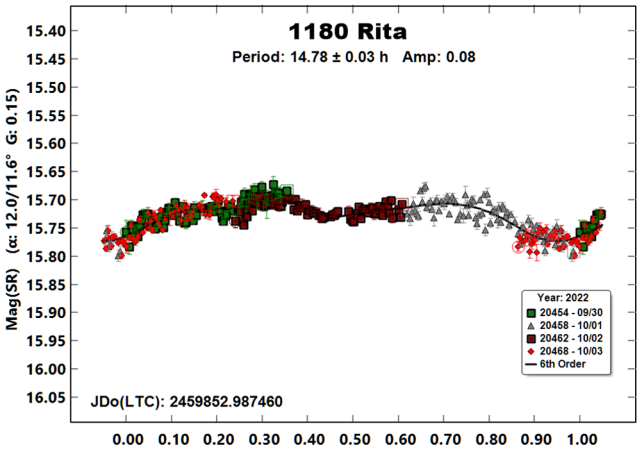

9661 Hohmann. The only previously reported period in the LCDB was from Waszczak et al. (2015), who found a period of 5.920 h. The period spectrum using our 2022 data shows two nearly equal solutions (based on minimum RMS fit to the Fourier curve), one near that by Waszczak et al. and the other at 5.248 h. The two periods differ by one-half rotation over 24-hours.

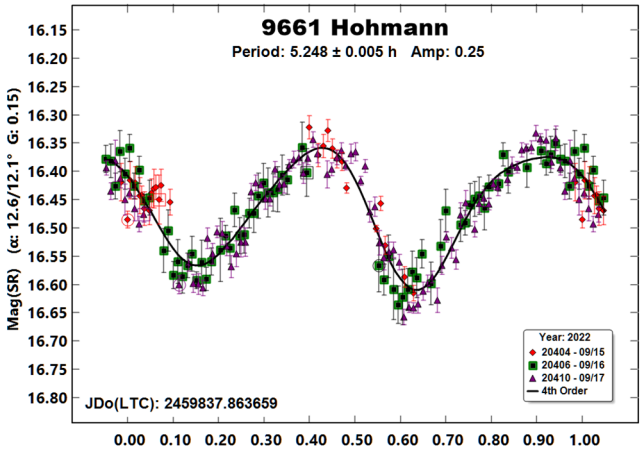

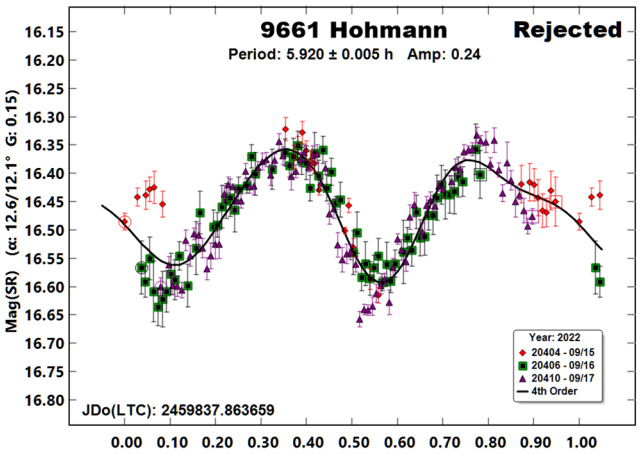

We plotted our data to the two possible solutions. The "Rejected" plot is for the period found by Waszczak et al. and shows significant deviations from the Fourier curve and a gap in coverage. Based on a comparison between the two, we feel confident in adopting 5.248 h as the correct result.

11739 Baton Rouge. Hasegawa et al. (2018) reported a period of 4.8 h for the 22-km Hilda. It is rated U = 2– in the LCDB, meaning rthe solution is barely reliable. Our observations in 2022 September allowed us to find what we believe to be a reliable period of 5.601 h.

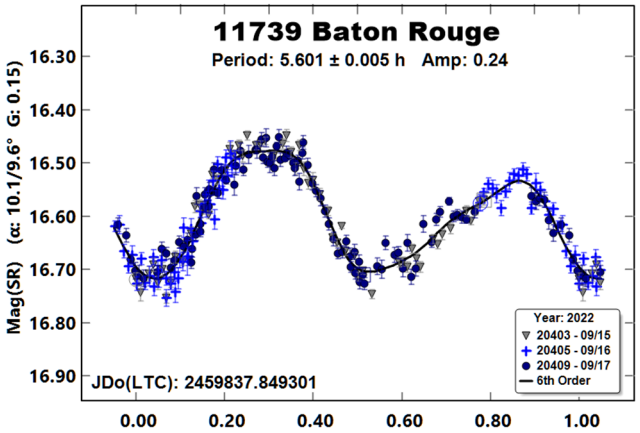

12896 Geoffroy. The only previous result in the LCDB was 5.68 h by Chang et al. (2016), but it is considered insufficiently reliable for statistical studies (U = 1+).

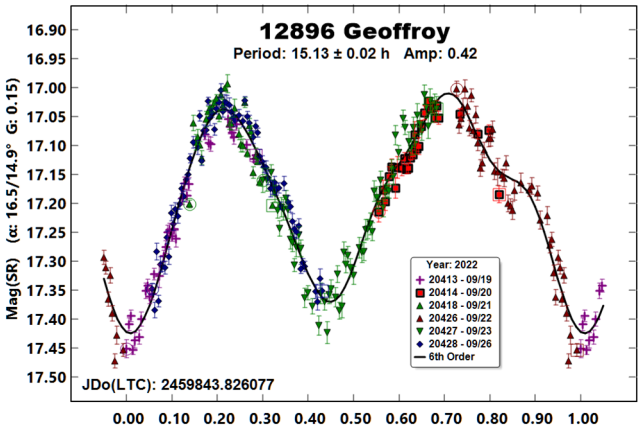

Number	Name	2022/mm/dd	Phase	L_{PAB}	B_{PAB}	Period(h)	P.E.	Amp	A.E.
1180	Rita	09/30-10/03	12.0,11.6	62	-4	14.78	0.03	0.08	0.01
9661	Hohmann	09/15-09/17	12.6,12.1	28	-9	5.248	0.005	0.27	0.02
11739	Baton Rouge	09/15-09/17	10.1,9.5	14	15	5.601	0.005	0.24	0.02
12896	Geoffroy	09/19-09/26	16.5,14.9	43	-1	15.13	0.02	0.42	0.03
12920	1998 VM15	09/19-10/01	12.5,10.2	46	0	12.881	0.003	0.30	0.02
14569	1998 QB32	08/17-08/29	11.2,7.4	354	1	2.5699	0.0005	0.09	0.01
21930	1999 VP61	09/15-09/26	1.7,5.6	348	1	-	-	0.02	0.02
41365	2000 AO98	07/24-08/08	5.5,2.2	315	6	13.148	0.003	0.21	0.03

Table II. Observing circumstances and results. The phase angle (α) is given at the start and end of each date range. The asterisk indicates that the phase angle reached an extremum over the span of the observations. L_{PAB} and B_{PAB} are the average phase angle bisector longitude and latitude (see Harris et al.. 1984).

Our observations in 2022 September covered a span of about a week. The resulting data set led to a period of 15.13 h. Given the large amplitude, the lightcurve is almost certainly to be bimodal (Harris et al., 2014), which was confirmed by that being the only solution to fit the data with complete coverage and proper spacing of the maximums and minimums.

(12920) 1998 VM15. Clark (2014) reported a period of 12.885 h for this 35-km Hilda. He subsequently revised it to 9.0511 h after newer observations in 2014 led to P = 9.1240 h (Clark, 2015). The period spectrum based on our 2022 data shows only a relatively weak solution for periods near 9 h. Our result and Clark's original period are in close agreement.

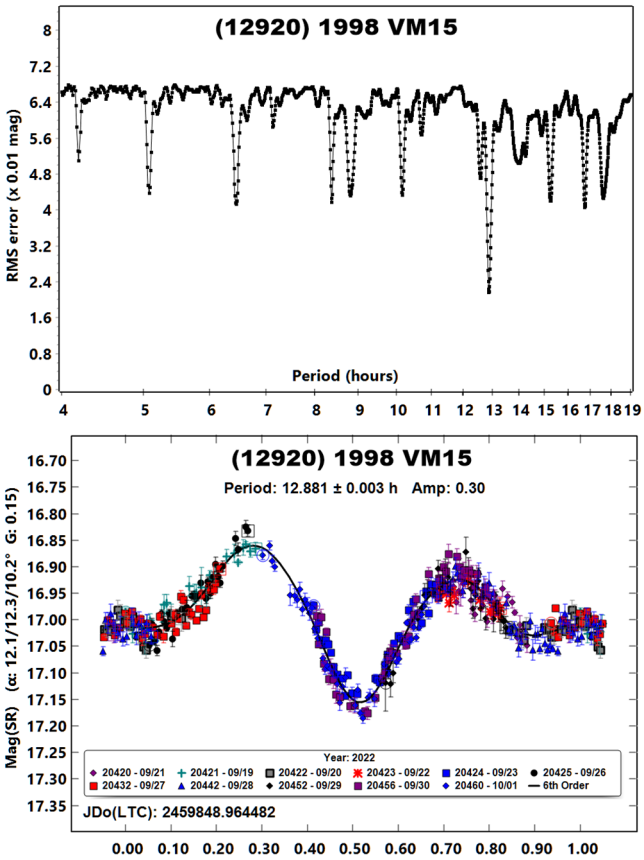

(14569) 1998 QB32. There were no previous period results in the LCDB. The low amplitude led to an ambiguous solution (see Harris et al., 2014).

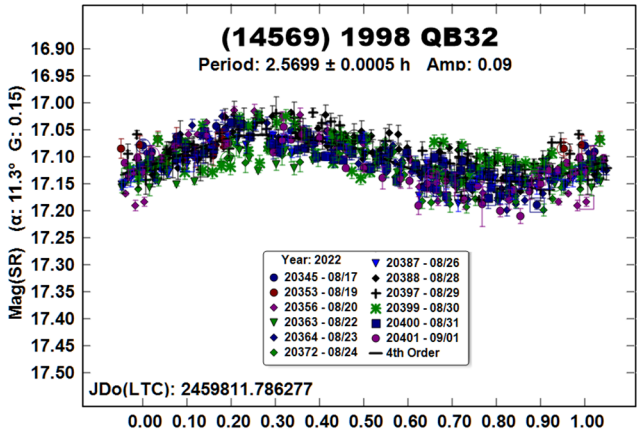

A split-halves plot using a period near 5 hours showed essentially identical halves and so a monomodal solution of 2.57 h was adopted. We note, however, that the double period near 5 h cannot be formally excluded and that both solutions lie below the spin barrier in the LCDB frequency-diameter plot.

(21930) 1999 VP61. There were no previous entries for a period in the LCDB. The estimated diameter is 17 km. A search from 2 to 200 hours, and then from 1 to 10 hours, on the combined and individual data sets found solutions only barely above the noise in the period spectrums. If there is a period to be found, it is well into the noise of the data. It's possible that this apparition was close to a pole-on view. A future apparition, with a more equatorial viewing aspect, might lead to a lightcurve with at least a modest amplitude.

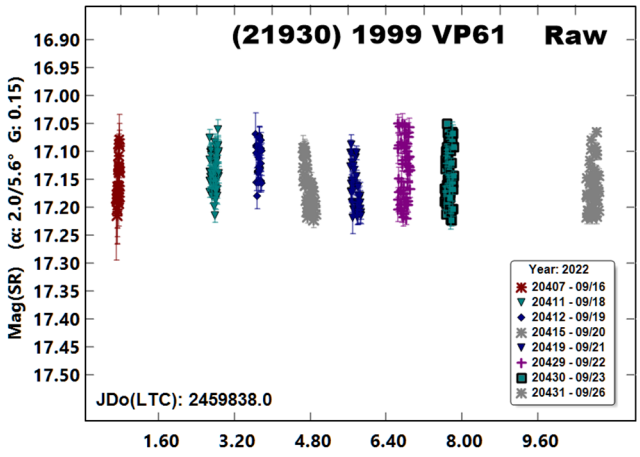

(41365) 2000 AO98. There were no previously reported periods in the LCDB. The period spectrum based on our 2022 data showed a few possibilities.

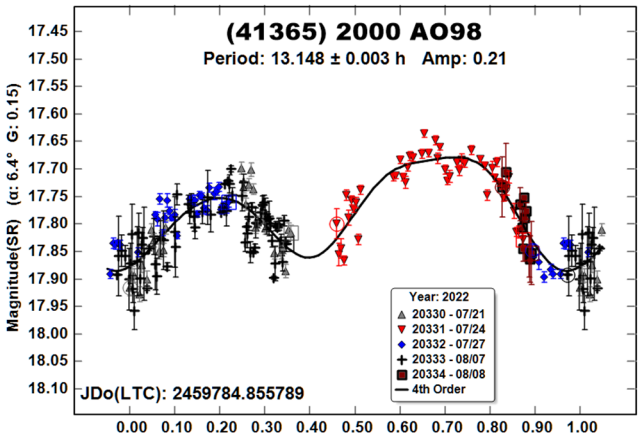

We adopted a period of 13.148 h since it produced a bimodal lightcurve with a reasonable spacing of the maximums and minimums, e.g., the two maximums were about 0.5 rotation phase apart. In addition, the two halves were significantly different, which made the half-period unlikely.

Acknowledgements

This work includes data from the Asteroid Terrestrial-impact Last Alert System (ATLAS) project. ATLAS is primarily funded to search for near earth asteroids through NASA grants NN12AR55G, 80NSSC18K0284, and 80NSSC18K1575; byproducts of the NEO search include images and catalogs from the survey area. The ATLAS science products have been made possible through the contributions of the University of Hawaii Institute for Astronomy, the Queen's University Belfast, the Space Telescope Science Institute, and the South African Astronomical Observatory. The authors gratefully acknowledge Shoemaker NEO Grants from the Planetary Society (2007, 2013). These were used to purchase some of the telescopes and CCD cameras used in this research.

References

Chang, C.-K.; Lin, H.-W.; Ip, W.-H.; Prince, T.A.; Kulkarni, S.R.; Levitan, D.; Laher, R.; Surace, J. (2016). "Large Super-fast Rotator Hunting Using the Intermediate Palomar Transient Factory." *Astrophys. J. Sup. Ser.* **227**, A20.

Clark, M. (2014). "Asteroid Photometry from the Preston Gott Observatory." *Minor Planet Bull.* **41**, 178-183.

Clark, M. (2015). Asteroid Photometry from the Preston Gott Observatory." *Minor Planet Bull.* **42**, 163-166.

Dahlgren, M.; Lahulla, J.F.; Lagerkvist, C.-I.; Lagerros, J.; Mottola, S.; Erikson, A.; Gonano-Beurer, M.; Di Martino, M. (1998). "A Study of Hilda Asteroids. V. Lightcurves of 47 Hilda Asteroids." *Icarus* **133**, 247-285.

Harris, A.W.; Young, J.W.; Scaltriti, F.; Zappala, V. (1984). "Lightcurves and phase relations of the asteroids 82 Alkmene and 444 Gyptis." *Icarus* **57**, 251-258.

Harris, A.W.; Pravec, P.; Galad, A.; Skiff, B.A.; Warner, B.D.; Vilagi, J.; Gajdos, S.; Carbognani, A.; Hornoch, K.; Kusnirak, P.; Cooney, W.R.; Gross, J.; Terrell, D.; Higgins, D.; Bowell, E.; Koehn, B.W. (2014). "On the maximum amplitude of harmonics on an asteroid lightcurve." *Icarus* **235**, 55-59.

Hasegawa, S.; Kuroda, D.; Kitazato, K.; Kasuga, T.; and 40 coauthors (2018). "Physical properties of near-Earth asteroids with a low delta-v: Survey of target candidates for the Hayabusa2 mission." *Pub. Astron. Soc. Japan* **70**, A114.

Rubincam, D.P. (2000). "Relative Spin-up and Spin-down of Small Asteroids." *Icarus* **148**, 2-11.

Tonry, J.L.; Denneau, L.; Flewelling, H.; Heinze, A.N.; Onken, C.A.; Smartt, S.J.; Stalder, B.; Weiland, H.J.; Wolf, C. (2018). "The ATLAS All-Sky Stellar Reference Catalog." *Astrophys. J.* **867**, A105.

Warner, B.D.; Stephens, R.D (2017). "Lightcurve Analysis of Hilda Asteroids at the Center for Solar System Studies: 2016 December thru 2017 April." *Minor Planet Bull.* **44**, 220-222.

Warner, B.D.; Stephens, R.D. (2018). "Lightcurve Analysis of Hilda Asteroids at the Center for Solar System Studies: 2018 April-June." *Minor Planet Bull.* **45**, 390-393.

Warner, B.D.; Stephens, R.D. (2022). "Lightcurve Analysis of Hilda Asteroids at the Center for Solar System Studies: 2021 September-December." *Minor Planet Bull.* **49**, 102-104.

Warner, B.D.; Harris, A.W.; Pravec, P. (2009). "The Asteroid Lightcurve Database." *Icarus* **202**, 134-146. Updated 2021 Dec. *http://www.minorplanet.info/lightcurvedatabase.html*

Waszczak, A.; Chang, C.-K.; Ofek, E.O.; Laher, R.; Masci, F.; Levitan, D.; Surace, J.; Cheng, Y.-C.; Ip, W.-H.; Kinoshita, D.; Helou, G.; Prince, T.A.; Kulkarni, S. (2015). "Asteroid Light Curves from the Palomar Transient Factory Survey: Rotation Periods and Phase Functions from Sparse Photometry." *Astron. J.* **150**, A75.

ON CONFIRMED AND SUSPECTED BINARY ASTEROIDS OBSERVED AT THE CENTER FOR SOLAR SYSTEM STUDIES: 2022 JUNE TO AUGUST

Brian D. Warner (CS3)
Center for Solar System Studies
446 Sycamore Ave.
Eaton, CO 80615 USA
brian@MinorPlanetObserver.com

Robert D. Stephens
Center for Solar System Studies (CS3)
Rancho Cucamonga, CA 91730

(Received: 2022 October 7)

Analysis of CCD photometric observations obtained in 2022 June to August of the inner main-belt asteroid 3533 Toyota and near-Earth asteroid (85804) 1998 WQ5 at the Center for Solar System Studies indicate that both asteroids are likely binary. For 3533, we found P1 = 2.9809 h and PORB = 16.070 h but, for the latter, solutions of 12.098 h and 24.2176 h cannot be formally excluded. (85804) 1998 WQ5 has P1 = 2.6761 h and PORB = 46.13 h. The estimated diameter ratio of the two bodies is >0.33.

CCD photometric observations of inner main-belt asteroid 3533 Toyota and near-Earth asteroid (85804) 1998 WQ5 were made at the Center for Solar System Studies in 2022 June to August. Data analysis makes it very likely that both objects are binary. This is based on there being a sufficiently distinct secondary period with its lightcurve showing what appear to be *mutual events* (occultations/eclipses) or a slightly elliptical body where the rotational and orbital periods are the same.

The observations were made with a 0.35-m Schmidt-Cassegrain and either an FLI Proline or Microline CCD camera as well as a 0.40-m Schmidt-Cassegrain with FLI Proline CCD camera. All cameras use a KAF-1001E chip, which has a pixel array of 1024×1024×24µ. The field-of-view and image scale were about 26×26 arcminutes and 1.5 arcsec/pixel, respectively, for the 0.35-m telescopes. The 0.4-m values were 20×20 arcminutes and 1.2 arcsec/pixel.

All lightcurve observations were unfiltered or with a clear filter, even though the clear filter can cause a 0.1-0.3 mag loss. The exposures varied depending on the asteroid's brightness and sky motion. Whether guiding on a field star or not, sometimes the asteroid was trailed on the image.

Measurements were made using *MPO Canopus*. The Comp Star Selector utility in *MPO Canopus* found up to five comparison stars of near solar-color for differential photometry. To reduce the number of adjusted nightly zero points and their amounts, the analysis of the data used the ATLAS catalog r´ (SR) magnitudes (Tonry et al., 2018). The rare zero-point adjustments of ≥ ±0.03 mag may be related to using unfiltered/clear observations, poor centroiding of the reference stars, not correcting for second-order extinction, or selecting a comp star that is an unresolved pair.

The Y-axis values are ATLAS SR "sky" (catalog) magnitudes. The two values in the parentheses are the phase angle (a) and the value of *G* used to normalize the data to the comparison stars used in the earliest session. This, in effect, corrected all the observations to appear that they were made at a single fixed date/time and phase angle, presumably leaving any variations due only to the asteroid's rotation and/or albedo changes. The X-axis shows rotational phase from -0.05 to 1.05. If the plot includes the amplitude, e.g., "Amp: 0.65", this is the amplitude of the Fourier model curve and *not necessarily the adopted amplitude for the lightcurve*.

References to previous works were taken from the asteroid lightcurve database (Warner et al., 2009), known as "LCDB" from here on. Since most listed rotation periods for the primary were very similar, only a few of the LCDB references have been used.

3533 Toyota. There are several previously reported periods for this asteroid, all with a single period close of 2.98 h, i.e., no indications of a satellite: Behrend (2006web); Pravec et al. (2009web; 2022web); Higgins (2011web); and Benishek (2020).

After several sessions, it was apparent that a second period was involved. Using the dual-period search in *MPO Canopus*, we found a primary period of P_1 = 2.9809 h and three possible secondary periods, each commensurate with an Earth Day (24 hours).

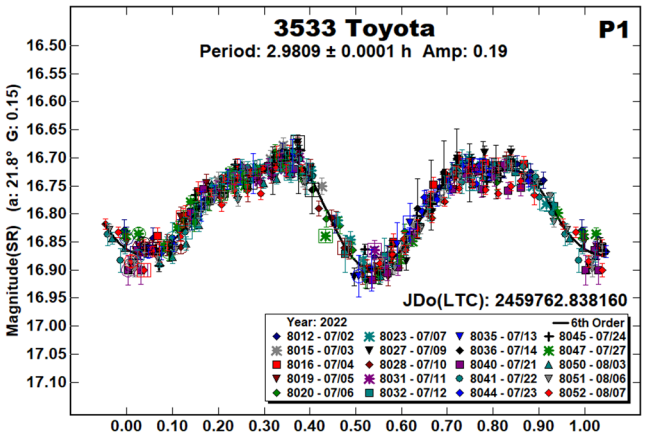

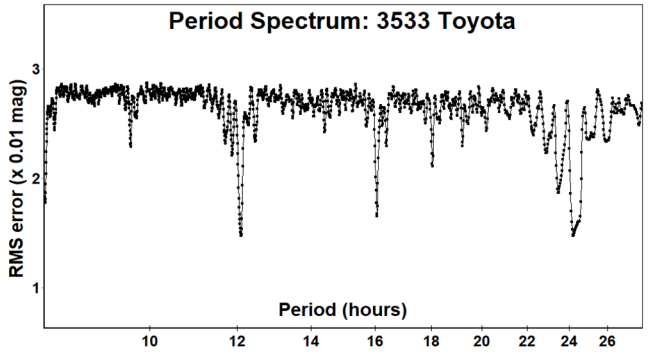

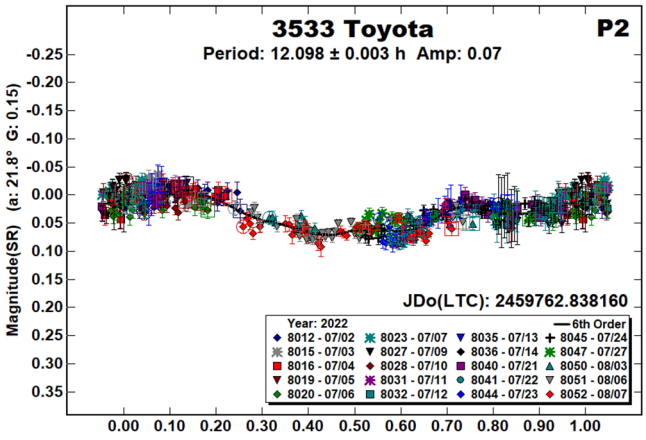

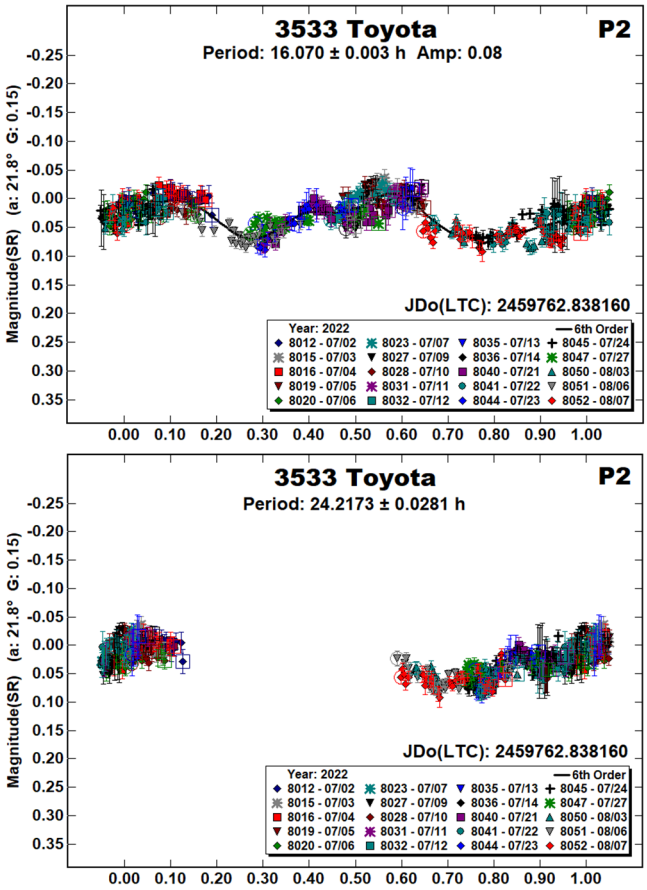

Finding a unique period for an Earth-day commensurate period from a single station is difficult at best. After nearly a month of observations, we adopted P_{ORB} = 16.070 h, primarily because it produces a nearly sinusoidal bimodal lightcurve, which can be expected if the satellite is a slightly elongated body with its rotation and orbital periods being the same. There are no obvious signs of *mutual events*, i.e., occultations and/or eclipses, so we cannot give an estimate of the relative diameters between the primary and secondary bodies.

(85804) 1998 WQ5. Oey (2006) reported a period of 3.0089 h for this NEA while Higgins (2011web) found 3.71 h. Our previous work (Warner, 2015) gave a period of 6.028 h. Analysis of our 2022 data rejected all three results.

The "NoSub" plot shows the data phased to a single period. The numerous points below the "main" curve are often a good sign of a secondary period, most likely a satellite.

Once again, a month's worth of observations was needed to resolve the system characteristics to our satisfaction. The primary period seemed to resolve itself after a short time. However, being monomodal at 2.6761 h (after subtracting the proposed secondary period), there was a possibility the true value was the double period, or about 5.35 h (see Harris et al., 2014). Since a good majority of small binary asteroids have primary rotation period on the order of 2-4 hours, we have adopted P_1 = 2.6761 h for the primary.

Once this was settled, the search for the secondary period continued, sometimes changing significantly with the addition of another session's data. Eventually, we were led to P_{ORB} = 46.13 h. Since there are nearly flat sections of the secondary period between the minima, we take those attenuations to be the result of mutual events and not just the rotation of an elliptical satellite.

We estimate the attenuations to be 0.11 mag and 0.17 mag in depth. Using the smaller value allows finding the approximate effective relative diameters of the two bodies (*Ds/Dp*). In this case, the ratio is on the order of 0.33 ± 0.03. This is a minimum value since neither minimum is flat-bottomed, i.e., the mutual event would be total.

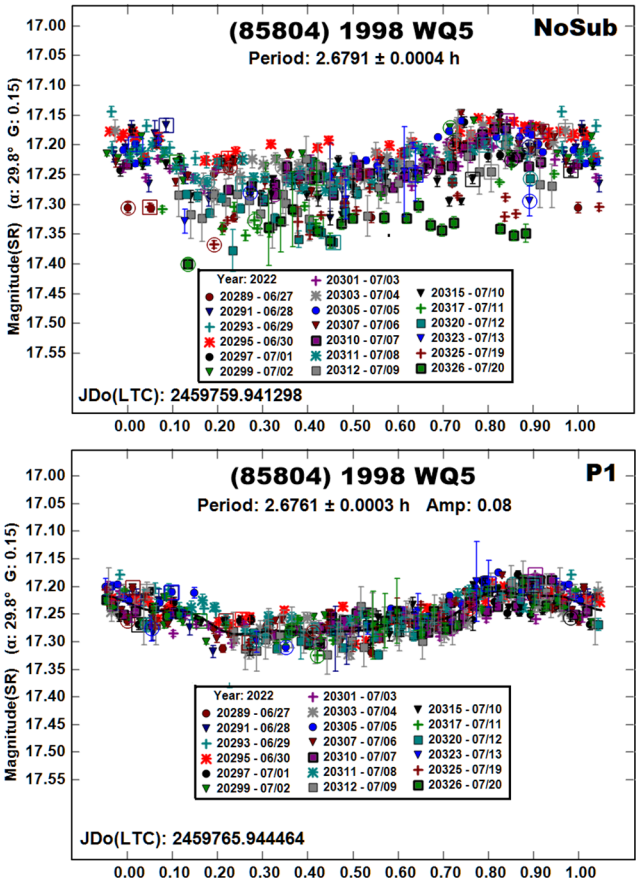

Number	Name	2022 mm/dd	Phase	L_{PAB}	B_{PAB}	Period(h)	P.E.	Amp	A.E.	Grp/Dr
3533	Toyota	07/02-08/07	21.8,9.5	329	5	2.9809	0.0001	0.19	0.01	MB-I
						*16.070	0.003	0.08	0.01	*UD*
85804	1998 WQ5	06/27-07/20	29.8,18.4	314	13	2.6761	0.0003	0.06	0.01	NEA
						46.13	0.02	0.17	0.01	*>0.33*

Table II. Observing circumstances. The first line for an asteroid gives the primary or dominant period. The second line gives the secondary period. * Indicates the preferred solution for the secondary period when more than one is found. The phase angle (α) is given at the start and end of each date range. L_{PAB} and B_{PAB} are, respectively the average phase angle bisector longitude and latitude (see Harris et al.,1984). For the Grp/Dr column, the first line gives the group/family: MB-I: inner main-belt, NEA: near-Earth asteroid. The code "UD" on the second line in the Grp/Dr column means "undetermined," primarily because there were no mutual events. Otherwise, the value is the ratio of the secondary-to-primary effective diameters.

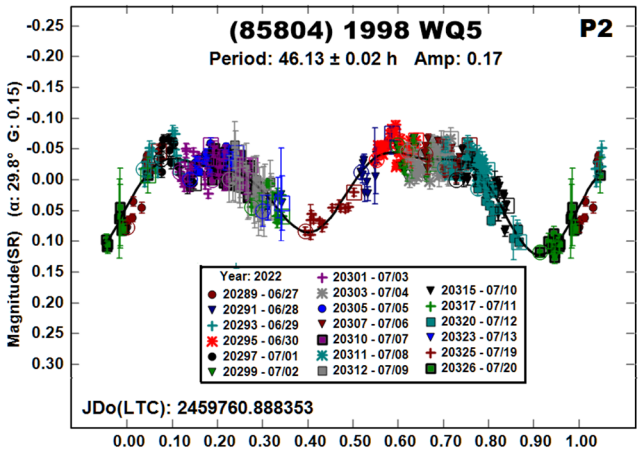

Acknowledgements

The authors gratefully acknowledge Shoemaker NEO Grants from the Planetary Society (2007, 2013). These were used to purchase some of the telescopes and CCD cameras used in this research. This work includes data from the Asteroid Terrestrial-impact Last Alert System (ATLAS) project. ATLAS is primarily funded to search for near earth asteroids through NASA grants NN12AR55G, 80NSSC18K0284, and 80NSSC18K1575; byproducts of the NEO search include images and catalogs from the survey area. The ATLAS science products have been made possible through the contributions of the University of Hawaii Institute for Astronomy, the Queen's University Belfast, the Space Telescope Science Institute, and the South African Astronomical Observatory. This paper made use of the services provided by the SAO/NASA Astrophysics Data System, which is operated by the Smithsonian Astrophysical Observatory under NASA Cooperative Agreement 80NSSC211M0056.

References

Behrend, R. (2006web). Observatoire de Geneve web site. *http://obswww.unige.ch/~behrend/page_cou.html*

Benishek, V. (2020). "Asteroid Photometry at Sopot Astronomical Observatory: 2019 September - 2020 March." *Minor Planet Bull*. **47**, 75-83.

Harris, A.W.; Pravec, P.; Galad, A.; Skiff, B.A.; Warner, B.D.; Vilagi, J.; Gajdos, S.; Carbognani, A.; Hornoch, K.; Kusnirak, P.; Cooney, W.R.; Gross, J.; Terrell, D.; Higgins, D.; Bowell, E.; Koehn, B.W. (2014). "On the maximum amplitude of harmonics on an asteroid lightcurve." *Icarus* **235**, 55-59.

Harris, A.W.; Young, J.W.; Scaltriti, F.; Zappala, V. (1984). "Lightcurves and phase relations of the asteroids 82 Alkmene and 444 Gyptis." *Icarus* **57**, 251-258.

Higgins, D.J. (2011web). *http://www.david-higgins.com/Astronomy/asteroid/lightcurves.htm* (no longer active).

Oey, J. (2006). "Lightcurve analysis of 10 asteroids from Leura Observatory." *Minor Planet Bull*. **33**, 96-99.

Pravec, P.; Wolf, M.; Sarounova, L. (2009web, 2022web). *http://www.asu.cas.cz/~ppravec/neo.htm*

Tonry, J.L.; Denneau, L.; Flewelling, H.; Heinze, A.N.; Onken, C.A.; Smartt, S.J.; Stalder, B.; Weiland, H.J.; Wolf, C. (2018). "The ATLAS All-Sky Stellar Reference Catalog." *Ap. J.* **867**, A105.

Warner, B.D. (2015). "Near-Earth Asteroid Lightcurve Analysis at CS3-Palmer Divide Station: 2014 October-December." *Minor Planet Bull*. **42**, 115-127.

Warner, B.D.; Harris, A.W.; Pravec, P. (2009). "The Asteroid Lightcurve Database." *Icarus* **202**, 134-146. Updated 2021 Dec. *http://www.minorplanet.info/lightcurvedatabase.html*

ROTATIONAL PERIOD AND LIGHTCURVE DETERMINATION OF TWO ASTEROIDS

Andrzej Armiński
Marina Sky Observatory, Nerpio (Z06)
P.O. Box 730, 70-952 Szczecin, Poland
aa@aarminski.com.pl

(Received: 2022 October 14)

Photometric observations were conducted of two main-belt asteroids. The results of lightcurve analysis gave sidereal rotation periods and amplitudes shown in the table below.

Reported here are lightcurve and period of rotation solutions for asteroids studied with Marina Sky Observatory 17-inch robotic telescope (Marina Sky Observatory, 2022). All images were taken with a Planewave CDK 0.432-m f/6.8 telescope and Finger Lake Instruments Proline 16803 CCD camera using Sloan r filter. The images were binned at 2×2 yielding an image scale of 1.278 arcsec/pixel and the field of view 43 × 43 arcmin. The exposure time of each image was 150 seconds. To remove Residual Bulk Image (RBI), the NRI pre-flash was applied before each exposure. Images were calibrated with bias, dark for -20°C and sky flat frames.

Astrometric plate solving of acquired images was achieved using *PinPoint* (DC3 Dreams, 2022) with star positions from ATLAS catalogue (Tonry et al., 2018). In photometry analysis, a couple dozen of carefully selected comparison stars sourced from ATLAS catalogue were used having Sloan r magnitudes in range 12 - 16, B-V color index in range 0.45 - 0.9 and SNR usually between 50 and 450.

Tycho Tracker software (Parrot, 2022) was used for data processing and photometric analysis. *The Top 50 Asteroids* website and associated database (Kluwak, 2022) was used as asteroid ephemeris generator during planning and observing.

(7353) Kazuya 1995 AC1. This main-belt (LCDB orbital group 521) asteroid was discovered at Nyukasa on 1995 January 06 by M. Hirasawa and S. Suzuki. The determined orbit (MPC Objects, 2022) has a semi-major axis of 2.5695868 au, eccentricity of 0.1751155, and inclination of 14.32936 degrees. According to JPL Small-Body Database (JPL, 2022) the diameter is 10.998 km, absolute magnitude H = 12.47, and geometric albedo 0.192.

The rotational period for this body has not been found in previously published data (Warner et al., 2009). Data were obtained during observations on 2022 October 01 and 04. The number of images used in the analysis for the two nights were 161 and 105 respectively. The sky motion during imaging was 0.52 - 0.55 arcsec/minute. The two full observational nights allowed establishing a period of rotation of 6.3815 ± 0.0015 h and Sloan r magnitude range 16.13 - 16.29.

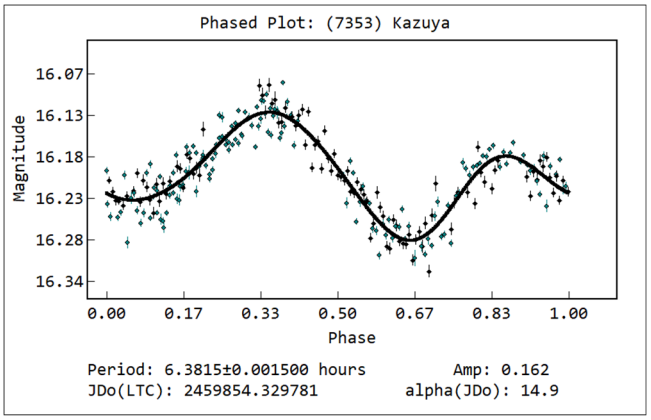

(10590) 1996 OP2. This inner main-belt (LCDB orbital group 9104), orbit type Phocaea asteroid was discovered at Campo Imperatore on 1996 July 24 by A. Boattini and A. Di Paola. The determined orbit (MPC Objects, 2022) has a semi-major axis of 2.4013510 au, eccentricity of 0.2429032, and inclination of 13.54323 degrees. According to JPL Small-Body Database (JPL, 2022) the diameter is 3.951 km, absolute magnitude H = 14.37, and geometric albedo 0.284.

The rotational period for this body has not been found in previously published data (Warner et al., 2009). Data were obtained on 2022 July 7-10. The number of images used in the analysis for the four nights were 23, 85, 88 and 55 respectively. The sky motion during imaging was 0.39 – 0.43 arcsec/minute. The four observational nights allowed establishing a bi-modal period of rotation of 7.1463 ± 0.0007 h and Sloan r magnitude range 16.18 - 16.42.

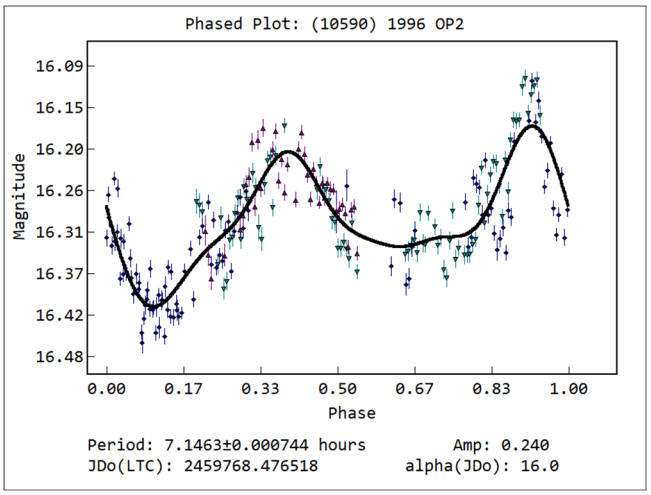

Number	Name	yyyy mm/dd	Phase	L_{PAB}	B_{PAB}	Period(h)	P.E.	Amp	A.E.	Grp
7353	Kazuya	2022 10/01-10/04	14.9,13.9	30	18	6.3815	0.0015	0.16	0.02	521
10590	1996 OP2	2022 07/07-07/10	15.7,16.0	300	18	7.1463	0.0007	0.24	0.04	MB-I

Table I. Observing circumstances and results. The phase angle is given for the first and last date. If preceded by an asterisk, the phase angle reached an extrema during the period. L_{PAB} and B_{PAB} are the approximate phase angle bisector longitude/latitude at mid-date range (see Harris et al., 1984). Grp is the asteroid family/group (Warner et al., 2009).

References

DC3 Dreams. (2022). PinPoint Astrometric Engine. *http://pinpoint.dc3.com*

Harris, A.W.; Young, J.W.; Scaltriti, F.; Zappala, V. (1984). "Lightcurves and phase relations of the asteroids 82 Alkmene and 444 Gyptis." *Icarus* **57**, 251-258.

JPL Small-Body Database. (2022). *https://ssd.jpl.nasa.gov/tools/sbdb_lookup.html#/?sstr=49937*

Kluwak, T. (2022). "Top 50 Asteroids for K80 Lusowko Platanus Observatory." *https://platanus.pl/services*

Marina Sky Observatory (2022). IAU code Z06. *http://marinasky.org*

MPC Objects. (2022). *https://minorplanetcenter.net/db_search/show_object?object_id=49937*

Parrot, D. (2022). Tycho Tracker software. *https://www.tycho-tracker.com*

Tonry, J.L.; Denneau, L.; Heinze, A.N.; Stalder, B.; Smith, K.W.; Smartt, S.J.; Stubbs, C.W.; Weiland, H.J.; Rest, A. (2018). "ATLAS: A High-cadence All-sky Survey System." *PASP* **130**, 064505.

Warner, B.D.; Harris, A.W.; Pravec, P. (2009). "The Asteroid Lightcurve Database." *Icarus* **202**, 134-146. Updated 2022, Sep. *http://www.minorplanet.info/lightcurvedatabase.html*

LIGHTCURVE ANALYSIS OF THREE ASTEROIDS

Thomas Chelius
Physics Department
University of Wisconsin River Falls
River Falls, WI 54022
tjchelius98@gmail.com

(Received: 2022 September 2 Revised: 2022 November 11)

Photometric observations were made of three main-belt asteroids in 2021 March at the Las Campanas Remote Observatory. The rotational period and amplitude of each asteroid were determined.

Photometric observations of three main-belt asteroids were taken on four nights over the span of five days in 2021 March using the Las Campanas Remote Observatory. The observatory uses a 0.3 m f8 Astro Physics Maksutov Cassegrain telescope. It uses a FLI Proline 16803 CCD Camera with FLI focuser and Filter wheel. The field of view is 52'×52' with a plate scale of 0.76" per pixel. Exposures were 300 seconds.

Data processing and analysis was done through *Tycho* v9.2 software (Parrott, 2022) to produce lightcurves. Comparison stars were used from the ATLAS catalog (Tonry et al., 2018). Previous data and measurements were found through the asteroid lightcurve database (LCDB, Warner et al., 2009).

4133 Heureka. This main-belt asteroid was discovered by L. Oterma at Turku in 1942. 38 images were taken on four nights producing a rotational period of 3.725 ± 0.001 h with an amplitude of 0.20 ± 0.03 mag. There were no previous LCDB measurements found for the period of this asteroid.

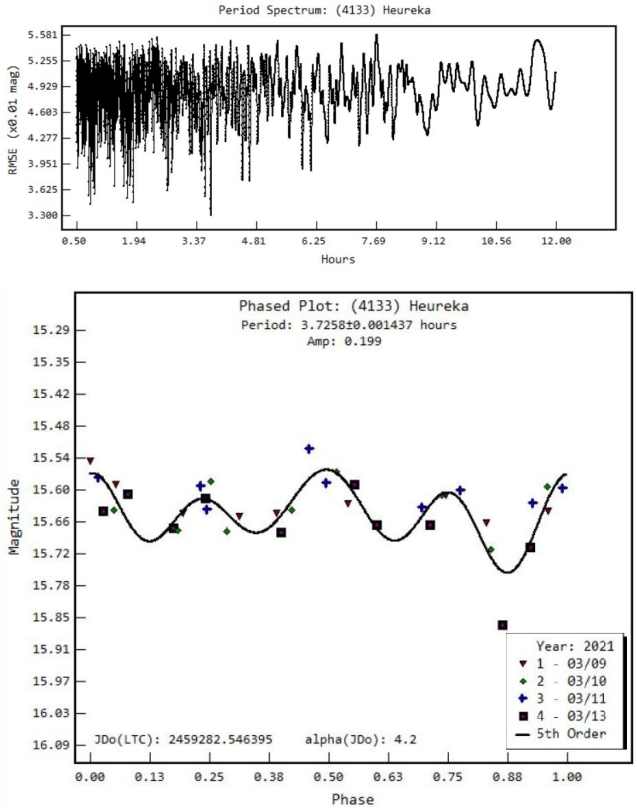

Number	Name	yyyy mm/dd	Phase	L_{PAB}	B_{PAB}	Period(h)	P.E.	Amp	A.E.	Grp
4133	Heureka	2021/03/09-03/13	*5.2,6.0	163	-5	3.726	0.001	0.20	0.03	MB
16452	Goldfinger	2021/03/09-03/13	*1.3,1.6	169	-1	3.867	0.001	0.31	0.03	MB
49483	1999 BP13	2021/03/09-03/13	*4.0,6.2	162	0	9.538	0.001	0.30	0.03	MB

Table I. Observing circumstances and results. The phase angle is given for the first and last date. If preceded by an asterisk, the phase angle reached an extrema during the period. L_{PAB} and B_{PAB} are the approximate phase angle bisector longitude/latitude at mid-date range (see Harris et al., 1984). Grp is the asteroid family/group (Warner et al., 2009).

16452 Goldfinger. This is another main-belt asteroid and was discovered by C.S. Shoemaker and E.M. Shoemaker at Palomar in 1989. A total of 37 images were taken on four nights to find a rotational period of 3.867 ± 0.001 h and an amplitude of 0.30 ± 0.03 mag. This is similar to the previous measurement on the LCDB of 3.884±0.001 h by Dose (2021).

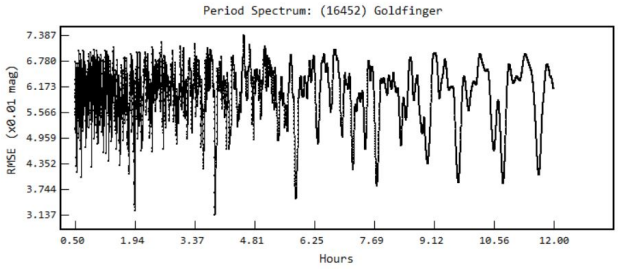

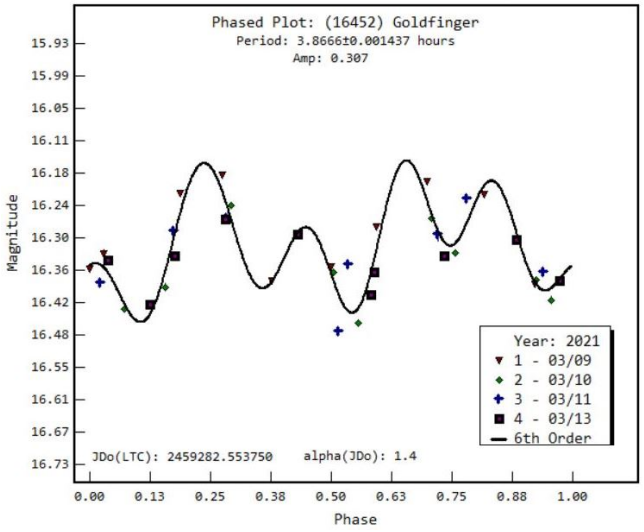

(49483) 1999 BP13. This main-belt asteroid was discovered by K. Korlevic at Visnjan in 1999. A total of 37 images from four nights were used to find a rotational period. The best solution derived from these measurements was a period of 9.538 ± 0.001 h and an amplitude of 0.30 ± 0.06 mag. The period spectrum also shows two other solutions with similar RMS. One is a period of 6.359 ± 0.001 h and the other is a period of 3.178 ± 0.001 h. A period of 6.359 ± 0.001 h would agree with the previous measurement found in the LCDB of 6.365 ± 0.005 h by Marchini et al. (2021).

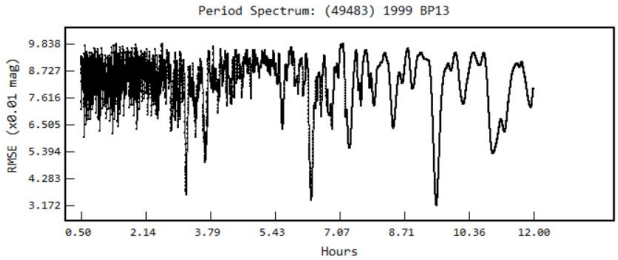

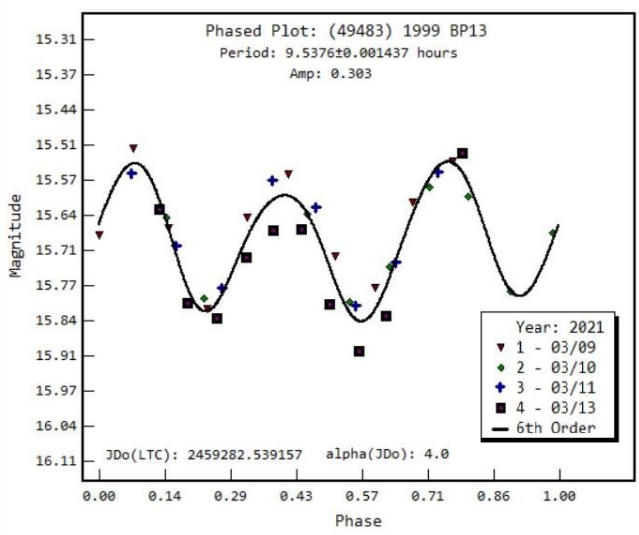

Acknowledgements

Funding was provided by the University of Wisconsin River Falls URSCA Undergraduate Stipends and Expenses (USE) Grant. The author would like to express his gratitude towards all those who helped in the learning process. This includes Dr. Matthew Vonk and Dr. Lowell McCann from the University of Wisconsin River Falls. This also includes the people from the Las Campanas Remote Observatory: Howard Hedlund, Andy Monson, Bryan Penprase, Michael Long, John E. Hoot, and Dave Jurasevich.

References

Dose, E.V. (2021). "Lightcurves of Fourteen Asteroids." *Minor Planet Bull.* **48**, 228-233.

Harris, A.W.; Young, J.W.; Scaltriti, F.; Zappala, V. (1984). "Lightcurves and phase relations of the asteroids 82 Alkmene and 444 Gyptis." *Icarus* **57**, 251-258.

JPL (2022). Small Body Data-Base Lookup. *https://ssd.jpl.nasa.gov/tools/sbdb_lookup.html#/*

Marchini, A.; Cavaglioni, L.; Privitera, C.A.; Papini, R.; Salvaggio, F. (2021). "Rotation Period Determination for Asteroids 2243 Lonnrot, (10859) 1995 GJ7, (18640) 1998 EF9 and (49483) 1999 BP13" *Minor Planet Bull.* **48**, 206-208.

Parrott, D. (2022). Tycho software, version 9.2. *https://www.tycho-tracker.com/*

Tonry, J.L.; Denneau, L.; Flewelling, H.; Heinze, A.N.; Onken, C.A.; Smartt, S.J.; Stalder, B.; Weiland, H.J.; Wolf, C. (2018). "The ATLAS All-Sky Stellar Reference Catalog." *Ap. J.* **867**, A105.

Warner, B.D.; Harris, A.W.; Pravec, P. (2009). "The Asteroid Lightcurve Database." *Icarus* **202**, 134-146. Updated 2021 Dec. *http://www.MinorPlanet.info/php/lcdb.php*

PHOTOMETRIC OBSERVATIONS AND ROTATION PERIODS OF ASTEROIDS 175 ANDROMACHE, 6569 ONDAATJE, AND 2006 NL. ROTATION PERIOD REVISION OF ASTEROID (7335) 1989 JA

Sergei Schmalz, Anastasia Schmalz, Viktor Voropaev Keldysh
Institute of Applied Mathematics of
Russian Academy of Sciences, Moscow, RUSSIA
sergiuspro77@gmail.com

Artyom Novichonok
Petrozavodsk State University, Petrozavodsk, RUSSIA

Alexandr Ivanov, Viktor Ivanov, Natalia Ivanova,
Anatoliy Barkov, Vadim Lysenko, Nikolay Yakovenko,
Nikita Gorbunov, German Kurbatov, Pavel Shchukin,
Kuban State University, Krasnodar, RUSSIA

Filippo Graziani, Riccardo di Roberto
GAUSS Srl, Rome, ITALY

(Received: 2022 October 15)

Photometric observations of asteroids 175 Andromache, 6569 Ondaatje, and 2006 NL were conducted in order to determine their synodic rotation period, the absolute brightness with its amplitude and estimate their diameter. For 175 Andromache we found P = 8.324 ± 0.004 h, H = 8.51 ± 0.05 mag, A = 0.40 ± 0.05 mag, D = 105.290 ± 1.170 km (for albedo a = 0.0631) and D = 86.265 ± 1.253 km (for albedo a = 0.094). For 6569 Ondaatje we found P = 5.954 ± 0.002 h, H = 16.44 ± 0.05 mag, A = 0.99 ± 0.05 mag, D = 1.770 ± 0.020 km (for albedo a = 0.15) and D = 1.533 ± 0.021 km (for albedo a = 0.20). For 2006 NL we found P = 6.503 ± 0.003 h, H = 19.65 ± 0.05 mag, A = 1.12 ± 0.05 mag, D = 0.404 ± 0.004 km (for albedo a = 0.15) and D = 0.350 ± 0.005 km (for albedo a = 0.20). We also revised our previously reported synodic rotation period of asteroid (7335) 1989 JA and determined it to be P = 2.588 ± 0.001 h.

We observed asteroids 175 Andromache, 6569 Ondaatje and 2006 NL in order to determine their synodic rotation period, the absolute brightness with its amplitude, and estimate their diameter. Observations took place at four observatories – Simeiz Observatory (MPC code 094) in Crimea, ISON-Kitab Observatory (MPC code 186) in Uzbekistan, Kuban State University Astrophysical Observatory (MPC code C40) in Russia, and ISON-Castelgrande Observatory (MPC code L28) in Italy.

For data processing we used the following software: *Tycho v.9.0.6* (Parrott, 2022) at C40; *APEX v.2021.01.4* (Kouprianov, 2008; Devyatkin et al., 2010) at L28; *Astrometrica v.4.11.1.442* (Raab, 2018) and *FoCAs v.3.66* (Roig et al., 2011) at 094 and 186. All images were calibrated with dark and flat-field frames. Photometry was done in the Gaia G band against reference stars from the Gaia DR3 catalog with near-solar color indices $(G_{BP} - G_{RP})$ = 0.818 ± 10% (Gaia Collaboration, 2022). For the calculation of the absolute brightness, we used a phase slope parameter G = 0.15. For the rotation period search we used a custom-written Python script with the PDM algorithm imported from the *PyAstronomy* package (Czesla et al., 2019); the underlying orbital data was retrieved from the NASA JPL Horizons System (JPL, 2022a) by the imported *Astroquery* package (Ginsburg et al., 2019).

For the conversion from Gaia G to Johnson-Cousins V band we used the transformation:

$$G - V = -0.02704 + 0.01424(G_{BP} - G_{RP}) - 0.2156(G_{BP} - G_{RP})^2 + 0.01426(G_{BP} - G_{RP})^3$$

where: G is Gaia G magnitude, V is Johnson-Cousins V magnitude, and $(G_{BP} - G_{RP})$ is Gaia BP-RP color index (ESA, 2022).

For the estimation of the asteroid diameter, we used the formula:

$$D = 10^{(3.1236 - 0.5\log(\alpha) - 0.2H)}$$

where D is asteroid diameter in km, α is the geometric albedo of the asteroid, and H is the absolute brightness of asteroid in Johnson-Cousins V magnitudes (JPL, 2022b).

Table I shows the observing circumstances and results.

175 Andromache was discovered on 1877 October 1 by J.C. Watson at Ann Arbor (Leuschner, 1936). It is a main-belt asteroid with a semi-major axis of a = 3.18 au, eccentricity e = 0.23, inclination i = 3.22°, and an orbital period of P = 5.68 years; its absolute magnitude has a value of H = 8.63 (MPC, 2022a), other reported values range from H = 8.06 (Warner, 2007) to H = 8.52 (Nugent et al., 2016). In the Asteroid Lightcurve Database (Warner et al., 2009), we found seven reported rotation periods for asteroid 175 Andromache: 7.109 h (Blanco et al., 2000), 7.102 ± 0.001 h (Warner et al., 2009), 8.326 ± 0.001 h (Warner et al., 2009), 8.324 ± 0.004 h (Warner et al., 2009), 8.3296 ± 0.0002 h (Warner et al., 2009), 8.325 ± 0.007 h (Warner et al., 2009), and 8.32801 ± 0.00002 h (Ďurech et al., 2020).

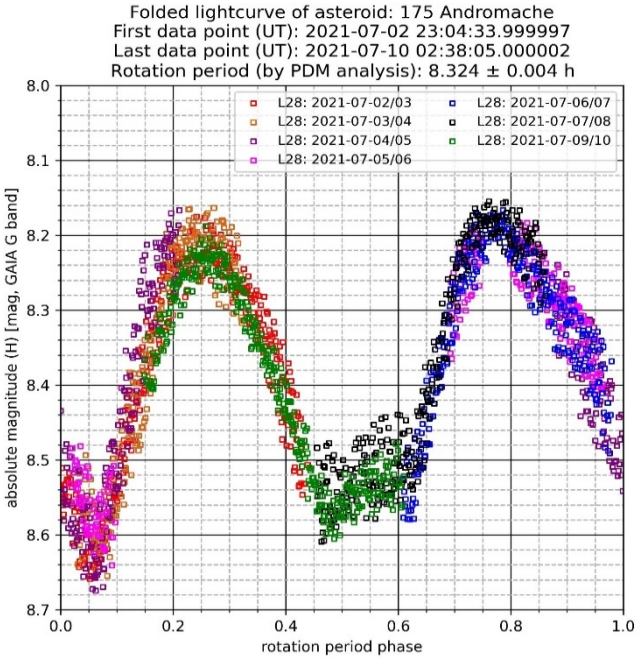

CCD photometric observations of asteroid 175 Andromache were carried out on seven nights in 2021 July 2-9 at one observatory – L28. We used a 0.22-m *f*/2.38 Newton-Hamilton telescope with a FLI PL 16803 CCD camera without filters at 1×1 binning, giving 3.54 arcsec/pix pixel scale, and 30 s exposure times during the nights 2021 July 2-9. In the course of the entire observation

campaign, the phase angle of 175 Andromache changed from 21.4° to 20.0°. For the analysis we collected 2105 usable data points.

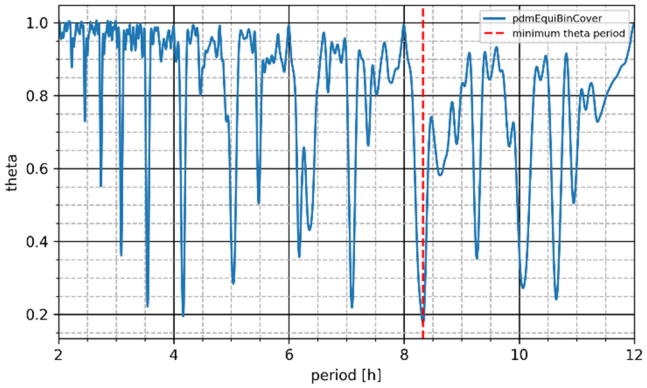

We found a synodic rotation period P = 8.324 ± 0.004 h, median absolute brightness H = 8.51 ± 0.05 mag in Johnson-Cousins V band, and brightness amplitude of the folded lightcurve A = 0.40 ± 0.05 mag. For albedo a = 0.0631 we estimated asteroid diameter D = 105.290 ± 1.170 km; using an albedo α = 0.094, we estimated asteroid diameter D = 86.265 ± 1.253 km. The PDM power spectrum covers a rotation period range between 2 and 12 hours with a red dashed line indicating the best probable rotation period corresponding to the one we found; other potential solutions either produced monomodal folded lightcurves, or didn't produce well-fitted folded lightcurves.

6569 Ondaatje was discovered on 1993 June 22 by J.E. Mueller; it was named in honor of Michael Ondaatje, a Canadian novelist, poet and writer, best known for his novel *The English Patient* (MPC, 2006a). It is a near-Earth asteroid of the Amor family with a semi-major axis of a = 1.63 au, eccentricity e = 0.22, inclination i = 22.64°, and an orbital period of P = 2.07 years; its absolute magnitude is H = 16.68 (MPC, 2022b). Other reported values are: H = 16.2 (Pravec et al., 1996), H = 16.443 ± 0.006 (Waszczak et al., 2015), and H = 16.00 (Carry et al., 2016). In the Asteroid Lightcurve Database (Warner et al., 2009), we found three reported rotation periods for asteroid 6569 Ondaatje: 5.959 h (Pravec et al., 1996), 5.916 ± 0.0052 h (Waszczak et al., 2015), and 5.295 ± 0.001 h (Warner and Stephens, 2020); also, a period of 5.96 ± 0.01 h has been reported by (Warner and Stephens, 2022).

CCD photometric observations of asteroid 6569 Ondaatje were carried out on five nights in 2020 June 27 to July 1 at two observatories, 186 and C40. At 186 we used a 0.36-m *f*/8 Ritchey-Chrétien telescope with a FLI ML 09000 CCD camera without filters at 2×2 binning, giving 1.72 arcsec/pix pixel scale, and 60-s exposure times during the nights 2020 June 28, 30 and July 1; at C40 we used a 0.51-m *f*/7.93 Ritchey-Chrétien telescope with a FLI PL 16803 CCD camera without filters at 3×3 binning, giving 1.37 arcsec/pix pixel scale, and 60-s exposure times during the nights 2020 June 27-30 and July 1. In the course of the entire observation campaign, the phase angle of 6569 Ondaatje changed from 26.6° to 21.4°. For the analysis we collected 722 usable data points.

We found a synodic rotation period P = 5.954 ± 0.002 h, median absolute brightness H = 16.44 ± 0.05 mag in Johnson-Cousins V band, and brightness amplitude of the folded lightcurve A = 0.99 ± 0.05 mag. For albedo a = 0.15, we estimated asteroid diameter D = 1.770 ± 0.020 km; for the albedo a = 0.20. we estimated asteroid diameter D = 1.533 ± 0.021 km. The next figures show the folded lightcurve of asteroid 6569 Ondaatje and the PDM power spectrum in a rotation period range between 2 and 12 hours with a red dashed line indicating the best probable rotation period at 2.977 h, which produced a monomodal folded lightcurve. However, the second-best probable rotation period at 5.954 h is the one that we consider the real rotation period; other potential solutions didn't produce well-fitted folded lightcurves.

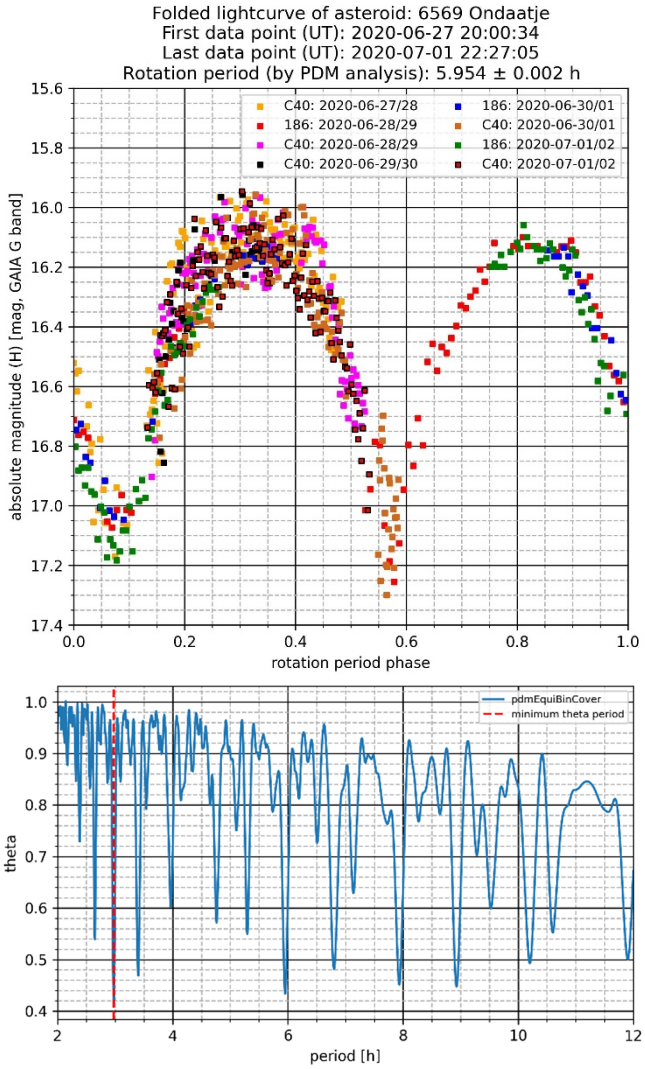

2006 NL was first observed on 2006 July 2 at the Lincoln Laboratory ETS, New Mexico (MPC, 2006b). It is a near-Earth asteroid of the Aten family with a semi-major axis of a = 0.85 au, eccentricity e = 0.58, inclination i = 20.09°, and an orbital period of P = 0.78 years; its absolute magnitude has a value of H = 19.97 (MPC, 2022c). In the Asteroid Lightcurve Database (Warner et al., 2009) we found three reported rotation periods for asteroid 2006 NL: 6.50 ± 0.02 h, 6.44 ± 0.05 h, and 6.503 ± 0.001 h (Warner and Stephens, 2021).

CCD photometric observations of asteroid 2006 NL were carried out on four nights in 2020 July 9-14 at two observatories, 094 and 186. At 094 we used a 1-m *f*/12.7 Cassegrain telescope with a FLI ML 09000 CCD camera without filters at 3×3 binning, giving 0.58 arcsec/pix pixel scale, and 15-s exposure times during the night 2020 July 9; at 186 we used a 0.36-m *f*/8 Ritchey-Chrétien telescope with a FLI PL 09000 CCD camera without filters at 2×2 binning, giving 1.72 arcsec/pix pixel scale, and 30-s exposure times during the nights 2020 July 12-14. In the course of the entire observation

campaign, the phase angle of 2006 NL changed from 56.8° to 30.8°. For the analysis we collected 1791 usable data points.

We found a synodic rotation period P = 6.503 ± 0.003 h, median absolute brightness H = 19.65 ± 0.05 mag in Johnson-Cousins V band, and brightness amplitude of the folded lightcurve A = 1.12 ± 0.05 mag. For albedo a = 0.15 we estimated asteroid diameter D = 0.404 ± 0.004 km; for the albedo a = 0.20, we estimated asteroid diameter D = 0.350 ± 0.005 km. The next figures show the folded lightcurve of asteroid 2006 NL and the PDM power spectrum in a rotation period range between 2 and 12 hours, with a red dashed line indicating the best probable rotation period at 3.251 h, which produced a monomodal folded light curve. However; the second-best probable rotation period at 6.503 h is the one that we consider the real rotation period; other potential solutions didn't produce a well-fitted folded lightcurve.

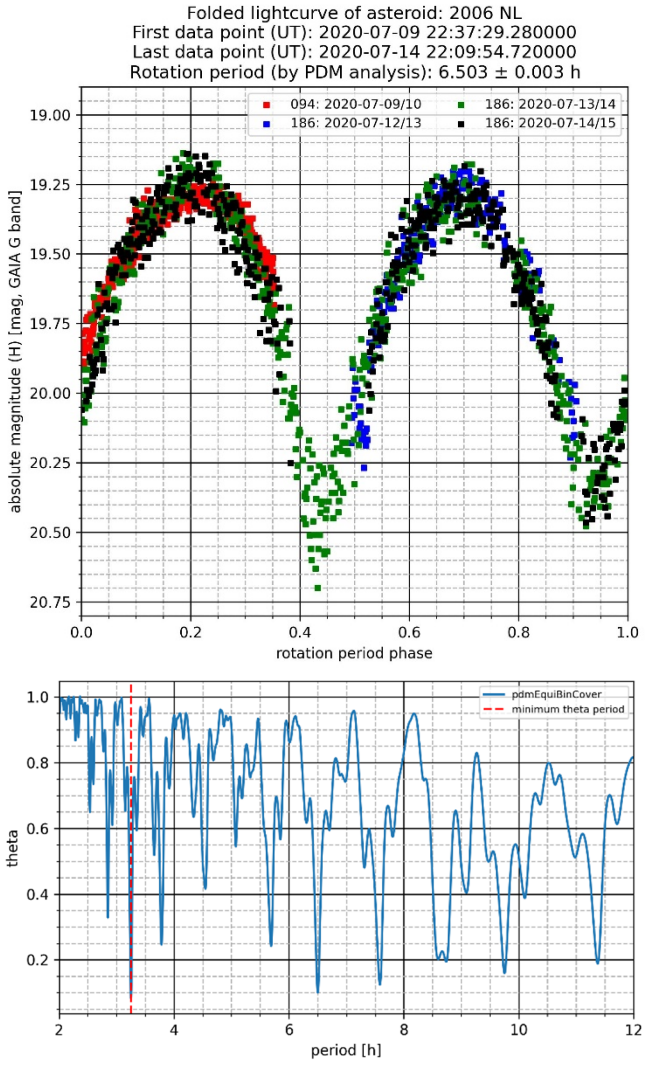

(7335) 1989 JA. In (Schmalz et al., 2022), we reported a synodic rotation period of P = 5.177 ± 0.005 h, indicating also a second-best probable solution with a rotation period of 2.589 h; This didn't produce a well-fitted folded lightcurve and, thus, was excluded as a possible solution. In our analysis we forgot the fact that (7335) 1989 JA was found to be a binary asteroid (Benner, 2022); hence we were getting a slightly changing brightness amplitude, which caused the misfit in the folded lightcurve. After considering the binary nature of asteroid with a 10-day long observational campaign and revising its analysis, we determine a synodic rotation period of P = 2.588 ± 0.001 h as the correct solution. Similar solutions have been reported: P = 2.590 ± 0.002 h (Loera-González et al., 2022) and P = 2.588 ± 0.001 h (Franco et al., 2022). The next figure shows the folded lightcurve of asteroid (7335) 1989 JA.

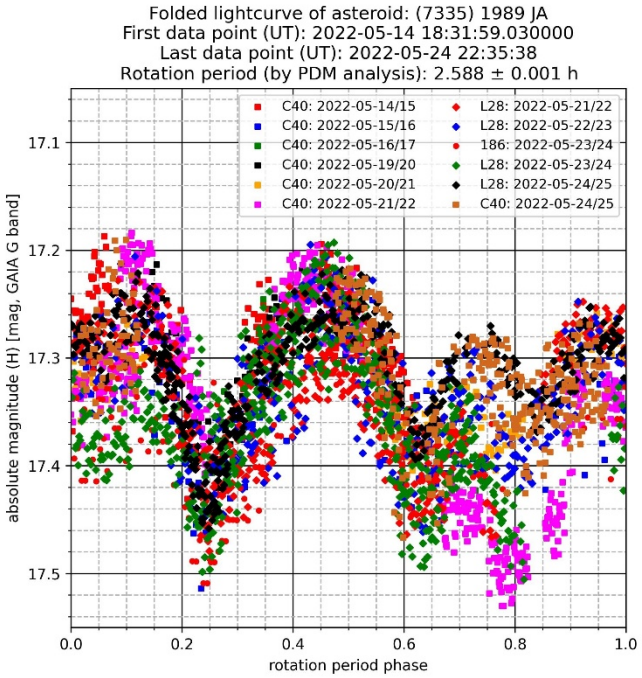

References

Benner, L.A.M. (2022). "Goldstone Radar Observations Planning: (7335) 1989 JA, 388945 2008 TZ3, and 467460 2006 JF42." *https://echo.jpl.nasa.gov/asteroids/1989JA/1989JA.2022.goldstone.planning.html*

Blanco, C.; Di Martino, M.; Riccioli, D. (2000). "New rotational periods of 18 asteroids." *Planetary and Space Science* **48**, 271-284.

Carry, B.; Solano, E.; Eggl, S.; DeMeo, F.E. (2016). "Spectral properties of near-Earth and Mars-crossing asteroids using Sloan photometry." *Icarus* **268**, 340-354.

Czesla, S.; Schröter, S.; Schneider, C.P.; Huber, K.F.; Pfeifer, F.; Andreasen, D.T.; Zechmeister, M. (2019). "PyA: Python astronomy-related packages." Astrophysics Source Code Library, record ascl:1906.010. *https://github.com/sczesla/PyAstronomy*

Devyatkin, A.V.; Gorshanov, D.L.; Kouprianov, V.V.; Verestchagina, I.A. (2010). "Apex I and Apex II software packages for the reduction of astronomical CCD observations." *Solar System Research* **44**, 68-80.

Ďurech, J.; Tonry, J.; Erasmus, N.; Denneau, L.; Heinze, A.N.; Flewelling, H.; Vančo, R. (2020). "Asteroid models reconstructed from ATLAS photometry." *Astronomy & Astrophysics* **643**, A59.

ESA (2022). "5.5.1 Relationships with other photometric systems." Gaia Data Release 3. Documentation Release 1.1. *https://gea.esac.esa.int/archive/documentation/GDR3/Data_processing/chap_cu5pho/cu5pho_sec_photSystem/cu5pho_ssec_photRelations.html*

Number	Name	20yy/mm/dd	Phase	L_{PAB}	B_{PAB}	Period(h)	P.E.	Amp	A.E.	D	Grp
175	Andromache	21/07/02-21/07/09	21.4,20.0	333	-3	8.324	0.004	0.40	0.05	105.290 86.265	MBA
6569	Ondaatje	20/06/27-20/07/01	26.6,21.4	294	9	5.954	0.002	0.99	0.05	1.770 1.533	NEA
7335	1989 JA	22/05/14-22/05/24	26.9,35.1	227	11	2.588	0.001	0.27	0.05	0.849 0.748	NEA
	2006 NL	20/07/09-20/07/14	56.8,30.8	283	22	6.503	0.003	1.12	0.05	0.404 0.350	NEA

Table I. Observing circumstances and results. The phase angle is given for the first and last exposure time. L_{PAB} and B_{PAB} are the approximate phase angle bisector longitude/latitude at mid-date range (see Harris et al., 1984). Grp is the asteroid family/group (Warner et al., 2009).

Franco, L.; Marchini, A.; Papini, R.; Bacci, P.; Maestripieri, M.; Ruocco, N.; Scarfi, G.; Iozzi, M.; Montigiani, M.; Mannucci, M.; Baj, G.; Valvasori, A.; Guido, E.; Galli, G.; Buzzi, L. (2022). "Collaborative asteroids photometry from UAI: 2022 April-June." *The Minor Planet Bulletin* **49**, 342-346.

Gaia Collaboration: Creevey O.L.; Sarro L.M.; Lobel A.; and 444 colleagues. (2022). "Gaia Data Release 3: A Golden Sample of Astrophysical Parameters." *Astronomy & Astrophysics* (accepted). *https://arxiv.org/abs/2206.05870*

Ginsburg, A.; Sipöcz, B.M.; Brasseur, C.E.; and 22 colleagues. "astroquery: An Astronomical Web-querying Package in Python." *The Astronomical Journal* **157**, A98.

Harris, A.W.; Young, J.W.; Scaltriti, F.; Zappala, V. (1984). "Lightcurves and phase relations of the asteroids 82 Alkmene and 444 Gyptis." *Icarus* **57**, 251-258.

JPL (2022a). Horizons. *https://ssd.jpl.nasa.gov/horizons/*

JPL (2022b). Asteroid Size Estimator. *https://cneos.jpl.nasa.gov/tools/ast_size_est.html*

Kouprianov, V. (2008). "Distinguishing features of CCD astrometry of faint GEO objects." *Advances in Space Research* **41**, 1029-1038.

Leuschner, A.O. (1936). "The Story of Andromache, an Unruly Planet." *Publications of the Astronomical Society of the Pacific* **48**, 55-81.

Loera-González, P.A.; Olguín, L.; Saucedo, J.C.; Contreras, M.E.; Nuñez-López, R.; Domínguez-González, R.; Angulo, O.E.; Chapetti, S.D.; Córdova, D.E.; Cortez, R.A.; Ramírez, M.A.; Vázquez, P.S. (2022). "Rotation periods for asteroids from Carl Sagan Observatory: 2021 November - 2022 May." *The Minor Planet Bulletin* **49**, 289-290.

MPC (2006a). *Minor Planet Circular*. **56958**. *https://minorplanetcenter.net/iau/ECS/MPCArchive/2006/MPC_20060613.pdf*

MPC (2006b). *Minor Planets and Comets Supplement*. **174738**. *https://minorplanetcenter.net/iau/ECS/MPCArchive/2006/MPS_20060711.pdf*

MPC (2022a). Orbits Database. *https://minorplanetcenter.net/db_search/show_object?object_id=175*

MPC (2022b). Orbits Database. *https://minorplanetcenter.net/db_search/show_object?object_id=6569*

MPC (2022c). Orbits Database. *https://minorplanetcenter.net/db_search/show_object?object_id=2006+NL*

Nugent, C.R.; Mainzer, A.; Bauer, J.; Cutri, R.M.; Kramer, E.A.; Grav, T.; Masiero, J.; Sonnett, S.; Wright, E.L. (2016). "NEOWISE Reactivation Mission Year Two: Asteroid Diameters and Albedos." *The Astronomical Journal* **152**, 63.

Parrott, D. (2022). Tycho software. *https://www.tycho-tracker.com*

Pravec, P.; Šarounová, L.; Wolf, M. (1996). "Lightcurves of 7 Near-Earth Asteroids." *Icarus* **124**, 471-482.

Raab, H. (2018) Astrometrica software. *http://www.astrometrica.at*

Roig, J.C.; Nogues, R.N.; Lorenz, E.S.; Gonzalez, J.L.S. (2011). *Fotometrica Con Astrometrica*, a Software Tool. *http://www.astrosurf.com/cometas-obs*

Schmalz, S.; Schmalz, A.; Voropaev, V.; and 18 colleagues. (2022). "Photometric observations and rotation periods of asteroids 2376 Martynov, (7335) 1989 JA, 12923 Zephyr, and (85184) 1991 JG1." *Minor Planet Bulletin* **49**, 291-295.

Warner, B.D. (2007). "Initial Results of a Dedicated H-G Project." *Minor Planet Bulletin* **34**, 113-119.

Warner, B.D.; Harris, A.W.; Pravec, P. (2009). "The Asteroid Lightcurve Database." *Icarus* **202**, 134-146. Updated 2022 Jul. *http://www.minorplanet.info/lightcurvedatabase.html*

Warner, B.D.; Stephens, R.D. (2020). "Near-Earth Asteroid Lightcurve Analysis at the Center for Solar System Studies: 2020 April - June." *Minor Planet Bulletin* **47**, 290-304.

Warner, B.D.; Stephens, R.D. (2021). "Near-Earth Asteroid Lightcurve Analysis at the Center for Solar System Studies: 2020 July - September." *Minor Planet Bulletin* **48**, 30-39.

Warner, B.D.; Stephens, R.D. (2022). "Near-Earth Asteroid Lightcurve Analysis at the Center for Solar System Studies: 2022 March - June." *The Minor Planet Bulletin* **49**, 274-279.

Waszczak, A.; Chang, C.-K.; Ofek, E.O.; Laher, R.; Masci, F.; Levitan, D.; Surace, J.; Cheng, Y.-C.; Ip, W.-H.; Kinoshita, D.; Helou, G.; Prince, T.A.; Kulkarni, S. (2015). "Asteroid Light Curves from the Palomar Transient Factory Survey: Rotation Periods and Phase Functions from Sparse Photometry." *Astron. J.* **150**, A75.

COLLABORATIVE ASTEROID PHOTOMETRY FROM UAI: 2022 JULY-SEPTEMBER

Lorenzo Franco
Balzaretto Observatory (A81), Rome, ITALY
lor_franco@libero.it

Marco Iozzi
HOB Astronomical Observatory (L63),
Capraia Fiorentina, ITALY

Giulio Scarfi
Iota Scorpii Observatory (K78), La Spezia, ITALY

Fabio Mortari, Davide Gabellini
Hypatia Observatory (L62), Rimini, ITALY

Nello Ruocco
Osservatorio Astronomico Nastro Verde (C82), Sorrento, ITALY

Paolo Fini, Guido Betti
Blessed Hermann Observatory (L73), Impruneta, ITALY

Alessandro Marchini
Astronomical Observatory, DSFTA - University of Siena (K54)
Via Roma 56, 53100 - Siena, ITALY

Pietro Aceti, Massimo Banfi
Seveso Observatory (C24), Seveso, ITALY

Giorgio Baj
M57 Observatory (K38), Saltrio, ITALY

Paolo Bacci, Martina Maestripieri
GAMP - San Marcello Pistoiese (104), Pistoia, ITALY

Mauro Bachini, Giacomo Succi
BSCR Observatory (K47), Santa Maria a Monte (PI), ITALY

Alessandro Coffano, Wladimiro Marinello
Osservatorio Serafino Zani (130), Lumezzane (BS), ITALY

Gianni Galli
GiaGa Observatory (203), Pogliano Milanese, ITALY

Nico Montigiani, Massimiliano Mannucci
Osservatorio Astronomico Margherita Hack (A57)
Florence, ITALY

(Received: 2022 October 13)

Photometric observations of six asteroids were made in order to acquire lightcurves for shape/spin axis modeling. The synodic period and lightcurve amplitude were found for 78 Diana, 198 Ampella, 895 Helio, 1060 Magnolia, 1543 Bourgeois, 1806 Derice. We also found color indices for 78 Diana, 198 Ampella, 895 Helio, 1060 Magnolia and H-G parameters for 198 Ampella.

Collaborative asteroid photometry was done inside the Italian Amateur Astronomers Union (UAI; 2022) group. The targets were selected mainly in order to acquire lightcurves for shape/spin axis modeling. Table I shows the observing circumstances and results.

The CCD observations of six asteroids were made in 2022 July-September using the instrumentation described in the Table II. Lightcurve analysis was performed at the Balzaretto Observatory with *MPO Canopus* (Warner, 2021). All the images were calibrated with dark and flat frames and converted to standard magnitudes using solar colored field stars from CMC15 and ATLAS catalogues, distributed with MPO Canopus. For brevity, the following citations to the asteroid lightcurve database (LCDB; Warner et al., 2009) will be summarized only as "LCDB".

78 Diana is a Ch-type (Bus & Binzel, 2002) middle main-belt asteroid. Collaborative observations were made over three nights. The period analysis shows a synodic period of P = 7.292 ± 0.003 h with an amplitude A = 0.10 ± 0.04 mag. The period is close to the previously published results in the LCDB. Multiband photometry was made by M. Scarfi (K78) on 2022 September 20. We found the color index (V-R) = 0.35 ± 0.04, consistent with a C-type asteroid (Shevchenko and Lupishko, 1998).

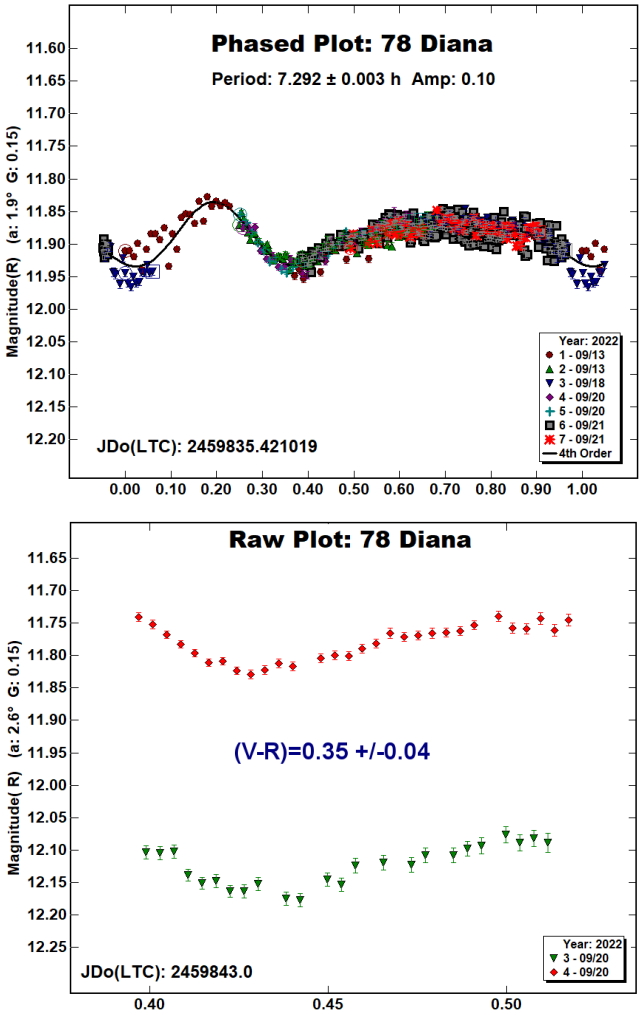

198 Ampella is an S-type (Bus & Binzel, 2002) inner main-belt asteroid. Collaborative observations were made over eleven nights. The period analysis shows a synodic period of P = 10.381 ± 0.001 h with an amplitude A = 0.07 ± 0.02 mag. The period is close to the previously published results in the LCDB. Multiband photometry was made by G. Baj (K38) on 2022 August 1. We found the color index (V-R) = 0.47 ± 0.03. The wide phase angles covered by the observations allowed us to determine the H-G parameters. The R band magnitudes were converted to V band adding the color index (V-R) and evaluating the half peak to peak magnitude using a Fourier model of the same order of the lightcurve plot (Buchheim, 2010). We found H = 8.61 ± 0.06 and G = 0.27 ± 0.06. Both the color index (V-R) and G value are close to an S-type asteroid (Shevchenko and Lupishko, 1998).

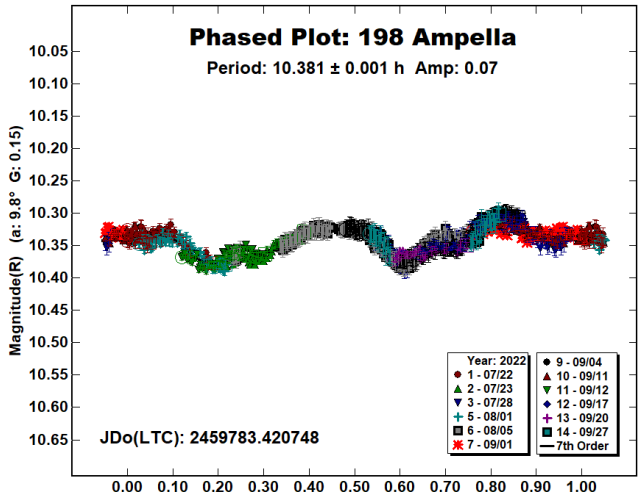

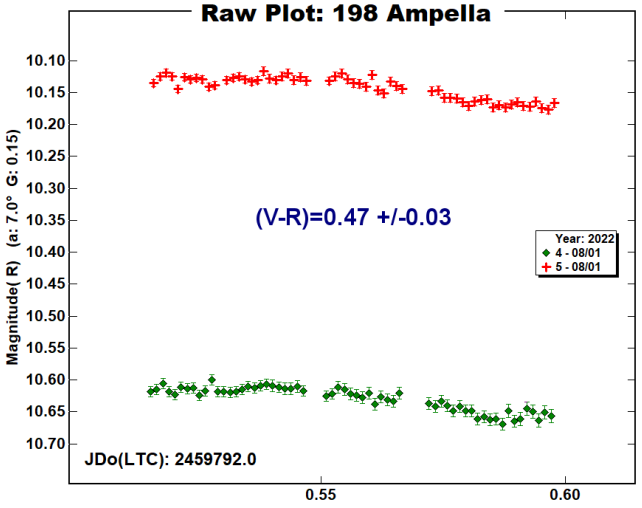

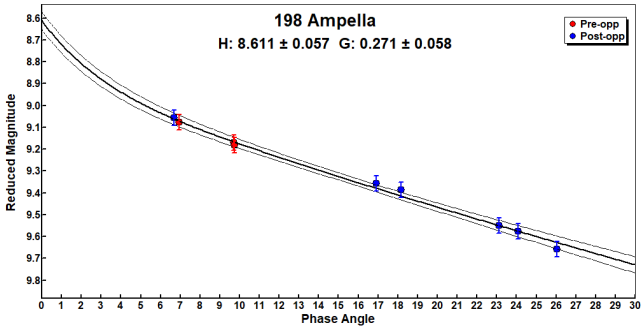

895 Helio is a B-type (Bus & Binzel, 2002) outer main-belt asteroid. Collaborative observations were made over eight nights. The period analysis shows a synodic period of P = 9.394 ± 0.001 h with an amplitude A = 0.09 ± 0.02 mag. The period is close to the previously published results in the LCDB. Multiband photometry was made by P. Bacci and M. Maestripieri (104) on 2022 August 1. We found color indices (B-V) = 0.66 ± 0.06; (V-R) = 0.37 ± 0.06, consistent with a low albedo asteroid (Shevchenko and Lupishko, 1998).

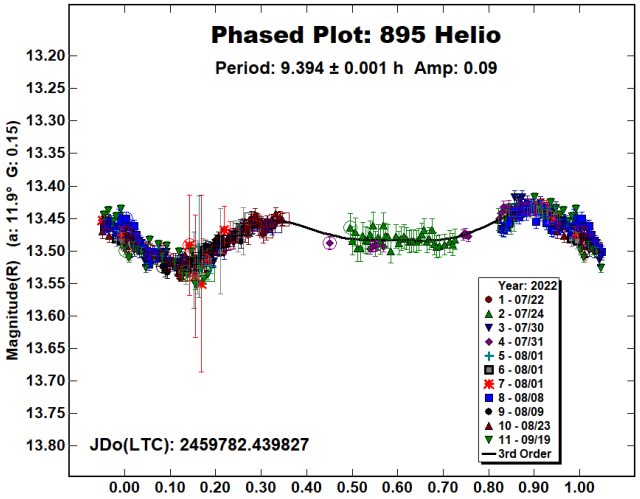

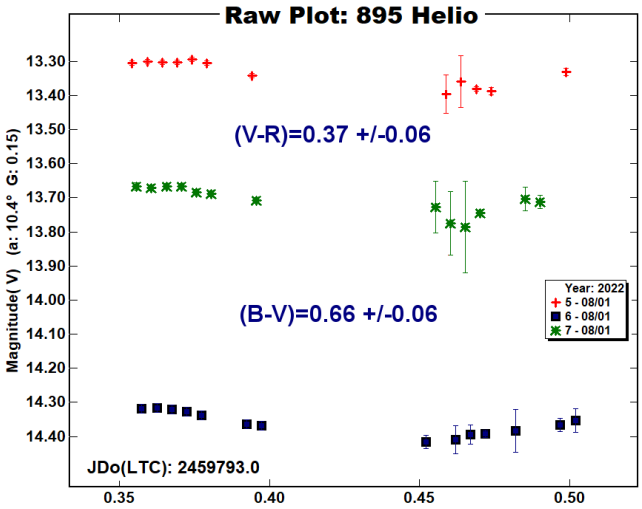

1060 Magnolia is a medium albedo inner main-belt asteroid. Collaborative observations were made over nine nights. We found a synodic period of P = 2.9116 ± 0.0004 h with an amplitude A = 0.06 ± 0.02 mag. The period is close to the previously published results in the LCDB. Multiband photometry was made by P. Bacci and M. Maestripieri (104) on 2022 August 1 and by M. Iozzi (L63) on 2022 August 13. We found color indices (B-V) = 0.87 ± 0.02; (V-R) = 0.49 ± 0.02, consistent with a medium albedo asteroid (Shevchenko and Lupishko, 1998).

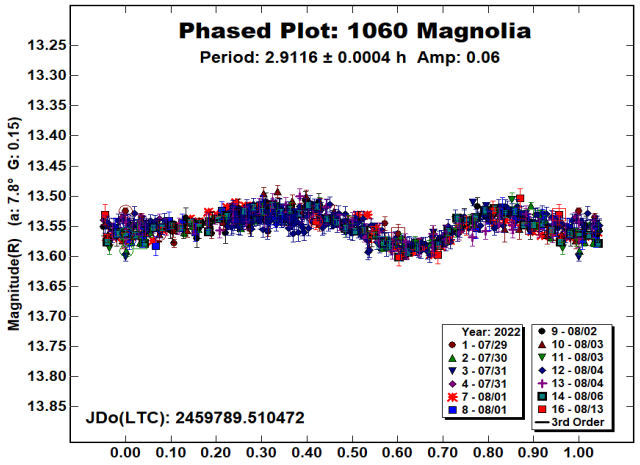

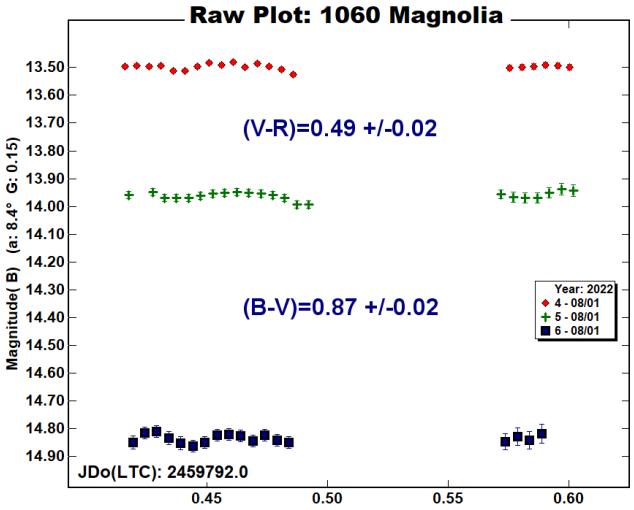

1543 Bourgeois is a medium albedo middle main-belt asteroid. Collaborative observations were made over ten nights. The period spectrum shows two solutions close to 18 and 36 hours. The split halves plot shows that the two halves are almost identical for the period of 35.6 h, so we prefer the monomodal solution of $P = 17.8 \pm 0.1$ h with an amplitude $A = 0.07 \pm 0.03$ mag. The period is quite different from the one reported on LCDB of 2.48 h.

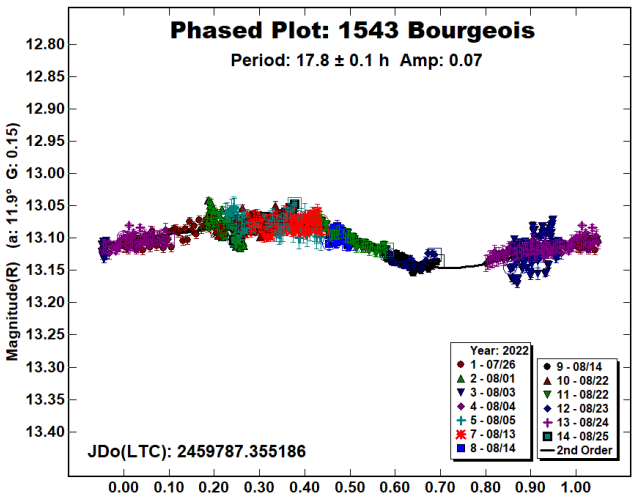

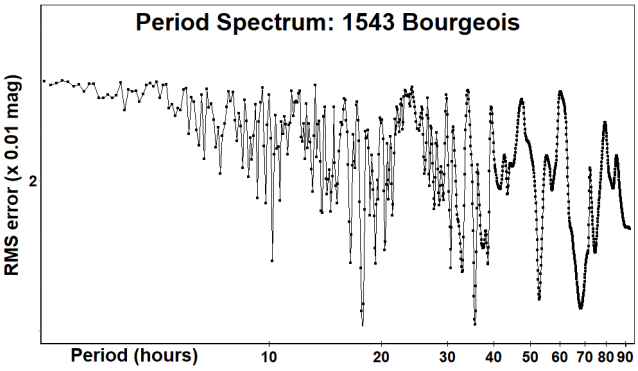

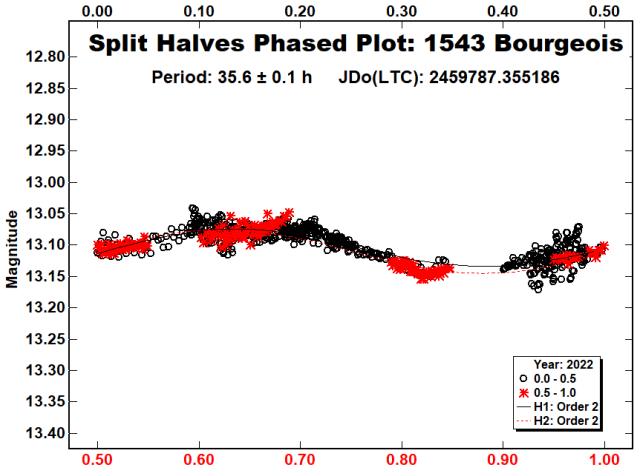

1806 Derice is a low albedo inner main-belt asteroid. Collaborative observations were made over five nights. We found a synodic period of $P = 3.223 \pm 0.001$ h with an amplitude $A = 0.12 \pm 0.03$ mag. The period is close to the previously published results in the LCDB.

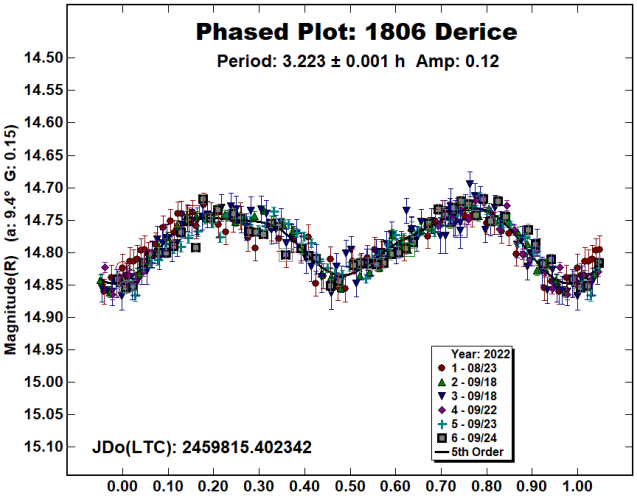

References

Buchheim, R.K. (2010). "Methods and Lessons Learned Determining the H-G Parameters of Asteroid Phase Curves." *Society for Astronomical Sciences Annual Symposium* **29**, 101-115.

Bus, S.J.; Binzel, R.P. (2002). "Phase II of the Small Main-Belt Asteroid Spectroscopic Survey - A Feature-Based Taxonomy." *Icarus* **158**, 146-177.

Harris, A.W.; Young, J.W.; Scaltriti, F.; Zappala, V. (1984). "Lightcurves and phase relations of the asteroids 82 Alkmene and 444 Gyptis." *Icarus* **57**, 251-258.

Shevchenko, V.G.; Lupishko, D.F. (1998). "Optical properties of Asteroids from Photometric Data." *Solar System Research*, **32**, 220-232.

Number	Name	2022 mm/dd	Phase	L_{PAB}	B_{PAB}	Period(h)	P.E.	Amp	A.E.	Grp
78	Diana	09/13-09/21	*1.7,2.9	353	4	7.292	0.003	0.10	0.04	MB-M
198	Ampella	07/22-09/27	*9.7,26.0	315	11	10.381	0.001	0.07	0.02	MB-I
895	Helio	07/22-09/19	*11.7,12.9	326	28	9.394	0.001	0.09	0.02	MB-O
1060	Magnolia	07/29-08/13	7.9,13.7	304	10	2.9116	0.0004	0.06	0.02	MB-I
1543	Bourgeois	07/26-08/25	*11.8,11.7	319	9	17.8	0.1	0.07	0.03	MB-M
1806	Derice	08/23-09/24	*9.4,8.0	348	5	3.223	0.001	0.12	0.03	MB-I

Table I. Observing circumstances and results. The first line gives the results for the primary of a binary system. The second line gives the orbital period of the satellite and the maximum attenuation. The phase angle is given for the first and last date. If preceded by an asterisk, the phase angle reached an extrema during the period. L_{PAB} and B_{PAB} are the approximate phase angle bisector longitude/latitude at mid-date range (see Harris et al., 1984). Grp is the asteroid family/group (Warner et al., 2009).

Observatory (MPC code)	Telescope	CCD	Filter	Observed Asteroids (#Sessions)
HOB Astronomical Observatory (L63)	0.20-m SCT f/6.0	ATIK 383L+	C,V, Rc	78(3),198(5),1060(3), 1543(4)
Iota Scorpii(K78)	0.40-m RCT f/8.0	SBIG STXL-6303e (bin 2x2)	V,Rc	78(1),895(4),1543(2), 1806(2)
Hypatia Observatory (L62)	0.25-m RCT f/5.3	MORAVIAN C2-7000A	Rc	198(5),1060(3)
Osservatorio Astronomico Nastro Verde (C82)	0.35-m SCT f/6.3	SBIG ST10XME (bin 2x2)	C	1060(2),1543(1),1806(3)
Blessed Hermann Observatory (L73)	0.30-m SCT f/6.0	QHY 174MGPS (bin 2x2)	Rc	78(1),1543(2)
Astronomical Observatory of the University of Siena(K54)	0.30-m MCT f/5.6	SBIG STL-6303e(bin 2x2)	Rc	1060(2),1543(1)
Seveso Observatory (C24)	0.30-m SCT f/10.0	MORAVIAN KAF 8300 (bin 3x3)	Rc	78(1),895(1)
M57 (K38)	0.35-m RCT f/5.5	SBIG STT1603ME	V,Rc	198(1),895(1)
GAMP (104)	0.60-m NRT f/4.0	Apogee Alta	B,V, Rc	895(1),1060(1)
BSCR Observatory (K47)	0.41-m NRT f/3.2	DTA Discovery 1600	C	895(1),1543(1)
Osservatorio Serafino Zani (130)	0.40-m RCT f/5.8	SBIG ST8 XME (bin 2x2)	C	1060(1)
GiaGa Observatory (203)	0.36-m SCT f/5.8	MORAVIAN G2-3200	Rc	1543(1)
Osservatorio Astronomico Margherita Hack (A57)	0.35-m SCT f/8.3	SBIG ST10XME (bin 2x2)	Rc	1806(1)

UAI (2022). “Unione Astrofili Italiani” web site. *https://www.uai.it*

Warner, B.D.; Harris, A.W.; Pravec, P. (2009) “The asteroid lightcurve database.” *Icarus* **202**, 134-146. Updated 2022 Oct. *https://minplanobs.org/alcdef/index.php*

Warner, B.D. (2021). MPO Software, MPO Canopus v10.8.5.0. Bdw Publishing. *http://minorplanetobserver.com*

ASTEROID PHOTOMETRY AND LIGHTCURVE

Milagros Colazo
Instituto de Astronomía Teórica y Experimental (IATE-CONICET), Argentina
Facultad de Matemática, Astronomía y Física, Universidad Nacional de Córdoba, Argentina
Grupo de Observadores de Rotaciones de Asteroides (GORA), Argentina, *https://aoacm.com.ar/gora/index.php*
milirita.colazovinovo@gmail.com

Damián Scotta, Raúl Melia, Giuseppe Ciancia, César Fornari, Mario Morales, Bruno Monteleone, Aldo Wilberger, Francisco Santos, Alberto García, Néstor Suárez, Ezequiel Bellocchio, Andrés Chapman, Ricardo Nolte, Matías Martini, Aldo Mottino, Carlos Colazo.

Grupo de Observadores de Rotaciones de Asteroides (GORA), Argentina

Observatorio Astronómico Giordano Bruno (MPC G05) - Piconcillo (Córdoba-España)

Observatorio Astronómico El Gato Gris (MPC I19) - Tanti (Córdoba-Argentina)

Observatorio Cruz del Sur (MPC I39) - San Justo (Buenos Aires-Argentina)

Observatorio de Sencelles (MPC K14) - Sencelles (Mallorca-Islas Baleares-España)

Osservatorio Astronomico "La Macchina del Tempo" (MPC M24) - Ardore Marina (Reggio Calabria-Italia)

Observatorio Los Cabezones (MPC X12) - Santa Rosa (La Pampa-Argentina)

Observatorio Galileo Galilei (MPC X31) - Oro Verde (Entre Ríos-Argentina)

Observatorio Antares (MPC X39) - Pilar (Buenos Aires-Argentina)

Observatorio Río Cofio (MPC Z03) - Robledo de Chavela (Madrid-España)

Observatorio AstroPilar (GORA APB) - Pilar (Buenos Aires-Argentina)

Specola "Giuseppe Pustorino 3" (GORA GC3) - Palizzi Marina (Reggio Calabria-Italia)

Observatorio Astronómico Aficionado Omega (GORA OAO) - Córdoba (Córdoba-Argentina)

Observatorio de Damián Scotta 1 (GORA ODS) - San Carlos Centro (Santa Fe-Argentina)

Observatorio Ricardo Nolte (GORA ORN) - Córdoba (Córdoba-Argentina)

Observatorio de Raúl Melia (GORA RMG) - Gálvez (Santa Fe-Argentina)

(Received: 2022 October 7 Revised: 2022 November 6)

Synodic rotation periods and amplitudes are reported for: 786 Bredichina, 795 Fini, 892 Seeligeria, 1343 Nicole, 2717 Tellervo, 3224 Irkutsk.

The presented periods and amplitudes of asteroid light curves are the product of collaborative work by GORA (Grupo de Observadores de Rotaciones de Asteroides) group. In all the studies we have applied relative photometry assigning V magnitudes to the calibration stars.

The image acquisition was performed without filters and with exposure times of a few minutes. All images used were corrected using dark frames and, in some cases, bias and flat-field were also used. Photometry measurements were performed using *FotoDif* software and for the analysis, we employed *Periodos* software (Mazzone, 2012).

Below, we present the results for each asteroid under study. The light curve figures contain the following information: the estimated period and period error and the estimated amplitude and amplitude error. In the reference boxes, the columns represent, respectively, the marker, observatory MPC code, or - failing that - the GORA internal code, session date, session offset, and several data points.

Targets were selected based on the following criteria: 1) those asteroids with magnitudes accessible to the equipment of all participants, 2) those with favorable observation conditions from Argentina or Spain and Italy, *i.e.*, with negative or positive declinations δ, respectively, and 3) objects with few periods reported in the literature and/or with light curve Database (LCDB) (Warner et al., 2009) quality codes (U) of less than 3.

786 Bredichina. This C-type asteroid, was discovered in 1914 by Kaiser Heidelberg. Several periods were measured for this asteroid with the following results: P = 18.61 ± 0.02 h (Gil-Hutton and Cañada, 2003), P = 27.88 h (Behrend, 2010web), and P = 29.434 ± 0.001 h (Garceràn et al., 2015). We have determined a period of 29.819 ± 0.013 h, consistent with the one proposed by Garceràn et al.

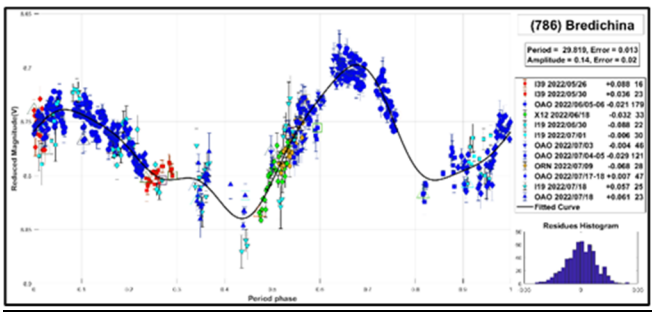

795 Fini. This asteroid was discovered in 1914 by Johann Palisa. The two more recent periods published in the literature correspond to P = 4.65 h with Δm = 0.02 mag (Pravec et al., 2012) and P = 26.9714 ± 0.0557 h with Δm = 0.06 mag (Waszczak et al., 2015). The results we obtained, P = 30.526 ± 0.008 h with Δm = 0.06 ± 0.01 mag, are consistent with the longer period proposed by Waszczak et al.

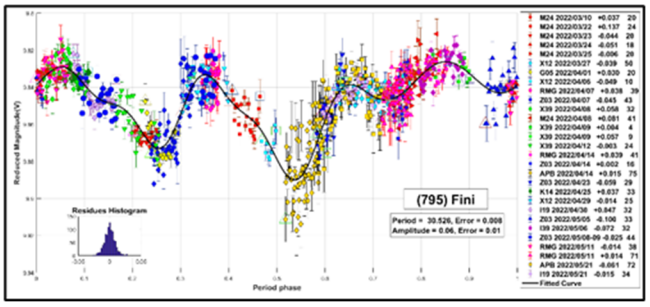

892 Seeligeria. This asteroid was discovered in 1918 by Maximilian Franz Wolf. We found two different periods reported in the literature: P = 41.40 ± 0.02 h with Δm = 0.15 ± 0.02 mag (Behrend, 2007web) and P = 15.78 ± 0.04 with Δm = 0.2 mag (Shipley et al., 2008). Our period P=16.693 ± 0.008 with Δm = 0.11± 0.01 mag well agrees with the one measured by Shipley et al.

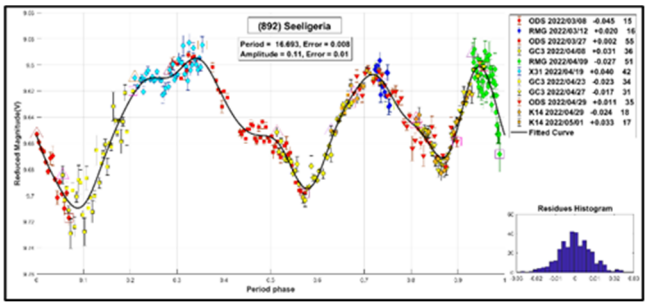

1343 Nicole. This asteroid was discovered in 1935 by Louis Boyer. We measured a period of 14.773 ± 0.011 h with Δm = 0.40 ± 0.02 mag. These results well agree with those reported by Waszczak et al. (2015), P = 14.7781 ± 0.0151 h with Δm = 0.42 mag and Aznar et al., (2016), P = 14.76 ± 0.01 h with Δm = 0.38 ± 0.02 mag. As a further contribution, our light curve provides almost full coverage of the rotational phase.

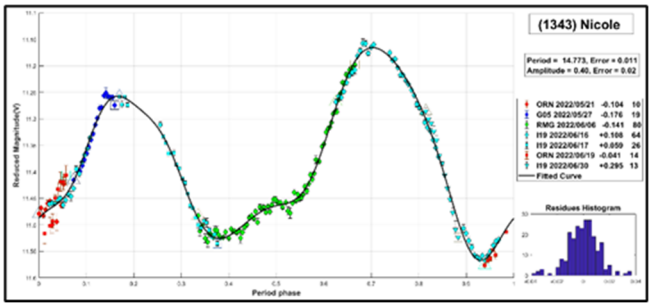

2717 Tellervo. This asteroid was discovered in 1940 by Liisi Oterma. We found in the literature two rather different periods calculated for this object: P = 8.428 ± 0.003 h with Δm = 0.40 ± 0.03 mag (Tomassini et al., 2013), and P = 4.213 h with Δm = 0.40 ± 0.03 mag (Scardella et al., 2016). The results we obtained are P = 4.222± 0.007 h and Δm = 0.11 ± 0.01 mag. Our period well agrees with the one measured by Scardella et al.

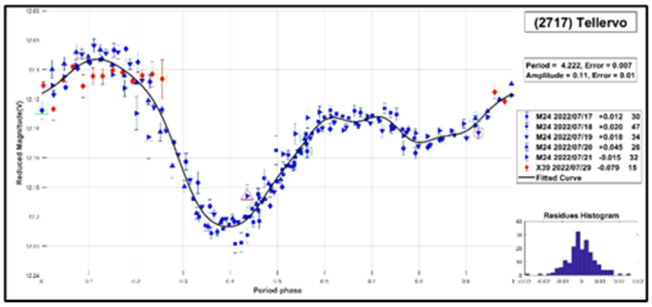

3224 Irkutsk. It was discovered in 1977 by Nikolái Chernyj. In the literature, we found only one period reported for this asteroid: P = 33.1404 ± 0.0630 h with Δm = 0.51 mag (Waszczak et al., 2015). Our study supports the aforementioned period and yielded the following data: P = 33.047 ± 0.014 h with Δm = 0.56 ± 0.02 mag.

Number	Name	yy/ mm/dd- yy/ mm/dd	Phase	L_{PAB}	B_{PAB}	Period(h)	P.E.	Amp	A.E.	Grp
786	Bredichina	22/05/26-22/07/19	*12.8,08.3	276	-2	29.819	0.013	0.14	0.02	MB-O
795	Fini	22/03/10-22/05/22	*13.7,18.0	199	-2	30.526	0.008	0.06	0.01	MB-O
892	Seeligeria	22/03/08-22/05/01	*8.3,11.1	189	7	16.693	0.008	0.11	0.01	MB-O
1343	Nicole	22/05/21-22/06/30	*7.5,13,0	253	-5	14.773	0.011	0.40	0.02	MB-I
2717	Tellervo	22/07/17-22/07/29	12.0,04,9	310	3	4.222	0.007	0.11	0.01	MB-I
3224	Irkutsk	22/04/02-22/05/22	*7.2,16.4	206	-2	33.047	0.014	0.56	0.02	MB-O

Table I. Observing circumstances and results. The phase angle is given for the first and last date. If preceded by an asterisk, the phase angle reached an extremum during the period. L_{PAB} and B_{PAB} are the approximate phase angle bisector longitude/latitude at mid-date range (see Harris et al., 1984). Grp is the asteroid family/group (Warner et al., 2009). MB-O: main-belt outer; MB-I: main-belt inner.

Observatory	Telescope	Camera
G05 Obs.Astr.Giordano Bruno	SCT (D=203mm; f=6.3)	CCD Atik 420 m
I19 Obs.Astr.El Gato Gris	SCT (D=355mm; f=10.6)	CCD SBIG STF-8300M
I39 Obs.Astr.Cruz del Sur	Newtonian (D=254mm; f=4.7)	CMOS QHY 174M
K14 Obs.Astr.de Sencelles	Newtonian (D=250mm; f=4.0)	CCD SBIG ST-7XME
M24 Oss.Astr.La Macchina del Tempo	RCT (D250mm; f=8.0)	CMOS ZWO ASI 1600MM
X12 Obs.Astr.Los Cabezones	Newtonian (D=200mm; f=5.0)	CMOS QHY 174M
X31 Obs.Astr.Galileo Galilei	RCT ap (D=405mm; f=8.0)	CCD SBIG STF-8300M
X39 Obs.Astr.Antares	Newtonian (D=250mm; f=4.72)	CCD QHY9 Mono
Z03 Obs.Astr.Río Cofio	SCT (D=254mm; f=6.3)	CCD SBIG ST-8XME
APB Obs.Astr.AstroPilar	Refractor (D=150mm; f=7.0)	CCD ZWO ASI 183
GC3 Specola Giuseppe Pustorino 3	RCT (D=400mm; f=5.7)	CCD Atik 383L+Mono
OAO Obs.Astr.Aficionado Omega	Newtonian (D=150mm; f=5.0)	CMOS QHY 174M
ODS Obs.Astr.de Damián Scotta 1	Newtonian (D=300mm; f=4.0)	CMOS QHY 174M
ORN Obs.Astr.de Ricardo Nolte	Newtonian (D=200mm; f=5.0)	CMOS POA Neptune-M
RMG Obs.Astr.de Raúl Melia	Newtonian (D=254mm; f=4.7)	CMOS QHY 174M

Table II. List of observatories and equipment.

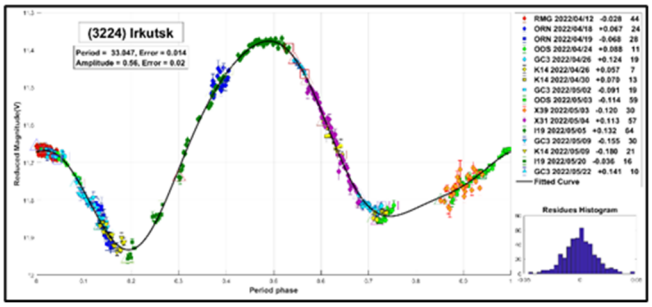

Acknowledgements

We want to thank Julio Castellano as we use his *FotoDif* program for preliminary analyses, Fernando Mazzone for his *Periodos* program, used in final analyses, and Matías Martini for his *CalculadorMDE_v0.2* used for generating ephemerides used in the planning stage of the observations. This research has made use of the Small Bodies Data Ferret (*http://sbn.psi.edu/ferret/*), supported by the NASA Planetary System. This research has made use of data and/or services provided by the International Astronomical Union's Minor Planet Center.

References

Aznar Macias, A.; Carreno Garcerain, A.; Arce Mansego, E.; Brines Rodriguez, P.; Lozano de Haro, J.; Fornas Silva, A.; Fornas Silva, G.; Mas Martinez, V.; Rodrigo Chiner, O. (2016). "Twenty-three Asteroids Lightcurves at Observadores de Asteroides (OBAS): 2015 October-December." *Minor Planet Bulletin* **43(2)**, 174-181.

Behrend, R. (2007web, 2010web). Observatoire de Geneve web site. *http://obswww.unige.ch/~behrend/page_cou.html*

Garceràn, A.C.; Macias, A.A.; Mansego, E.A.; Rodriguez, P.B.; de Haro, J.L. (2015). "Lightcurve Analysis of Six Asteroids." *Minor Planet Bulletin* **42(4)**, 235-237.

Gil-Hutton, R.; Cañada, M. (2003). "Photometry of fourteen main belt asteroids." *Revista Mexicana de Astronomía y Astrofísica* **39**, 69-76.

Harris, A.W.; Young, J.W.; Scaltriti, F.; Zappala, V. (1984). "Lightcurves and phase relations of the asteroids 82 Alkmene and 444 Gyptis." *Icarus* **57(2)**, 251-258.

Mazzone, F.D. (2012). Periodos software, version 1.0. *http://www.astrosurf.com/salvador/Programas.html*

Pravec, P.; Wolf, M.; Sarounova, L. (2012web) Ondrejov Asteroid Photometry Project website. *http://www.asu.cas.cz/~ppravec/neo.htm*.

Scardella, M.; Tomassini, A.; Franceshini, F. (2016). "Rotational Period Determination of 2717 Tellervo and (9773) 1993 MG1." *Minor Planet Bulletin* **43(2)**, 186.

Shipley, H.; Dillard, A.; Kendall, J.; Reichert, M.; Sauppe, J.; et al. (2008). "Asteroid Lightcurve Analysis at the Oakley Observatory – September 2007." *Minor Planet Bulletin* **35(5)**, 119-122.

Tomassini, A.; Scardella, M.; La Caprara, G. (2013). "Lightcurve of 2717 Tellervo." *Minor Planet Bulletin* **40(2)**, 108-109.

Warner, B.D.; Harris, A.W.; Pravec, P. (2009). "The Asteroid Lightcurve Database." *Icarus* **202**, 134-146. Updated 2022 Aug. *http://www.minorplanet.info/lightcurvedatabase.html*

Waszczak, A.; Chang, C.K.; Ofek, E.O.; Laher, R.; Masci, F.; Levitan, D.; Kulkarni, S. (2015). "Asteroid light curves from the Palomar Transient Factory survey: rotation periods and phase functions from sparse photometry." *The Astronomical Journal* **150(3)**, 75.

SYNODIC PERIOD DETERMINATION OF SEVEN MAIN-BELT ASTEROIDS FROM MALTESE OBSERVATORIES

Stephen M. Brincat
Flarestar Observatory (MPC 171)
Fl.5/B, George Tayar Street,
San Gwann SGN 3160, MALTA
stephenbrincat@gmail.com

Charles Galdies
Znith Observatory
Naxxar NXR 2217, MALTA

Martin Mifsud
Manikata Observatory
Manikata MLH 5013, MALTA

Winston Grech
Antares Observatory
Fgura FGR 1555, MALTA

(Received: 2022 September 30)

Photometric observations of seven asteroids were acquired from four Maltese observatories in order to derive or update published synodic periods and lightcurve amplitudes of the asteroids: 1461 Jean-Jacques, 2030 Belyaev, 2149 Schwambraniya, 3114 Ercilla, (7357) 1995 UJ7, 12919 Tomjohnson, and (20895) 2000 WU106.

Photometric observations of seven asteroids were carried out from four observatories located on the Maltese mainland. From our observations, we determined the synodic period for the following asteroids: 1461 Jean-Jacques, 2030 Belyaev, 2149 Schwambraniya, 3114 Ercilla, 12919, Tomjohnson, and (20895) 2000 WU106. Our observatories used the configurations shown in Table 1. All of our images were dark subtracted and flat-fielded.

Observatory	Telescope	CCD	Asteroids (#Sessions)
Flarestar (MPC 171)	0.25-m SCT	Moravian G2-1600	2030 (5) 2149 (2) 7357 (6) 12919 (5)
Znith	0.2-m SCT	Moravian G2-1600	2149 (1) 3114 (4)
Manikata	0.2-m SCT	SBIG ST-9	1461 (5) 2149 (1)
Antares	0.27-m SCT	SBIG ST-11000	2149 (3)

Table 1 - Instrumentation. SCT: Schmidt-Cassegrain Telescope.

All telescopes and cameras were controlled remotely over the Internet either from a location near the telescope or through remote programing. All observatories employed the *Sequence Generator Pro* Software (Binary Star Software) for observatory control and ancillary equipment. Photometric reduction, lightcurve construction, and analyses were derived through *MPO Canopus* software using version 10.8.6.11(Warner, 2017). The Comparison Star Selector (CSS) feature of *MPO Canopus* was used to select comparison stars of near-solar color. In cases where the asteroid passed in proximity of a background star, we used the *MPO Canopus* "StarBGone" routine to deduct the background signal from that of the asteroid. Our magnitude measurements were all carried out through a clear filter with framework magnitude bandpass based on the ATLAS catalogue through the Red (R) bandpass. As a result, our measurements are based on the 'CR' bandpass.

1461 Jean-Jacques is an outer main-belt asteroid that was discovered on 1937 December 30 by M. Laugier at Nice. The discoverer named this minor planet after her son Jean-Jacques (Schmadel, 2012). The estimated diameter was derived to be 35.145 ± 0.172 km diameter based on an absolute magnitude H = 10.15 and orbits the sun with a semi-major axis of 3.126 au. Its orbit has an eccentricity of 0.049 and a period of 5.52 years (JPL, 2022).

1461 Jean-Jacques was observed from Manikata Observatory during five nights on 2022 June 5-20. Our results yielded a synodic period of 8.2788 ± 0.0027 h and amplitude of 0.31 ± 0.05 mag. Our lightcurve results are in line with Ďurech et al., (2020) in the Asteroid Lightcurve Data Base (LCDB; Warner et al, 2009).

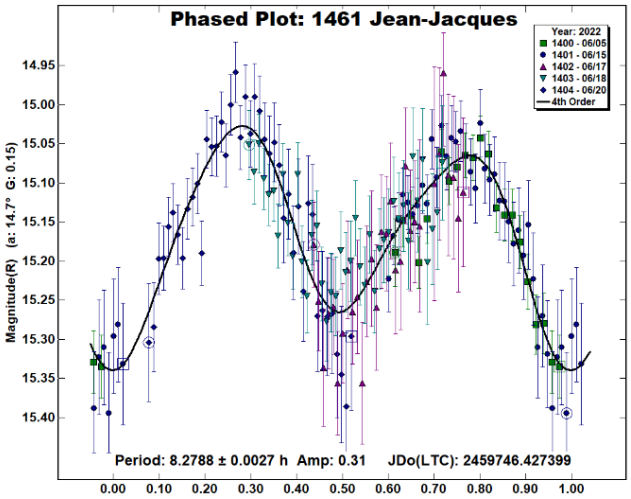

2030 Belyaev is an inner main-belt asteroid that was discovered in 1969 Oct. 8 by L.I. Chernykh at Nauchnyj. It was named in honor of Colonel Pavel Ivanovich Belyaev (1925-1970), a Soviet cosmonaut and commander of the spaceship Voskhod 2. A lunar crater was also named 'Belyaev' for his honor (Schmadel, 2012).

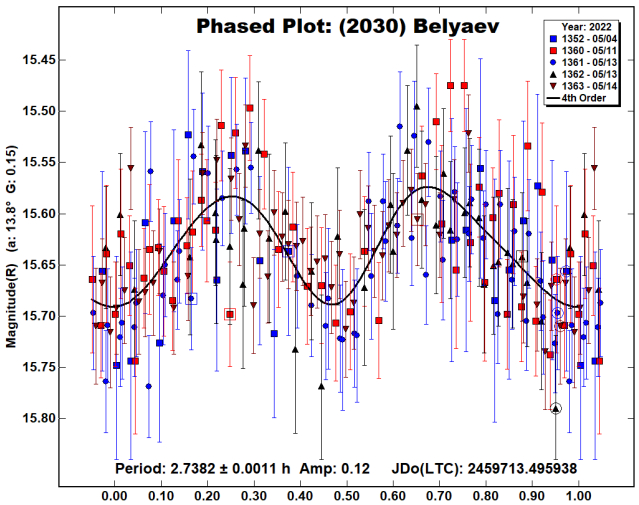

This minor planet orbits the sun with a semi-major axis of 2.247 au, eccentricity 0.093, and orbital period of 3.37 years (JPL, 2022). The JPL Small-Bodies Database Browser does not list the diameter of (2030) Belyaev, however an absolute magnitude of H = 13.63 is quoted (JPL, 2022).

We observed 2030 Belyaev for five nights from 2022 May 4-14 from Flarestar Observatory. Our results yielded a synodic rotation period of 2.7382 ± 0.0011 h and amplitude of 0.12 ± 0.07 mag. The LCDB did not contain any references of the synodic period for this asteroid.

2149 Schwambraniya is an inner main-belt asteroid that was discovered on 1977 March 22 by N.S. Chernykh at Nauchnyj. It has been named for the 'wonderland' created by the characters in L.A. Kassil's children's novel, "*Conduite and Schwambraniya*" (Schmadel, 2012). The estimated diameter of 2149 Schwambraniya was derived to be 11.180 ± 0.122 km diameter based on an absolute magnitude H = 11.89. This asteroid orbits the sun at a semi-major axis of 2.549 au, an eccentricity of 0.107, and a period of 4.07 years (JPL, 2022).

The asteroid was observed by our group on seven nights from 2022 May 17 to June 5. Our analysis has yielded the lowest RMS rotational period of 5.676 ± 0.001 h with an amplitude of 0.21 ± 0.07 mag ("P1" figure).

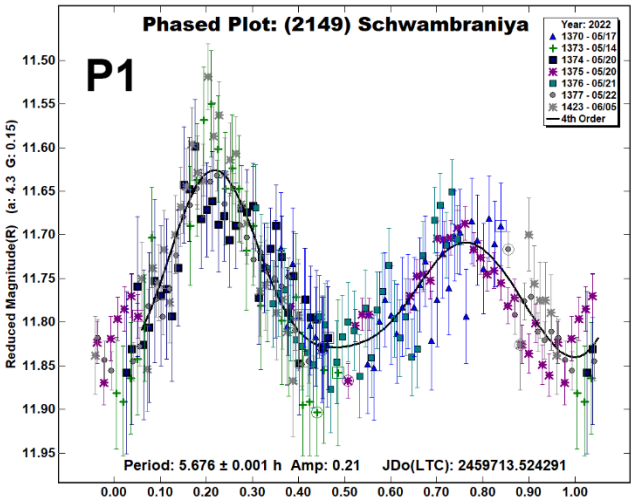

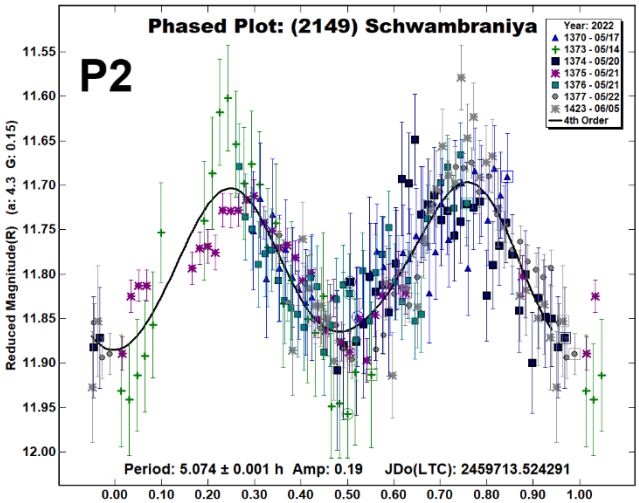

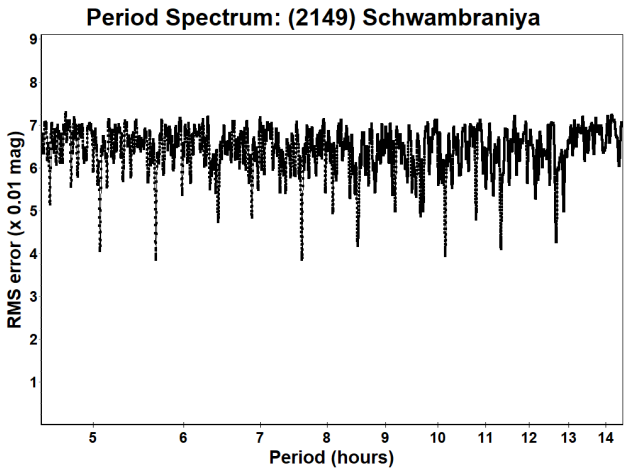

The LCDB shows a period of 5.070 ± 0.0034 h (Waszczak, 2015) with a rating of U = 2. Ďurech et al. (2020) also yields a sidereal period of 5.07348 ± 0.00001 h with an Q = R quality value in the LCDB, showing that a retrograde rotation has been determined but not specific pole position.

Our period spectrum also includes a relative minimum at the above mentioned 5.074 h period but when the data are phased to this period (P2 figure), the RMS value of 4.057 is higher than that of the derived period of 5.676 (RMS 3.857). The third lowest minima shown in the period spectrum displays a period of 7.611 ± 0.001 h that exhibits a trimodal lightcurve when data are phased to this period.

3114 Ercilla is main-belt asteroid that belongs to the 2004 Hertha family. It was discovered by C. Torres at Cerro El Roble on 1980 March 19. Ercilla is named in memory of Don Alonso de Ercilla y Zuniga (1533-1594), a Spanish poet and soldier who distinguished himself in the campaign in Chile against the Araucanians and is considered by many as the first chronicler of the history of Chile.

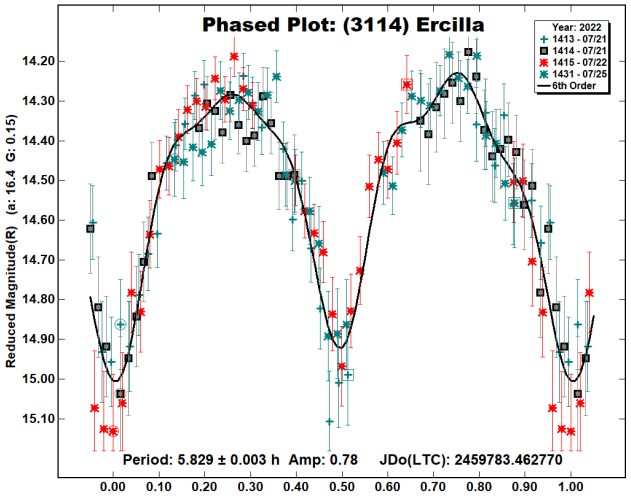

The estimated diameter of 3114 Ercilla was derived to be 5.040 ± 0.048 km based on an absolute magnitude H = 13.96 and orbits the sun with a semi-major axis of 2.419 au. Its orbit has an eccentricity of 0.197 and a period of 3.76 years (JPL, 2022).

Observations were conducted by Znith Observatory over four nights: 2022 July 21-25. Our results indicate a synodic period of 5.829 ± 0.003 h and amplitude of 0.78 ± 0.05 mag. The LCDB did not contain any references of the synodic period for this asteroid.

(7357) 1995 UJ7 is an inner main-belt asteroid that was discovered on 1995 October 27 by S. Ueda and H. Kaneda at Kushiro, Japan. The estimated diameter of (7357) is estimated to be 3.992 ± 0.308 km based on an absolute magnitude H = 14.03. The asteroid orbits the sun at a semi-major axis of 2.268 au and eccentricity of 0.182. The orbital period of 3.41years (JPL, 2022).

(7357) was observed from Flarestar Observatory on six nights during the period from 2022 July 27 to August 9. We derived its synodic period to be 2.803 ± 0.0004 h with an amplitude of 0.16 ± 0.07 mag. The Asteroid Lightcurve Database (LCDB; Warner et al., 2009) did not show any reference period for this asteroid.

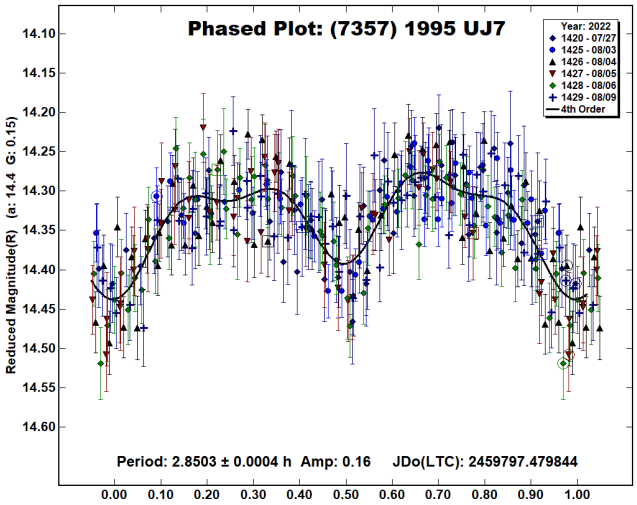

12919 Tomjohnson is an inner main-belt asteroid that was discovered on 1998 November 11 by the Catalina Sky Survey. This asteroid was named after Thomas J. Johnson (1923-2012) who developed a technique for creating Schmidt telescope correctors that allowed the mass production of Schmidt-Cassegrain telescopes. In 1978 the Optical Society of America awarded him the David Richardson Medal for this work.

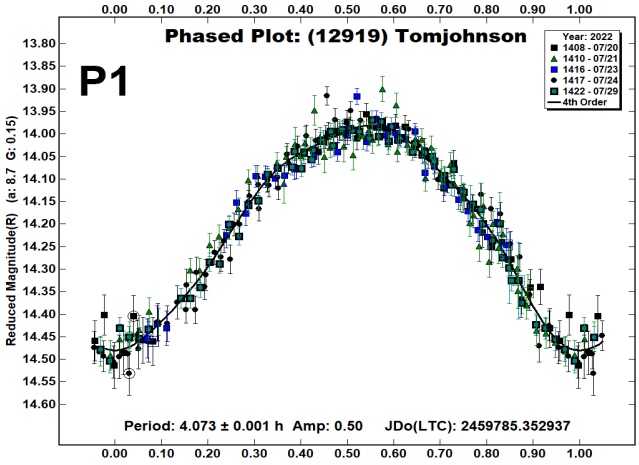

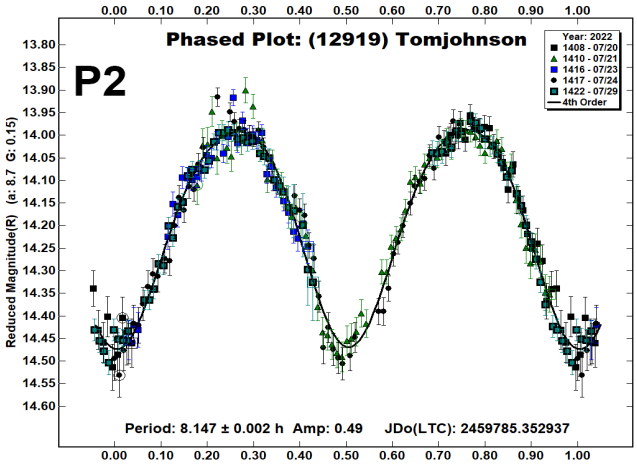

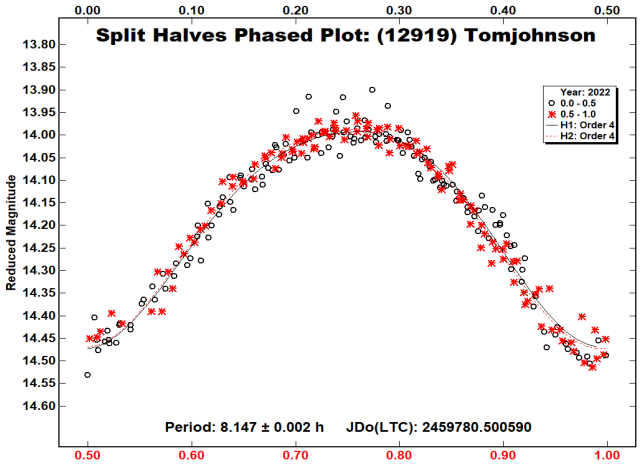

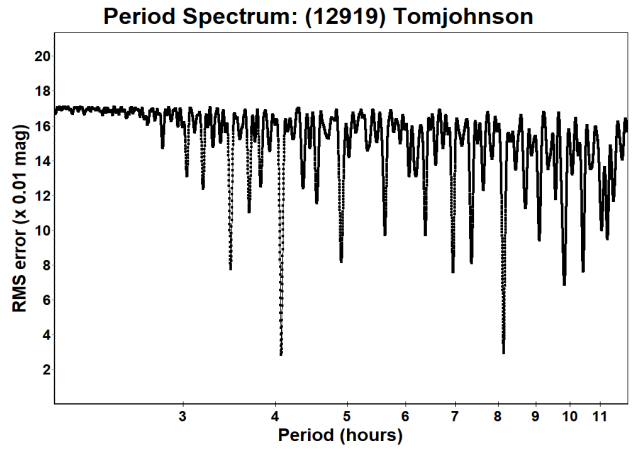

The diameter of this asteroid is estimated to be 4.882 ± 0.468 km based on H = 14.03. The asteroid orbits at a semi-major axis of 2.273. The eccentricity is 0.281 and the orbital period is 3.42 years (JPL, 2022).

We observed the asteroid on five nights from Flarestar Observatory and derived its synodic period to be 4.073 ± 0.001 h with a lightcurve amplitude of 0.50 ± 0.03 mag. A second period was also derived at 8.147 ± 0.002 h with an amplitude of 0.49 ± 0.03 mag; however, on inspection through split-half analysis, the average shape of both phases of the light curve are very identical and hence we believe that the correct synodic period of this asteroid is 4.073 ± 0.001 h. The former period solution (P1) also has a slightly lower RMS residual, at 2.8515 and 2.944 (P2) respectively. The LCDB did not show any reference period for this asteroid.

Number	Name	2022 mm/dd	Phase	L_{PAB}	B_{PAB}	Period(h)	P.E.	Amp	A.E.	Grp
1461	Jean-Jacques	07/05-07/20	17.9,18.2	214	14	8.2788	0.0027	0.31	0.05	MB
2030	Belyaev	05/04-05/14	13.8,8.7	246	4	2.7382	0.001	0.12	0.07	MB
2149	Schwambraniya	05/17-06/05	4.2,13.0	229	2	5.676	0.001	0.21	0.07	MB
3114	Ercilla	07/21-07/25	16.5,14.5	324	2	5.829	0.003	0.78	0.05	MB
7357	1995 UJ7	07/27-08/09	13.9,6.4	325	1	2.803	0.0004	0.16	0.07	MB
12919	Tomjohnson	07/20-07/29	8.4,6.3	306	8	4.073	0.001	0.50	0.03	MB
20895	2000 WU106	07/18-07/25	6.7,2.7	304	2	7.301	0.001	0.72	0.07	MB

Table I. Observing circumstances and results. Pts is the number of data points. The phase angle is given for the first and last date. LPAB and BPAB are the approximate phase angle bisector longitude and latitude at mid-date range (see Harris et al., 1984). Grp is the asteroid family/group (Warner et al., 2009).

20895 2000 WU106 is an inner main-belt asteroid that was discovered in 2000 November 20 by Lincoln Near-Earth Asteroid Research (LINEAR) at Socorro, USA. The minor planet has an absolute magnitude H = 14.64 and orbits the sun with a semi-major axis of 2.184 au, eccentricity of 0.199, and a period of 3.223 years (JPL, 2022).

This asteroid was observed from Flarestar Observatory from 2022 July 18-25. We derived its synodic period to be 7.301 ± 0.001 h with an amplitude of 0.72 ± 0.07 mag. The LCDB did not show any reference period for this asteroid.

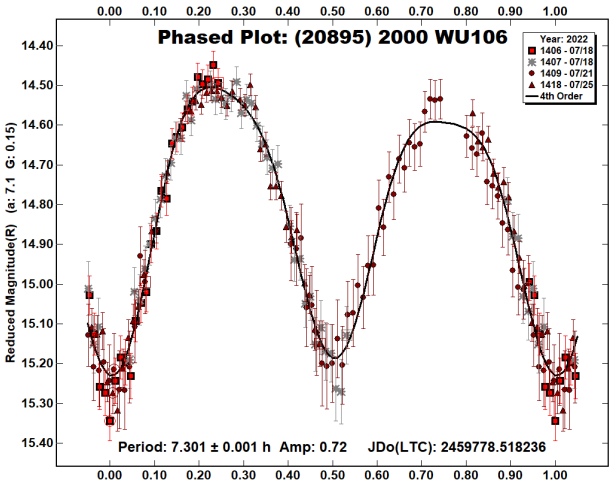

Acknowledgements

We would like to thank Brian Warner for his work in the development of *MPO Canopus* and for his efforts in maintaining the CALL website (Warner, 2016; Warner et al., 2009).

This research has made use of the JPL's Small-Body Database.

References

Ďurech, J.; Tonry, J.; Erasmus, N.; Denneau, L.; Heinze, A.N.; Flewelling, H.; and Vančo, R. (2020). "Asteroid models reconstructed from ATLAS photometry." *Astron. Astrophys.* **643**, A59.

Harris, A.W.; Young, J.W.; Scaltriti, F.; Zappala, V. (1984). "Lightcurves and phase relations of the asteroids 82 Alkmene and 444 Gyptis." *Icarus* **57**, 251-258.

JPL (2022). Small-Body Database Browser - JPL Solar System Dynamics web site. Last accessed: 15 September 2022. *http://ssd.jpl.nasa.gov/sbdb.cgi*

Schmadel, L.D. (2012). Catalogue of Minor Planet Names and Discovery Circumstances. In *Dictionary of Minor Planet Names* (pp. 11-1309). Springer, Berlin, Heidelberg.

Warner, B.D. (2016). Collaborative Asteroid Lightcurve Link website. Last accessed: 26 September 2018. *http://www.minorplanet.info/call.html*

Warner, B.D., (2017). MPO Software, *MPO Canopus* version 10.8.6.11. Bdw Publishing. *http://www.minorplanetobserver.com/*

Warner, B.D.; Harris, A.W.; Pravec, P. (2009). "The Asteroid Lightcurve Database." *Icarus* **202**, 134-146. Updated 2021 June. *https://minplanobs.org/MPInfo/php/lcdbsummaryquery.php*

Waszczak, A.; Chang, C.-K.; Ofek, E.O.; Laher, R.; Masci, F.; Levitan, D.; Surace, J.; Cheng, Y.-C.; Ip, W.-H.; Kinoshita, D.; Helou, G.; Prince, T.A.; Kulkarni, S. (2015). "Asteroid Light Curves from the Palomar Transient Factory Survey: Rotation Periods and Phase Functions from Sparse Photometry." *Astron. J.* **150**, A75.

MAIN-BELT ASTEROIDS OBSERVED FROM CS3: 2022 JULY-SEPTEMBER

Robert D. Stephens
Center for Solar System Studies (CS3)
11355 Mount Johnson Ct., Rancho Cucamonga, CA 91737 USA
rstephens@foxandstephens.com

Daniel R. Coley
Center for Solar System Studies (CS3)
Corona, CA

Thomas M. Mathis
Carina Software & Instruments
Danville, CA

Brian D. Warner
Center for Solar System Studies (CS3)
Eaton, CO

(Received: 2022 October 6 Revised: 2022 November 19)

CCD photometric observations of seven main-belt asteroids were obtained at the Center for Solar System Studies (CS3) from 2022 July-September. Two revised periods from observations obtained in 2003 and 2018 are also reported. 4429 Chinmoy appears to be in non-principal axis rotation ("tumbling"). Our analysis found an additional, unexpected short period, low amplitude lightcurve. (101465) 1998 WL12 also appears to be tumbling. It was not possible to establish the true periods of rotation and precession for either asteroid.

The Center for Solar System Studies (CS3) has nine telescopes which are normally used in program asteroid family studies. The focus is on near-Earth asteroids, Jovian Trojans and Hildas. When it is not the season to study a family, or when a nearly full moon is too close to the family targets being studied, targets of opportunity amongst the main-belt families were selected.

Table I lists the telescopes and CCD cameras that were used to make the observations. Images were unbinned with no filter and had master flats and darks applied. The exposures depended upon various factors including magnitude of the target, sky motion, and Moon illumination.

Telescope	Camera
0.35-m f/10 Schmidt-Cass	FLI Microline 1001E
0.35-m f/10 Schmidt-Cass	FLI Proline 1001E
0.40-m f/10 Schmidt-Cass	FLI Proline 1001E
0.50-m F/8.1 R-C	QHY600 CMOS

Table I: List of CS3 telescope/CCD camera.

Image processing, measurement, and period analysis were done using *MPO Canopus* (Bdw Publishing), which incorporates the Fourier analysis algorithm (FALC) developed by Harris (Harris et al., 1989). The Comp Star Selector feature in *MPO Canopus* was used to limit the comparison stars to near solar color. Night-to-night calibration was done using field stars from the ATLAS catalog (Tonry et al., 2018), which has Sloan *griz* magnitudes that were derived from the GAIA and Pan-STARR catalogs and are "native" magnitudes of the catalog. Those adjustments are usually ≤ ±0.03 mag. The rare greater corrections may have been related in part to using unfiltered observations, poor centroiding of the reference stars, and not correcting for second-order extinction.

The Y-axis values are ATLAS SR "sky" magnitudes. The two values in the parentheses are the phase angle (a) and the value of *G* used to normalize the data to the comparison stars used in the earliest session. This, in effect, made all the observations seem to be made at a single fixed date/time and phase angle, leaving any variations due only to the asteroid's rotation and/or albedo changes. The X-axis shows rotational phase from -0.05 to 1.05. If the plot includes the amplitude, e.g., "Amp: 0.65", this is the amplitude of the Fourier model curve and *not necessarily the adopted amplitude for the lightcurve*.

For brevity, only some of the previously reported rotational periods may be referenced. A complete list is available at the asteroid lightcurve database (LCDB; Warner et al., 2009).

3153 Lincoln. Periods have been reported for this Vestoid using survey data. Using dense TESS data, Pál et al. (2020) reported a period of 4.81947 h. Using sparse ATLAS data, Erasmus et al. (2020) reported a period of 15.997 h, close to a 3:1 alias of the Pál et al. result. Our result this year confirmed the Pál et al. period and illustrates the issue of using sparse data while assuming a bimodal lightcurve.

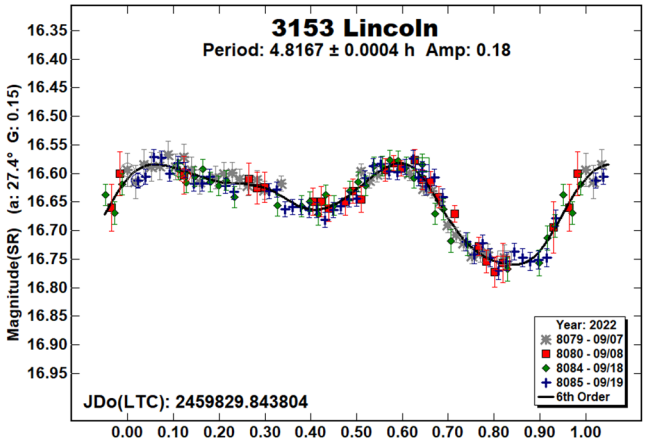

3893 DeLaeter. Finding a reliable period for this inner main-belt asteroid has been difficult in the past due to the asymmetric shape of its lightcurve and low-quality data. We observed it three times before with varying results (Stephens, 2004, 9.73 h; Warner, 2014, 5.633 h; Stephens, 2019, 9.61 h). This year we were able to obtain a high-quality dataset covering the entire phased lightcurve three times. The period spectrum suggests only two possibilities: near 14 h and 18 h. Upon inspection, the 18 h period is not plausible.

The original 2003 images no longer exist, but we were able to rephase that lightcurve to a period near 14.41 h resulting in a low amplitude lightcurve. With such a low amplitude, it is possible that a lightcurve could have a single minimum/maximum pair, or three or more pairs (Harris et al., 2014). The 2014 data were of too low a quality to rephase to a useful lightcurve, but we remeasured the 2018 data using ATLAS SR magnitudes and were able to find a 14.490 h period with an asymmetric lightcurve.

We think we can pronounce 'case closed' for 3893 DeLaeter. The next opportunities to observe it are in 2025, and particularly in 2026 when it will be mag 15.1.

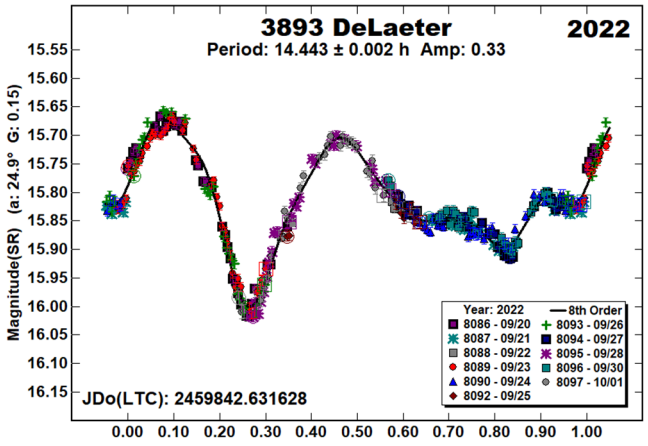

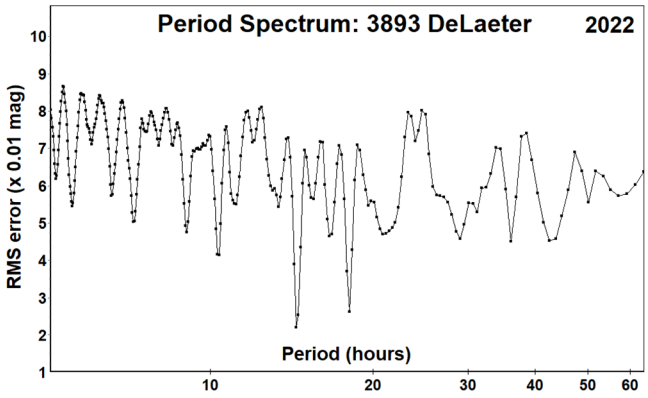

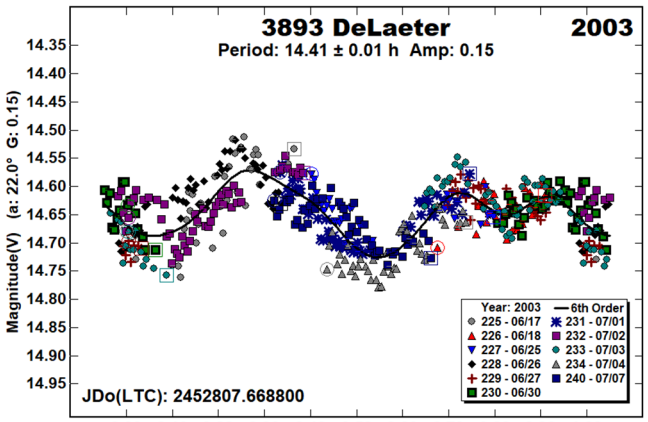

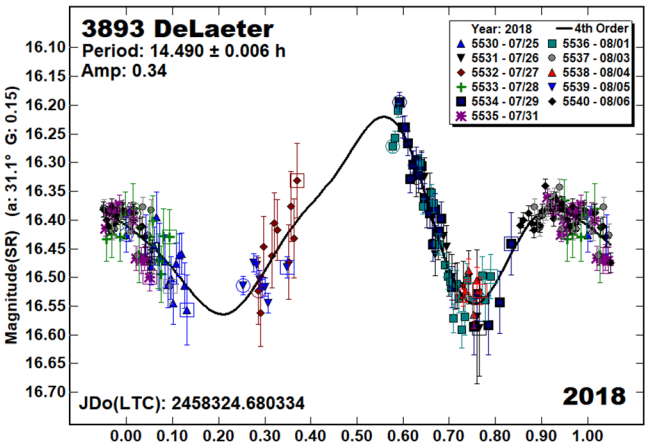

4429 Chinmoy. There are no previous periods reported in the LCDB for this member of the Hertha dynamical family (Nesvorny et al., 2015; Nesvorny, 2015). We were requested to observe it by Szabolcs Nyari. It was apparent from our first night of observations that Chinmoy had a long period. Deviations in the period suggested it to be tumbling, which *MPO Canopus* cannot properly analyze. Even so, we used it to extract the dominant period and another that, when subtracted from the full data set, allowed a good fit to a bimodal lightcurve with P_1 = 44.99 h. The other period, P_2 = 50.35 h, is likely an integral ratio (1/P) of the true frequency, an artifact of holding the first period constant while searching for a second and insufficient data. Proper analysis would have the two periods solved simultaneously. The periods are long enough to suspect that the asteroid has been in a tumbling state for some time. Based on a general rule of thumb (Pravec et al., 2005, 2014), the damping time for the asteroid, given its size and periods, would be slightly more than 1 Gyr.

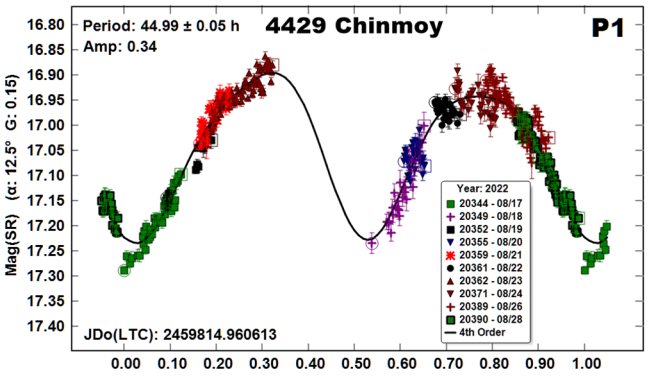

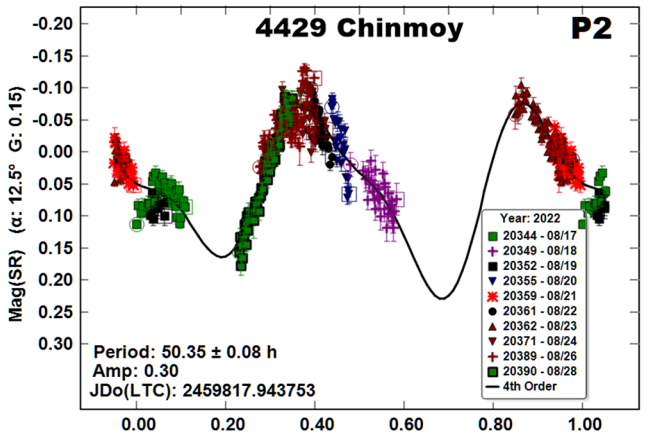

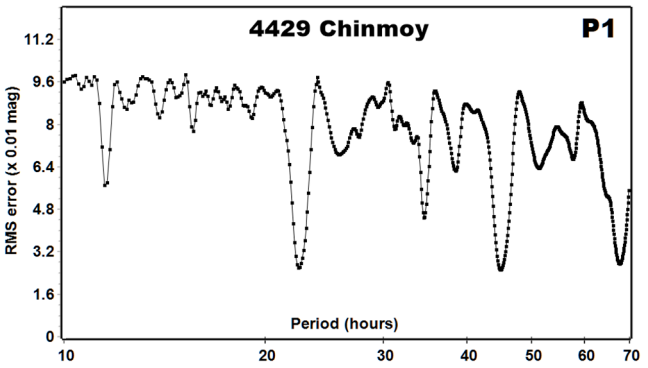

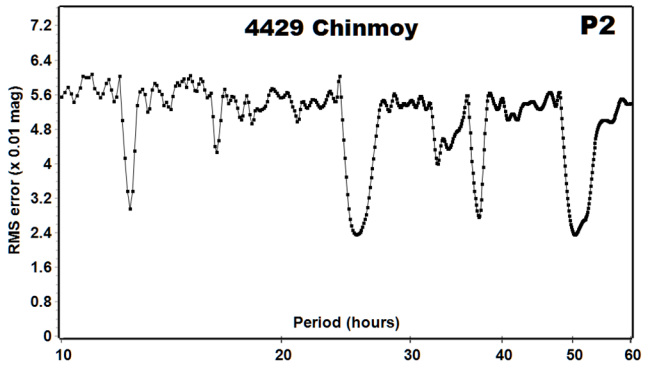

7334 Sciurus. This Vestoid has been observed twice in the past. Pravec (2011web) observed it finding a period of 4.0659 h. Using Gaia data (DR2), Colazo et al. (2021) reported a period of 4.067 h. Our result this year is in good agreement with those prior findings.

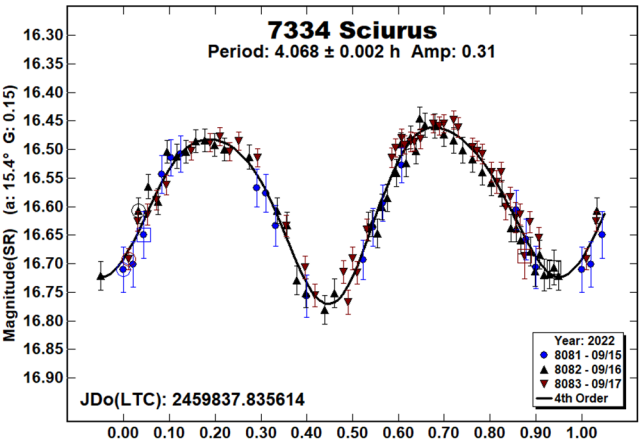

(10548) 1992 PJ2. As part of the Photometric Survey of Binary Near-Earth Asteroids (Pravec et al., 2006; Pravec et al., 2007web) reported a period of 4.01838 h for this Mars-crosser. Our period of 4.068 h this year is in good agreement with that prior result.

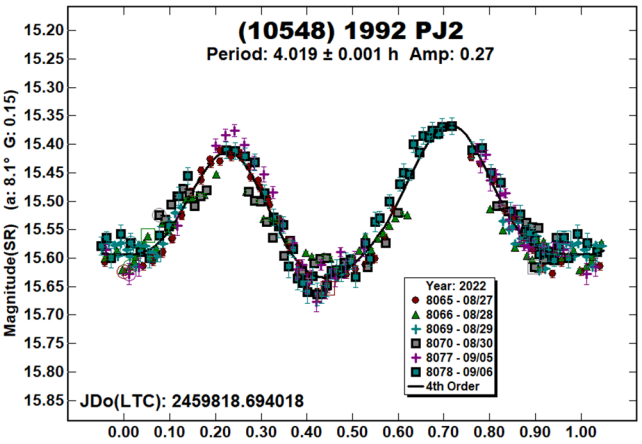

(89486) 2001 XL31. There are no previous entries in the LCDB for this Mars-crosser. The result of 7.026 h is assured since each of the four sequential nights covered the complete lightcurve.

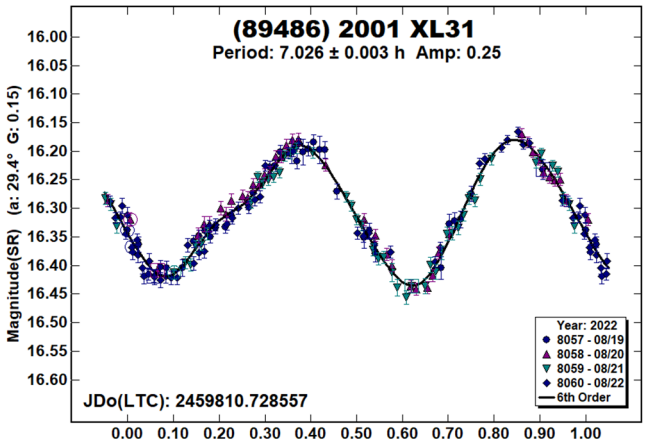

(101465) 1998 WL12. There are no previous periods reported in the LCDB for this Mars-crosser. From the first night of observations, it was apparent that it had a long period. It seems likely from the period and diameter of 1.9 km that this is a tumbler (Pravec et al. 2005). *MPO Canopus* cannot fully analyze this type of object. Even so, we were 200able to extract a dominant period of 230.1 h. Subtracting that dominant period allowed us to find a secondary period of 77.6 h. Given that this has a 3:1 integral ratio with P_1 suggests the idea of P_2 being a harmonic artifact of the Fourier analysis.

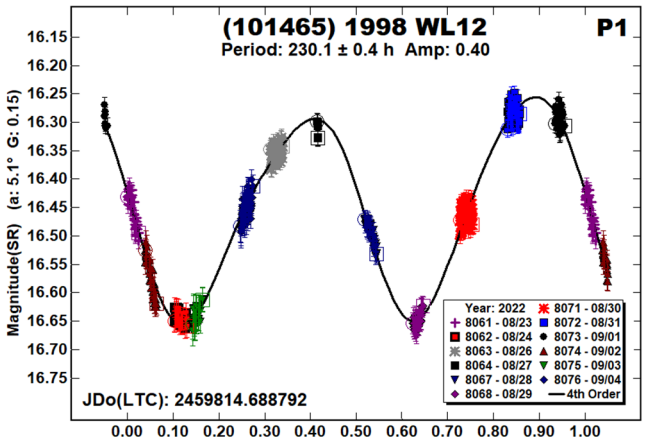

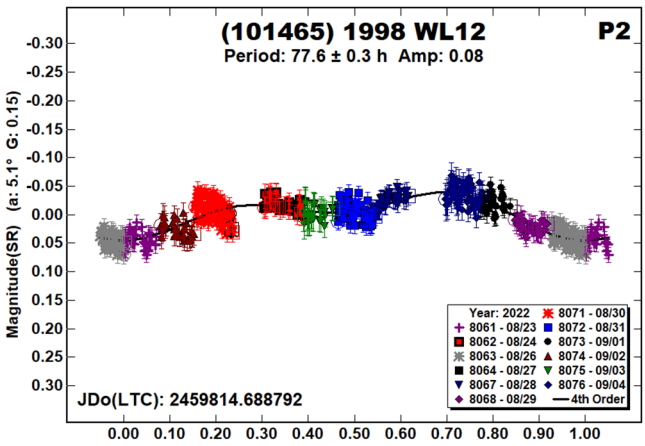

Number	Name	2022/mm/dd	Phase	L_{PAB}	B_{PAB}	Period(h)	P.E.	Amp	A.E.
3153	Lincoln	09/07-09/19	27.4,25.5	46	-1	4.8167	0.0004	0.18	0.01
3893	DeLaeter	09/20-10/01	24.9,26.8	327	21	14.443	0.002	0.33	0.02
		2003/06/17-07/07	22.0, 25.2	266	33	[R]14.41	0.01	0.15	0.05
		2018/07/25-08/06	31.1, 32.8	256	29	[R]14.490	0.006	0.34	0.05
4429	Chinmoy	08/17-08/28	12.4,6.6	344	0	[T]44.99	0.05	0.37	0.05
						50.35	0.08	0.30	0.05
7334	Sciurus	09/15-09/17	15.4,14.5	18	-5	4.068	0.002	0.31	0.02
10548	1992 PJ2	08/27-09/06	8.1,12.0	306	7	4.019	0.001	0.27	0.02
89486	2001 XL31	08/19-08/22	29.4,29.2	345	29	7.026	0.003	0.25	0.01
101465	1998 WL12	08/23-09/04	5.1,11.5	329	5	[T]230.1	0.4	0.40	0.05
						77.6	0.3	0.08	0.02

Table II. Observing circumstances and results. [R]Revised period. [T]Dominant period for a tumbling asteroid. The phase angle is given for the first and last date. If preceded by an asterisk, the phase angle reached an extremum during the period. L_{PAB} and B_{PAB} are the approximate phase angle bisector longitude/latitude at mid-date range (see Harris et al., 1984). If more than one line for an asteroid, the first line gives the dominant solution and has a [T] superscript. Subsequent lines are additional, not alternate, periods. See the text for more details.

Acknowledgements

This work includes data from the Asteroid Terrestrial-impact Last Alert System (ATLAS) project. ATLAS is primarily funded to search for near earth asteroids through NASA grants NN12AR55G, 80NSSC18K0284, and 80NSSC18K1575; byproducts of the NEO search include images and catalogs from the survey area. The ATLAS science products have been made possible through the contributions of the University of Hawaii Institute for Astronomy, the Queen's University Belfast, the Space Telescope Science Institute, and the South African Astronomical Observatory. The authors gratefully acknowledge Shoemaker NEO Grants from the Planetary Society (2007, 2013). These were used to purchase some of the telescopes and CCD cameras used in this research.

References

Colazo, M.; Duffard, R.; Weidmann, W. (2021). "The determination of asteroid H and G phase function parameters using Gaia DR2." *Monthly Notices of RAS.* **504**, 761-768.

Erasmus, N.; Navarro-Meza, S.; McNeill, A.; Trilling, D.E.; Sickafoose, A.A.; Denneau, L.; Flewelling, H.; Heinze, A.; Tonry, J.L. (2020). "Investigating Taxonomic Diversity within Asteroid Families through ATLAS Dual-band Photometry." *Ap. J. Suppl. Ser.* **247**, A13.

Harris, A.W.; Young, J.W.; Scaltriti, F.; Zappala, V. (1984). "Lightcurves and phase relations of the asteroids 82 Alkmene and 444 Gyptis." *Icarus* **57**, 251-258.

Harris, A.W.; Young, J.W.; Bowell, E.; Martin, L.J.; Millis, R.L.; Poutanen, M.; Scaltriti, F.; Zappala, V.; Schober, H.J.; Debehogne, H.; Zeigler, K.W. (1989). "Photoelectric Observations of Asteroids 3, 24, 60, 261, and 863." *Icarus* **77**, 171-186.

Harris, A.W.; Pravec, P.; Galad, A.; Skiff, B.A.; Warner, B.D.; Vilagi, J.; Gajdos, S.; Carbognani, A.; Hornoch, K.; Kusnirak, P.; Cooney, W.R.; Gross, J.; Terrell, D.; Higgins, D.; Bowell, E.; Koehn, B.W. (2014). "On the maximum amplitude of harmonics on an asteroid lightcurve." *Icarus* **235**, 55-59.

Nesvorny, D. (2015). "Nesvorny HCM Asteroids Families V3.0." NASA Planetary Data Systems, id. EAR-A-VARGBET-5-NESVORNYFAM-V3.0.

Nesvorny, D.; Broz, M.; Carruba, V. (2015). "Identification and Dynamical Properties of Asteroid Families." In *Asteroids IV* (P. Michel, F. DeMeo, W.F. Bottke, R. Binzel, Eds.). Univ. of Arizona Press, Tucson, also available on astro-ph.

Pál, A.; Szakáts, R.; Kiss, C.; Bódi, A.; Bognár, Z.; Kalup, C.; Kiss, L.L.; Marton, G.; Molnár, L.; Plachy, E.; Sárneczky, K.; Szabó, G.M.; Szabó, R. (2020). "Solar System Objects Observed with TESS - First Data Release: Bright Main-belt and Trojan Asteroids from the Southern Survey." *Ap. J.* **247**, A26.

Pravec, P.; Harris, A.W.; Scheirich, P.; Kušnirák, P.; Šarounová, L.; Hergenrother, C.W.; Mottola, S.; Hicks, M.D.; Masi, G.; Krugly, Yu.N.; Shevchenko, V.G.; Nolan, M.C.; Howell, E.S.; Kaasalainen, M.; Galád, A.; Brown, P.; Degraff, D.R.; Lambert, J.V.; Cooney, W.R.; Foglia, S. (2005). "Tumbling asteroids." *Icarus* **173**, 108-131.

Pravec, P.; Scheirich, P.; Kusnirák, P.; Sarounová, L.; Mottola, S.; Hahn, G.; Brown, P.; Esquerdo, G.; Kaiser, N.; Krzeminski, Z.; and 47 colleagues (2006). "Photometric survey of binary near-Earth asteroids." *Icarus* **181**, 63-93.

Pravec, P.; Wolf, M.; Sarounova, L. (2007web, 2011web). *http://www.asu.cas.cz/~ppravec/neo.htm*

Pravec, P.; Scheirich, P.; Ďurech, J.; Pollock, J.; Kusnirak, P.; Hornoch, K.; Galad, A.; Vokrouhlicky, D.; Harris, A.W.; Jehin, E.; Manfroid, J.; Opitom, C.; Gillon, M.; Colas, F.; Oey, J.; Vrastil, J.; Reichart, D.; Ivarsen, K.; Haislip, J.; LaCluyze, A. (2014). "The tumbling state of (99942) Apophis." *Icarus* **233**, 48-60.

Stephens, R.D. (2004). "Photometry of 683 Lanzia, 1101 Clematis, 1499 Pori, 1507 Vaasa, and 3893 DeLaeter." *Minor Planet Bull.* **31**, 4-6.

Stephens, R.D. (2019). "Asteroids Observed from CS3: 2018 July - September." *Minor Planet Bul.* **46**, 66-71.

Tonry, J.L.; Denneau, L.; Flewelling, H.; Heinze, A.N.; Onken, C.A.; Smartt, S.J.; Stalder, B.; Weiland, H.J.; Wolf, C. (2018). "The ATLAS All-Sky Stellar Reference Catalog." *Astrophys. J.* **867**, A105.

Warner, B.D. (2014). "Asteroid Lightcurve Analysis at CS3-Palmer Divide Station: 2014 March-June." *Minor Planet Bull.* **41**, 235-241.

Warner, B.D.; Harris, A.W.; Pravec, P. (2009). "The Asteroid Lightcurve Database." *Icarus* **202**, 134-146. Updated 2021 Dec. *http://www.minorplanet.info/lightcurvedatabase.html*

PHOTOMETRY OF 10 ASTEROIDS AT SOPOT ASTRONOMICAL OBSERVATORY: 2022 MAY - OCTOBER

Vladimir Benishek
Belgrade Astronomical Observatory
Volgina 7, 11060 Belgrade 38, SERBIA
vlaben@yahoo.com

(Received: 2022 October 14)

Lightcurves and synodic rotation periods established for 10 asteroids using photometric observations carried out at Sopot Astronomical Observatory in the time span 2022 May - October are presented in this paper.

Photometric observations of 10 asteroids were conducted at Sopot Astronomical Observatory (SAO) from 2022 May through 2022 October in order to determine the asteroids' synodic rotation periods. For this purpose, two 0.35-m *f*/6.3 Meade LX200GPS Schmidt-Cassegrain telescopes were employed. The telescopes are equipped with a SBIG ST-8 XME and a SBIG ST-10 XME CCD cameras. The exposures were unfiltered and unguided for all targets. Both cameras were operated in 2×2 binning mode, which produces image scales of 1.66 arcsec/pixel and 1.25 arcsec/pixel for ST-8 XME and ST-10 XME cameras, respectively. Prior to measurements, all images were corrected using dark and flat field frames.

Photometric reduction was conducted using *MPO Canopus* (Warner, 2018). Differential photometry with up to five comparison stars of near solar color ($0.5 \leq B\text{-}V \leq 0.9$) was performed using the Comparison Star Selector (CSS) utility. This helped ensure a satisfactory quality level of night-to-night zero-point calibrations and correlation of the measurements within the standard magnitude framework. Field comparison stars were calibrated using standard Cousins R magnitudes derived from the Carlsberg Meridian Catalog 15 (VizieR, 2022) Sloan r' magnitudes using the formula: R = r' - 0.22 in all cases presented in this paper. In some instances, small zero-point adjustments were necessary in order to achieve the best match between individual data sets in terms of achieving the most favorable statistical indicators of Fourier fit goodness.

Lightcurve construction and period analysis was performed using *Perfindia* custom-made software developed in the R statistical programming language (R Core Team, 2020) by the author of this paper. The essence of its algorithm is reflected in finding the most favorable solution for rotational period by minimizing the *residual standard error* of the lightcurve Fourier fit.

The lightcurve plots presented in this paper show so-called 2% error for rotational periods, i.e., an error that would cause the last data point in a combined data set by date order to be shifted by 2% (Warner, 2012) and represented by the following formula:

$$\Delta P = (0.02 \cdot P^2) / T$$

where P and T are the rotational period and the total time span of observations, respectively. Both of these quantities must be expressed in the same units. Table I gives the observing circumstances and results.

Observations and Results

1252 Celestia. There is an apparent match between the only previous rotation period determination by Worman (1995, 10.636 h) and the bimodal period (P = 10.63 ± 0.02 h) derived from the SAO data obtained in 2022 July over 6 nights.

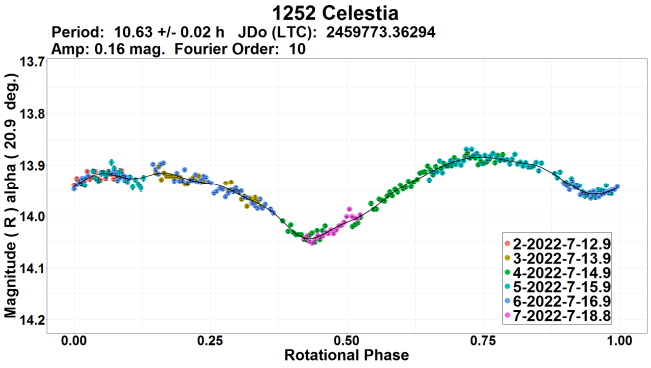

2454 Olaus Magnus. Two previous rotation periods in the Asteroid Lightcurve Database (LCDB; Warner et al., 2009) records are as follows: 3.804 h (Vargas, 2013) and a sidereal one determined by Durech et al. (2020, 3.80436 h). Observations carried out at SAO on 3 nights in 2022 July yielded a bimodal period result (P = 3.805 ± 0.002 h) in complete agreement with previous ones.

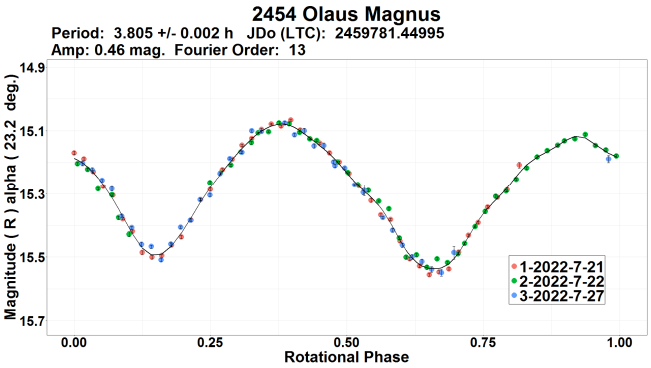

3977 Maxine. The only previously known rotation period determination result by Franco et al. (2014, 3.081 h) is completely identical to the newly determined period of P = 3.081 ± 0.007 h obtained from the SAO data acquired over 2 consecutive nights in 2022 August.

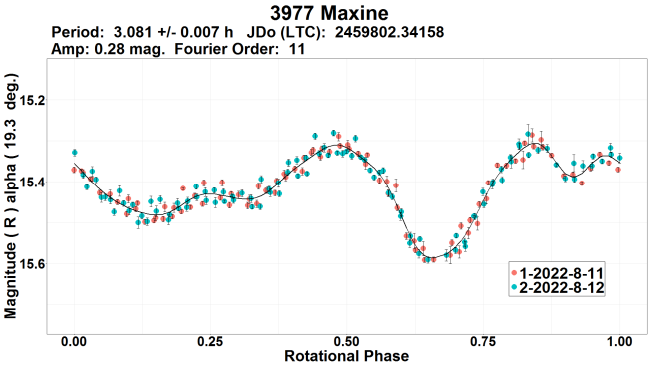

5736 Sanford. A search of the LCDB database found a value of 3.1846 h (Pravec, 2011web) as the only previously determined rotation period. Period analysis carried out upon the 2022 July SAO observations shows a statistically equal rotation period result of P = 3.1842 ± 0.0006 h.

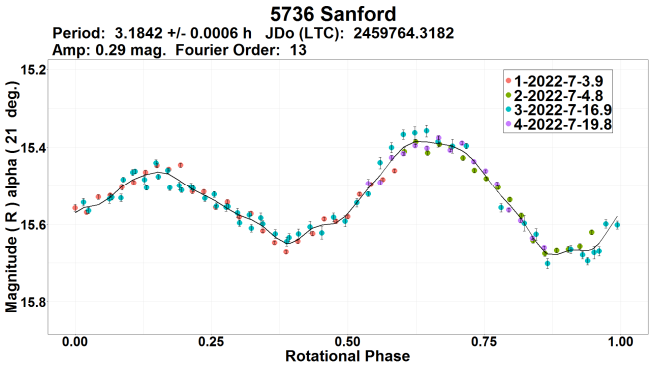

7189 Kuniko. Waszczak et al. (2015) found a rotation period of 2.922 h. SAO data obtained in late 2022 August indicate a concordant result of P = 2.924 ± 0.002 h.

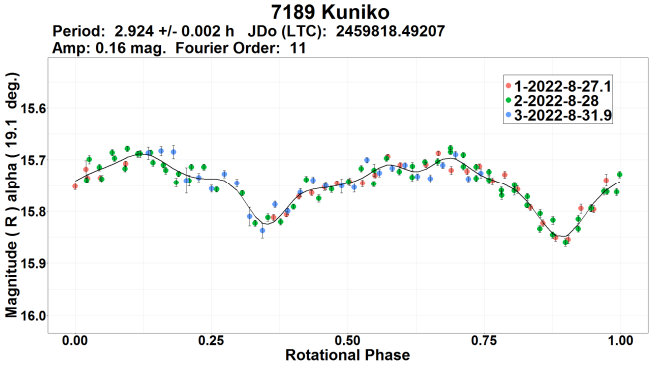

7365 Sejong. Rotation period result of P = 2.5804 ± 0.0002 h found from the SAO data collected over 7 nights in 2022 June - July is fully accordant with the previous period determinations by Pravec (2019web, 2.5802 h), Polakis (2020, 2.579 h) and slightly different from the period obtained by Yeh et al. (2020, 2.59 h).

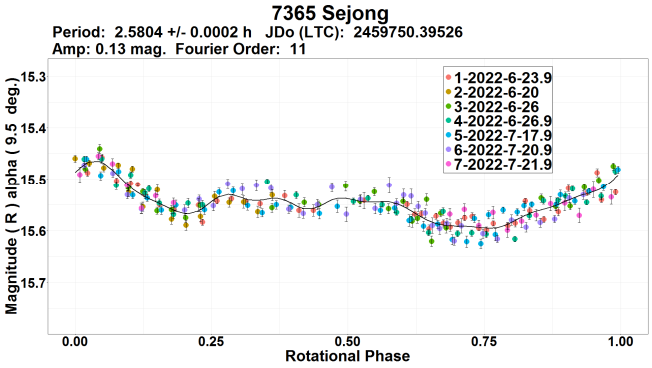

13520 Felicienrops. No clearly defined rotation periods found in the LCDB database. Observations conducted in 2022 June - July point to a fairly plausible low-amplitude lightcurve solution associated with a period of P = 2.9270 ± 0.0005 h.

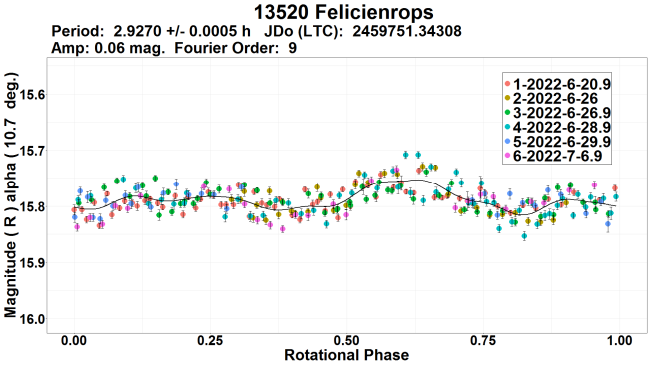

(16556) 1991 VQ1. According to the LCDB database records the result of this rotation period determination could be considered the first one for this asteroid. Data collected over 3 nights in early 2022 October yield a unique relatively short rotational period of P = 2.653 ± 0.002 h.

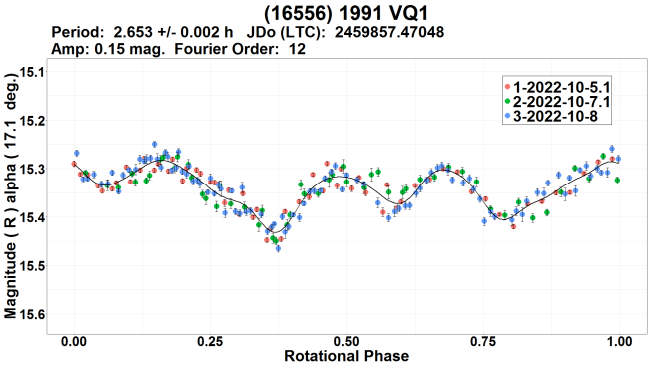

(25332) 1999 KK6. The result for a rotation period of P = 2.451 ± 0.001 h derived from the 2022 May SAO photometric data is consistent with the vast majority of rotation period results previously obtained for this Hungaria family asteroid found in the LCDB, for example: 2.4531 h (Warner, 2008); 2.453 h (Warner, 2013); 2.4531 h (Warner, 2016); 2.452 h (Dose, 2021).

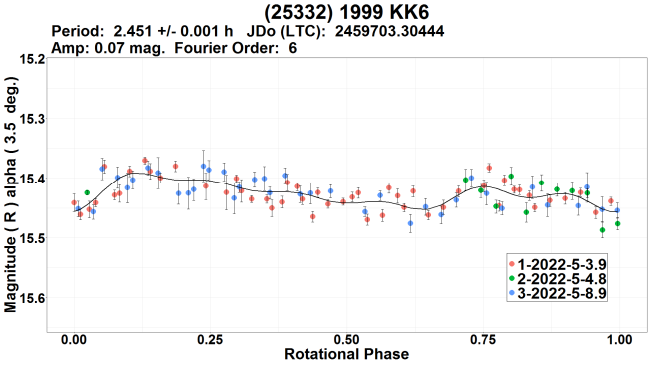

Number	Name	20yy/mm/dd	Phase	L_{PAB}	B_{PAB}	Period (h)	P.E.	Amp	A.E.	Grp
1252	Celestia	22/07/12-22/07/18	22.1,22.6	257	36	10.63	0.02	0.16	0.01	PAL
2454	Olaus Magnus	22/07/20-22/07/27	23.2,20.7	330	7	3.805	0.002	0.46	0.02	MAT
3977	Maxine	22/08/10-22/08/12	19.3,18.9	356	13	3.081	0.007	0.28	0.02	EUN
5736	Sanford	22/07/03-22/07/19	21.0,25.2	276	29	3.1842	0.0006	0.29	0.02	PHO
7189	Kuniko	22/08/26-22/08/31	19.1,16.7	2	-1	2.924	0.002	0.16	0.02	MB-I
7365	Sejong	22/06/19-22/07/21	8.0,22.2	262	10	2.5804	0.0002	0.13	0.02	MB-I
13520	Felicienrops	22/06/20-22/07/07	*10.7,11.2	276	17	2.9270	0.0005	0.06	0.03	MB-I
16556	1991 VQ1	22/10/04-22/10/08	17.1,15.5	34	-8	2.653	0.002	0.15	0.02	MB-I
25332	1999 KK6	22/05/03-22/05/08	3.5,7	218	0	2.451	0.001	0.07	0.03	HUN
29798	1999 CP79	22/07/21-22/07/24	11.0,10.1	319	9	5.01	0.01	0.41	0.03	EUN

Table I. Observing circumstances and results. Phase is the solar phase angle given at the start and end of the date range. If preceded by an asterisk, the phase angle reached an extrema during the period. L_{PAB} and B_{PAB} are the average phase angle bisector longitude and latitude. Grp is the asteroid family/group (Warner *et al.*, 2009): PAL = Pallas, MAT = Matterania, HUN = Hungaria, MB-I = main-belt inner, PHO = Phocaea, EUN = Eunomia.

(29798) 1999 CP79. No prior rotation period determination results were known. Three datasets obtained in 2022 July reveal an unambiguous bimodal solution for period of P = 5.01 ± 0.01 h.

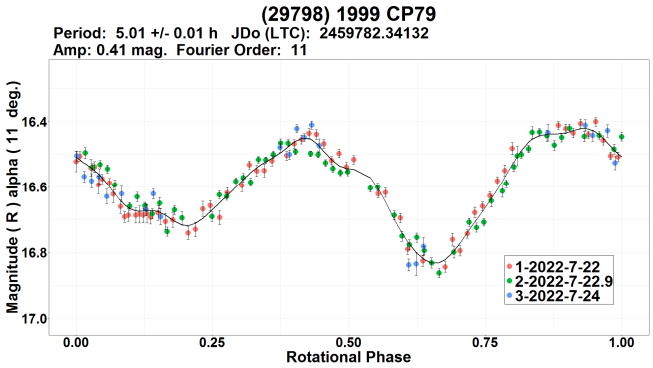

Acknowledgements

Observational work at Sopot Astronomical Observatory is generously supported by Gene Shoemaker NEO Grants awarded by the Planetary Society in 2018 and 2022.

References

Dose, E.V.(2021). „Lightcurves of Nineteen Asteroids.“ *Minor Planet Bull.* **48**, 69-76.

Durech, J.; Tonry, J.; Erasmus, N.; Denneau, L.; Heinze, A.N.; Flewelling, H.; Vančo, R. (2020). “Asteroid models reconstructed from ATLAS photometry.” *Astron. Astrophys.* **643**, A59-A63.

Franco, L.; Tomassini, A.; Scardella, M. (2014). “The Rotation Period of 3977 Maxine.” *Minor Planet Bull.* **41**, 1.

Polakis, T. (2020). “Photometric Observations of Ten Minor Planets.” *Minor Planet Bull.* **47**, 13-17.

Pravec, P. (-2011web, -2019web). Photometric Survey for Asynchronous Binary Asteroids web site. *http://www.asu.cas.cz/~ppravec/newres.txt*

R Core Team (2020). R: A language and environment for statistical computing. R Foundation for Statistical Computing. Vienna. Austria. *https://www.R-project.org/*

Vargas, A. (2013). “Synodic Period for 2454 Olaus Magnus from Frank T. Etscorn Observatory. ” *Minor Planet Bull.* **40**, 61.

VizieR (2022). *http://vizier.u-strasbg.fr/viz-bin/VizieR*

Warner, B.D. (2008). “Asteroid Lightcurve Analysis at the Palmer Divide Observatory: September-December 2007.” *Minor Planet Bull.* **35**, 67-71.

Warner, B.D.; Harris, A.W.; Pravec, P. (2009). “The Asteroid Lightcurve Database.” *Icarus* **202**, 134-146. Updated 2021 Dec. *http://www.minorplanet.info/lightcurvedatabase.html*

Warner, B.D. (2012). *The MPO Users Guide: A Companion Guide to the MPO Canopus/PhotoRed Reference Manuals*. BDW Publishing, Eaton, CO.

Warner, B.D. (2013). “Rounding Up the Unusual Suspects.” *Minor Planet Bull.* **40**, 36-42.

Warner, B.D. (2016). “Asteroid Lightcurve Analysis at CS3-Palmer Divide Station: 2015 December - 2016 April.” *Minor Planet Bull.* **43**, 227-233.

Warner, B.D. (2018). MPO Canopus software, version 10.7.11.3. *http://www.bdwpublishing.com*

Waszczak, A.; Chang, C.-K.; Ofek, E.O.; Laher, R.; Masci, F.; Levitan, D.; Surace, J.; Cheng, Y.-C.; Ip, W.-H.; Kinoshita, D.; Helou, G.; Prince, T.A.; Kulkarni, S. (2015). “Asteroid Light Curves from the Palomar Transient Factory Survey: Rotation Periods and Phase Functions from Sparse Photometry.” *Astron. J.* **150**, A75.

Worman, W.E. (1995). “CCD Photometry of 1252 Celestia.” *Minor Planet Bull.* **22**, 39-40.

Yeh, T.-S.; Li, B.; Chang, C.-K.; Zhao, H.-B.; Ji, J.-H.; Lin, Z.-Y.; Ip, W.-H. (2020). “The Asteroid Rotation Period Survey Using the China Near-Earth Object Survey Telescope (CNEOST).” *The Astronomical Journal* **160**, id. 73.

LIGHTCURVES OF NINETEEN ASTEROIDS

Eric V. Dose
3167 San Mateo Blvd NE #329
Albuquerque, NM 87110
mp@ericdose.com

(Received: 2022 October 15 Revised: 2022 November 12)

We present lightcurves, synodic rotation periods, and G slope value (H-G) estimates for nineteen asteroids.

We present asteroid lightcurves obtained via the workflow process described by Dose (2020) and as later improved (Dose, 2021a). This workflow applies to each image an ensemble of typically 20-60 nearby comparison ("comp") stars selected from the ATLAS refcat2 catalog (Tonry et al., 2018). Custom diagnostic plots and the abundance of comp stars allow for rapid identification and removal of outlier, variable, and poorly measured comp stars.

The product of this custom workflow is one night's time series of absolute magnitudes for the target asteroid, all on Sloan r' (SR) catalog basis. These magnitudes are imported directly into *MPO Canopus* software (Warner, 2021) where they are adjusted for distances and phase-angle dependence, fit by Fourier analysis including identifying and ruling out of aliases, and plotted. Phase-angle dependence is corrected with a H-G model, using the G slope value minimizing best-fit RMS error across all nights' data. No nightly zero-point adjustments (DeltaComps in *MPO Canopus* terminology) were made to any session herein, other than by adjusting the G slope value (H-G phase model).

Lightcurve Results

Nineteen asteroids were observed from New Mexico Skies Observatory at 2310 meters elevation in southern New Mexico. Images were acquired with a 0.35 m SCT reduced to f/7.7; a SBIG STXL-6303E camera cooled to -35 C and fitted with an Exoplanet/Blue Blocker (BB) filter (Astrodon); and a PlaneWave L-500 mount. The equipment was operated remotely via ACP software (DC-3 Dreams, version 8.3), running plan files generated for each night by the author's python scripts (Dose, 2020). Exposures were autoguided, and exposure times targeted 3-4 millimagnitudes uncertainty in asteroid instrumental magnitude, subject to a minimum exposure of 150 seconds to ensure suitable comp-star photometry, and to a maximum of 900 seconds.

FITS images were plate-solved by *PinPoint* (DC-3 Dreams) or *TheSkyX* (Software Bisque) and were calibrated using temperature-matched, median-averaged dark images and recent flat images of a flux-adjustable flat panel. Every photometric image was visually inspected; the author excluded all images with poor tracking, obvious interference by cloud or moon, or having stars, satellite tracks, cosmic ray artifacts, or other apparent light sources within 10 arcseconds of the target asteroid. Images passing these screens were submitted to the workflow. The BB filter, a yellow filter with relatively sharp wavelength cut-off, requires only a modest first-order transform to the standard Sloan r' passband. Using this BB filter, rather than a clear filter or no filter, improves night-to-night reproducibility to a degree outweighing any loss of signal-to-noise ratio.

In this work, "period" refers to an asteroid's synodic rotation period, "SR" denotes the Sloan r' passband, and "mmag" denotes millimagnitudes (0.001 magnitude).

282 Clorinde. This inner main-belt asteroid has numerous published rotation periods (6.42 h, Binzel and Mulholland, 1983; 12.142 h, Behrend, 2018web; 49.365 h, Ďurech et al., 2020; 49.352 h, Bonamico and van Belle, 2021; and 49.350 h, Pilcher, 2022). We confirm the more recent reports with our determination of 49.280 ± 0.006 h. Our lightcurve is built from 12 nights' data taken over 12 weeks; a large number of nights is needed to obtain full coverage as the period is rather close to two sidereal days. The lightcurve shape is clearly bimodal. Our best estimate of G (H-G phase model) is 0.03; Fourier fit RMS error is 7 mmag.

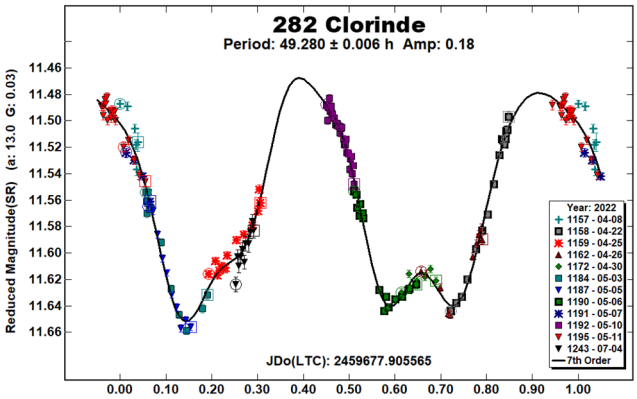

414 Liriope. For this outer main-belt asteroid, the author confirms the most recent period determinations (11.005 h, Colazo et al., 2020; 11.0065 h, Pál et al., 2020; 11.007 h, Dose, 2021c) with a new determination of 11.004 ± 0.001 h, derived from observations at a new viewing aspect (phase angle bisector). This new lightcurve (PAB = 209° longitude, 11° latitude) and the author's 2021 lightcurve (PAB = 147° longitude, 7° latitude) are remarkably similar in shape and amplitude, suggesting that 414 Liriope's rotational axis may be nearly aligned with the ecliptical axis. The present Fourier fit RMS error is 8 mmag; G value (H-G model) of roughly 0.16 gave optimum fit.

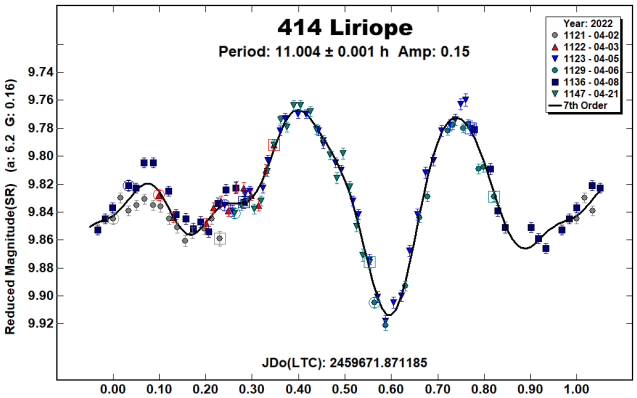

866 Fatme. New observations and period solution of 23.215 ± 0.001 h for this outer main-belt asteroid decidedly fail to confirm previous period reports, including the author's own from 2021 (20.03 h, Stephens, 2002; 9.4 h, Behrend, 2004web; 9.36 h, Behrend, 2012web; 20.7 h, Aznar Macias et al., 2016; 5.800 h, Polakis, 2018b; 11.600 h, Dose, 2021b). The new Fourier fit RMS error is 8 mmag, and best G value is approximately 0.08.

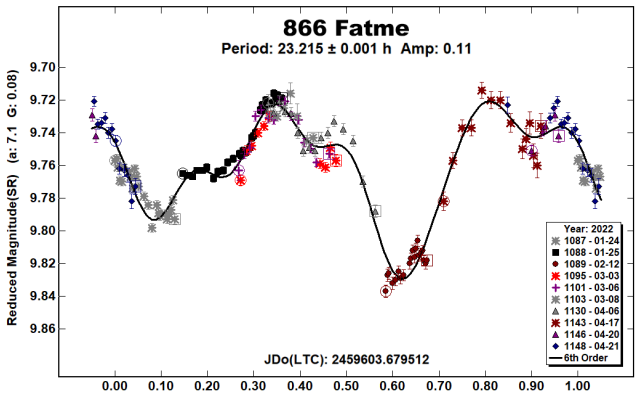

A split-halves plot of the new observations appears clearly support a bimodal interpretation. But the author's 2021 lightcurve at exactly half the present period appeared bimodal as well. And beyond that: Polakis' 2018 lightcurve with period 5.800 h, which is *one quarter* of the present solution, could itself be interpreted as bimodal. The author speculates that the asteroid's shape could be quite unusual but has no explanation for how these three relatively high-quality lightcurves could differ in such a manner. Most likely, this is a tale of caution where bi-modality assumptions fail for low amplitude objects (see Harris et al., 2014.).

866 Fatme clearly needs careful observation at future apparitions, and given the period's proximity to 24 (or 12) h, we recommend apparitions at very favorable latitude, in order to maximize session lengths. The next such apparitions are July 2024 for the Southern Hemisphere and March 2028 for the Northern Hemisphere.

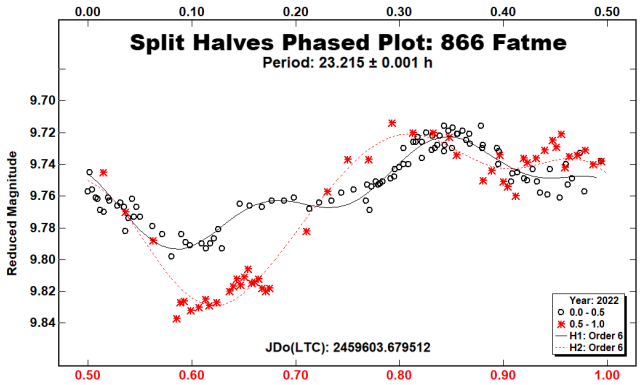

1051 Merope. We determine a synodic period of 13.710 ± 0.001 h for this Alauda-family, outer main-belt asteroid. Our result, built from 11 nights' data, agrees with that of Waszczak et al. (13.717 h, 2015) but differs from two other published solutions (27.2 h, Carbo et al., 2009; 6.85563 h, Pál et al., 2020). Our Fourier fit RMS error is 14 mmag; best G value was approximately -0.09. All positive values of G gave markedly worse fits.

The author notes that the 4 published periods show the same 1:2:4 pattern found for 866 Fatme mentioned above, though the 27.2 h lightcurve suffered incomplete phase coverage.

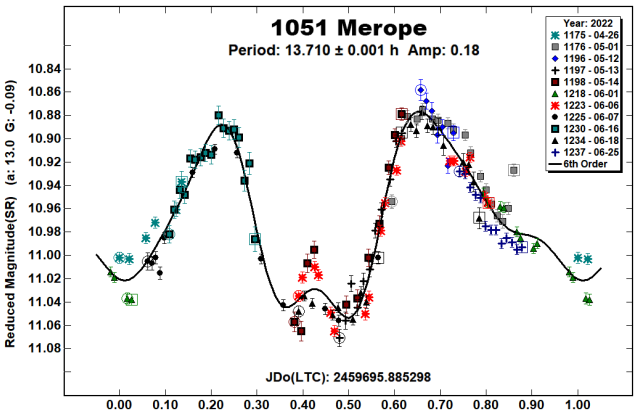

In our period spectrum, the 13.710 h solution dominates.

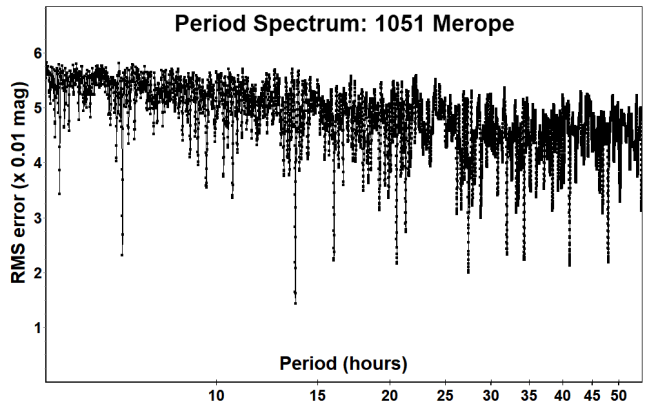

1237 Genevieve. This middle main-belt asteroid has had several reported rotation periods, all near 16.4 or 24.8 hours (16.37 h, Binzel, 1987; 24.82 h, Behrend, 2005web; 16.48 h, Polakis, 2018b; 24.6982 h, Ďurech et al., 2019; 16.31 h, Polakis, 2022). We report a period of 12.346 ± 0.004 h on a monomodal basis, which would give 24.692 h on a bimodal basis. Our lightcurve gave no indication of shape differences in alternating phases, nor does the amplitude of 0.21 magnitudes point clearly toward either basis, so the monomodal vs. bimodal nature of our lightcurve remains ambiguous. Our best G estimate is 0.15, the MPC nominal value, and Fourier RMS error is 9 mmag.

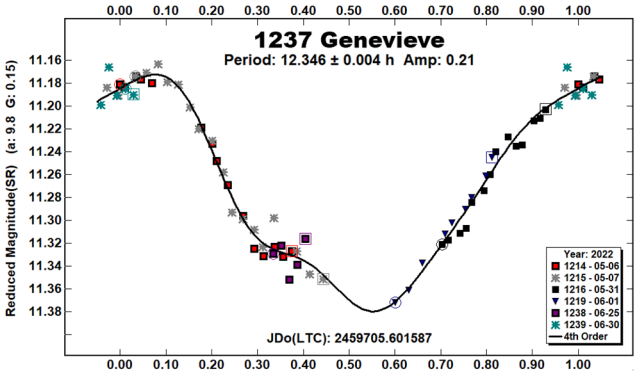

Our period spectrum disfavors rotation period estimates near 16 hours, which is an alias by ½ period per 24 hours of both period estimates 12 hours and 24 hours. This asteroid seems to call for a multi-longitude observation campaign, or a campaign benefiting from unusually favorable asteroid declination (and thus long observing sessions) to attempt to relieve the aliasing that apparently plagues single-location observation campaigns of 1237 Genevieve.

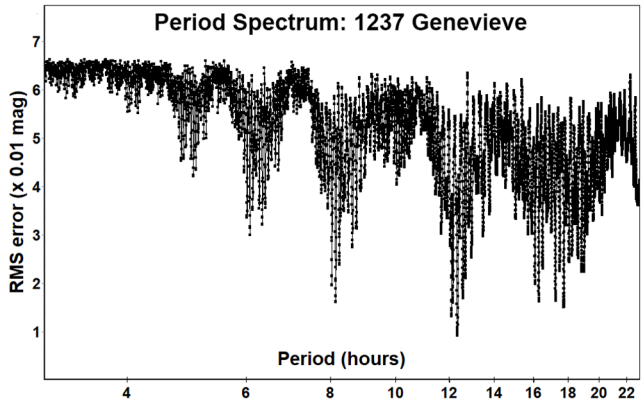

1255 Schilowa. This outer main-belt asteroid has had several rotation period reports in some disagreement (29.536 h, Behrend, 2005web; 29.7 h, Behrend, 2006web; > 24 h, Behrend, 2009web; 29.4674 h, Hanuš et al., 2013; 76.275 h, Polakis, 2018a; 38.4733 h, Pál et al., 2020). Our determination of 76.707 ± 0.019 h agrees approximately with that of Polakis and differs from the others. We note that Pál's period is half of ours, but that our lightcurve is clearly bimodal in shape. Our RMS error is 8 mmag, and our G value estimate is 0.02.

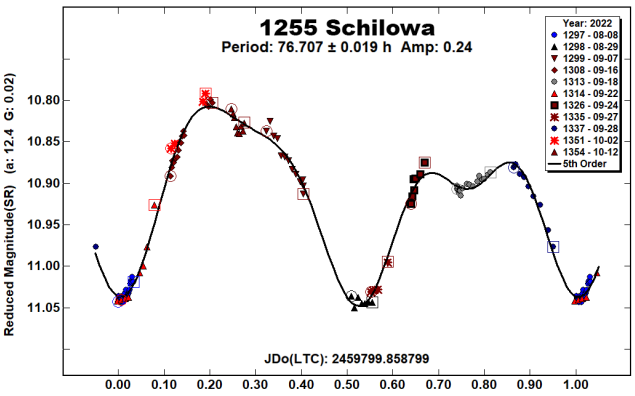

Previously reported periods near 29.6 h are an alias of our result by ½ period per sidereal day; the substantial number of our observing sessions has eliminated that alias from our period spectrum.

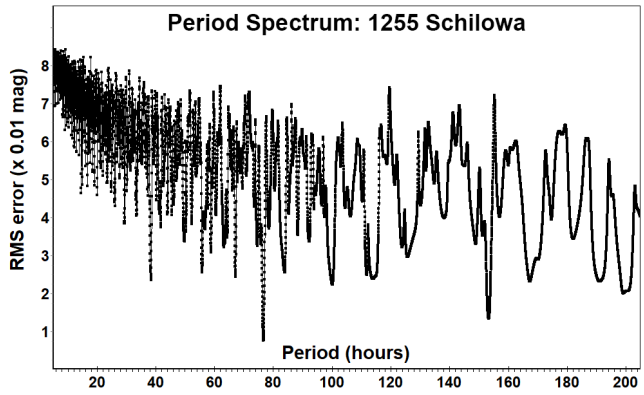

1261 Legia. For this outer main-belt asteroid, we find a period of 25.727 ± 0.002 h, differing from the sole known previous report of 8.693 h (Behrend, 2005web). Our RMS error is 16 mmag; G value of 0.07 minimized the fit error.

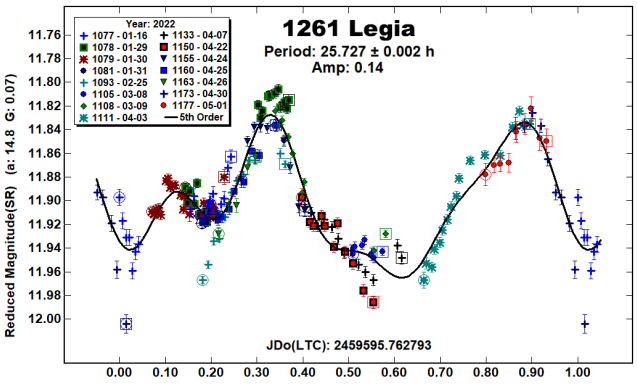

Our length of observation campaign (15 nights over 15 weeks) yields a period spectrum that supports our proposed period solution. The period spectrum does not support the previously reported period near 8.7 h.

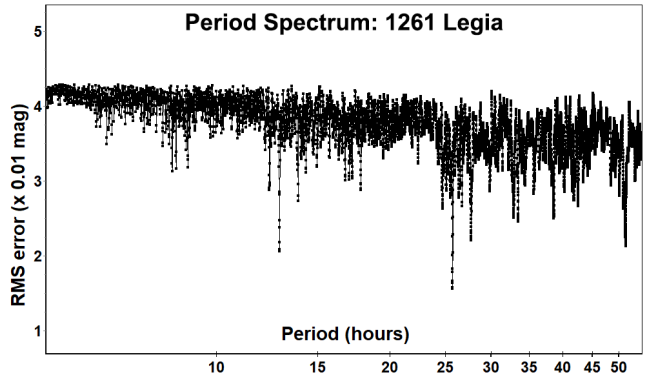

1300 Marcelle. Previous period reports (>12 h, Behrend, 2008 web; 17.9536 h, Pál et al., 2020) did not prepare us for the very long period estimate of 566.57±0.44 h that emerged from our 16 nights (across 14 weeks, about 3.8 period cycles) of observations of this outer main-belt asteroid. We have an unfortunate gap in observations around the major minimum (phase 0.93 in the lightcurve), but rest of the lightcurve is well covered, and the RMS error is only 17 mmag, or about 5% of the amplitude found. G value of 0.09 optimized the fit.

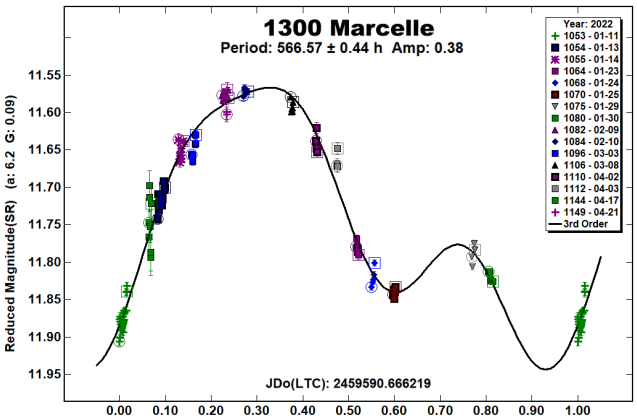

Number	Name	yyyy mm/dd	Phase	L_{PAB}	B_{PAB}	Period(h)	P.E.	Amp	A.E.	Grp
282	Clorinde	2022 04/08-07/04	*13.8,21.5	224	11	49.280	0.006	0.18	0.04	MB-I
414	Liriope	2022 04/02-04/21	*6.3,3.5	209	11	11.004	0.001	0.15	0.02	MB-O
866	Fatme	2022 01/24-04/21	*7.2,17.2	142	8	23.215	0.001	0.11	0.03	MB-O
1051	Merope	2022 04/26-06/25	*13.1,12.8	247	26	13.710	0.001	0.18	0.04	ALA
1237	Genevieve	2022 05/06-06/30	9.4,21.1	206	5	12.346	0.004	0.21	0.03	MB-M
1255	Schilowa	2022 06/08-10/12	*21.7,14.5	341	10	76.707	0.019	0.24	0.03	MB-O
1261	Legia	2022 01/16-05/01	*15.0,21.7	154	3	25.727	0.002	0.14	0.05	MB-O
1300	Marcelle	2022 01/11-04/21	*6.3,21.2	124	9	566.570	0.440	0.38	0.05	MB-O
1582	Martir	2022 03/08-04/29	*6.0,17.0	171	14	12.376	0.001	0.61	0.03	MB-O
1585	Union	2022 07/19-10/12	*11.0,21.1	320	4	12.800	0.001	0.22	0.04	MB-O
1605	Milankovitch	2022 09/24-10/04	10.2,6.8	24	-6	11.608	0.004	0.10	0.02	EOS
1724	Vladimir	2022 05/06-06/24	*10.9,11.7	248	15	12.569	0.002	0.26	0.04	MB-O
1904	Massevitch	2022 04/30-05/05	7.7,6.5	232	13	5.396	0.001	0.34	0.02	MB-O
2088	Sahlia	2022 04/02-05/02	11.0,22.3	174	0	59.550	0.008	0.90	0.03	FLO
2802	Weisell	2022 05/15-06/16	19.2,21.8	184	10	21.086	0.003	0.47	0.05	MB-O
3431	Nakano	2022 07/13-09/05	*15.0,4.4	332	4	9.056	0.002	0.13	0.03	MB-O
4429	Chinmoy	2022 09/05-10/14	*2.7,19.3	347	1	731.710	5.020	0.46	0.06	NYS
4901	O Briain	2022 07/27-09/06	*20.5,6.9	333	6	1.325	0.001	0.08	0.03	2076
12919	Tomjohnson	2022 07/18-09/24	*9.6,28.3	312	8	8.149	0.001	0.52	0.04	MB-I

Table I. Observing circumstances and results. The phase angle is given for the first and last date. If preceded by an asterisk, the phase angle reached an extrema during the period. L_{PAB} and B_{PAB} are the approximate phase angle bisector longitude/latitude at mid-date range (see Harris et al., 1984). Grp is the asteroid family/group (Warner et al., 2009).

Despite the gap in lightcurve phase coverage, our period spectrum appears to rule out periods shorter than about 300 h.

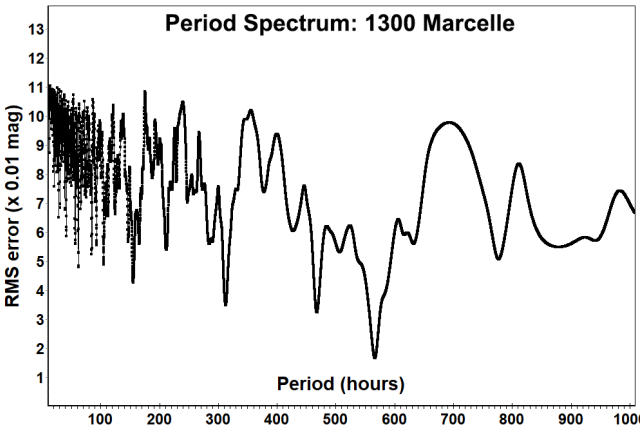

1582 Martir. This relatively well-studied outer main-belt asteroid has recently been found to have synodic rotation period near 12.37 h (12.37670 h, Ďurech et al., 2018; 12.366 h, McNeill et al., 2019; 12.3754 h, Pál et al., 2020; 12.372 h, Stephens and Warner, 2021); earlier reports differed (15.757 h, Warner, 2000; 15.668 h, Warner, 2006; 9.84 h, Warner, 2010). We were fortunate to observe 1582 Martir while its lightcurve amplitude was greater than previously reported, and we confirm the more recent reports with our period of 12.376 ± 0.001 h. Our Fourier fit RMS error is 16 mmag; G value of 0.04 minimized that fit error.

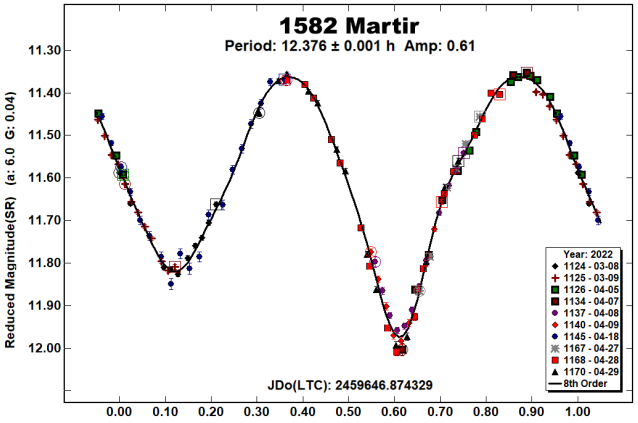

Our lightcurve coverage is complete despite the period's proximity to ½ sidereal day. The resulting period spectrum is reassuring, with signals only at multiples of half our proposed period. It does not support periods near 9.8 h (an alias of our solution by ½ period per 24 h) or near 15.6 h.

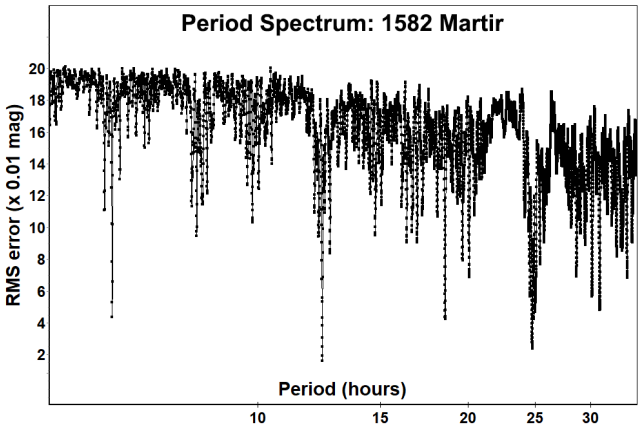

1585 Union. Of the rotation period reports for this relatively bright outer main-belt asteroid (9.38 h, Binzel, 1987; 24 h, Behrend, 2004web; 12.798 h, Polakis, 2019; 12.7993 h, Ďurech et al., 2020; 12.7988 h, Pál et al., 2020) we confirm the more recent of these with our estimate of 12.800 ± 0.001 h. The lightcurve shape is clearly bimodal. Our Fourier fit RMS error is 11 mmag, and our best estimate of G is 0.17.

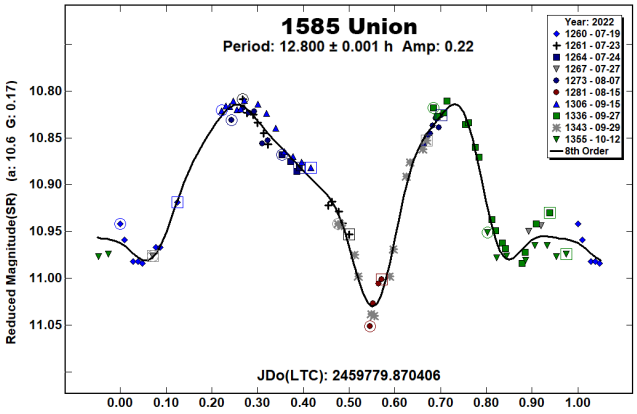

1605 Milankovitch. Our new rotation period estimate for this outer main-belt asteroid agrees with two published periods (11.60 h, Cooney, 2005; 11.63 h, Behrend, 2006web) but differs from two others (11.111 h, Carreño et al., 2020; 5.80104 h, Pál et al., 2020).

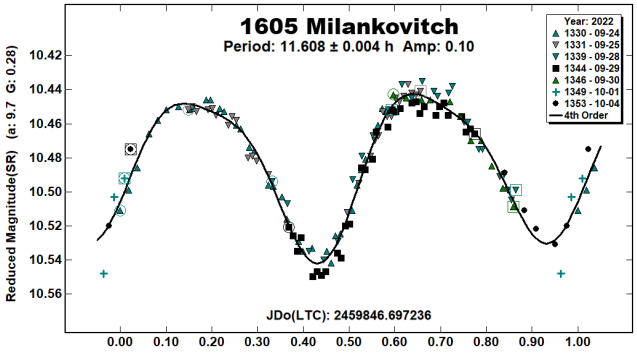

The period spectrum strongly disfavors other period candidates that are not multiples of our estimate. The published estimate of 11.111 h cannot readily be explained as an alias of our result.

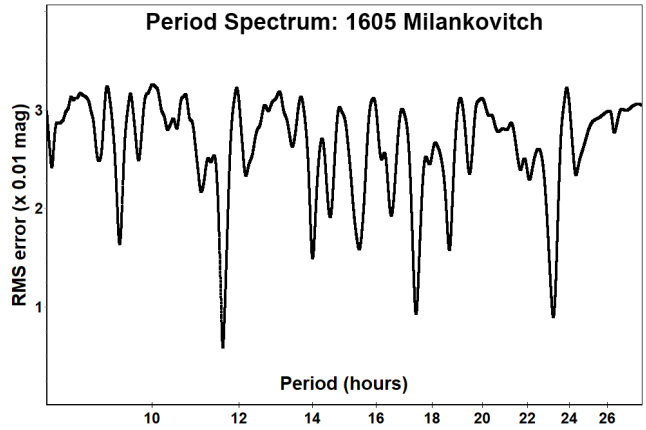

At the aspect from which our observations were taken, the lightcurve is very probably bimodal; in particular, the minima do not quite coincide in magnitude.

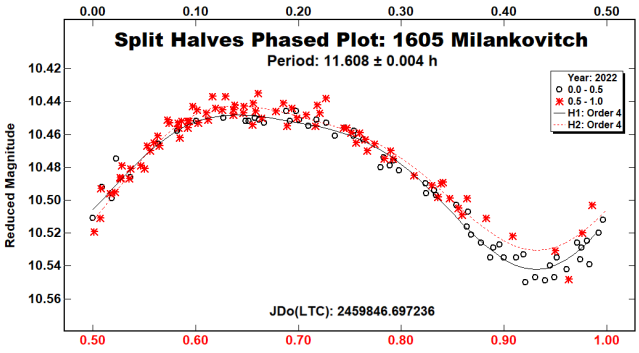

1724 Vladimir. For this outer main-belt asteroid, we confirm previous period reports, all with LCDB uncertainty codes of 2 (12.57 h, Benishek, 2011web; 12.582 h, Benishek, 2015; 12.574 h and 12.557 h, Waszczak et al., 2015; 12.56792 h, Ďurech et al., 2020), with our determination of 12.569 ± 0.002 h. Our Fourier fit RMS error is 17 mmag; G value of 0.04 minimized that fit error.

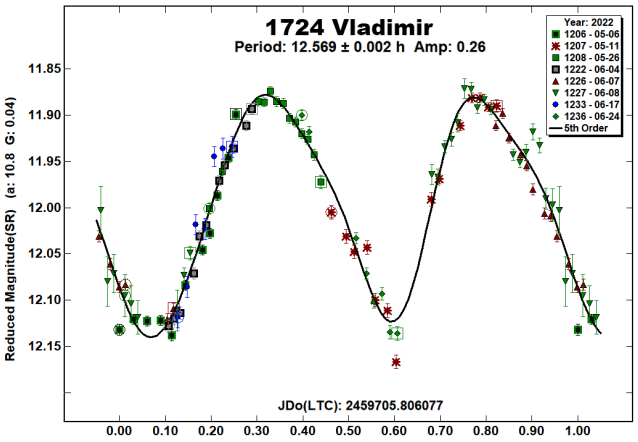

1904 Massevitch. For this outer main-belt asteroid, we confirm previous period reports (5.394 h, Bohn et al., 2015; 5.395389 h, Ďurech et al., 2019) with our finding of 5.3961 ± 0.0006 h. RMS fit error is 12 mmag; G value of 0.30 optimized the fit.

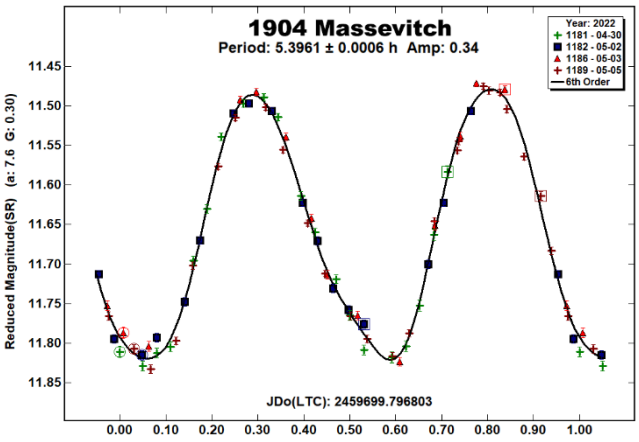

The period spectrum has secondary signals at multiples of half of our proposed period; the deepest minimum is at our proposed period.

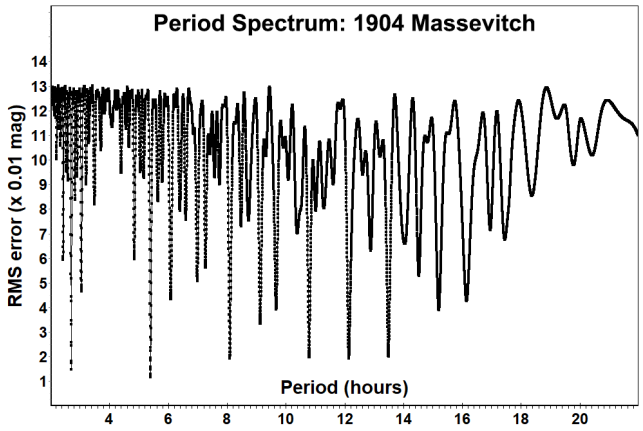

2088 Sahlia. This Flora-family asteroid has had three period reports, all differing (10.37 h, Binzel and Mulholland, 1983; 36.717 h, Erasmus et al., 2020; 58.3 h, Podlewska-Gaca et al., 2021). We generally confirm the most recent with our estimate of 59.550 ± 0.008 h. RMS error is 24 mmag; G value of 0.27 optimizes the Fourier fit.

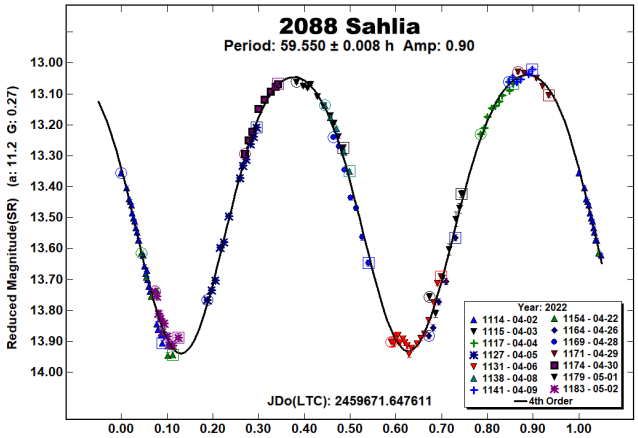

The very high lightcurve amplitude persuades us to adopt the bimodal interpretation at 59.550 h. Our period spectrum does not support previously reported periods near 10.4 h or 36.7 h (which is an alias of the present solution by exactly ¼ period per 24 h). Given the period's proximity to 60 h (2.5 days), this asteroid will benefit from longer observing sessions at apparitions of favorable latitude, of which the next will be August 2023 for the Southern Hemisphere and January 2025 for the Northern Hemisphere.

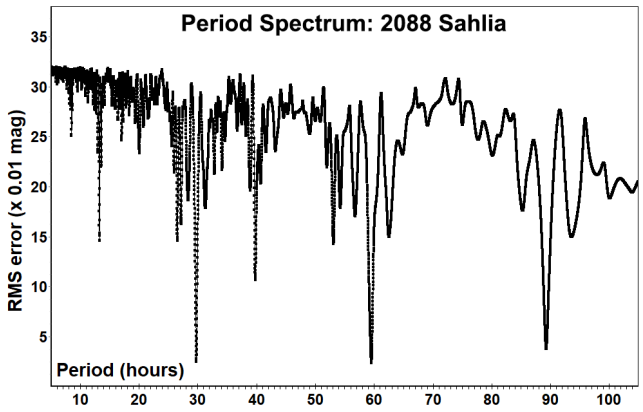

2802 Weisell. For this outer main-belt asteroid we report a period of 21.086 ± 0.003 h, in agreement with three previous reports (21.11 h, Behrend, 2006web; 21.078 h, Behrend, 2011web; 21.0966 h, Ďurech et al., 2019) but differing from two others (14.683 h, Brinsfield, 2011; 37.705 h, Hanuš et al., 2016).

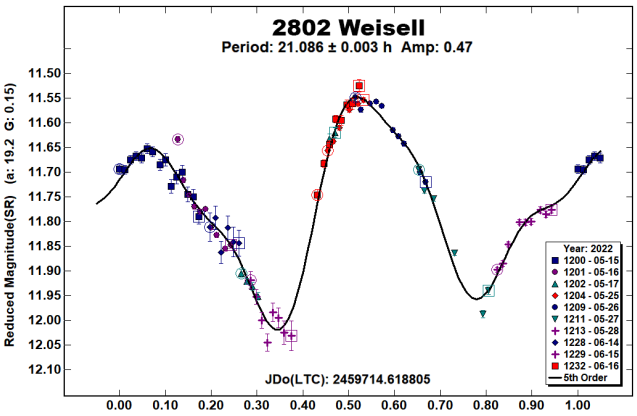

The period spectrum's strongest signal is at the proposed period, and the next-largest is at three-halves the proposed period. It does not support periods near 14.68 h or 37.7 h, both in fact being aliases of our solution by ½ period per 24 h.

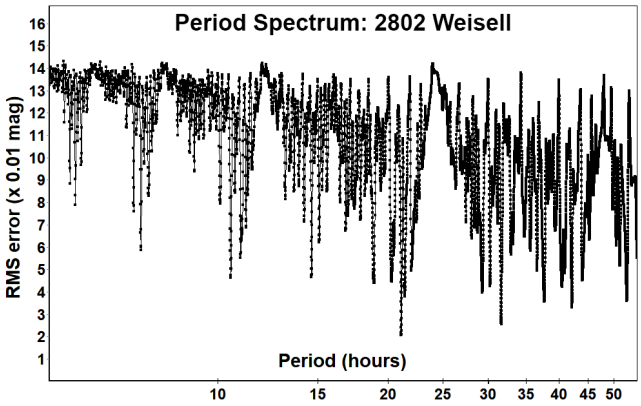

3431 Nakano. All known previous rotation period reports (8.90 h, Warner, 2003; 9.2 h, Warner, 2011; 9.0863 h, Brincat, 2017web; 9.0563 h, Brincat and Galdies, 2018; 9.05427 h, Ďurech et al., 2020) for this outer main-belt asteroid are near 9 hours, and our period estimate of 9.056 ± 0.002 h confirms them. The lightcurve shape is clearly bimodal. Fourier fit RMS error is 10 mmag, and our best estimate of G is 0.11.

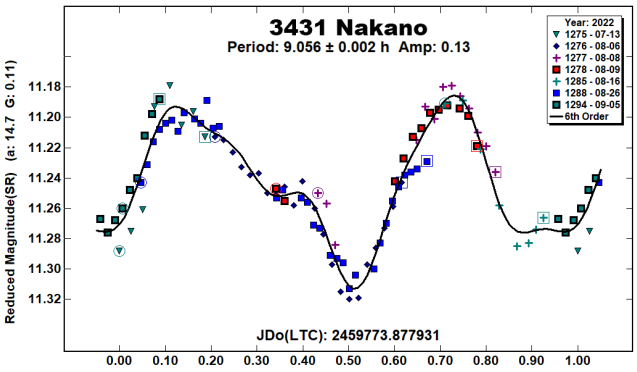

4429 Chinmoy. No previous period reports were found for this relatively faint Hertha/Nysa-family asteroid. We propose a

bimodal-basis rotation period of 731.7 ± 5.0 h, based on observations over 15 nights. The observation campaign covered only 40 calendar days, or about 1.3 rotation periods, but the large apparent amplitude helped us discern the lightcurve shape early on. The Fourier fit RMS error is 35 mmag; we could not distinguish the G value from MPC's default value of 0.15.

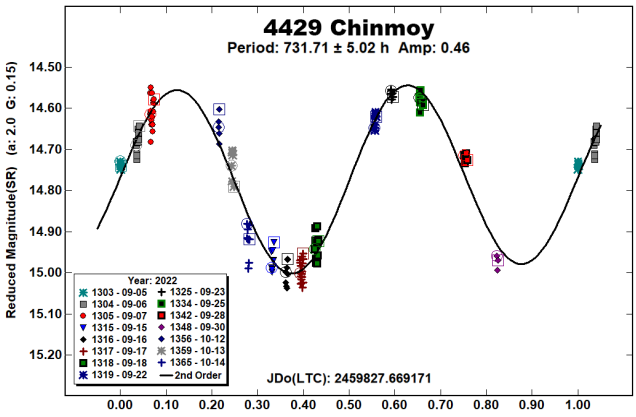

The minimum in our period spectrum actually falls at 366 h, that is, at half our proposed period estimate, but the lightcurve's large amplitude persuades us to adopt the bimodal value instead. In any case, periods shorter than about 300 h appear to be ruled out.

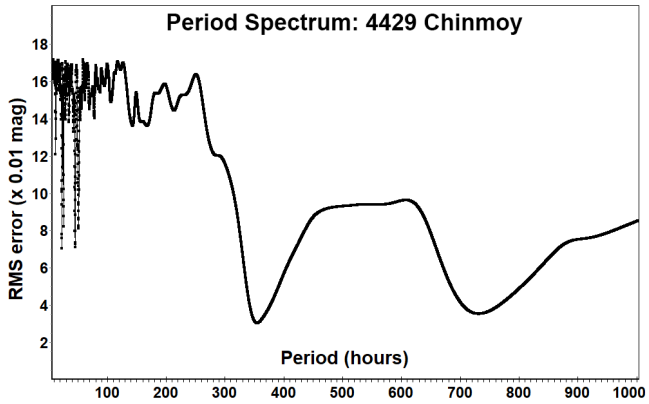

4901 O Briain. This Levin-family asteroid has no known rotation period reports. Our estimate of 1.3250 ± 0.0005 h on a monomodal basis would classify this asteroid squarely as a fast rotator, but interpreting the lightcurve as bimodal would render it a more normal case. Neither the split-halves plot nor the amplitude of 0.08 magnitudes helps to decide between monomodal and bimodal possibilities and thus the true, physical rotation rate. Our Fourier fit RMS error is 16 mmag, and our G estimate is 0.29.

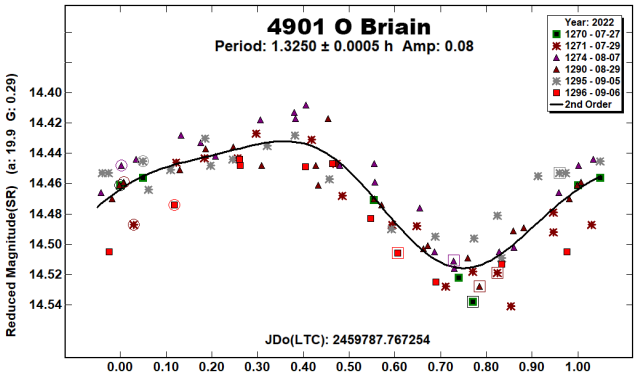

The period spectrum strongly supports our proposed period estimate, but it does not help in choosing between monomodal and bimodal lightcurve interpretations. The possibility of (4901) O Briain's being a fast rotator makes it an attractive candidate for future observation campaigns.

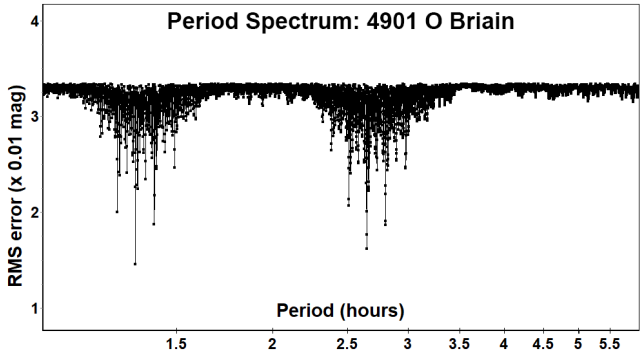

12919 Tomjohnson. This inner main-belt asteroid has no known rotation period reports. Despite the unfavorable declination for our observing site which served to limit duration of our observing sessions, we obtained an estimated period of 8.149 ± 0.001 h. The relatively large lightcurve amplitude lends confidence to the bimodal interpretation as suggested by the differing brightnesses of alternating minima. Fourier fit RMS error is 28 mmag, and our G estimate is 0.12.

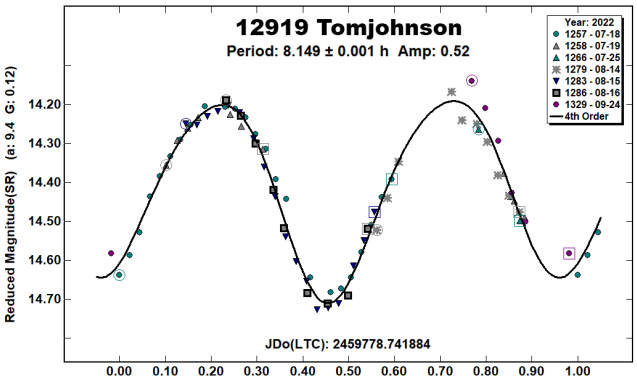

The four major signals within the period spectrum comprise a series of 1, 1.5, 2, and 2.5 times our proposed period. Despite the period's proximity to 8 hours (one-third day), other aliases have been suppressed by the use of data from seven nights variously spaced.

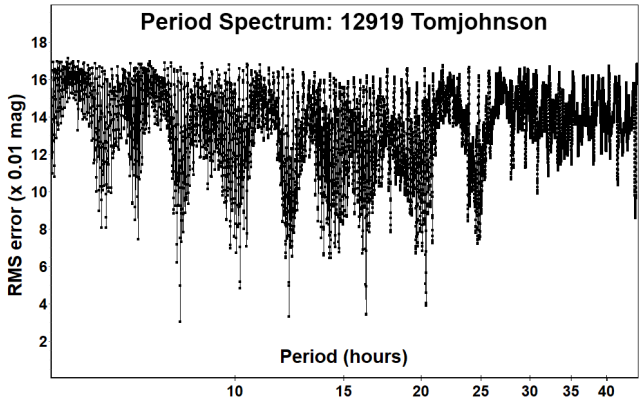

Acknowledgements

The author thanks authors of and contributors to the ATLAS paper (Tonry et al., 2018) for providing openly and without cost the ATLAS refcat2 catalog release. This current work also makes extensive use of the python language interpreter and of several supporting packages (notably: astropy, ccdproc, ephem, matplotlib, pandas, photutils, requests, and statsmodels), all made available openly and without cost.

References

Aznar Macías, A.; Carreno Garcerain, A.; Arce Masego, E.; Brines Rodriques, P.; Lozano de Haro, J.; Fornas Silva, A.; Fornas Silva, G.; Mas Martinez, V.; Rodrigo Chiner, O.; Herrero Porta, D. (2016). "Twenty-one Asteroid Lightcurves at Group Observadores de Asteroides (OBAS): Late 2015 to Early 2016." *Minor Planet Bull*. **43**, 257-263.

Behrend, R. (2004web, 2005web, 2006web, 2008web, 2009web, 2011web, 2012web, 2018web). Observatoire de Genève web site. *http://obswww.unige.ch/~behrend/page_cou.html*

Benishek, V. (2011web). *http://beoastrophot.freehostia.com* Web page not accessible July 2022; data retrieved from LCDB entry.

Benishek, V. (2015). "Rotation Period Determinations for 1724 Vladimir, 3965 Konopleva, and 9222 Chubey." *Minor Planet Bull.* **42**, 143-144.

Binzel, R.P.; Mulholland, J.D. (1983). "A photoelectric lightcurve survey of small main belt asteroids." *Icarus* **56**, 519-533.

Binzel, R.P. (1987). "A photoelectric survey of 130 asteroids." *Icarus* **72**, 135-208.

Bohn, L; Hibbler, B.; Stein, G.; Ditteon, R. (2015). "Asteroid Lightcurve Analysis at the Oakley Southern Sky Observatory: 2014 September." *Minor Planet Bull.* **42**, 89-90.

Bonamico, R.; van Belle, G. (2021). "Determining the Rotational Period of Main-Belt Asteroid 282 Clorinde." *Minor Planet Bull*. **48**, 210.

Brincat (2017web). As retrieved October 2022 from the Lightcurve Database (LCDB), reference to web page not available.

Brincat, S.M.; Galdies, C. (2018). "Photometric Observations of Main-Belt Asteroids 1968 Mehltretter, 2681 Ostrovskij & 3431 Nakano." *Minor Planet Bull*. **45**, 244-245.

Brinsfield, J.W. (2011). "Asteroid Lightcurve Analysis at the Via Capote Observatory: 1st Quarter 2011." *Minor Planet Bull.* **38**, 154-155.

Carbo, L.; Green, D.; Kragh, K.; Krotz, J.; Meiers, A.; Patino, B.; Pligge, Z.; Shaffer, N.; Ditteon, R. (2009). "Asteroid Lightcurve Analysis at the Oakley Southern Sky Observatory: 2008 October thru 2009 March." *Minor Planet Bull.* **36**, 152-157.

Carreño, A.; Fornas, G.; Arce, E.; Mas, V. (2020). "Twelve Main Belt Asteroids, One Near Earth and One Potentially Hazardous Asteroid Lightcurves at Asteroids Observers (OBAS) - MPPD: 2017 May - 2019 Jan." *Minor Planet Bull.* **47**, 7-10.

Colazo, L.C.; Fornari, C.; Santucho, M.; Mottino, A.; Colazo, C.; Melia, R.; Suarez, N.; Vasconi, N.; Arias, D.; Stechina, A.; Scotta, D.; García, J.; Pittari, C.; Ferrero, G. (2020). "Asteroid Photometry and Lightcurve Analysis at GORA's Observatories - Part II." *Minor Planet Bull*. **47**, 337-339.

Cooney, W.R., Jr. (2005). "Lightcurve Results for Minor Planets 228 Agathe, 297 Caecillia, 744 Aguntina, 1062 Ljuba, 1605 Milankovitch, and 3125 Hay." *Minor Planet Bull*. **32**, 15-16.

Dose, E. (2020). "A New Photometric Workflow and Lightcurves of Fifteen Asteroids." *Minor Planet Bull*. **47**, 324-330.

Dose, E. (2021a). "Lightcurves of Nineteen Asteroids." *Minor Planet Bull*. **48**, 69-76.

Dose, E. (2021b). "Lightcurves of Eighteen Asteroids." *Minor Planet Bull.* **48**, 125-132.

Dose, E.V. (2021c). "Lightcurves of Fourteen Asteroids." *Minor Planet Bull.* **48**, 228-233.

Ďurech, J.; Hanuš, J.; Alí-Lagoa, V. (2018). "Asteroid models reconstructed from the Lowell Photometric Database and WISE data." *Astron. Astrophys.* **617**, A57.

Ďurech, J.; Hanuš, J.; Vančo, R. (2019). "Inversion of asteroid photometry from *Gaia* DR2 and the Lowell Observatory photometric database." *Astron. Astrophys.* **631**, A2.

Ďurech, J.; Tonry, J.; Erasmus, N.; Denneau, L.; Heinze, A.N.; Flewelling, H.; Vančo, R. (2020). "Asteroid models reconstructed from ATLAS photometry." *Astron. Astrophys.* **643**, A59.

Erasmus, N.; Navarro-Meza, S.; McNeill, A.; Trilling, D.E.; Sickafoose, A.A.; Denneau, L.; Flewelling, H.; Heinze, A.; Tonry, J.L. (2020). "Investigating Taxonomic Diversity within Asteroid Families through ATLAS Dual-band Photometry." *Astrophys J. Suppl. Series* **247**, 13.

Hanuš, J.; Ďurech, J.; Broz, M.; Marciniak, A.; Warner, B.D. and 115 colleagues (2013). "Asteroids' physical models from combined dense and sparse photometry and scaling of the YORP effect by the observed obliquity distribution." *Astron. Astrophys.* **551**, A67.

Hanuš, J.; Ďurech, J.; Oszkiewicz, D.A.; Behrend, R.; Carry, B. and 164 colleagues (2016). "New and updated convex shape models of asteroids based on optical data from a large collaboration network." *Astron. Astrophys.* **586**, A108.

Harris, A.W.; Young, J.W.; Scaltriti, F.; Zappalà, V. (1984). "Lightcurves and phase relations of the asteroids 82 Alkmene and 444 Gyptis." *Icarus* **57**, 251-258.

Harris, A.W.; Pravec, P.; Galad, A.; Skiff, B.A.; Warner, B.D.; Vilagi, J.; Gajdos, S.; Carbognani, A.; Hornoch, K.; Kusnirak, P.; Cooney, W.R.; Gross, J.; Terrell, D.; Higgins, D.; Bowell, E.; Koehn, B.W. (2014). "On the maximum amplitude of harmonics on an asteroid lightcurve." *Icarus* **235**, 55-59.

McNeill, A.; Mommert, M.; Trilling, D.E.; Llama, J.; Skiff, B. (2019). "Asteroid Photometry from the Transiting Exoplanet Survey Satellite: A Pilot Study." *Astrophys J. Suppl. Series* **245**, 29.

Pál, A.; Szakáts, R.; Kiss, C.; Bódi, A.; Bognár, Z.; Kalup, C.; Kiss, L.L.; Marton, G.; Molnár, L.; Plachy, E.; Sárneczky, K.; Szabó, G.M.; Szabó, R. (2020). "Solar System Objects Observed with TESS - First Data Release: Bright Main-belt and Trojan Asteroids from the Southern Survey." *Ap. J.* **247**, A26.

Pilcher, F. (2022). "Lightcurves and Rotation Periods of 233 Asterope, 240 Vanadis, 275 Sapientia, 282 Clorinde, 414 Liriope, and 542 Susanna." *Minor Planet Bull.* **49**, 346-349.

Podlewska-Gaca, E.; Poleski, R.; Bartczak, P.; McDonald, I.; Pál, A. (2021). "Determination of Rotation Periods for a Large Sample of Asteroids from the K2 Campaign 9." *Astrophys. J. Suppl. Series* **255**, 4.

Polakis, T. (2018a). "Lightcurve Analysis for Eleven Main-Belt Asteroids." *Minor Planet Bull.* **45**, 199-203.

Polakis, T. (2018b). "Lightcurve Analysis for Fourteen Main-Belt Minor Planets." *Minor Planet Bull.* **45**, 347-352.

Polakis, T. (2019). "Lightcurves of Twelve Main-Belt Minor Planets." *Minor Planet Bull.* **46**, 287-292.

Polakis, T. (2022). "Lightcurves for Sixteen Minor Planets." *Minor Planet Bull.* **49**, 298-303.

Stephens, R.D. (2002). "Photometry of 866 Fatme, 894 Erda, 1108 Demeter, and 3443 Letsungdao." *Minor Planet Bull.* **29**, 2-3.

Stephens, R.D.; Warner, B.D. (2021). "Main-Belt Asteroids Observed from CS3: 2020 July to September." *Minor Planet Bull.* **48**, 56-69.

Tonry, J.L.; Denneau, L.; Flewelling, H.; Heinze, A.N.; Onken, C.A.; Smartt, S.J.; Stalder, B.; Weiland, H.J.; Wolf, C. (2018). "The ATLAS All-Sky Stellar Reference Catalog." *Astrophys. J.* **867**, A105.

Warner, B.D. (2000). "Lightcurve Parameters for 1582 Martir." *Minor Planet Bull.* **27**, 53-54.

Warner, B.D. (2003). "Lightcurve Analysis of Asteroids 331, 795, 886, 1266, 2023, 3285, and 3431." *Minor Planet Bull.* **30**, 61-64.

Warner, B.D. (2006). "Asteroid Lightcurve Analysis at the Palmer Divide Observatory - Late 2005 and Early 2006." *Minor Planet Bull.* **33**, 58-62.

Warner, B.D.; Harris, A.W.; Pravec, P. (2009). "The asteroid lightcurve database." *Icarus* **202**, 134-146. *https://minplanobs.org/MPInfo/php/lcdb.php*

Warner, B.D. (2010). "Upon Further Review: II. An Examination of Previous Lightcurve Analysis from the Palmer Divide Observatory." *Minor Planet Bull.* **37**, 150-151.

Warner, B.D. (2011). "Upon Further Review: III. An Examination of Previous Lightcurve Analysis from the Palmer Divide Observatory." *Minor Planet Bull.* **38**, 21-23.

Warner, B.D. (2021). *MPO Canopus* Software, version 10.8.4.11. BDW Publishing. *http://www.bdwpublishing.com*

Waszczak, A.; Chang, C.-K.; Ofek, E.O.; Laher, R.; Masci, F.; Levitan, D.; Surace, J.; Cheng, Y.-C.; Ip, W.-H.; Kinoshita, D.; Helou, G.; Prince, T.A.; Kulkarni, S. (2015). "Asteroid Light Curves from the Palomar Transient Factory Survey: Rotation Periods and Phase Functions from Sparse Photometry." *Astron. J.* **150**, A75.

LOWELL OBSERVATORY NEAR-EARTH ASTEROID PHOTOMETRIC SURVEY (NEAPS): PAPER 5

Brian A. Skiff
Lowell Observatory
1400 West Mars Hill Road
Flagstaff AZ 86001 USA
bas@lowell.edu

Kyle P. McLelland
Northern Arizona University

Jason J. Sanborn
Lowell Observatory
Lowell Discovery Telescope

Bruce W. Koehn
Edward Bowell
Lowell Observatory (retired)

(Received: 2022 August 11)

New photometry and lightcurves are shown for 107 asteroids observed mainly between 2009 and 2012 using four telescopes at Lowell Observatory. The data have not been previously published in detail. This completes work on the NEAPS program.

Previous reports in this series (Skiff et al., 2019a, Paper 3; Skiff et al., 2019b, Paper 4) gave revised or new results for more than 200 asteroids observed mainly at the end of a 12-year project to discover and characterize NEOs (Koehn and Bowell, 2000). The present work completes the NEAPS program, covering an especially concentrated period of observing 2009-2012. The same four Lowell Observatory telescopes were involved as described previously, and the personnel also the same. The two workhorse instruments were the 0.55-m *f*/1.9 LONEOS Schmidt (MPC observatory code 699) and robotic 0.7-m *f*/8 reflector (code 688 for this and other Lowell telescopes located at its Anderson Mesa site). The Schmidt was operated unfiltered, while the 0.7-m was used with an R_c filter. Both telescopes are now closed. In addition, the 1.1-m *f*/8 Hall and 1.8-m Perkins reflectors were occasionally employed. Further details about the instrumentation, data-acquisition, and reductions can be found in the previous papers.

Following image-preparation (bias correction and flat-fielding) using local software, all the data have been reduced through *MPO Canopus*, and adjusted as well as possible to the standard Sloan r′ system using improved photometry for the comparison stars. These were tied largely to the Pan-STARRS survey catalogue (Magnier et al., 2016). No color transformations were involved, only zero-point adjustment to asteroidal-color reference stars. These are preferably G/K dwarfs somewhat redder than the Sun. The phased lightcurves show apparent magnitudes reckoned from the first night by *MPO Canopus*. The primary maximum is set to phase zero in order to make it convenient to compare lightcurve morphologies at different apparitions or viewing geometries. The lightcurves shown below for (47035) 1998 WS are an example of this.

In preparing these results, the LCDB (Warner et al., 2009) was queried in 2022 Aug. Some of our lightcurves were previously posted to the CALL site; the results here supersede those interim reports, and are not mentioned unless necessary.

599 Luisa. Despite having only two relatively short runs on this main-belt asteroid in 2011 May, there is enough curvature to fit our incomplete 0.7-m data with the period first found by Debehogne et al. (1977). The RMS scatter is 0.010 mag.

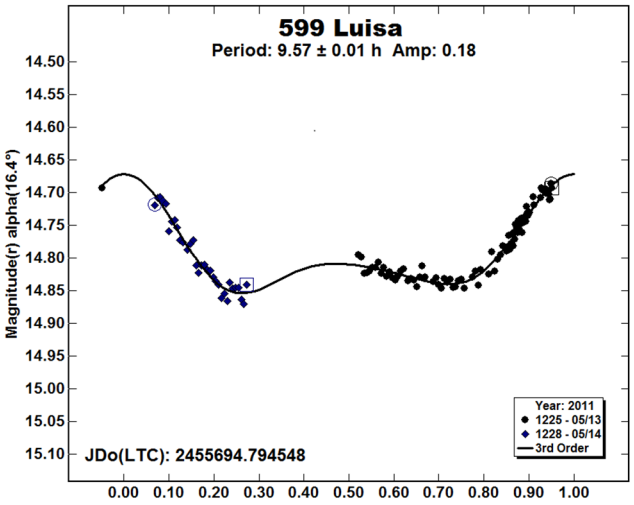

1151 Ithaka. At least three other observers besides ourselves got lightcurves for this main-belt object in 2011 Aug-Sep (Aymami, 2012; Franco et al., 2012; Pravec, 2011web). Everyone agrees on the period and that the asteroid exhibited a quadrimodal lightcurve at that apparition. We contribute data taken with the Schmidt for about seven hours on 2011 Sep 8 using 8-second exposures. After averaging the data into three-image 2-minute bins, the RMS scatter is 0.013 mag.

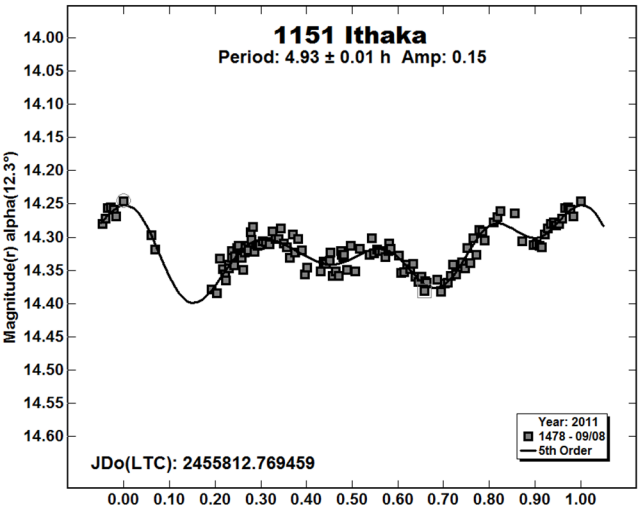

1355 Magoeba. There is obviously small-amplitude cyclic variation on a short timescale in this Hungaria, but our single-night 7-hour Schmidt run in 2011 Jul is insufficient to say much beyond that. The five comparison stars are constant with RMS scatter averaging only 0.009 mag Various periods near 3, 6, and 32 hours have been suggested (e.g., Warner, 2010; Stephens and Warner, 2020).

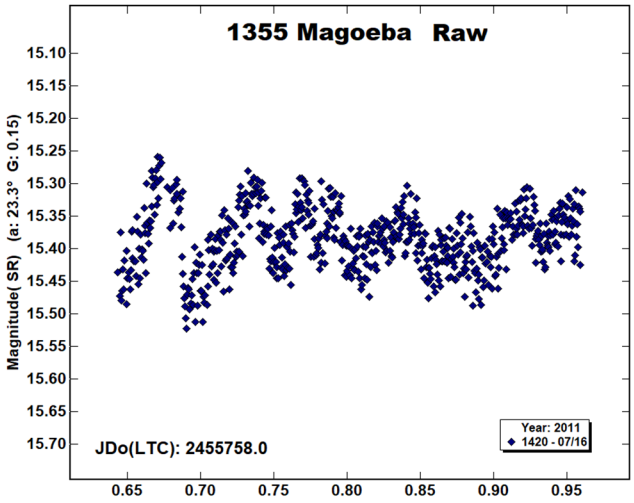

1374 Isora. Five consecutive nights in 2011 Mar using the 0.7-m telescope were inadequate to define the small amplitude lightcurve of this Mars-crosser. Stephens (2014) gave a tentative period of 37 h. Our data are too uncertain to confirm this, but a phased lightcurve at a very weak minimum in the periodogram near it is shown, likely merely coincidental. The RMS scatter of this fit is 0.05 mag.

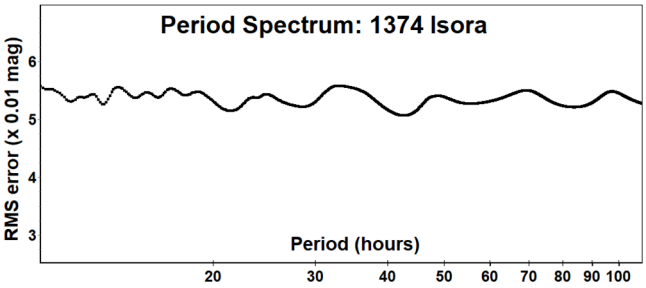

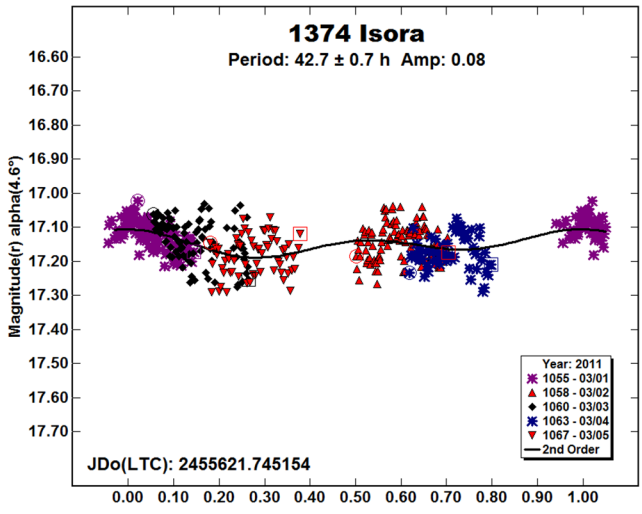

1501 Baade. Two nights on this main-belt asteroid using the 0.7-m telescope in 2011 Oct do not quite give complete rotational phase coverage, but the period is reasonably well-defined. As early as 2003 Oct, Ivarsen et al. (2004) determined a similar period. At about the same time, Maleszewski and Clark (2004) seem to have found a 10-hour 2:3 alias. The RMS scatter on the fit to our data is 0.011 mag.

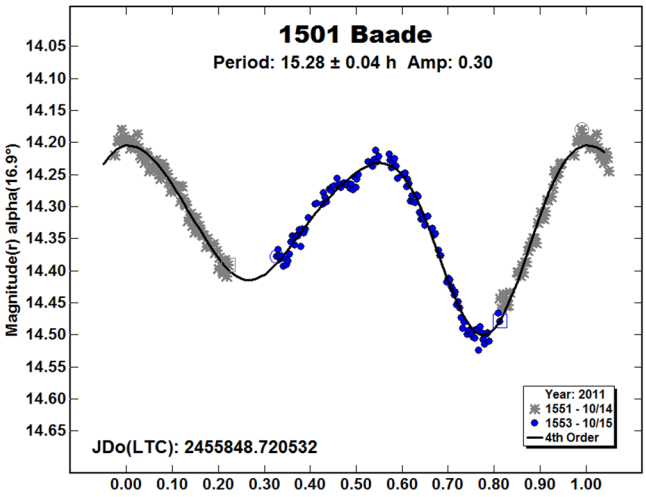

2060 = 95P Chiron. The earliest lightcurve of the first known Centaur was by Bus et al. (1989), who found the rotation period near 5.9 h, mainly from 1.8-m Perkins telescope CCD data taken in 1986 Nov-Dec. A few years later, Bus et al. (1991) identified cometary CN emission in spectra taken with the same telescope. In 2009 Nov, as part of monitoring the object for possible cometary activity, we obtained five 3-minute exposures on two nights using the Schmidt. These adjust to Sloan r′ mag 17.92 ± 0.03 (UT 2009 Nov 20.1) and 17.97 ± 0.03 (UT 2009 Nov 21.1).

We also attempted to get a complete lightcurve in 2017 Sep, again using the 1.8-m telescope. This was not entirely successful partly due to poor weather, and also the very small lightcurve amplitude at the time. A phased plot is shown here with the 150-second exposures binned into three-image 8-minute averages. The RMS scatter on the order-2 fit is 0.014 mag.

Perhaps due to the very small amplitude, the last high-precision lightcurve was obtained in 1996 by Lazzaro et al. (1997).

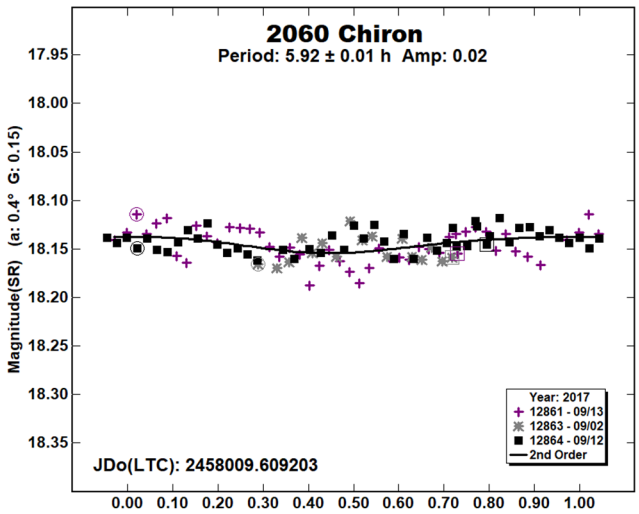

2714 Matti. Wisniewski et al. (1997) published a preliminary period of 9 ± 2 hours for this main-belt Flora. From four nights of 0.7-m data in 2012 May, we refine this to 9.27 hours. The RMS scatter on the fit is 0.012 mag with three-image 4-minute averaging.

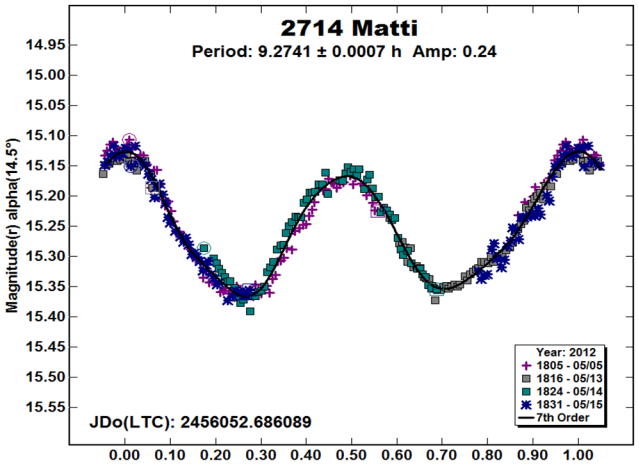

3512 Eriepa. This ordinary main-belt asteroid was discovered by then-MIT student Joe Wagner in 1984 Jan on Lowell "Pluto Camera" plates. Ditteon et al. (2004) first determined the rotation period. Three nights of photometry using the 0.7-m telescope in 2011 Jan yielded a smooth lightcurve of moderate amplitude. The RMS scatter from the 90-second exposures is 0.026 mag. The morphology is quite distinct from the earlier result since the PAB longitude and phase-angle are quite a bit different.

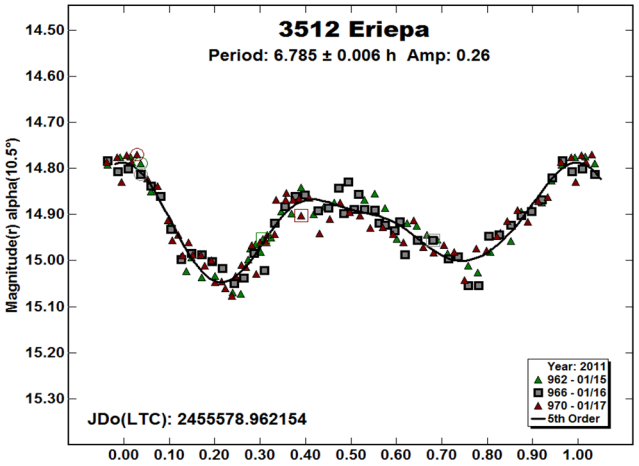

3988 Huma. Our data for this Amor were taken on 2011 Jul 2 using the 0.7-m telescope (R_c filter), then Jul 22 and 23 using the Schmidt (unfiltered). The results are noisy but yield a first look at the rotation period. The RMS scatter is 0.05 mag.

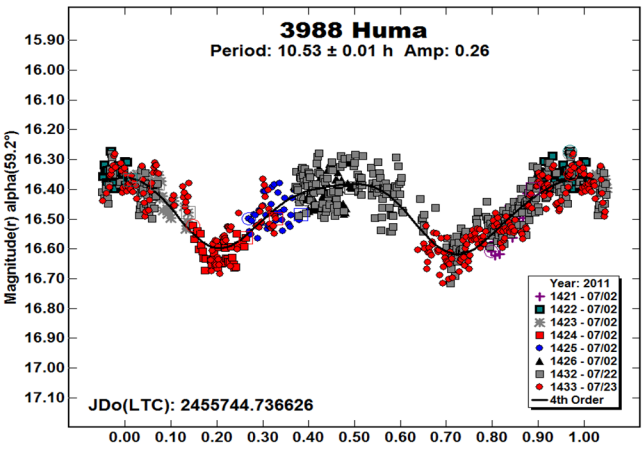

4015 = 107P Wilson-Harrington. This Apollo-type NEO was discovered as a faint comet on 1.2-m Schmidt plates taken in the early days of the first Palomar Observatory Sky Survey, but subsequently lost. It was rediscovered as 1979 VA by "Glo" Helin, also at Palomar. Though well-observed at that apparition, no cometary activity was noticed. The identification of the two objects was made by Ted Bowell while tracing 1979 VA back to the 1949 POSS prints, and the linkage made by Brian Marsden (Marsden, 1992). Cometary activity has not been observed since.

We made several attempts to get a lightcurve using the Schmidt during 2009, but none was satisfactory. We show results from a single 4-hour run in 2010 Jan using the 1.1-m telescope. The derived period is somewhat shorter than the series itself, so is provisional. However, Harris and Young (1983) and Urakawa et al. (2011) found periods of 3.56 and 3.57 hours, respectively, well within our formal uncertainty. The RMS scatter on the fitted curve is 0.023 mag.

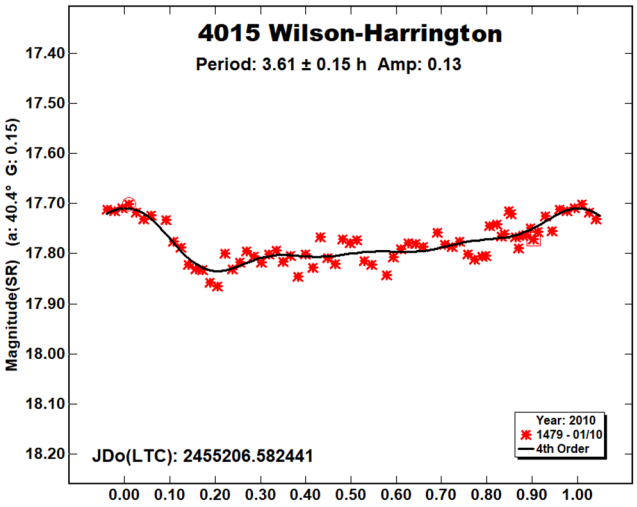

4103 Chahine. A series covering several weeks in 2018 Feb-Mar was obtained for this Phocaea using the 0.7-m telescope with 4- and 5-minute exposures. These produced a long-period lightcurve having significant tumbling aspect.

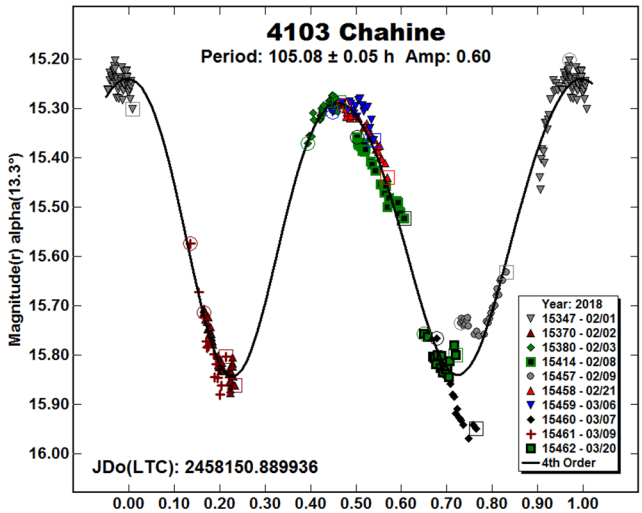

The period shown matches very nearly the one derived from TESS data by Pál et al. (2020), where the tumbling component was overlooked. Similar results from an apparition in late 2020 have been given by Polakis (2021) and Owings (2021). The RMS scatter is 0.035 mag, but this results from the incomplete model fit; the nightly internal errors are better. We include in the database three isolated nights from 2011 using the Schmidt; these show only the broad nightly trends.

4132 Bartok. Now a much-observed Phocaea, we got three nights on this asteroid in 2011 Apr using both the Schmidt (unfiltered) and 0.7-m telescope (R_c filter). Almost 20 hours were spent on-target and a total of 400 frames acquired. The period is very close to subsequent determinations (e.g., Warner, 2014b); the RMS scatter on the fit is 0.032 mag.

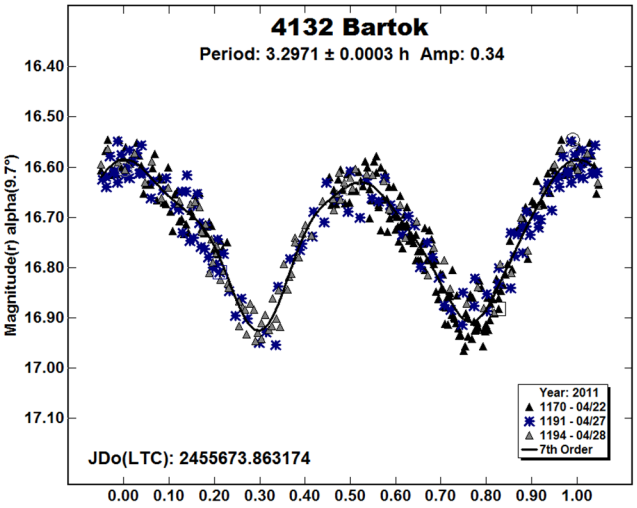

4287 Trisov. This main-belt Flora has a previously published period from ATLAS survey data by Ďurech et al (2020). Three nights of 0.7-m telescope data in 2011 Mar, including a ten-day gap, allow the rotation period to be determined accurately. The RMS scatter is 0.04 mag.

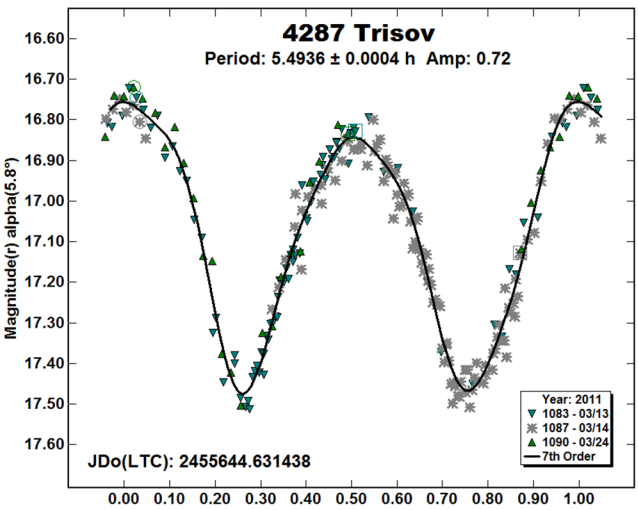

4666 Dietz. Several groups besides ourselves observed this Phocaea during 2011 Jun (e.g., Ferro, 2011). The object was later found to be binary or triple with mutual events (Oey et al., 2018). Our two nights of Schmidt data show no evidence of this. The RMS scatter on the fit is 0.014 mag after averaging the 12- and 15-second exposures in three-image 3-minute bins.

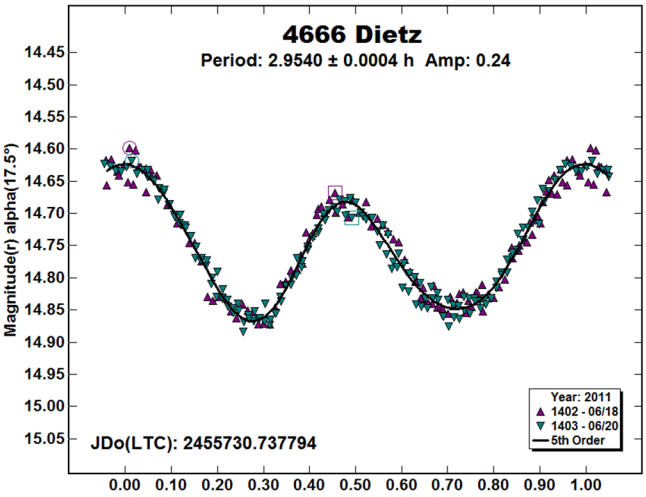

(5131) 1990 BG. Warner (2015) published a rotation period of 20.9 h for this Apollo, later modified in the LCDB to 37.2 ± 0.5 h, obviously uncertain. Our Schmidt data from 2009 Nov-2010 Jan also suggest a slow rotation roughly at double the revised Warner value. The asteroid was quite faint, so our data are likewise uncertain. The RMS scatter is 0.04 mag.

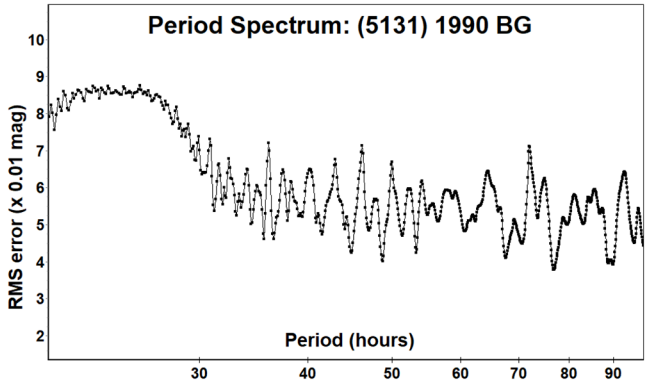

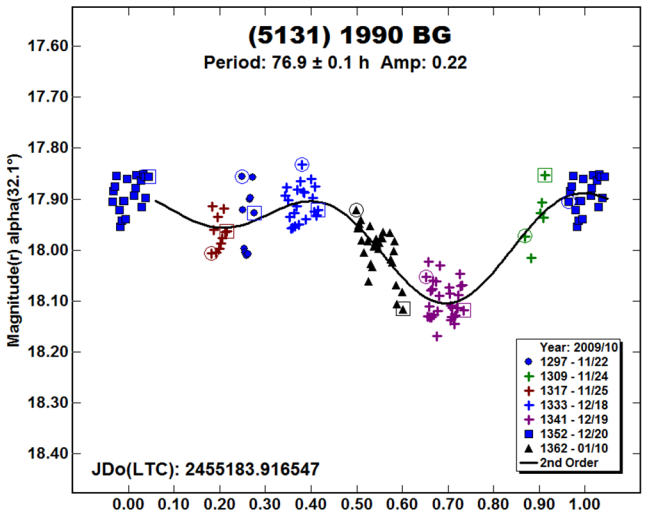

5209 Oloosson. Unfortunately, we devoted only two nights to this Jupiter Trojan using the 0.7-m telescope in 2011 Feb. The period is long enough that we obtained only partial lightcurve coverage. The fit shown here merely lets the two nights of data phase together without forcing. The RMS scatter is 0.025 mag. There is no photometry shown in the LCDB.

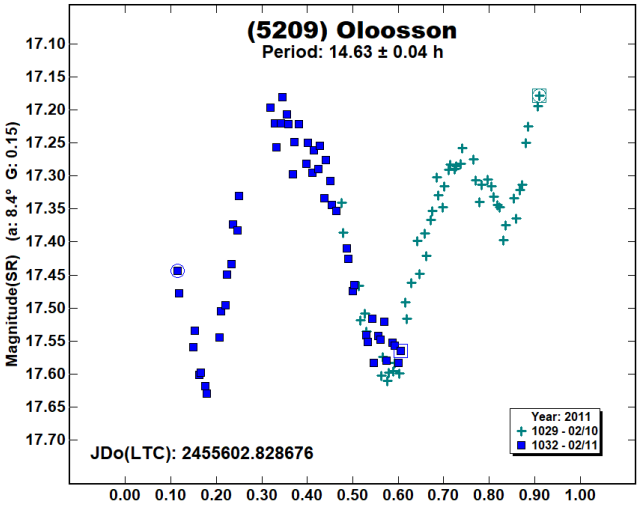

(5496) 1973 NA. Our first attempt on this asteroid was on 2011 Jan New Year's Eve and New Year's night, when we obtained data using the Schmidt and the 1.1-m telescope. Remarkably, but disappointingly, the 15-hour combined dataset showed a completely flat lightcurve. It didn't help that it was 1.3 mag fainter than the initial prediction. Six months later the asteroid was at high phase-angle, and we tried again on three nights using the Schmidt. This produced a short-period lightcurve of modest amplitude. The two series are displayed below.

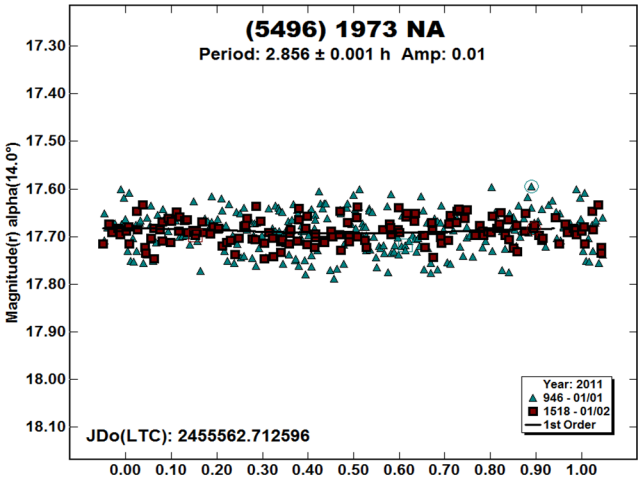

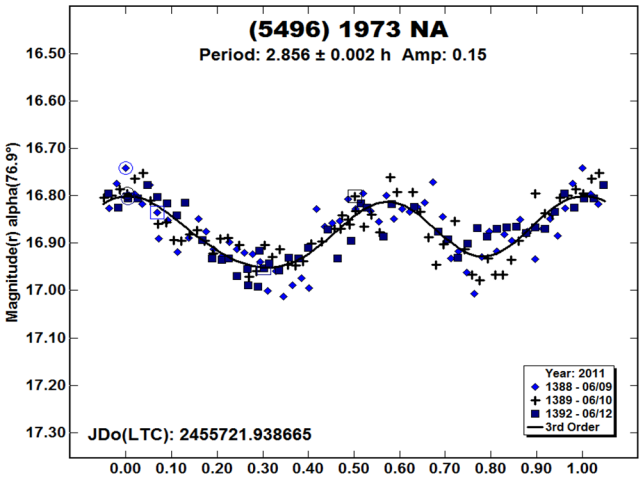

The 2011 Jan plot shows the data force-fit to the period determined in the second run. The RMS scatter is 0.037 mag, so any variation was less than one-third the noise level. The second lightcurve is plotted at the same vertical scale, and has RMS scatter of 0.034 mag following averaging the data into three-image 4-minute bins. This Apollo has been mostly fainter than mag 19 since 2011, so there is no other published photometry.

5621 Erb. These data are apparently the only lightcurve photometry available for this Mars-crosser. We observed it on three nights at the end of 2011 Aug using the 0.7-m telescope and 90-second exposures. The lightcurve has small amplitude and quadrimodal form. The RMS scatter on the fit is 0.015 mag.

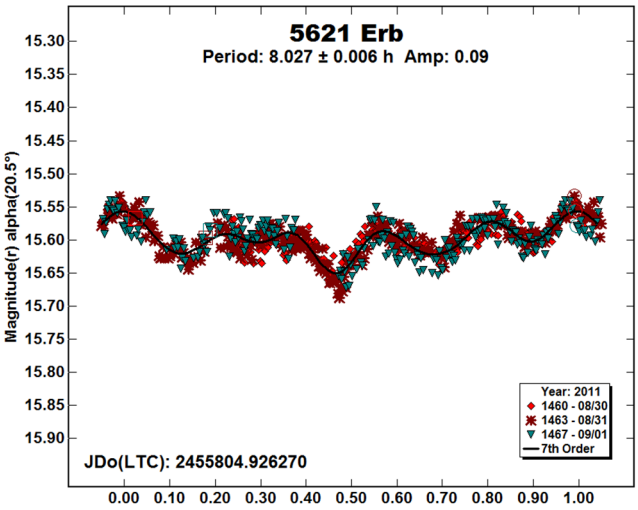

5626 Melissabrucker. We obtained data for this Amor spanning five months in 2009 using the Schmidt. Only the data from 2009 Jul are useful for characterizing the small-amplitude lightcurve. The asteroid brightened from Sloan r′ mag 16.9 up to 15.5 through the month, and exposures were gradually reduced from 90 to 45 seconds. The results confirm the most recent period determinations by Warner and Stephens (2020) from their 2020 Feb and revised 2019 lightcurve data. Note that the morphology of their 2020 Feb lightcurve is identical to the one shown here, which was done at PAB longitude very nearly 180° away. The present data have RMS scatter of 0.013 mag, as good as the best previous data.

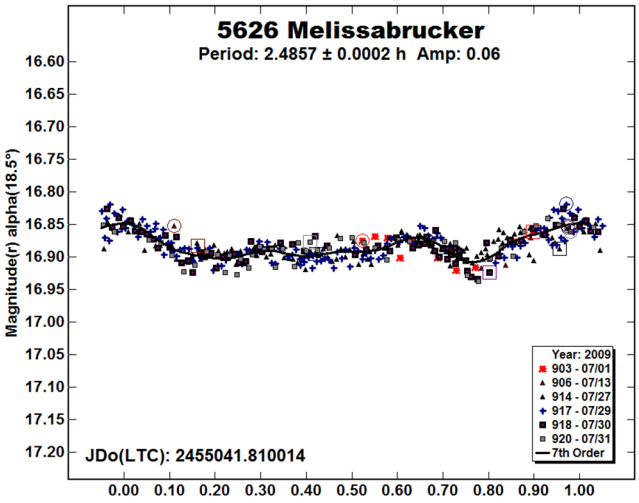

5682 Beresford. Two previous photometric studies have been published for this Mars-crosser. Kamél (1998) was not able to determine a period from data taken in autumn 1997, probably due to the small lightcurve amplitude. In 2004 Koff (2005) found a period of about 7.5 hours from somewhat noisy data. Benishek (2022) concluded that the half-period was preferred, but suggested some ambiguity remained. From our two nights of 0.7-m data in 2011 Oct, including an 8.4-hour run the first night, we also find a better fit to the shorter period, though we agree the longer one is not utterly excluded. The RMS scatter on the fit is 0.011 mag.

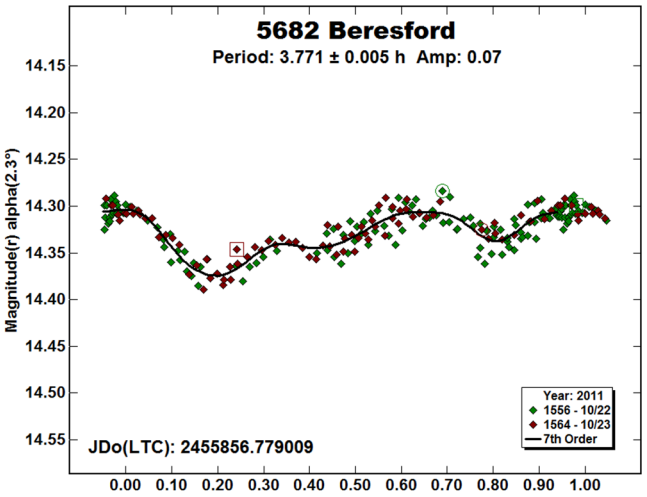

5736 Sanford. The only previously available lightcurves for this Phocaea are those of Pravec et al. (Pravec, 2011web), which were done in summer of 2011. We also obtained three nights at Full Moon in 2011 Jul using the Schmidt.

Two of these were satisfactory, and are shown in the first phased plot below. The data are binned into four-image 3-minute averages; the RMS scatter is 0.038 mag Our period matches that of Pravec et al. Another Schmidt night two weeks later without Moonlight (and smaller phase-angle) gave much better results. We fit the data in the 4.7-hour run to the previously determined period. The RMS here is 0.021 mag with no binning.

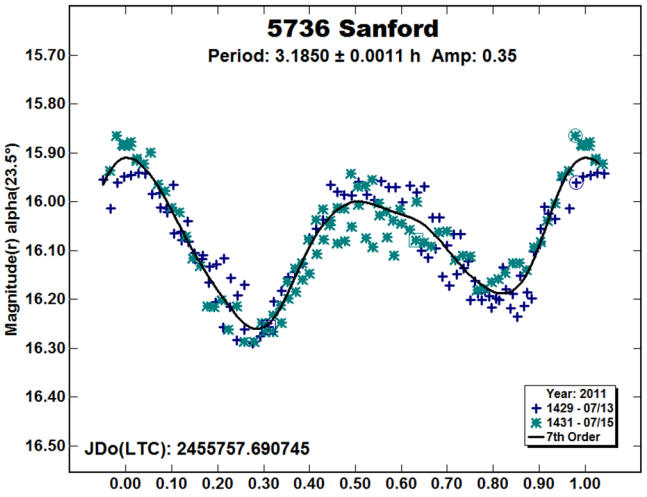

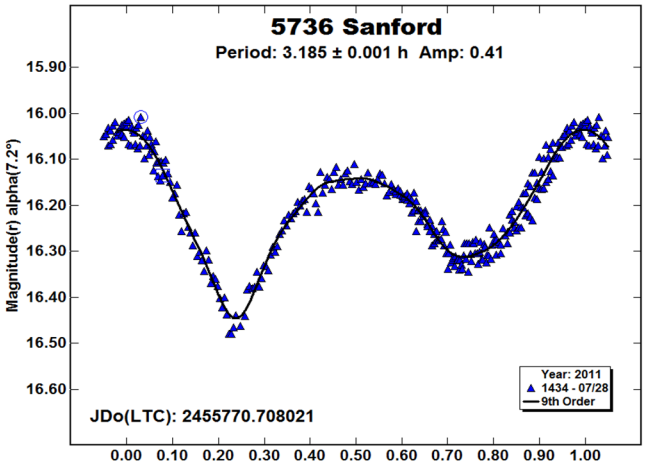

7002 Bronshten. Warner and Stephens (2019) showed that this Mars-crosser was a binary with a relatively short secondary orbital period. Our 0.7-m telescope data on three nights in 2011 Oct (about 8 hours each night) are more scattered than expected, so likely exhibit some distortion from modest tumbling or mutual events. The phased plot shows only the short period of the primary component; the RMS scatter is 0.027 mag, which includes the scatter from the secondary period.

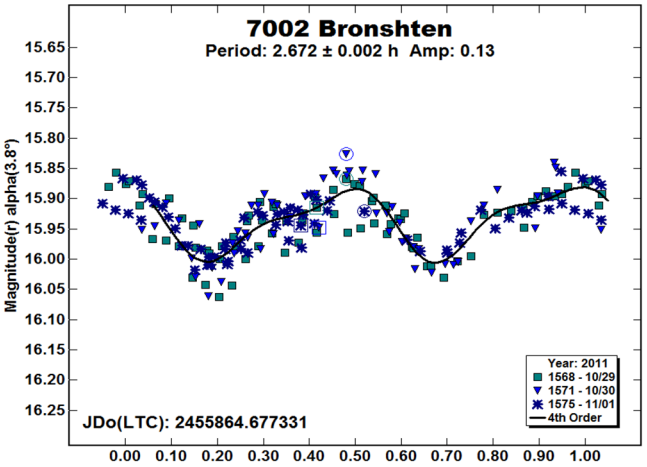

7750 McEwen. The first published of several studies obtained in 2011 for this asteroid was by Lee Owings (2012).

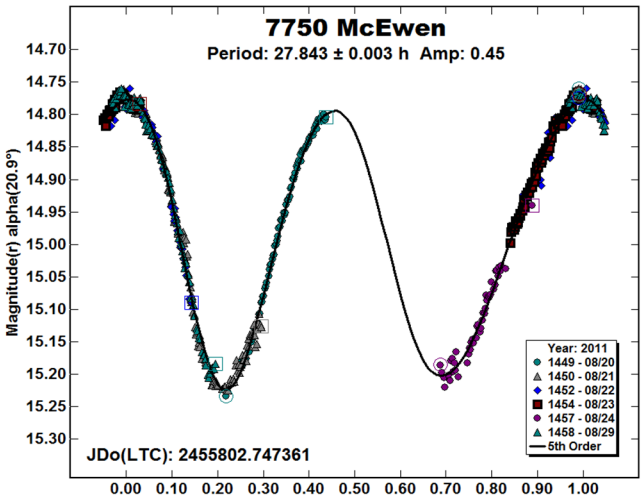

The main-belt object has a moderately-long rotation period and smooth lightcurve. Our series was done 2011 Aug using the 0.7-m telescope during a break in the Arizona summer monsoon, and we lack complete rotational phase coverage. The RMS scatter on the fit is 0.011 mag.

7757 Kameya. Warner (2005) published the only previous data on this Phocaea, showing an ambiguous period near 6 h. However, the first of our two 2011 Jul nights on the target spans 6.8 h, yet there is only a monotonic decline in brightness. The additional partial night three days later has a similar slope. The data comprise about three-hundred eighty 1-minute exposures using the 0.7-m telescope. A period of many tens of hours is indicated.

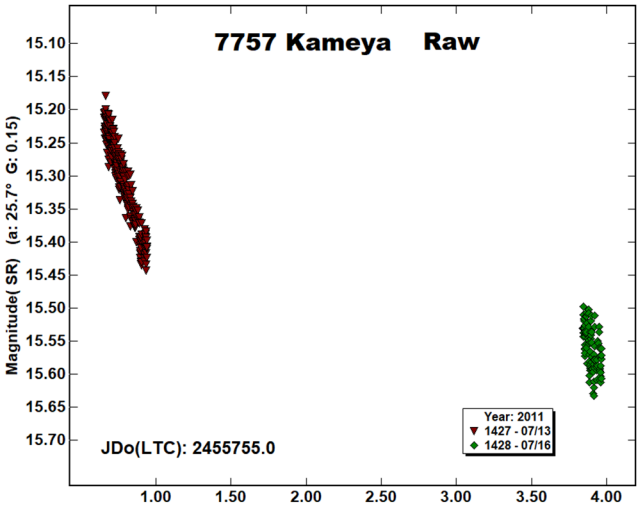

7784 Watterson. Our four nights for this Phocaea span more than a month in 2011 Sep-Oct. The 0.7-m telescope was used with 90-second exposures throughout. The data are highly consistent and no zero-point adjustments were needed. The phased plot shows the data averaged into three-image 5-minute bins. The RMS scatter is 0.024 mag. Benishek (2022) finds that a period near 5 h is preferred in his data, but fitting our data to that period gives significantly larger residuals. Because of the fairly small amplitude, a series with better internal errors will be required to resolve the uncertainty.

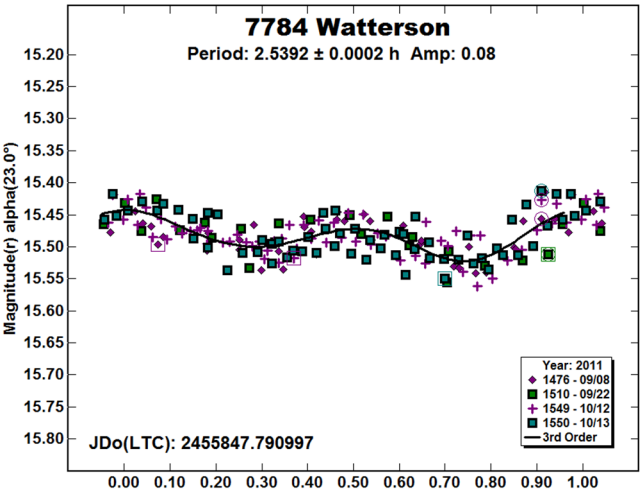

12225 Yanfernandez. Three nights of data in 2011 May using the 0.7-m telescope on this main-belt Flora show only slow variations. The fit here is probably indicative of a period of some tens of hours. The notional RMS scatter is 0.018 mag.

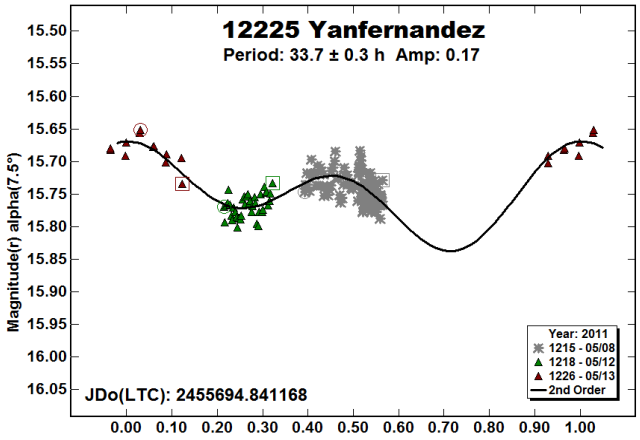

(13819) 1999 SX5. Two nights in 2011 Mar on this 4-km Mars-crosser showed only small variation relative to the noise in 0.7-m telescope data. The period fit is uncertain since the full amplitude is barely at the 3-sigma level. The RMS scatter is 0.035 mag. Behrend (2020web) shows data phased to a very similar period.

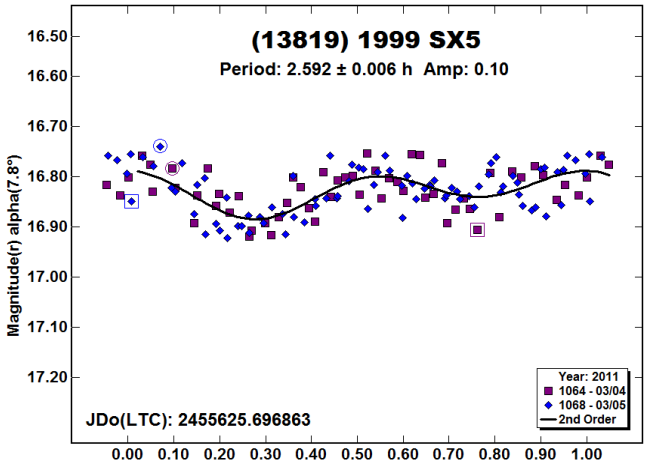

14335 Alexosipov. We observed this main-belt Flora on two nights in 2011 Oct using the 0.7-m telescope. The period is quite certain, matching that from TESS data (Pál et al., 2020) within errors, but with different PAB longitude; the amplitude here is much smaller. The RMS scatter on the fit is 0.014 mag.

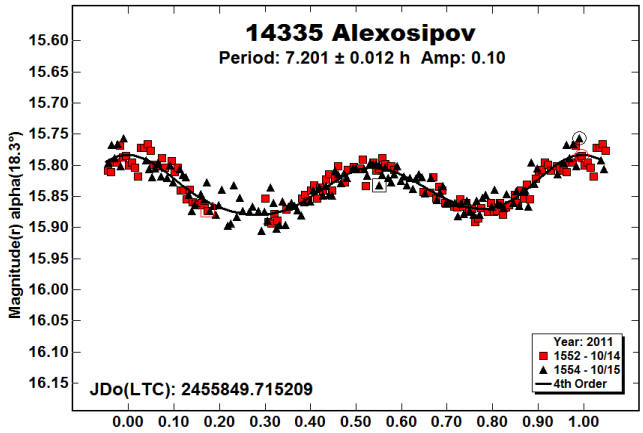

14764 Kilauea. Our two 2011 Jun solstice nights using the Schmidt were insufficient to cover the fairly long periods of this Hungaria, now known to be tumbling (Warner et al., 2012b). The lightcurve shows a notional fit to the data, but this is *not* the rotation period.

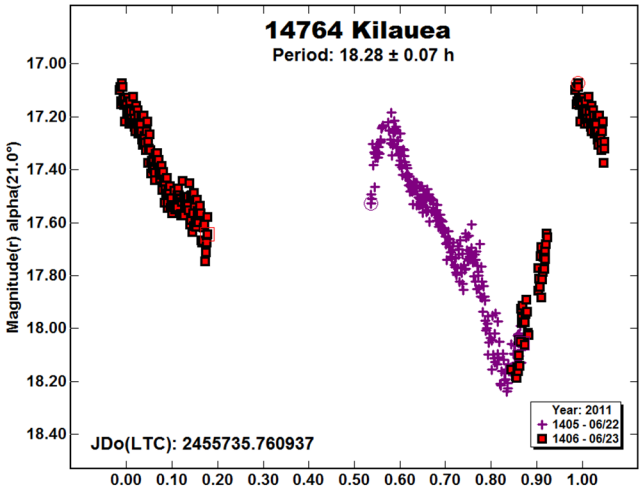

15673 Chetaev. This Mars-crosser has no previous lightcurve study. On six of seven consecutive nights in 2011 Oct-Nov we got runs of about 8 hours duration using the 0.7-m telescope. These were sufficient only to outline the variation approximately. The period is of order 100 hours with fairly large amplitude. We do not really have enough coverage to say whether or not there is tumbling, which might be expected. The RMS scatter on the fit is 0.030 mag.

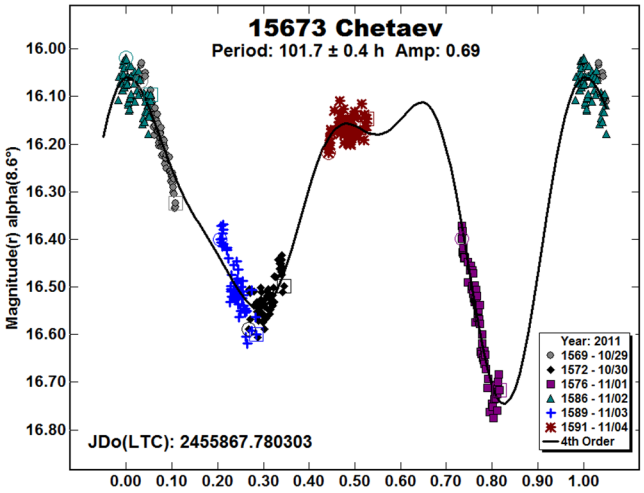

17744 Jodiefoster. Three nights in 2011 Aug using the 0.7-m telescope allowed us to find that the period of this Mars-crosser is relatively long, many tens of hours. The fit shown here is tentative only; the RMS scatter is 0.021 mag.

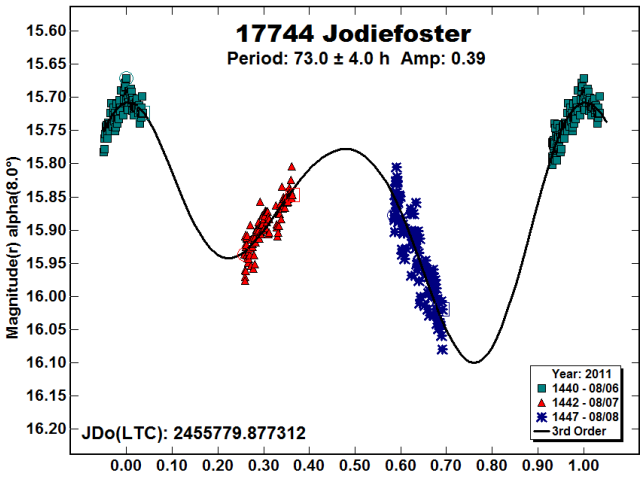

(18081) 2000 GB126. Two nights were spent on this Phocaea in 2011 Apr using the 0.7-m telescope; each run of 90-second exposures extended beyond 8½ hours. The lightcurve is well defined, with RMS scatter on the fit of 0.019 mag.

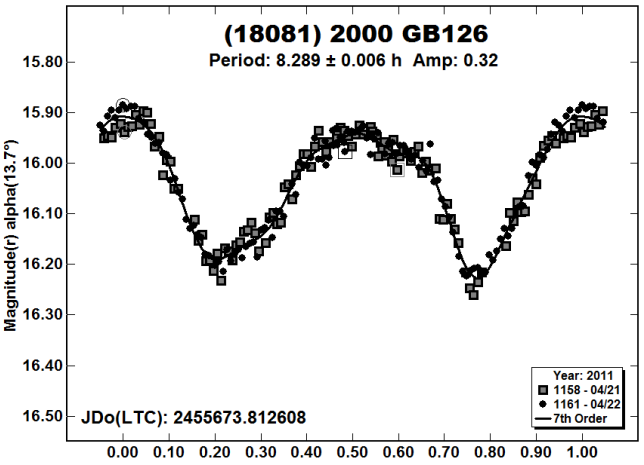

(18882) 1999 YN4. The LCDB shows no photometry for this Amor. We obtained two nights of 1.1-m telescope data in 2010 Dec. The (better) second night shows an ordinary short-period lightcurve. The previous night is somewhat less good, and we are unable to tell whether there is some problem with the data or if there is an indication of weak tumbling or a dimming event. A binary companion would not be unexpected in this period range.

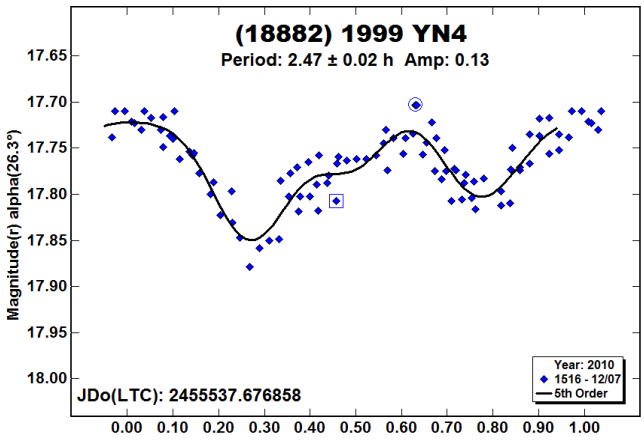

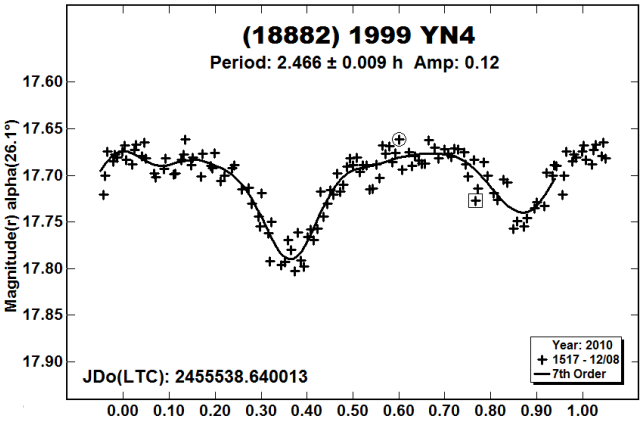

We show phased plots separately for the two nights. The RMS scatter is 0.018 mag for Dec 7, and 0.013 mag for Dec 8. Warner and Stephens (2022b) give a period of 2.35 h from somewhat noisier data (RMS ~0.03 mag).

19379 Labrecque. Using data from René Roy, Behrend (2007web) gave a provisional period of 8.3 h for this Phocaea. Our single 4.5-hour run using the 1.1-m telescope in 2012 Feb shows a period of only 2.6 h. It is reasonable to be skeptical, though there is repeat coverage between phases 0.7 and 0.1, as shown below, so the period seems secure, if imprecise. The RMS scatter is 0.009 mag versus ~0.05 mag for the Behrend data.

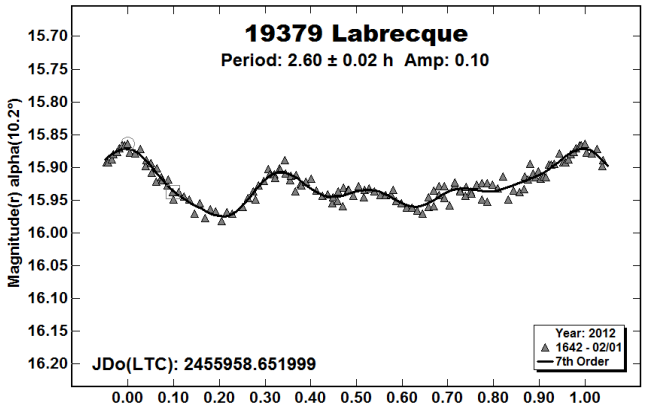

(23183) 2000 OY21. These data for this 1-km Amor were overlooked for our Paper 4 (Skiff et al., 2019b), which shows three nights taken one month prior.

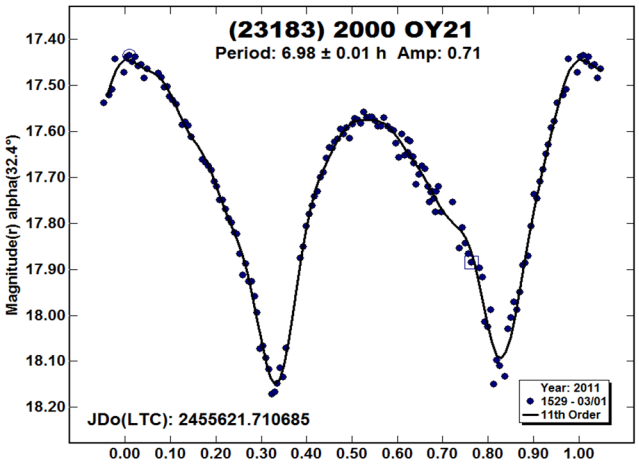

An 8-hour run on 2011 Mar 1 using the 1.1-m telescope fits the Paper 4 period (also cf. Warner, 2016b). The RMS scatter is 0.021 mag, about the same as the earlier data, but the asteroid was more than 1.5 mag fainter. The slight jog near phase 0.7, which seemed anomalous in our previous lightcurve, is present here also.

(23552) 1994 NB. Two wide-field surveys have produced rotation periods for this Phocaea: Waszczak et al. (2015) using Palomar Transient Factory data and Pál et al. (2020) from the TESS spacecraft. Both yield periods similar to ours, which is from 0.7-m telescope data in 2012 Apr (the same date-range as the PTF result). The RMS scatter on the fit is 0.029 mag.

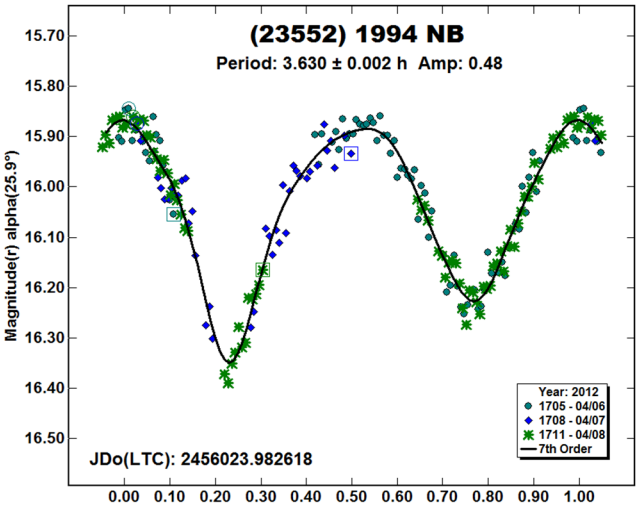

(24475) 2000 VN2. Without saying so explicitly, Melton et al. (2012) saw only a small variation in brightness in this Amor. We got a single night using the 0.7-m telescope in 2011 Dec, which we show to give an indication of the range and that the period must indeed be very long, many tens of hours. The RMS scatter on the trend is about 0.007 mag. The asteroid has not been observed otherwise.

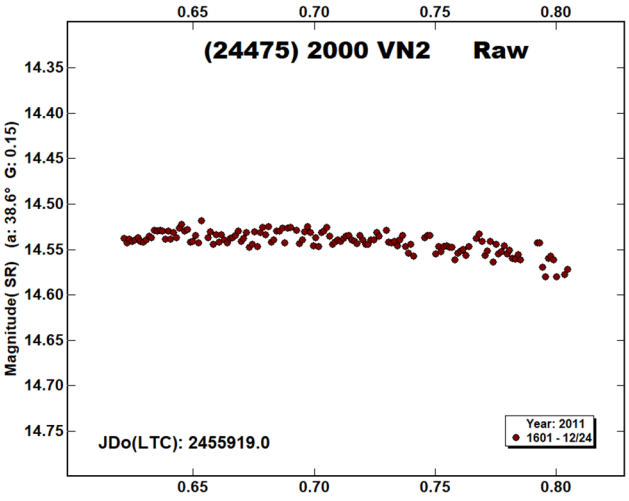

27810 Daveturner. The very long period of this Hungaria was described by Warner et al. (2011), which includes the series shown below. Sparse observations were obtained on nine consecutive nights in 2011 Feb using the 0.7-m telescope. A raw plot, now adjusted to Sloan r′ mags, traces the very slow, smooth variation over the interval.

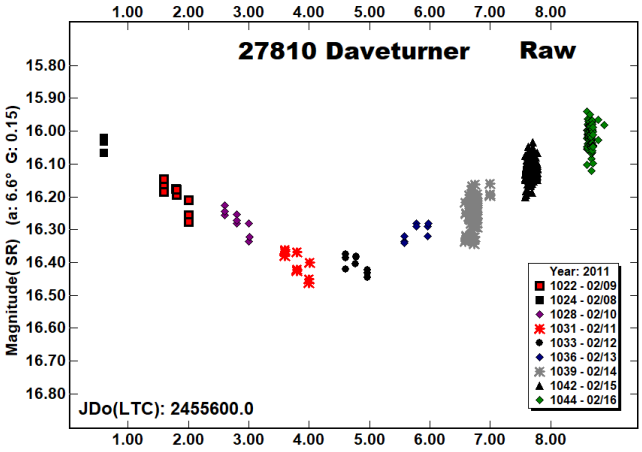

(29168) 1990 KJ. Pravec (2011web) found this Phocaea to be binary from extensive observations taken during the same 2011 apparition as we observed. Our data are more limited in time and have much lower precision. We show a lightcurve fit to Schmidt data with the 15- and 20-second exposures averaged into three-image 3-minute bins. The RMS scatter is 0.031 mag.

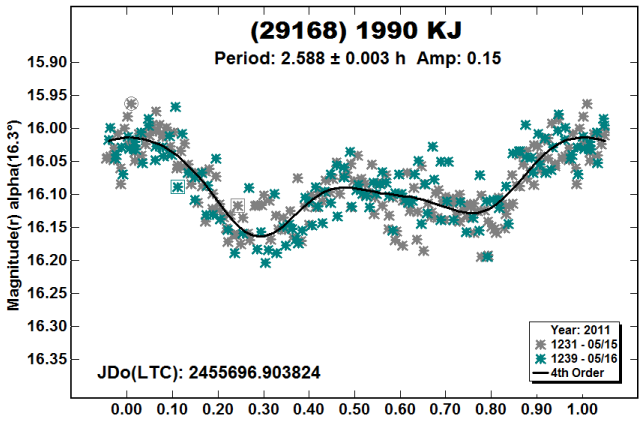

(30019) 2000 DD. Brian Warner (2012a) obtained the first correct rotation period for this Hungaria, including a revision of his earlier 2006 data. Our three nights in 2011 Oct using the 0.7-m telescope allowed us to find the same period within errors. The RMS scatter on the fit is 0.022 mag.

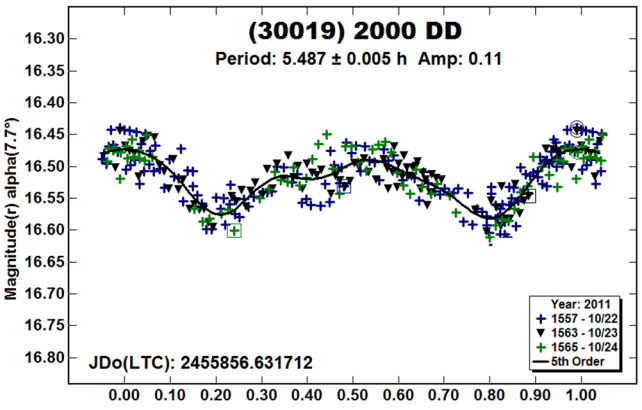

30722 Biblioran. Two long nights using the 0.7-m telescope in 2014 Nov each sparsely covered more than three rotations of this main-belt asteroid. The lightcurve is well-defined, with RMS scatter of 0.016 mag.

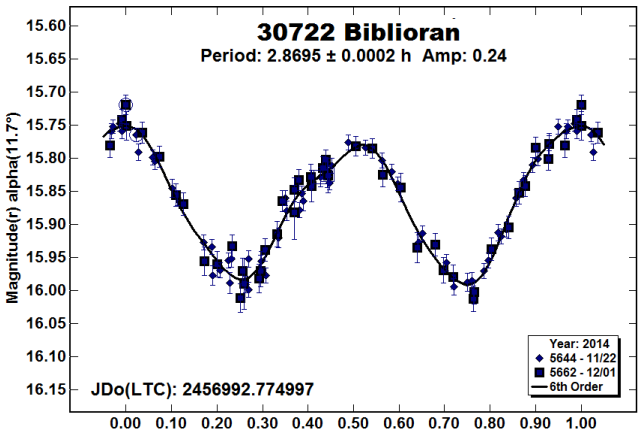

(31425) 1999 BF3. Previously (Skiff, 2011web) we used the data here to suggest a period of 5.9 h for this main-belt asteroid, assigned a rating of U = 1+ in the LCDB. The observations were taken in 2011 Apr with the 0.7-m telescope, and are now adjusted more closely to Sloan r′ mags. Re-examination of the data suggests a longer period by a 3:2 ratio, but with only two nights, there is the possibility that we simply have not covered the entire rotation cycle of the small-amplitude lightcurve (i.e., reliability still U = 1+ or 2-). The RMS scatter on the fit is 0.022 mag.

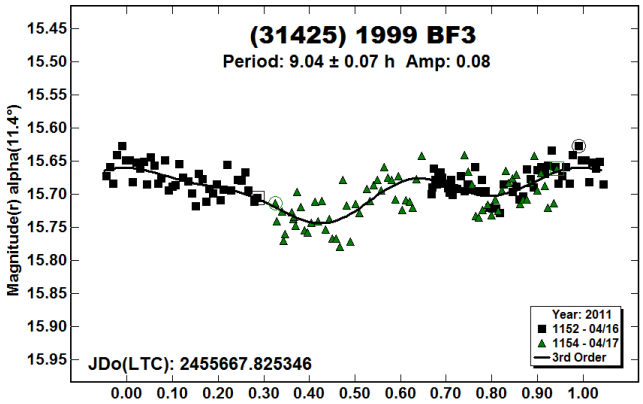

(32802) 1990 SK. This Phocaea turned out to have a short period. Three consecutive nights of 8-hour runs using the 0.7-m telescope in 2011 Nov allowed the variations to be well defined thanks to covering more than three rotational cycles each night. The RMS scatter on the fit is 0.017 mag.

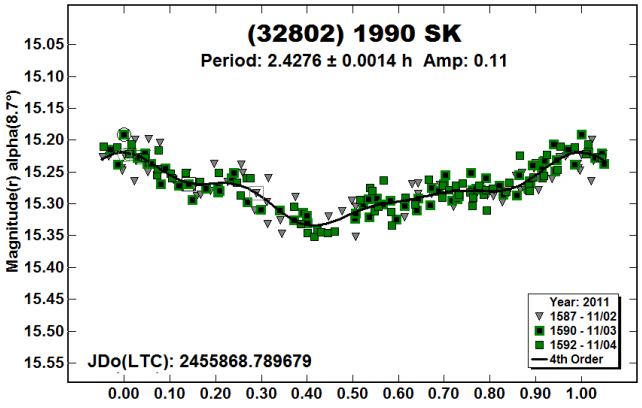

(32906) 1994 RH. Despite some clouds, we got more than one rotational cycle of observations on this Amor using the 0.7-m telescope on two nights in 2012 Jan. The lightcurve has a short period and moderately-small amplitude. The RMS scatter on the fit is 0.020 mag. We covered about 1.5 cycles each night, so the period was evident from visual inspection of the raw series. The period is contrary to Warner (2022a), who gave a period of 9.9 h from much noisier data (RMS 0.04 mag).

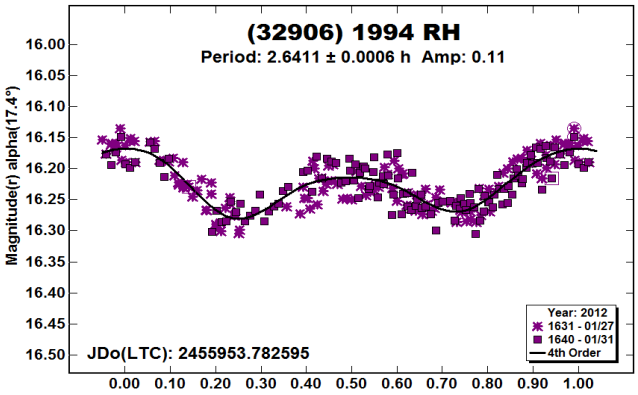

(34759) 2001 QL151. We obtained four nights of data using the Schmidt for this Mars-crosser as it moved at far-northern Declinations in 2011 Jan. Despite some slight peculiarities in the nightly series (likely instrumental in nature), the period seems to be well-determined. The RMS scatter on the fit is 0.021 mag after averaging the 20-second exposures in batches of three.

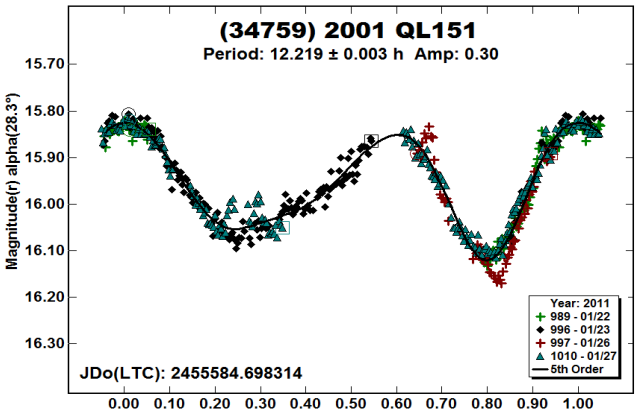

(36284) 2000 DM8. Linder et al. (2013) published the first lightcurve for this Apollo using data taken the week prior to ours. The Schmidt data cover two nights in 2011 Feb. The phased lightcurve shows the 30-second exposures binned into three-image 3-minute averages. The RMS scatter is 0.033 mag.

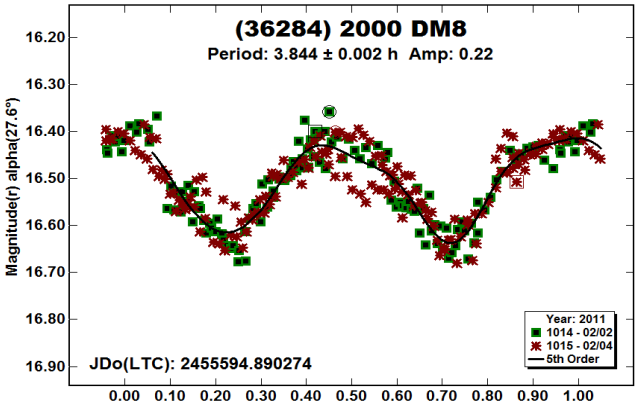

(41434) 2000 GB82. Two nights of 0.7-m photometry in 2011 Oct, with runs of over 7 hours each, revealed a smooth lightcurve of moderate amplitude for this Mars-crosser. The RMS scatter on the fit is 0.017 mag.

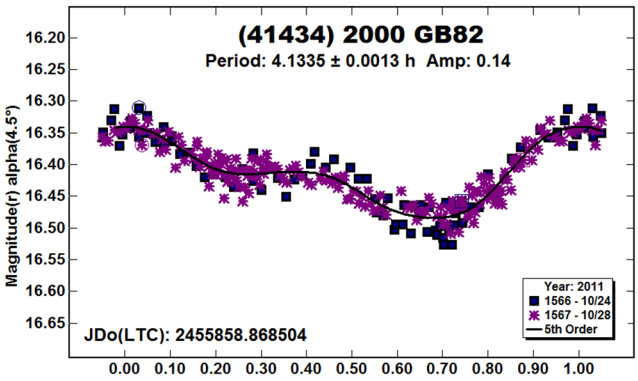

(43750) 1981 QG3. The orbit of this main-belt asteroid has moderate eccentricity, which brings it in to a perihelion distance of 1.85 AU. Relatively short summer-solstice runs in 2014 Jun show a period near 12½ hours, but the 12-day baseline did not allow the rotational phase coverage to shift enough to get a complete lightcurve. The period is nevertheless well-determined. The RMS scatter is 0.020 mag from 5-minute exposures using the 0.7-m telescope. Our period confirms the one by Ďurech et al. (2020) from sparse ATLAS photometry.

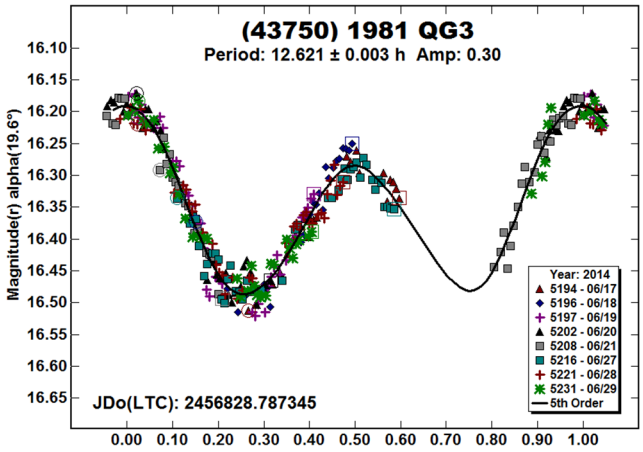

(44262) 1998 QR51. After taking data over five consecutive nights in 2011 Jan using the 0.7-m telescope, it became clear that this Phocaea was a long-period tumbler, so observing was abandoned.

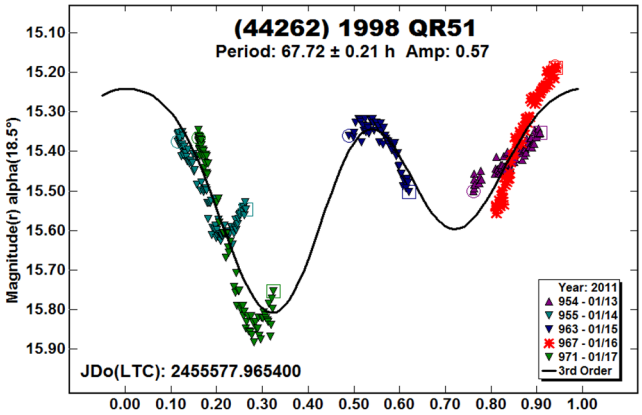

The lightcurve shows an approximate dominant period, but clearly the object requires much more extended observation. Pál et al (2020) show a period of about 77 h from TESS data. Although this is not present in our data, it is not significant, since the tumbling nature is not dealt with in either case.

(47035) 1998 WS. Warner et al. (2012a) previously published a pole-orientation and shape-model for this Mars-crosser based on data spanning a single apparition from near opposition to evening quadrature. Our data were part of this, comprising seven nights of 0.7-m data (60- and 90-second exposures) in 2012 Feb-Apr.

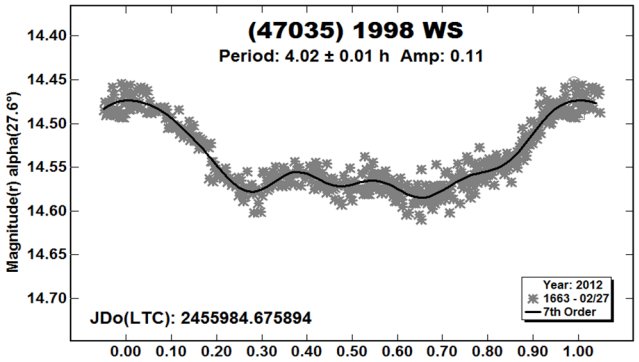

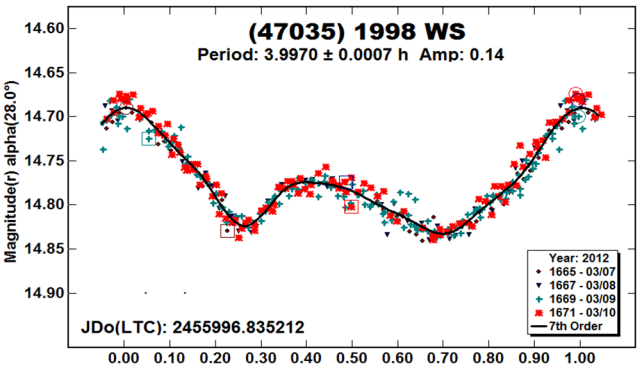

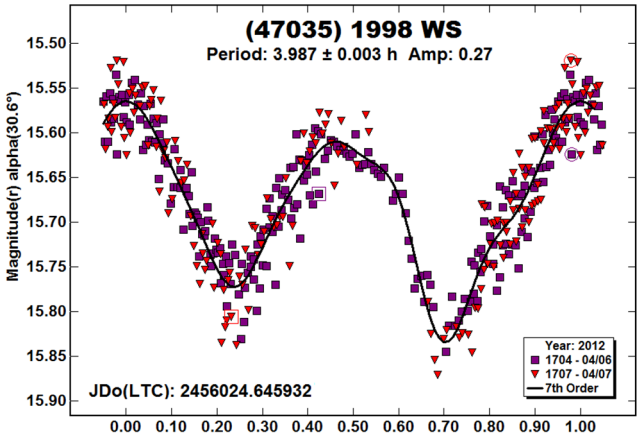

We have now adjusted the data more closely to Sloan r′, and show each group of nights separately, plotted at the same vertical scale. The first night covered nearly 10 hours, about 2½ rotational cycles, and the character is essentially monomodal with a broad minimum. Two weeks later the lightcurve was a typical bimodal one of moderate amplitude. Finally, in early April the amplitude had doubled – and all this with little change in phase angle. The RMS scatters on the plots are 0.010, 0.010 (with three-image, 5-minute averaging), and 0.028 mag.

(54660) 2000 UJ1. Student observer Emily Bevins followed this fast-moving (about 7° per day) Amor with the Schmidt for 5½ hours on 2009 Nov 9. The data (ninety 14-second exposures) were reduced with four sets of comparison stars. The rotation period turns out to be about the same length as the data-series, and ordinarily this would be suspicious. However, the large amplitude in this case removes the ambiguity, so the short run merely makes the period itself uncertain compared to having multiple nights.

We adjusted the zero-points of each session by measuring one or two overlapping frames in each batch against the two sets of comp stars. The RMS scatter on the fit is 0.034 mag.

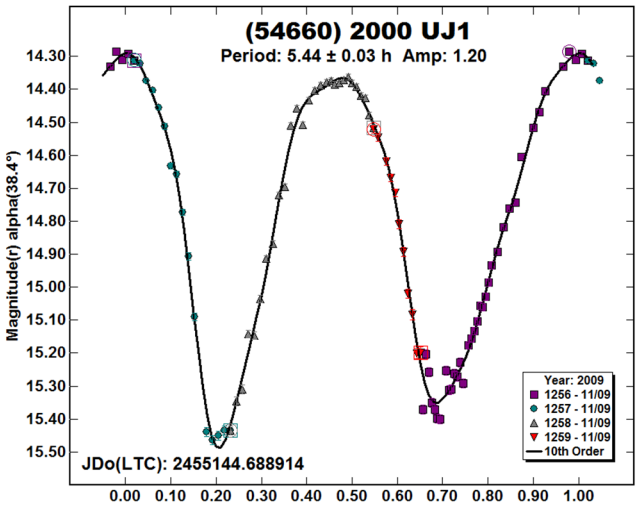

55854 Stoppani. Warner (2011) published the first lightcurve for this Hungaria from data taken shortly after ours. We obtained runs of more than 7½ hours (~2.5 rotational cycles) on consecutive nights in 2011 Apr using the 0.7-m telescope. The RMS scatter is 0.029 mag; the somewhat over-fit Fourier curve seems to be required to trace the sharp minima.

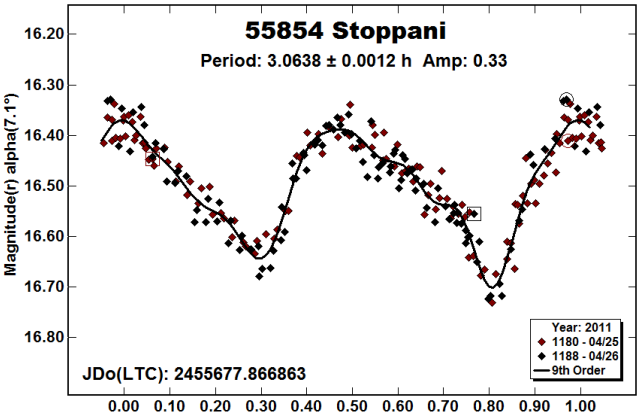

(66008) 1998 QH2. Warner (2016a) showed a lightcurve for this Apollo (a LONEOS discovery) of 7.09 h, assigned quality U = 2+. The periodogram of our two nights of 1.1-m telescope data in 2010 Sep does not show this period, but instead a somewhat shorter one. The RMS scatter on the plot is 0.020 mag.

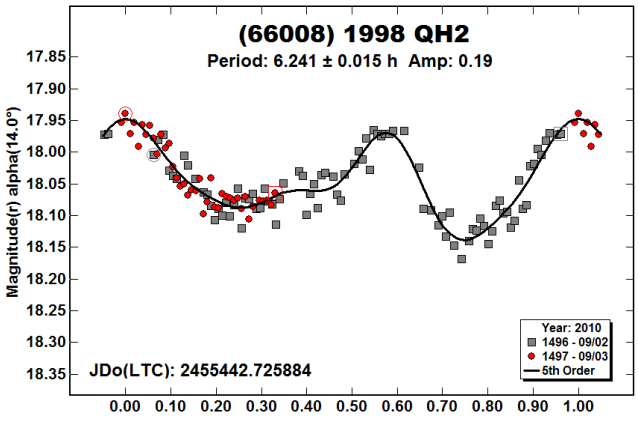

(75079) 1999 VN24. Three nights of 0.7-m data in 2011 Apr yielded a complete, well-defined lightcurve of moderate amplitude for this Mars-crosser. The 90-second exposures gave RMS scatter of 0.021 mag. We thus confirm the period by Waszczak et al. (2015) from sparse PTF data taken about the same time.

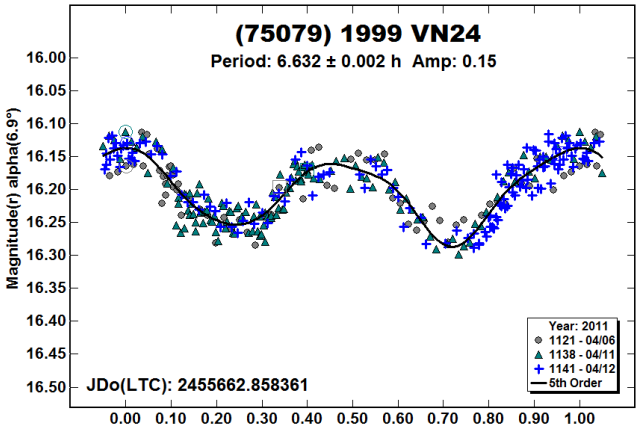

(77645) 2001 KX66. Using both the 0.7-m telescope (three nights, R_c filter) and Schmidt (final night, unfiltered), we obtained runs on this Phocaea of between 7½ and 8 hours duration in 2011 Apr-May, covering more than two rotational cycles each night. The period is thus well-determined despite the RMS scatter of 0.04 mag.

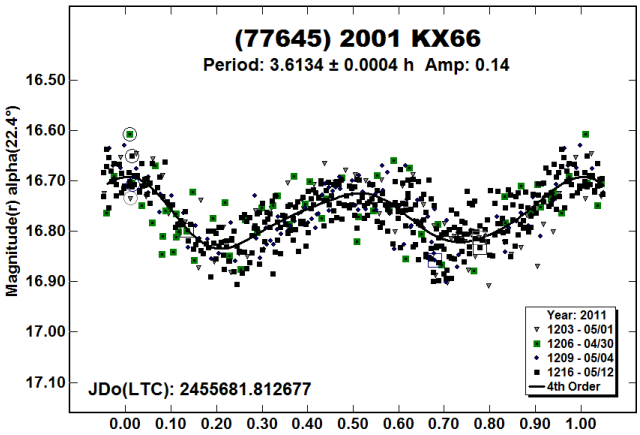

(81298) 2000 GW1. Three nights in 2011 Jun using 60-second exposures on the Schmidt gave a nearly complete large-amplitude lightcurve for this Phocaea. The RMS scatter on the fit is 0.05 mag due to the faintness at minimum. Two subsequent nights are more problematic; one was somewhat cloudy, and the other clear but the data showed a smooth but peculiar form. These are shown in the raw plot below. There is no previous lightcurve photometry published.

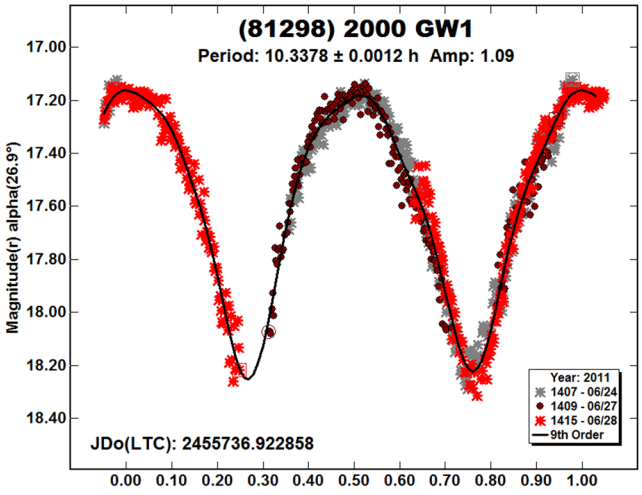

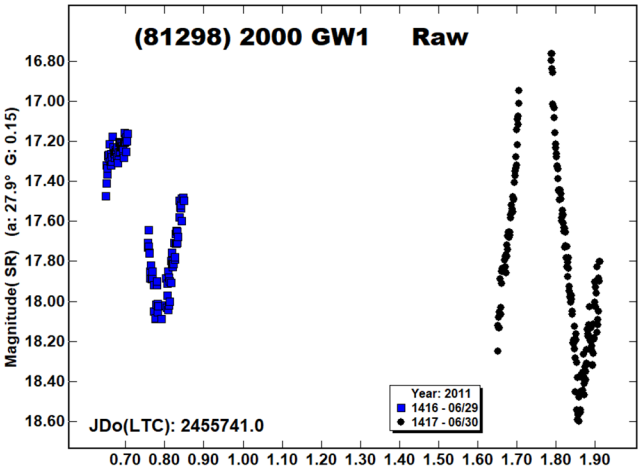

(85953) 1999 FK21. This 0.6-km Aten is a known tumbler (Pravec, 2019web), which we observed on seven nights in 2011 Mar-Apr using the Schmidt. Comprising nearly 2600 frames of 20- and 30-second exposures, this photometry will be analyzed together with further data by Pravec et al. in a separate publication, so for now we show a raw plot of our coverage.

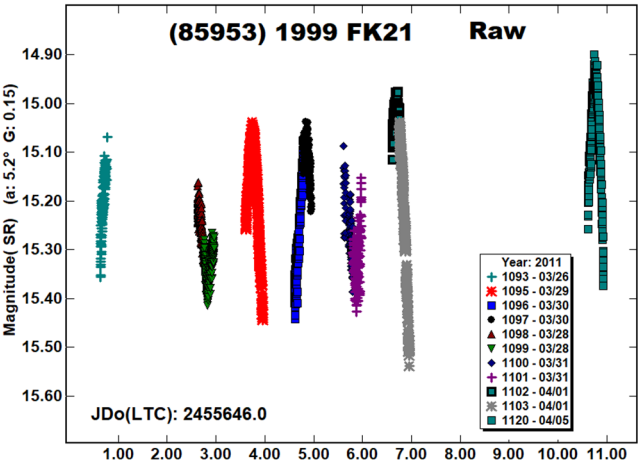

(103067) 1999 XA143. We obtained three nights of sparse data for this Apollo using the Schmidt in 2010 Jan. The lightcurve is only roughly outlined, but the period determination seems reliable due to the 6-day baseline, and is not far from previous work, starting with Galád et al. (2005). The RMS scatter on the fit is 0.04 mag.

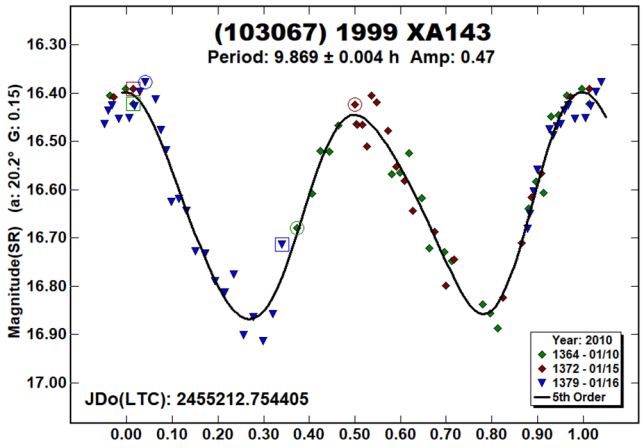

(136617) 1994 CC. This Apollo is now known to be a triple, having two small satellites identified in radar data (Brozović et al., 2011). We observed the object in 2009 Sep and Oct using the Schmidt, but it was really too faint for the telescope given the small amplitude. However, data from the first lunation fit a period close to the rotation period for the primary determined by Brozović et al (2.389 h). The RMS scatter is 0.05 mag.

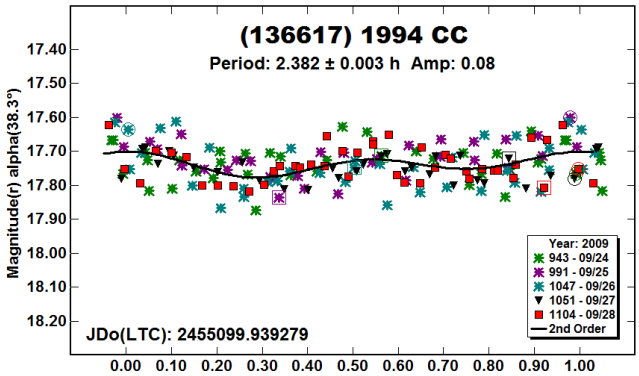

(138524) 2000 OJ8. Our data over two nights in 2011 Sep using the 0.7-m telescope had barely high-enough precision to see the small-amplitude short-period quadrimodal lightcurve in this Amor. Luckily there are data from Pravec (2011web) on the same nights confirming the period. The RMS on the phased plot is 0.020 mag.

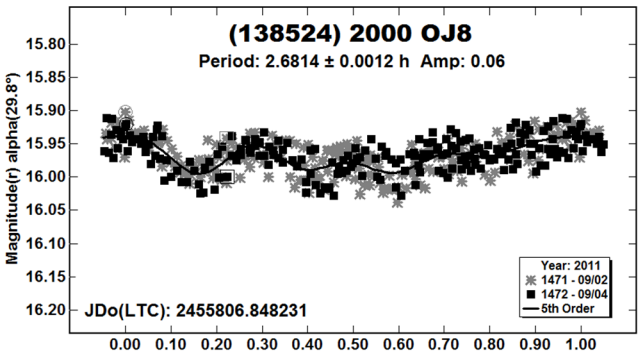

(141018) 2001 WC47. Over three lunations in 2012 Mar-May, we obtained lightcurve fragments using the 0.7-m telescope for what seems to be a long-period tumbling Amor. Based on data from the same apparition, Warner (2012b) suggested a period of 16.5 hours. However, any periodicity cannot be so short as that, since the example 7½-hour run shown below has only a broad maximum.

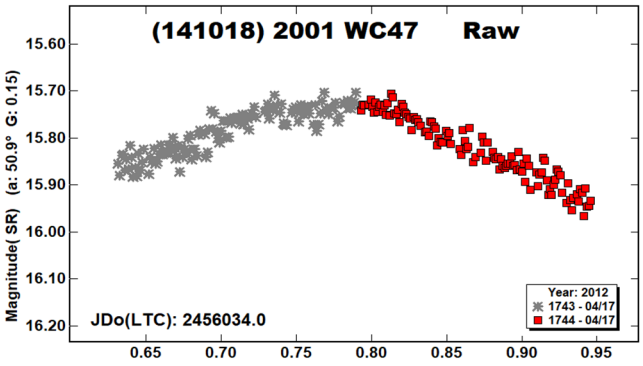

(143487) 2003 CR20. Schmidt data were obtained for this Apollo over a seven-night interval in 2009 Sep. The 90-second exposures yielded a somewhat noisy lightcurve with a period of about 7 h; the RMS scatter on the fit is 0.04 mag.

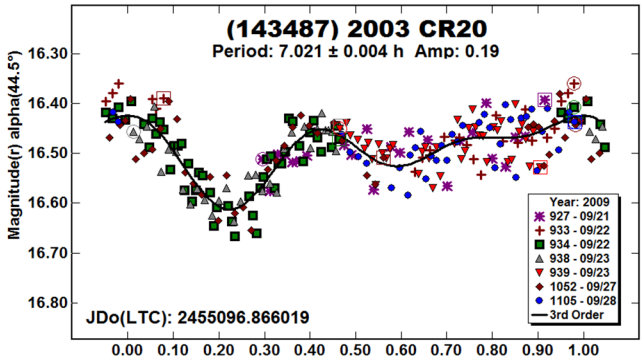

(152664) 1998 FW4. We obtained three nights of data in 2009 Sep for this Apollo using the Schmidt (20- to 30-second exposures), which gave barely enough rotational phase coverage for this somewhat slow rotator. The RMS scatter on the fit is 0.017 mag. The period we derive is similar to, but somewhat shorter than that of Warner (2014a), whose data cover a longer baseline. From a more recent run, Warner and Stephens (2022a) indicate things might be ambiguous.

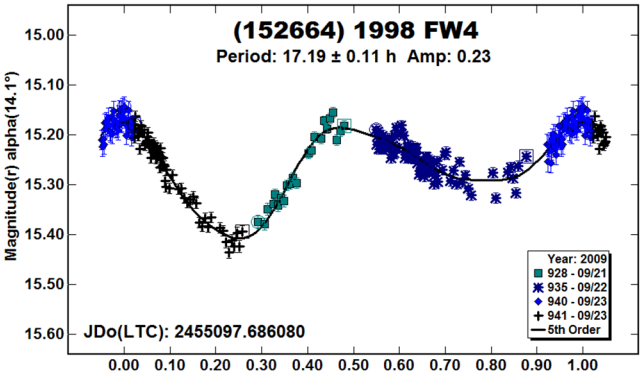

(159402) 1999 AP10. Our Schmidt data for this Amor span four months at the end of the 2009 into 2010. The first three nights were combined with other photometry acquired during the same range of dates and published by Franco et al. (2010). This group and Hasegawa et al. (2018) both obtained periods near 7.91 hours. Reanalysis of our complete series, after adjustment of the comparisons stars and including additional nights, show periods about 0.01 h longer – perhaps not a significant difference, but other later observers also get 7.92 h. The three lightcurves here are from 2009 Sep and Dec, and a final single-night run in 2010 Jan. The RMS scatter on all three plots, shown at the same vertical scale, is between 0.015 and 0.020 mag.

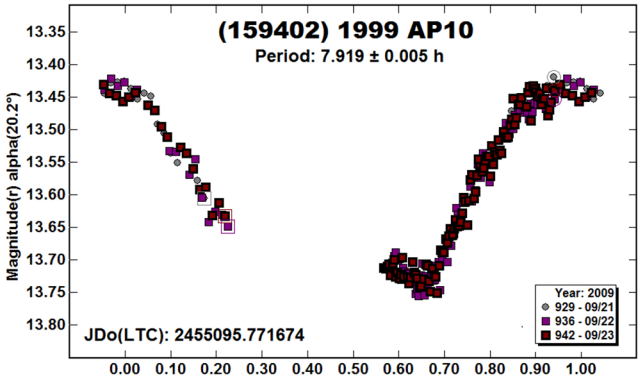

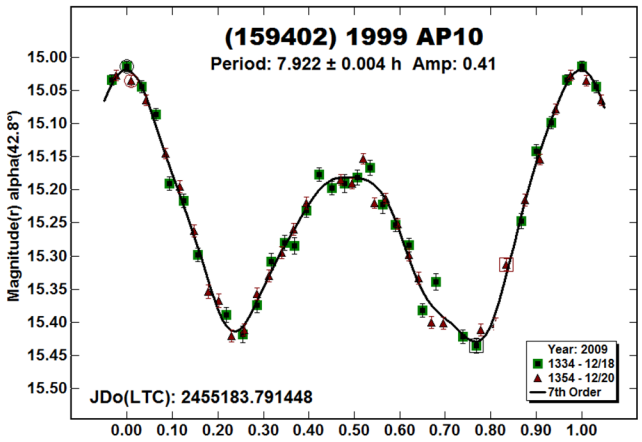

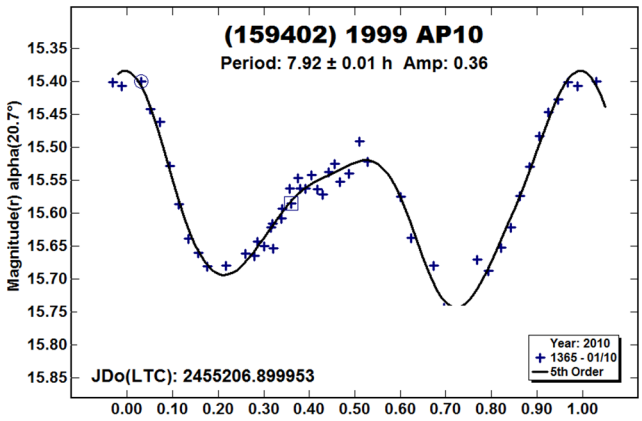

(160092) 2000 PL6. Three nights in 2011 Oct using the 0.7-m telescope showed a fairly short period lightcurve of modest amplitude for this Amor. The RMS scatter on the fit is 0.024 mag. We obtained two additional nights using the Schmidt, but they are much less good.

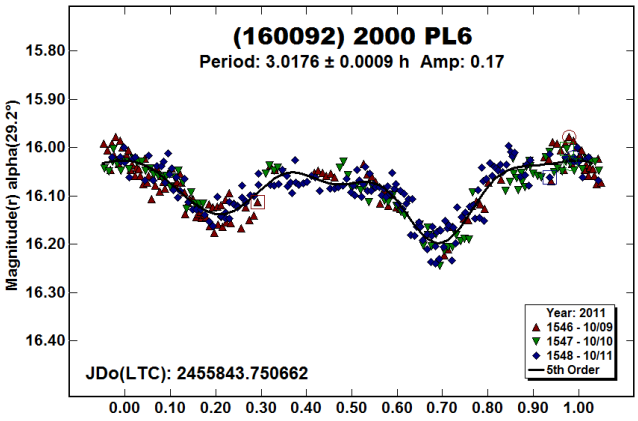

(163081) 2002 AG29. Pravec (2019web) has given the first rotation period (19.64 h) for this Apollo. Our Schmidt data from 2011 Oct are somewhat ragged and do not cover the secondary maximum, which could explain the slightly different period-determination. The RMS scatter is 0.019 mag with three-image 4-minute averaging.

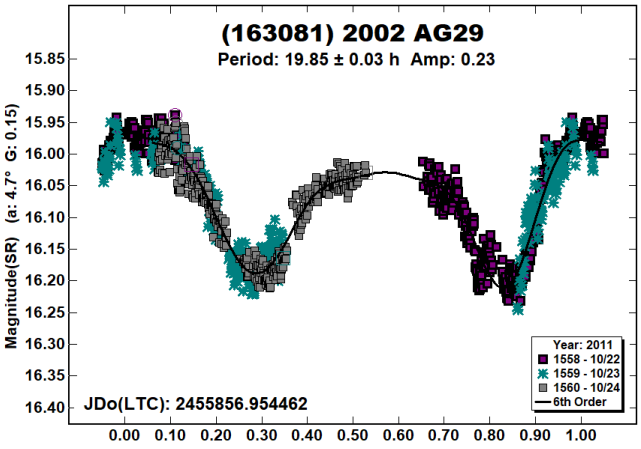

(178783) 2001 BY2. Despite getting three full-night runs in 2011 Jan of between 8.5- and 9-hours duration using the 1.1-m telescope, we caught only one extremum properly on this Mars-crosser. The nightly trends, however, constrain the period fairly well. The RMS scatter on the rough fit is 0.016 mag. A more realistic uncertainty on the period is perhaps 1 to 2 hours, compared to the smaller formal error shown in the lightcurve legend.

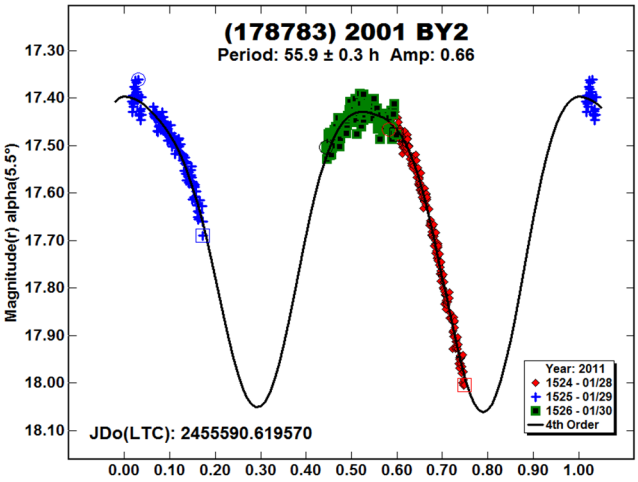

(181882) 1999 RF14. Our photometry from 2011 Mar for this Mars-crosser is problematic. There is a short-term wobble of about 0.1-mag amplitude, but also a longer-term slow variation. This could be a very wide binary, and the small, short variation is from the rotation of a companion, but otherwise the data are inscrutable. We have four nights of Schmidt data and three more 8-hour runs using the 1.1-m telescope. An example of the (better) 1.1-m data is shown.

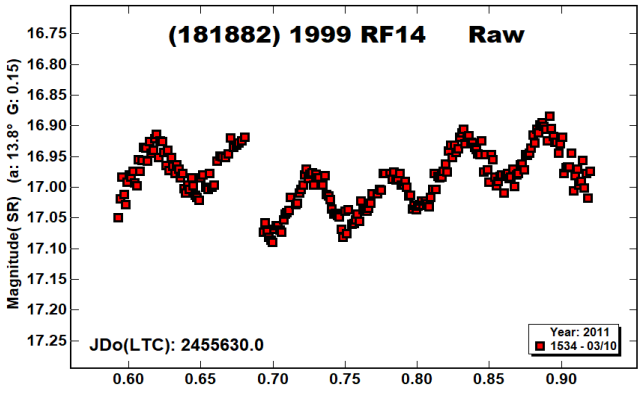

(188174) 2002 JC. This Aten was passing near the north ecliptic pole in 2011 May when we got three nights of photometry using the Schmidt. The fairly short period is unambiguous, with RMS scatter of 0.033 mag after averaging the data in three-image 4-minute bins. Our period determination is very similar to previous results, starting with Polishook and Brosch (2008). The alternative 2.74-h period suggested by Warner (2014b) is not present in our data.

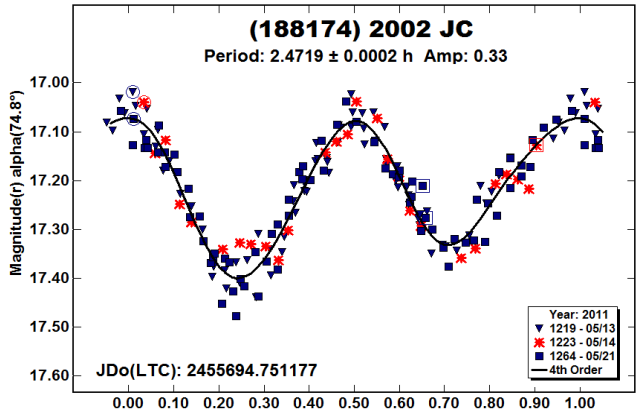

(218863) 2006 WO127. The LCDB cites a short, high-precision rotation period and spin-axis for this Apollo (Ďurech et al., 2018).

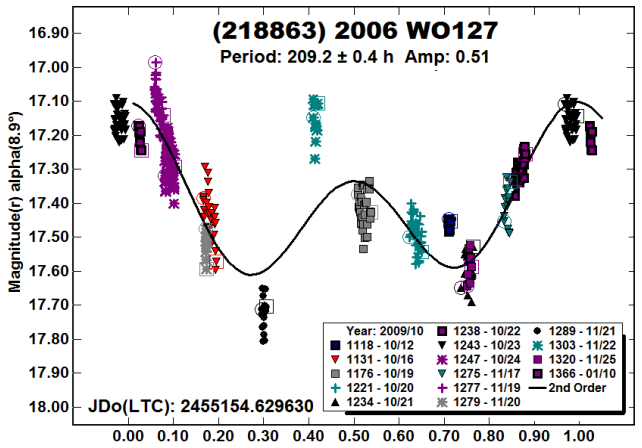

In our many nights of Schmidt data from 2009 Oct to 2010 Jan there is no such short cycle present unless the amplitude is quite small. Instead, we see evidence for a long-period tumbler. The data show a persistent cycle-length of roughly 210 hours, but surely other components are involved.

(222073) 1999 HY1. Previously Warner (2017) found a period for this Amor of 10.37 h with some uncertainty. Two nights of Schmidt data in 2009 Oct, totaling 16 h on target, with similarly-poor internal precision near the faint working limit of the telescope, suggests instead half this period with similar lightcurve morphology. The RMS scatter on the fit is 0.05 mag.

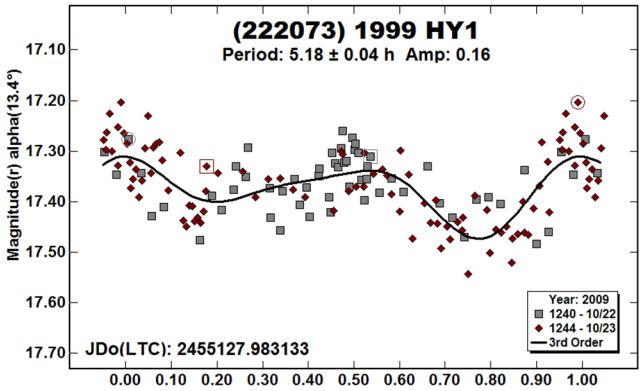

(241370) 2008 LW8. The two short 2010 Jun nights we obtained on this Apollo were insufficient to cover the rotation period. Indeed, the simple fit shown here is possibly half the true period of the very-small-amplitude lightcurve. The 3-minute exposures using the 1.1-m telescope have an RMS scatter of 0.012 mag.

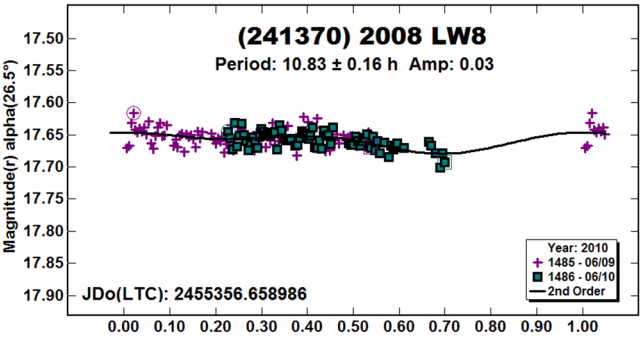

(253841) 2003 YG118. We got only a 5-hour Schmidt run on one night in 2011 Feb for this Apollo.

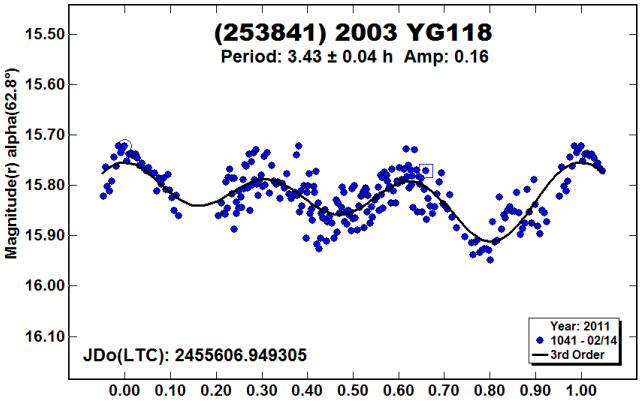

Previously (Skiff, 2011web), we used the same data to fit a double-mode period of 2.27 h, rated U = 2- in the LCDB. This is unlikely given the relatively large size of the object. We give here a tri-modal version that is probably not better (still quality 2-), but brings the period into a more likely range. The RMS scatter is 0.033 mag.

(274138) 2008 FU6. Warner (2014b) showed data for this Apollo from 2014 suggesting a short period of about 2.85 h along with a possible secondary period of 12.7 h. We cannot reproduce this in our single-night 3-hour run with the Schmidt in 2011 Apr. A quadrimodal period of 2.66 h with small amplitude is shown here, which could be spurious. The RMS scatter on the fit is 0.018 mag.

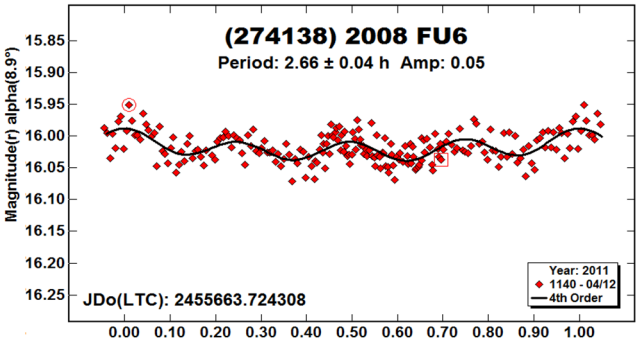

(276741) 2004 EM66. Observation of this Mars-crosser in 2011 Apr was hampered by clouds on three nights using the 0.7-m telescope. After adjusting the comparison stars to Sloan r′, we find an undistinguished moderate-amplitude lightcurve. The RMS scatter on the fit is 0.027 mag.

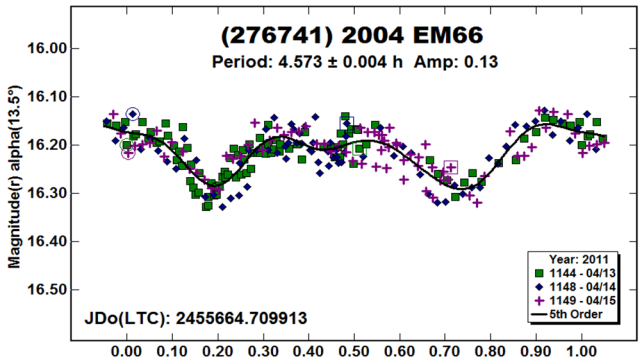

(302831) 2003 FH. This Apollo was followed using the Schmidt on three consecutive nights in 2011 Oct, though the runs were not especially long.

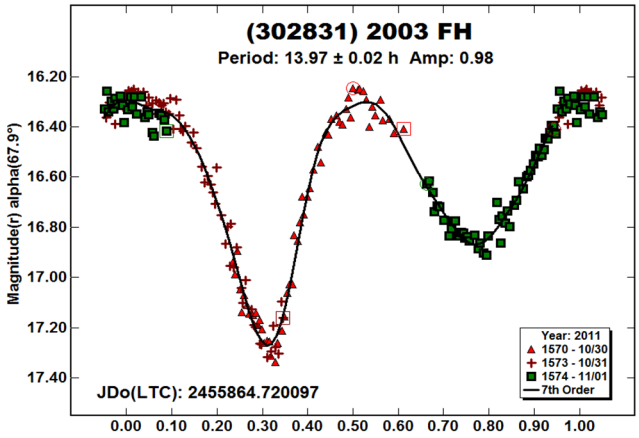

The data fit a period close to 14 hours with fairly large amplitude. The lightcurve has the 45-second exposures binned as three-image 4-minute averages; the RMS is 0.05 mag.

(307190) 2002 EK130. This Mars-crosser was discovered with the LONEOS Schmidt. Using that telescope we obtained three nights of data in 2011 Aug. Though quite noisy, an 8.25 h period seems possible with low confidence. The RMS scatter is 0.033 mag after binning the data into three-image 4-minute averages.

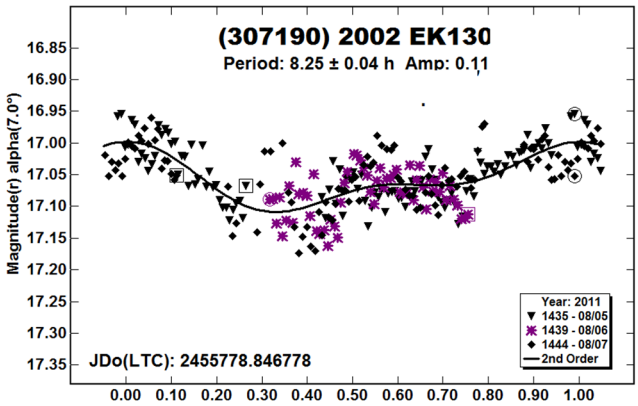

(307544) 2003 EJ16. We followed this Mars-crosser, another LONEOS discovery, on only one night with the 1.1-m telescope in 2010 Mar. The 7-hour run of 3-minute exposures allows only a tentative and uncertain period determination due to the very small amplitude. The RMS scatter on the fit is 0.022 mag.

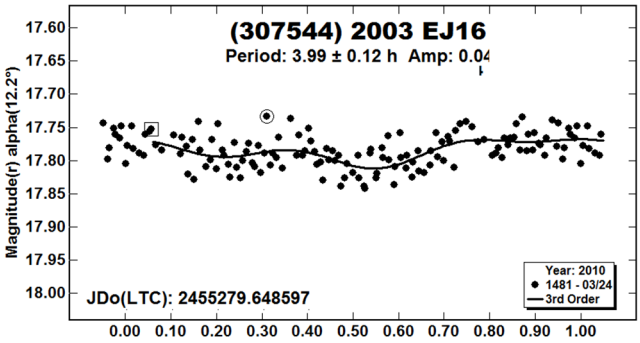

(326683) 2002 WP. The earliest published lightcurves for this 0.5-km Amor date from the 2016 apparition (e.g., Behrend, 2016web).

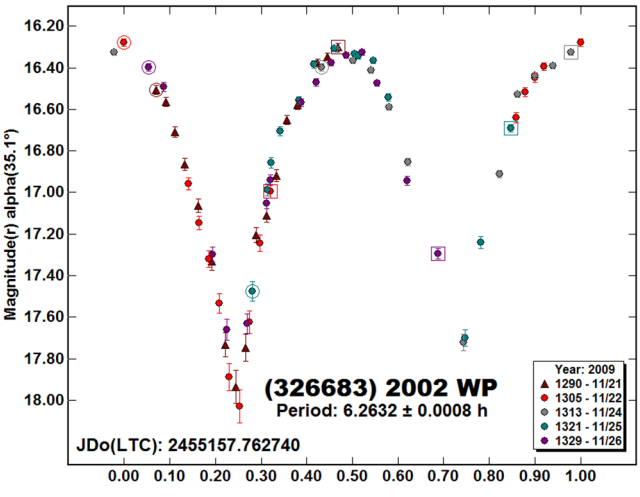

Seven years prior, we obtained data over two lunations using the Schmidt. Coverage in 2009 Nov allowed the period to be determined accurately; our 2009 Dec data are incomplete. The amplitude is 1.65 ± 0.03 mag, larger than previously observed, and the RMS scatter is 0.05 mag.

(351545) 2005 TE15. This Apollo has no previous photometric results in the LCDB. Although it was near the faint limit of the Schmidt, we observed it on four nights at the time of its 2009 Sep close approach. The lightcurve is rather noisy (RMS scatter 0.05 mag), but shows that it is a moderately-slow rotator.

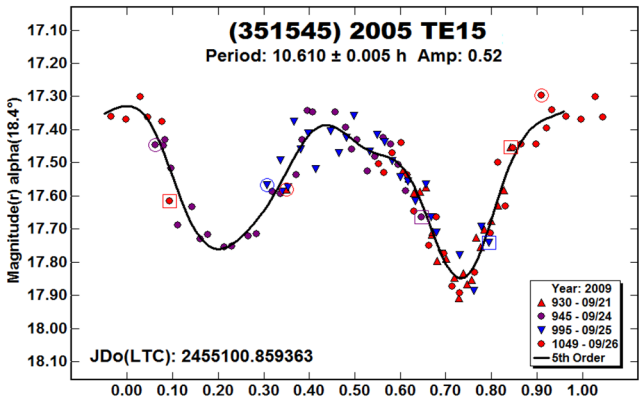

(366833) 2005 MC. Three nights of sparse data in 2009 Nov using the Schmidt with 3-minute exposures give only a tentative rotation period for this Amor. The RMS scatter is 0.05 mag.

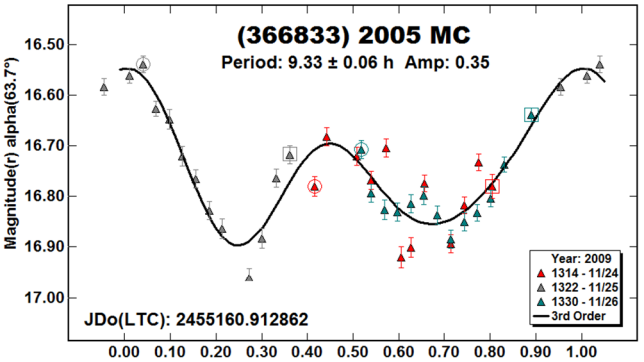

(385343) 2002 LV. We got only sparse data on two nights in 2009 Jul for this Apollo using the Schmidt. We force-fit the data to the period first found by Pravec (2002web). The RMS scatter on this rough fit is 0.05 mag.

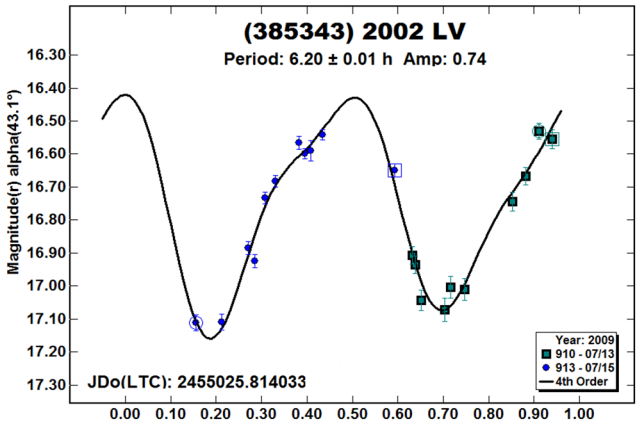

(387632) 2002 PD40. We obtained lightcurves at two stages during the 2010 apparition using the 1.1-m telescope: a single 8-hour run in April, then five consecutive nights in early July. The latter series defines the lightcurve and period of this Mars-crosser to a high degree. The lower phase-angle April lightcurve is obviously different in morphology and of smaller amplitude. The RMS scatter on the two lightcurves, which are plotted at the same vertical scale, is 0.015 and 0.013 mag, respectively.

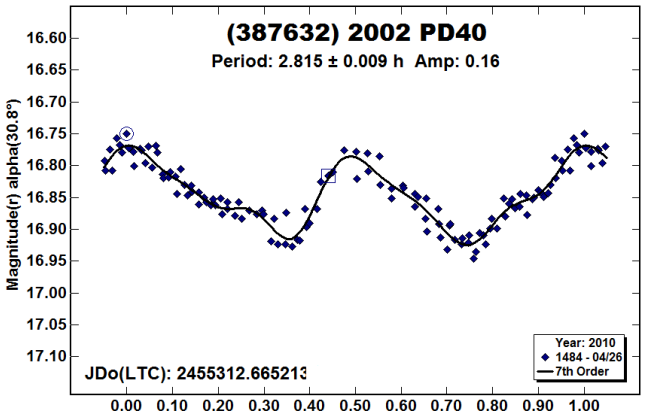

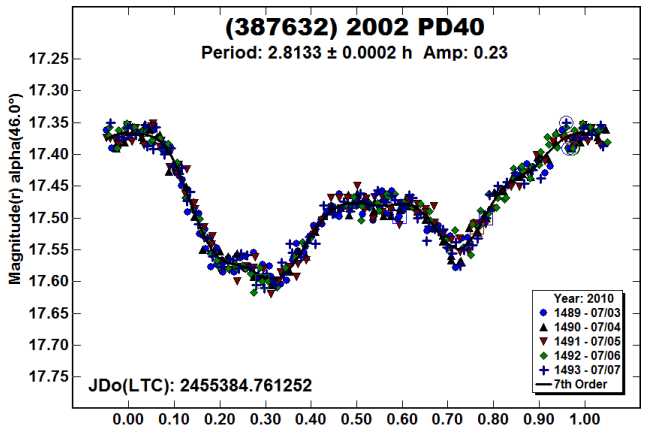

(407656) 2011 SL102. Three good nights in 2011 Dec using the 0.7-m telescope on this Amor yielded what look like parts of a large-amplitude lightcurve with period slightly longer than a day.

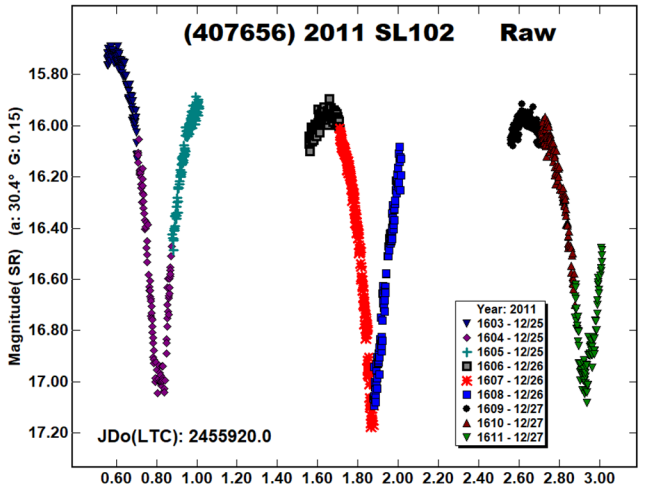

Each nightly run is nearly 11 hours long. The data, however, do not phase well with any period. We are confident that the photometric zero-points are consistent to within a few percent for the series, precluding a problem with the maximum on the first night being ~0.2 mag brighter than the following two. Neither do the shapes and slopes of the second and third nights match when those nights are aligned on their maxima. Perhaps some tumbling is involved, but we simply do not have enough coverage to say much more.

(420187) 2011 GA55. Two 7-hour runs using the Schmidt on this Amor in 2011 Aug showed a short-period lightcurve of modest amplitude. The phased plot has the 679 measurements from 45-second exposures binned into 230 three-image 4-minute averages; the resulting RMS is 0.031 mag.

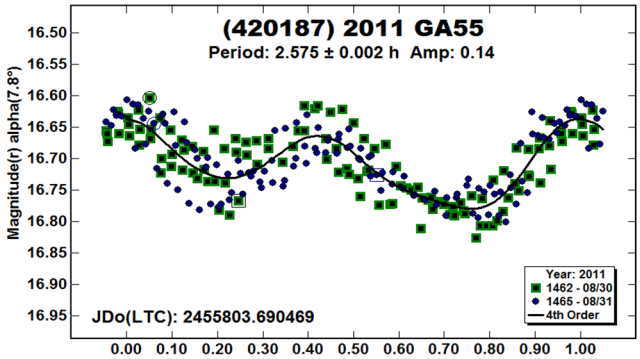

(448972) 2011 VY15. We observed this Amor on two consecutive nights with the 0.7- and 1.1-m telescopes in 2012 Mar, getting about 9 hours total on the target and more than a full cycle each night. The period is short and has small amplitude. The RMS scatter on the fit is 0.017 mag.

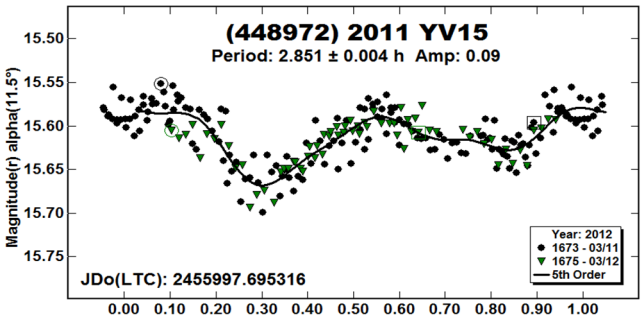

(451397) 2011 EZ78. Our series using the Schmidt in 2011 May-Jun on this Amor showed that it was a probable binary or tumbler with lightcurves that did not repeat from night-to-night.

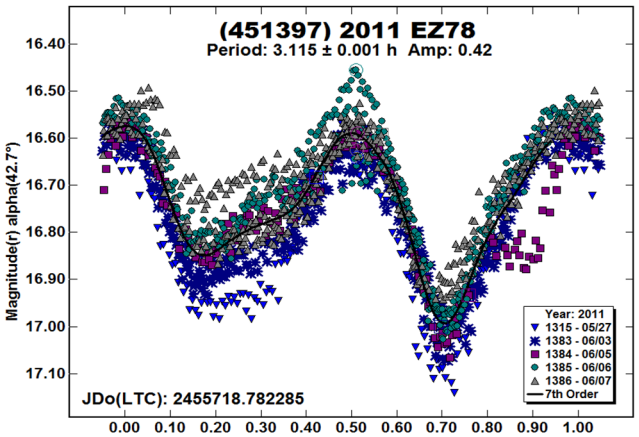

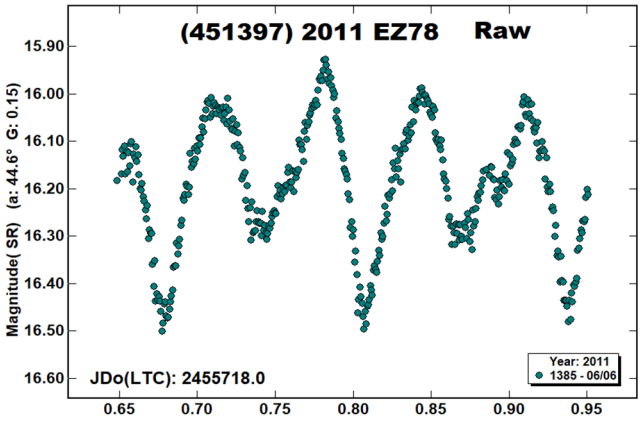

The dominant period is shown in the first plot, which phases all the data, and in which what look like mutual events can be seen. The second plot is a single full night run, showing that the lightcurve does not repeat even on a short timescale (the RMS scatter in this plot is about 0.02 mag). Pravec (2011web) suggests a possible second period of about 55 h along with unconfirmed attenuation events.

(483504) 2002 XN14. Sparse data for this Apollo on three nights using the Schmidt in 2009 Dec allow only an approximate and uncertain determination of the rotation period. The lightcurve here is the only bimodal solution in the periodogram. The RMS scatter on the fit is 0.032 mag. There is no other published photometry.

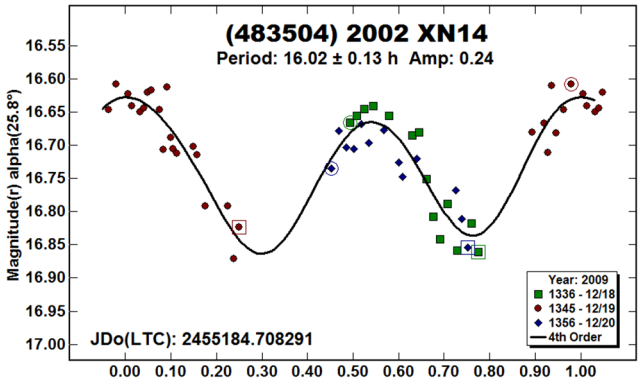

(523654) 2011 SR5. Our two nights of Schmidt data in 2011 Sep, starting the night after this Apollo was discovered, were relatively noisy and lack temporal coverage to get a reliable rotation period. We show a *tentative* solution, which could well be wrong. The RMS scatter, with the points averaged into three-image 4-minute bins, is 0.029 mag.

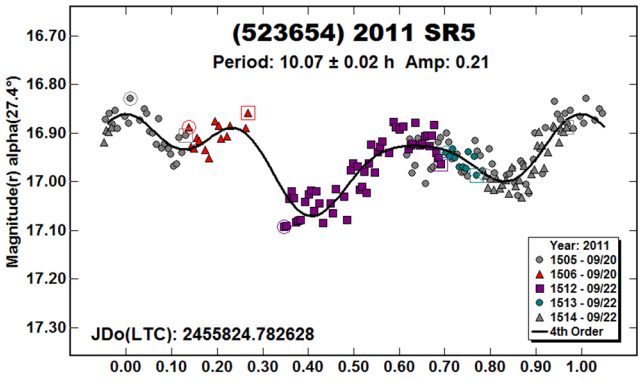

(524196) 2001 QP181. After four nights of Schmidt observing in 2011Apr we found no periodicity expressed in the data, so abandoned observing it. A period we gave previously (Skiff, 2011web) is spurious. The Amor is a likely tumbler with a complex lightcurve. The raw data-plot shows the series we obtained; at this magnitude level the typical RMS scatter is 0.04 mag.

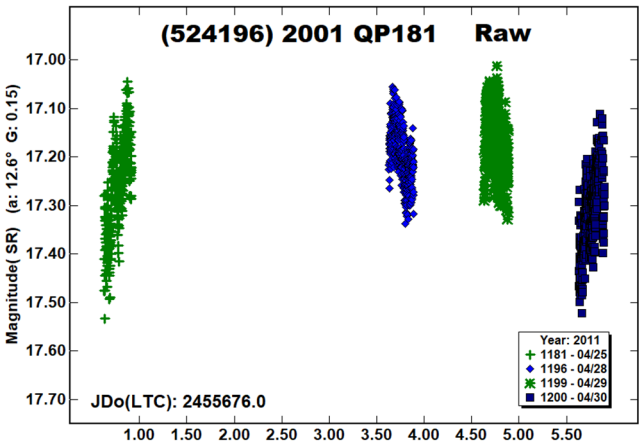

(530520) 2011 LT17. We followed this 150-meter Apollo for 6½ hours on 2011 Jun 11 (essentially dusk-to-dawn) using 30-second exposures on the Schmidt. The period is fairly short, but not unusually so for a small object. The RMS scatter on the fit is 0.04 mag after averaging the images by pairs.

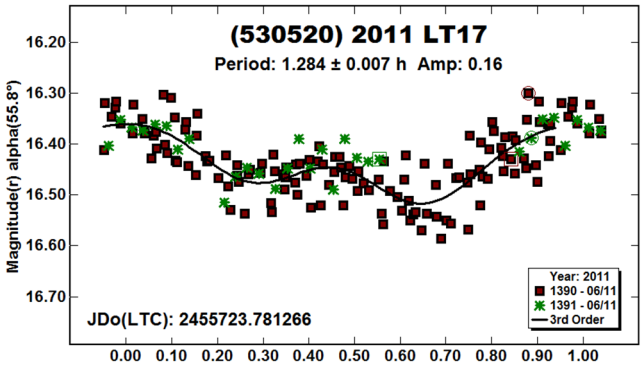

(612050) 1997 GL3. Pravec et al. (1998) first remarked upon the "several bumps and wiggles" in the complex lightcurve for this Apollo. They concluded that the period was 7.57 h, but consider that either the shape may not be symmetrical with respect to a 180° rotation, or that the body is in an excited rotational state.

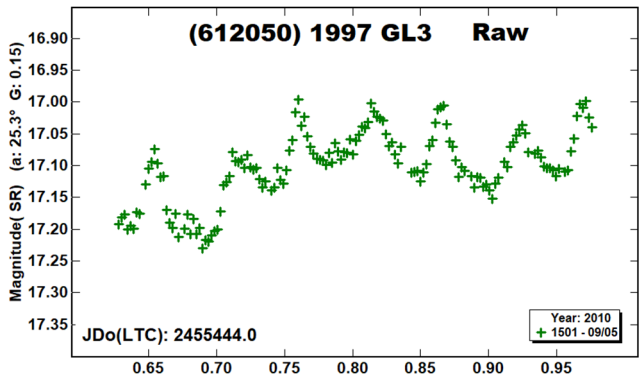

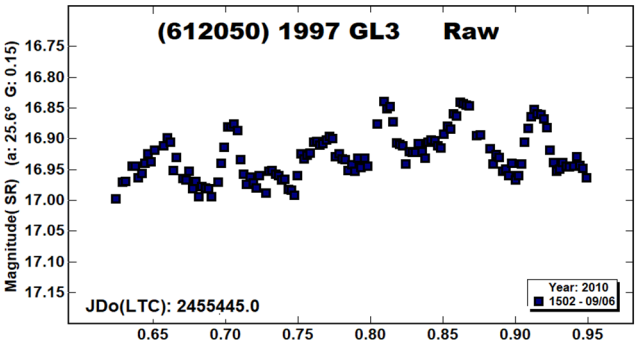

Our two nights of 1.1-m telescope data in 2010 Sep, each about 8 hours long, do not fit the 7.57-h period very well, and each night's series is subtly different. The phase-angle was also significantly higher (Pravec about 8° versus our 25°). We thus show the two raw plots. As can be seen from the point-by-point consistency, the internal precision is quite good (~0.015 mag RMS).

2000 CP101. Our single-night 3½-hour run in 2011 Aug showed only one pair of extrema for this Apollo. This suggests a period in the range of 10-12 hours, but we can say no more from these 45-second exposures with the Schmidt.

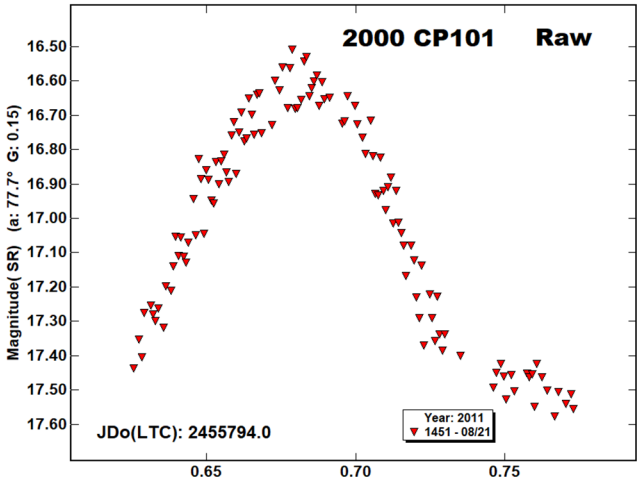

2009 MC9. This Amor was another object near the faint limit of the Schmidt. Our four nights of data in 2009 Sep (90-second exposures) produced a lightcurve similar to that of Behrend (2009web) from data by Silvano Casulli. The RMS scatter on the fit is 0.05 mag.

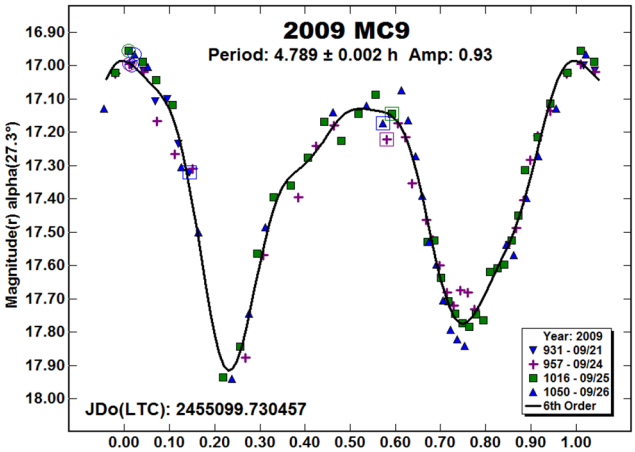

2009 NH. Albino Carbognani (2011) observed this Amor in 2009 Aug, a few weeks after our first observations. The asteroid was fairly faint, and so data from our two nights with the Schmidt are somewhat noisy, with RMS scatter of 0.04 mag. We nevertheless obtained a period similar to Carbognani's.

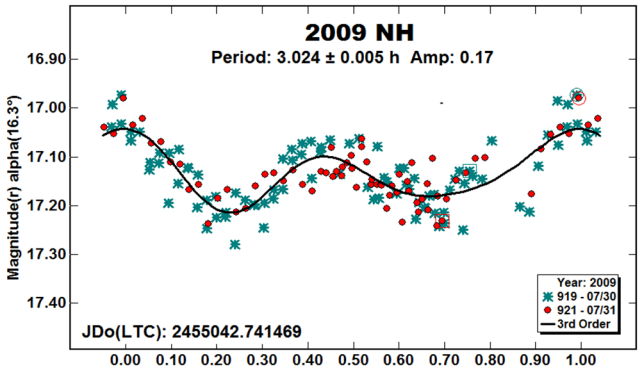

2009 WV25. This small Apollo was observed three days after discovery in 2009 Nov for only 3 hours using the Schmidt. The period derived is also 3 hours, which we consider to be suspect. The RMS error on the fit is 0.08 mag. The LCDB shows that Bill Ryan (unpublished) observed it on the same night from Magdalena Ridge Observatory, assigning an approximate period of 5 hours, possibly tumbling, and amplitude 1.24 mag, compared to 1.1 mag here. The object was last observed for astrometry in 2014, and will not be coming around again for many years.

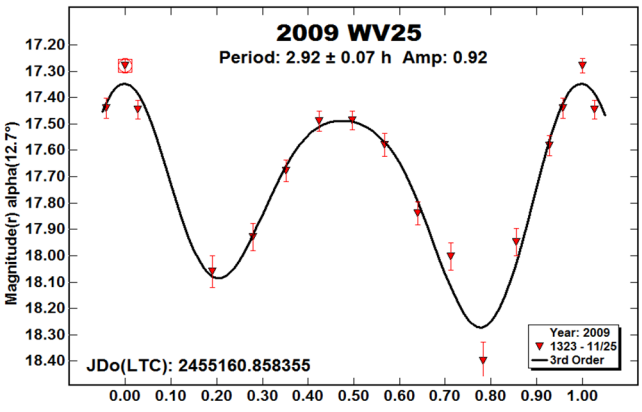

2011 CG2. Even at maximum this Apollo was at the faint working limit of the Schmidt using 45- and 60-second exposures.

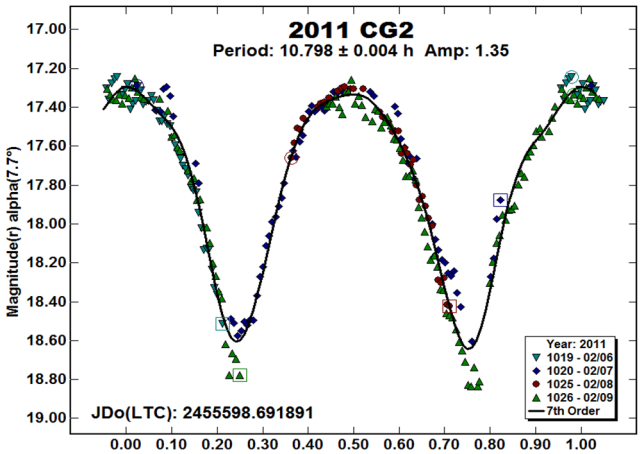

We show the lightcurve from 2011 Feb, shortly after discovery, and apparently the only such. The data below mag 18.5 are very poor, but the period seems to be secure thanks to the large amplitude. The RMS scatter on the fit is 0.08 mag after averaging the data in three-image 5-minute bins.

2011 CY46. We obtained two nights of data for this Apollo in 2011 Mar, about a month after discovery. The 45-second exposures using the Schmidt yielded a well-defined lightcurve of fairly large amplitude. The RMS scatter on the fit is 0.026 mag.

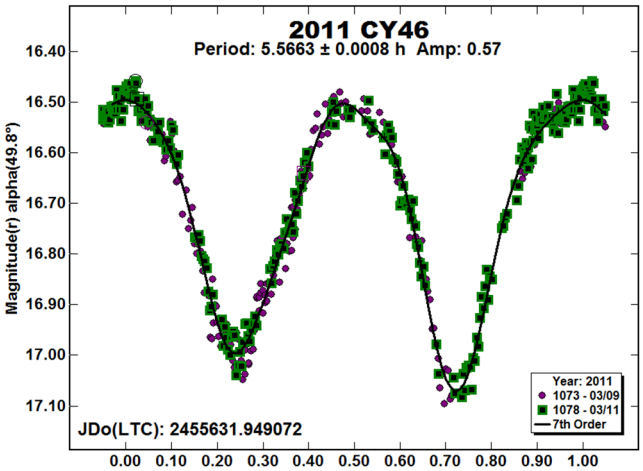

2011 GM62. We caught this small, fast-moving Apollo using the Schmidt for about 3½ hours on 2011 Apr 22 using 30-second exposures. The data span one maximum, so we infer only that the period could be in the range of 8 hours or so. At the high phase-angle involved, the amplitude is large.

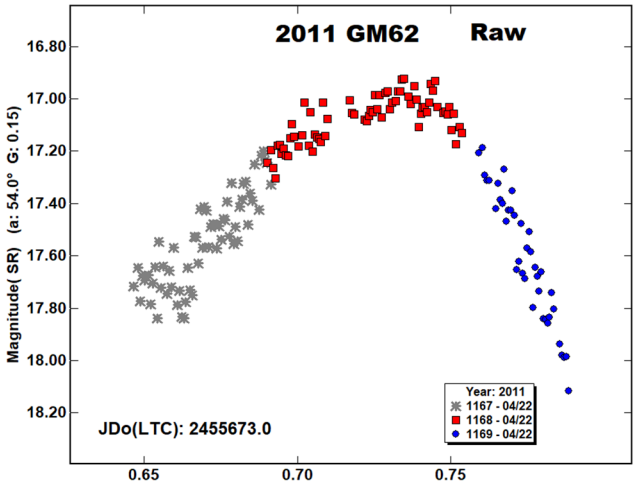

2011 GP59. This small (30 to 40 meters) Aten was observed for 6 hours on 2011 Apr 11 using the Schmidt. The period is very short, about 7.3 minutes, and the amplitude very large. Because the asteroid faded to near the telescope detection limit during the minima, the 45-second exposures gave very noisy data, saved only by the large amplitude. The lightcurve is displayed (warts and all) with error bars on the individual points to show how rapidly the errors increase as a function of magnitude. The RMS scatter on the fit is 0.21 mag(!). It is worth noting that the exposures were one-tenth the period, which reduces the apparent amplitude of the lightcurve (cf. Pravec et al., 2000).

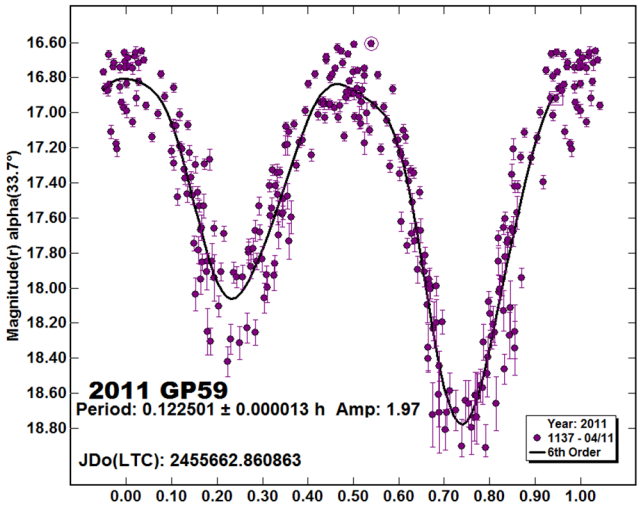

2011 HS. This 200-meter Apollo was another faint object observed using the Schmidt on the two nights following discovery in 2011 Apr. It turned out to be a tumbler, so the lightcurves do not repeat in any regular way night-to-night. The large phase-angle made the amplitudes very large, with rapid brightness changes on a short timescale. The two raw plots are shown to indicate the variation. The asteroid has not been observed since 2011 Jun.

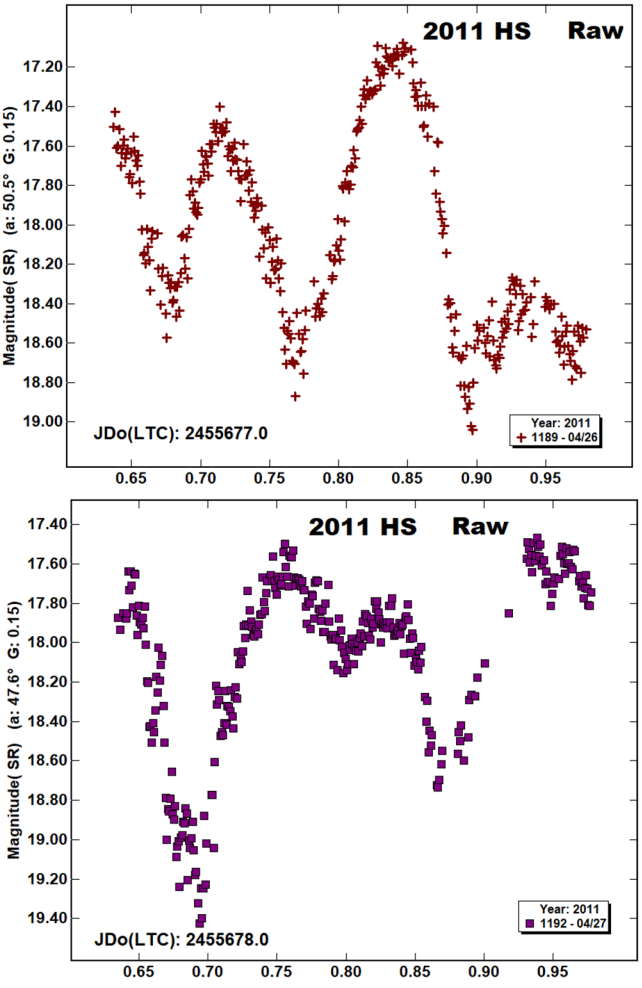

2011 KE. We obtained only rather poor and incomplete data for this Apollo using the Schmidt right after discovery in 2011 May. The period must be near 8 h, but with significant uncertainty. After binning the data into three-image 4-minutes averages, the RMS scatter is 0.06 mag.

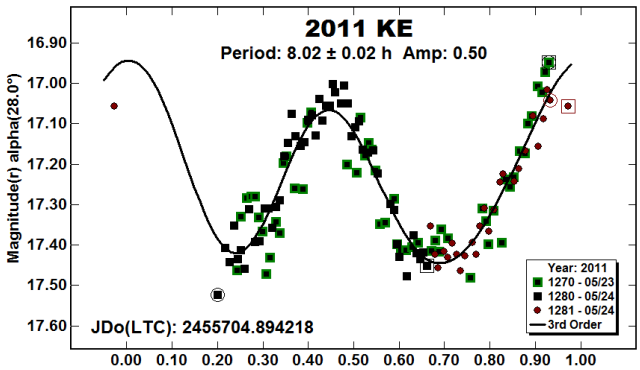

2011 LJ19. This fairly small Apollo has not been observed since 2011 Nov. We followed it on three nights in 2011 Sep using the Schmidt. The lightcurve morphology changed significantly each night, so we show three phased plots at the same vertical scale. The period has been fixed to that determined from the combined dataset, which has a realistic uncertainty of perhaps 0.01 h. On the first two nights the data are 30-second exposures and have RMS scatter of 0.04 and 0.035 mag. The final night, when the asteroid was fading, we averaged the 45-second exposures in three-image 4-minute bins; the RMS here is 0.034 mag.

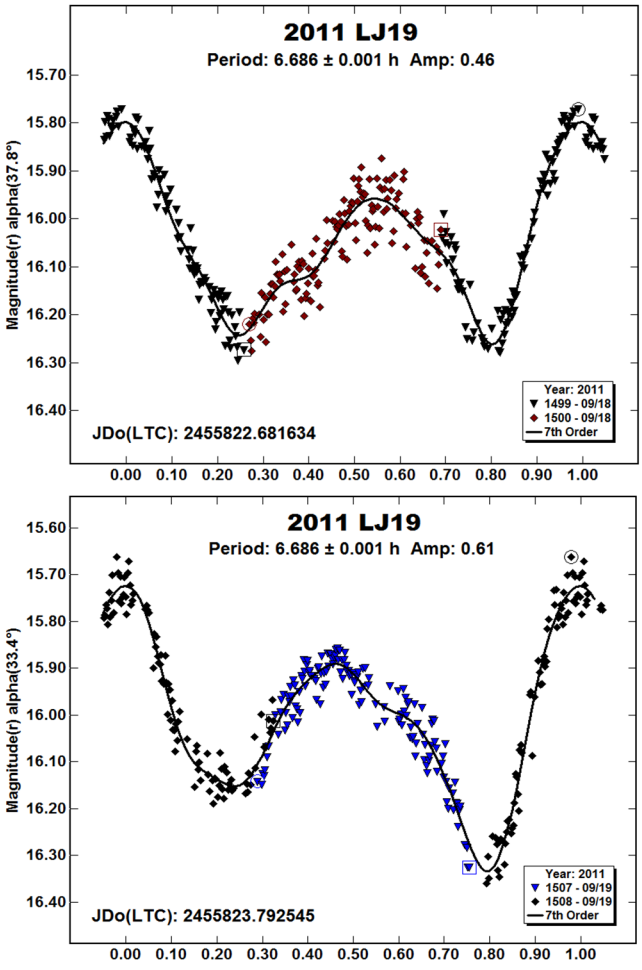

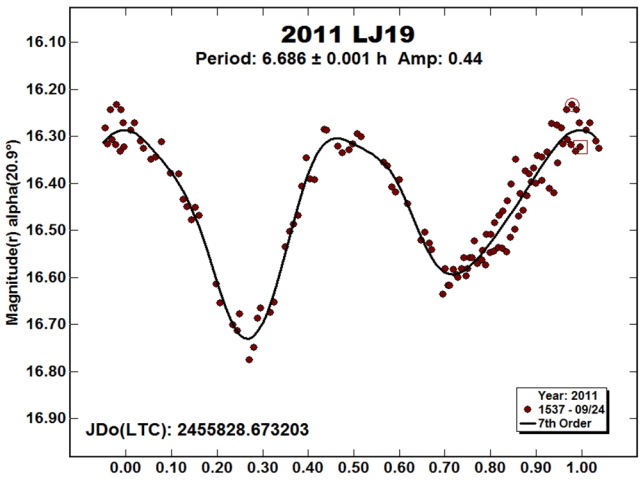

2011 MD. Several groups caught this very small (~6-meter) Apollo (Mommert et al., 2014) on the same nights in 2011 Jun. Our Schmidt data yield an unambiguous period of about 11½ minutes on two nights. The double period (cf. Vaduvescu et al., 2017) is excluded by a split-halves plot. The lightcurve morphology changed only slightly on the two nights, though on the second night it was brightening rapidly during the run. The RMS scatter on the phased plots, which are at the same vertical scale, is 0.09 and 0.06 mag, respectively.

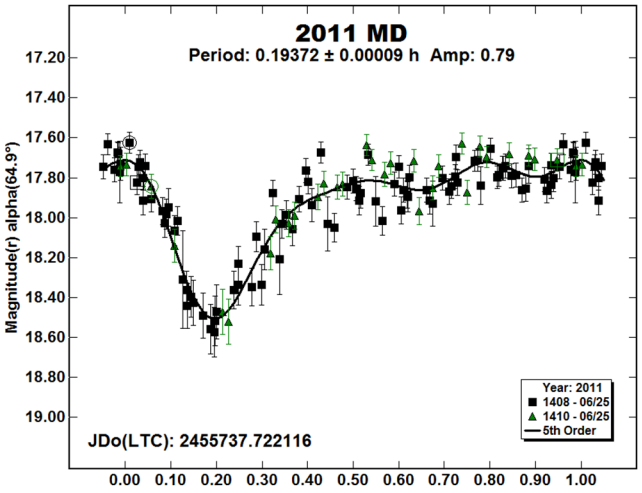

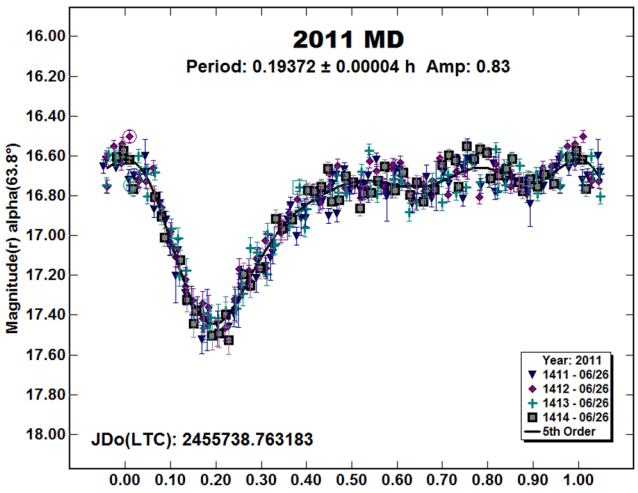

2011 OQ5. Our single 8-hour run in 2011 Sep with the 1.1-m telescope on this Amor revealed a regular bimodal lightcurve with some overlap in rotational phase coverage. The RMS scatter on the fit is 0.017 mag.

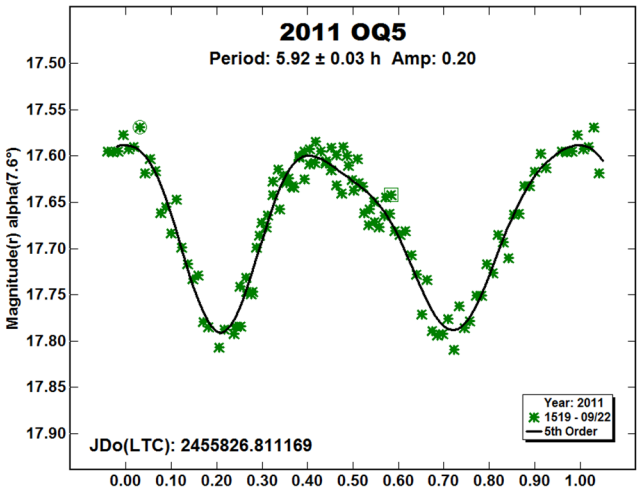

2011 PT1. We obtained a single-night 10-hour run on this Amor using the Schmidt in 2011 Sep. This shows a possible 8.3-hour period barely above the noise, which we consider tentative. If real, a single-mode 4-hour period is not excluded. The RMS scatter is 0.04 mag, so this is only a 2-sigma detection.

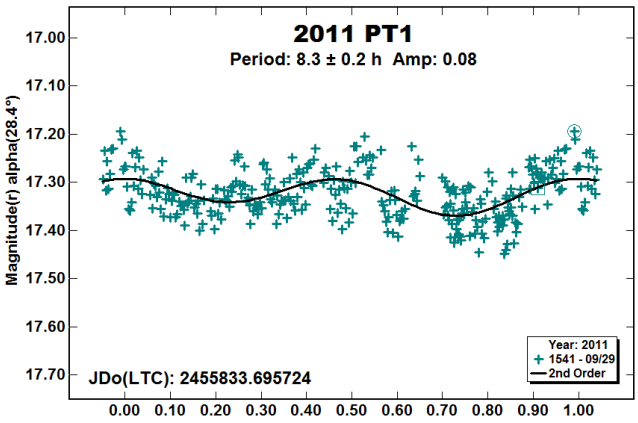

Incidental photometry

The following table shows objects for which we obtained only a few data-points, noisy data, or only a fraction of a rotational lightcurve for long-period objects. These resulted from interruptions by weather, the asteroid simply being too faint (often much fainter than predicted), or bad planning. The data are all adjusted to Sloan r′ as with the objects above.

455 Bruchsalia	5066 Garradd
5518 Mariobotta	(5646) 1990 TR2
6461 Adam	6485 Wendeesther
8648 Salix	(10145) 1994 CK1
11152 Oomine	(17274) 2000 LC16
24761 Ahau	(25362) 1999 TH24
(37336) 2001 RM	38628 Huya
49699 Hidetakasato	79360 Sila-Nunam
(86067) 1999 RM28	(105106) 2000 LS14
(123920) 2001 DW99	136108 Haumea
(138937) 2001 BK16	(143947) 2003 YQ117
(152563) 1992 BF	(162181) 1999 LF6
(162483) 2000 PJ5	(214088) 2004 JN13
(215442) 2002 MQ3	(217796) 2000 TO64
(217807) 2000 XK44	(263976) 2009 KD5
(363067) 2000 CO101	(366774) 2004 TB18
(416680) 2004 XD50	(429094) 2009 SG2
(490581) 2009 WZ104	2006 UR
2009 RN	2009 SH2
2011 CH71	

Acknowledgements

Funding for the Near-Earth Asteroid Photometric Survey (NEAPS) from 2008 to 2010 was provided by NASA grant NNX08AR28G awarded to Ted Bowell. Since then, Skiff has been supported in this activity by the Lowell Observatory research fund. We also gratefully acknowledge Sasha Brownsberger (now at Harvard Univ.), who transformed the old image-preparation code to IDL based on Marc Buie's algorithms. Student observers included Emily K. Bevins, Jared Nelson, and Graham Vickowski. The Lowell technical staff were *sine qua non* for maintenance of telescopes, domes, camera electronics, computer systems, and software – especially Larry Wasserman, Ralph Nye, Ted Dunham, Peter Collins, and Len Bright. The first author is also grateful to the Lowell library and its archivist Lauren Amundson for providing access to printed journals so that references could be browsed in-person. Tom Polakis provided considerable help with MS Word details and valuable editorial advice. We thank Brian Warner for his help with *MPO Canopus* and lightcurve interpretation.

This research has made extensive use of the VizieR catalogue access tool provided by the CDS, Strasbourg, France. Indeed, we would not have attempted it if this indispensable utility did not exist. Database wizards Cécile Loup and Patricia Vannier have been especially helpful in this regard.

References

Aymami, J.M. (2012). "CCD photometry and lightcurve analysis of main belt asteroids 1077 Campanula and 1151 Ithaka from Observatori Carmelita." *Minor Planet Bull*. **39,** 29.

Behrend, R. (2007web, 2009web, 2016web, 2020web). *http://obswww.unige.ch/~behrend/page_cou.html*.

Benishek, V. (2022). "CCD Photometry of 29 Asteroids at Sopot Astronomical Observatory: 2020 July - 2021 September." *Minor Planet Bull.* **49**, 38-44.

Brozović, M.; Benner, L.A.M.; Taylor, P.A.; and 17 colleagues (2011). "Radar and optical observations and physical modeling of triple near-Earth asteroid (136617) 1994 CC." *Icarus* **216**, 241-256.

Bus, S.J.; Bowell, E.; Harris, A.W.; Hewitt, A.V. (1989). "2060 Chiron: CCD and electronographic photometry." *Icarus* **77,** 223-238.

Bus, S.J.; A'Hearn, M.F.; Schleicher, D.G.; Bowell, E. (1991). "Detection of CN emission from (2060) Chiron." *Science* **251**, 774-777.

Carbognani, A. (2011). "Lightcurves and periods of eighteen NEAs and MBAs." *Minor Planet Bull*. **38**, 57-63.

Debehogne, H.; Surdej, A.; Surdej, J. (1977). "Photoelectric lightcurves of minor planet 599 Luisa and 128 Nemesis during the 1976 opposition." *Astron. Astrophys. Suppl. Ser*. **30**, 375-379.

Ditteon, R.; Hirsch, B.; Kirkpatrick, E.; Kramb, S.; Kropf, M.; Meehl, J.; Stanfield, M.; Tollefson, E.; Twarek, A. (2004). "2003-04 winter observing campaign at Rose-Hulman Institute. Results for 797 Montana, 3227 Hasegawa, 3512 Eriepa, 4159 Freeman, 5234 Sechenov, and (5892) 1981 YS1." *Minor Planet Bull.* **31,** 54-56.

Ďurech, J.; Hanuš, J.; Alí-Lagoa, V. (2018). "Asteroid models reconstructed from the Lowell Photometric Database and WISE data." *Astron. Astrophys.* **617**, A57.

Ďurech, J.; Tonry, J.; Erasmus, N.; Denneau, L.; Heinze, A.N.; Flewelling, H.; Vančo, R. (2020). "Asteroid models reconstructed from ATLAS photometry." *Astron. Astrophys.* **643**, A59.

Ferro, A. (2011). "Lightcurve determination of 3151 Talbot and 4666 Dietz." *Minor Planet Bull*. **38,** 223-224.

Franco, L.; Carbognani, A.; Wiggins, P.; Koehn, B.W.; Schmidt, R. (2010). "Collaborative lightcurve photometry of near-Earth asteroid (159402) 1999 AP10." *Minor Planet Bull*. **37**, 83-85.

Franco, L.; Ferrero, A.; Durkee, R.I. (2012). "Lightcurve photometry and H-G parameters for 1151 Ithaka." *Minor Planet Bull*. **39**, 47-48.

Galád, A.; Pravec, P.; Kušnirák, P.; Gajdoš, Š.; Kornoš, L; Világi, J. (2005). "Joint lightcurve observations of 10 near-Earth asteroids from Modra and Ondřejov." *Earth, Moon, & Planets* **97**, 147-193.

Harris, A.W.; Young, J.W. (1983). "Asteroid rotation IV. 1979 observations." *Icarus* **54**, 59-109.

Number	Name	yyyy mm/dd	Phase	L_{PAB}	B_{PAB}	Period(h)	P.E.	Amp	A.E.	Grp
599	Luisa	2011 05/14	14.7	24	-1	9.57	0.01	0.18	0.01	MBO
1151	Ithaka	2011 09/08	12.6	333	10	4.93	0.01	0.15	0.01	MBO
1355	Magoeba	2011 07/16	23.3	304	33					HUN
1374	Isora	2011 03/01-03/05	5.4	150	-3	42.7	0.7	0.08	0.03	MC
1501	Baade	2011 10/14-10/15	17.2	354	-3	15.28	0.04	0.30	0.01	MBO
2060	Chiron	2017 09/02-09/13	0.7	357	4	5.92	0.02	0.02	0.01	CEN
2714	Matti	2012 05/05-05/15	16.8	205	9	9.2741	0.0007	0.24	0.01	MBO
3512	Eriepa	2011 01/15-01/17	10.1	131	2	6.785	0.006	0.26	0.02	MBO
3988	Huma	2011 07/01-07/23	67	306	41	10.53	0.01	0.26	0.03	NEO
4015	Wilson-Harrington	2010 01/10	40.3	60	1	3.61	0.15	0.13	0.02	NEO
4103	Chahine	2018 02/01-03/20	13.3,18.1	135	30	105.	2.	0.60	0.05	PHO
4132	Bartok	2011 04/22-04/28	9.3	224	22	3.2971	0.0003	0.34	0.02	PHO
4287	Trisov	2011 03/11-03/24	8.2	162	7	5.4936	0.0004	0.72	0.03	MBO
4666	Dietz	2011 06/18-06/20	17.8	252	19	2.9540	0.0004	0.24	0.01	PHO
5131	1990 BG	2009 11/22-2010 01/10	32.1,22.8	127	0	76.9	0.1	0.22	0.03	NEO
5209	Oloosson	2011 02/10-02/11	8.4	99	6	14.6	0.1	0.50	0.05	TRO-J
5496	1973 NA	2011 01/01-01/02	14.0	108	17	2.86	0.01	0.00	0.01	NEO
5496	1973 NA	2011 06/09-06/12	76.0	314	23	2.856	0.002	0.15	0.02	NEO
5621	Erb	2011 08/30-09/01	20.1	1	9	8.027	0.006	0.09	0.01	MC
5626	Melissabrucker	2009 07/01-07/31	18.6,4.2	310	4	2.4857	0.0002	0.06	0.01	NEO
5682	Beresford	2011 10/22-10/23	1.8	31	1	3.771	0.005	0.07	0.01	MC
5736	Sanford	2011 07/13-07/15	23.7	272	28	3.1850	0.0011	0.35	0.03	PHO
5736	Sanford	2011 07/28	27.8	275	29	3.185	0.001	0.41	0.02	PHO
7002	Bronshten	2011 10/29-11/01	3.0	39	-3	2.672	0.002	0.13	0.02	MC
7750	McEwen	2011 08/20-08/29	20.0	340	25	27.843	0.003	0.45	0.01	MBO
7757	Kameya	2011 07/13-07/16	25.6	303	33					PHO
7784	Watterson	2011 09/08-10/13	*23.1,24.5	347	27	2.5392	0.0002	0.08	0.01	PHO
12225	Yanfernandez	2011 05/08-05/13	6.5	234	7	33.7	0.3	0.17	0.01	MBO
13819	1999 SX5	2011 03/04-03/05	8.0	153	11	2.592	0.006	0.10	0.03	MC
14335	Alexosipov	2011 10/14-10/15	18.6	356	-2	7.201	0.012	0.10	0.01	MBO
14764	Kilauea	2011 06/22-06/23	21.2	246	25			1.2	0.1	HUN
15673	Chetaev	2011 10/29-11/04	16.3	45	8	102.	1.	0.69	0.02	MC
17744	Jodiefoster	2011 08/06-08/08	7.7	321	5	73.	4.	0.39	0.02	MC
18081	2000 GB126	2011 04/21-04/22	13.9	193	22	8.289	0.006	0.32	0.02	PHO
18882	1999 YN4	2010 12/07-12/08	26.1	88	32	2.466	0.009	0.12	0.01	NEO
19379	Labrecque	2012 02/01	10.2	126	15	2.60	0.02	0.10	0.01	PHO
23183	2000 OY21	2011 03/01	32.4	136	35	6.98	0.01	0.71	0.02	NEO
23552	1994 NB	2012 04/04-04/08	25.8	168	28	3.630	0.002	0.48	0.02	PHO
24475	2000 VN2	2011 12/24	38.4	66	7					NEO
27810	Daveturner	2011 02/09-02/16	7.7	136	8					HUN
29168	1990 KJ	2011 05/15-05/16	16.3	229	25	2.588	0.003	0.15	0.02	PHO
30019	2000 DD	2011 10/22-10/24	7.8	28	11	5.487	0.005	0.11	0.02	HUN
30722	Biblioran	2014 11/22-12/01	3.9	49	14	2.8695	0.0002	0.24	0.01	MBO
31425	1999 BF3	2011 04/16-04/17	11.3	218	13	9.04	0.07	0.08	0.02	MBO
32802	1990 SK	2011 11/02-11/04	8.2	50	-1	2.4276	0.0014	0.11	0.01	PHO
32906	1994 RH	2012 01/27-01/31	17.0	122	16	2.6411	0.0006	0.11	0.02	NEO
34759	2001 QL151	2011 01/22-01/27	28.0	109	37	12.219	0.003	0.30	0.02	MC
36284	2000 DM8	2011 02/02-02/04	10.6	148	2	3.844	0.002	0.22	0.02	NEO
41434	2000 GB82	2011 10/24-10/28	3.0	35	0	4.1335	0.0013	0.14	0.01	MC
43750	1981 QG3	2011 06/17-06/29	20.6	254	24	12.621	0.003	0.30	0.02	MBO
44262	1998 QR51	2011 01/13-01/17	18.3	114	25	68.	1.	0.6	0.1	PHO
47035	1998 WS	2012 02/27	27.6	133	31	4.02	0.01	0.11	0.01	MC
47035	1998 WS	2012 03/07-03/10	28.2	136	28	3.9970	0.0007	0.14	0.01	MC
47035	1998 WS	2012 04/06-04/07	30.6	146	18	3.987	0.003	0.27	0.02	MC
54660	2000 UJ1	2009 11/09	38.6	24	5	5.44	0.03	1.20	0.02	NEO
55854	Stoppani	2011 04/25-04/26	7.0	216	10	3.0638	0.0012	0.33	0.02	HUN
66008	1998 QH2	2010 09/02-09/03	13.9	358	-8	6.241	0.015	0.19	0.02	NEO
75079	1999 VN24	2011 04/06-04/12	8.0	189	9	6.632	0.002	0.15	0.02	MC
77645	2001 KX66	2011 04/30-05/12	22.5	230	30	3.6134	0.0004	0.14	0.03	PHO
81298	2000 GW1	2011 06/24-06/28	27.2	249	33	10.3378	0.0012	1.09	0.03	PHO
85953	1999 FK21	2011 03/26-04/05	5.1,33.8	180	6			0.6	0.1	NEO
103067	1999 XA143	2010 01/10-01/16	18.8	129	5	9.87	0.01	0.47	0.03	NEO
136617	1994 CC	2009 09/24-09/27	36.6	32	11	2.382	0.003	0.08	0.03	NEO
138524	2000 OJ8	2011 09/02-09/04	29.9	359	14	2.6814	0.0012	0.06	0.02	NEO
141018	2001 WC47	2012 04/17	50.9	183	17					NEO

Table I. Observing circumstances and results. The phase angle is given for the first and last date. If preceded by an asterisk, the phase angle reached an extrema during the period. L_{PAB} and B_{PAB} are the approximate phase angle bisector longitude/latitude at mid-date range (see Harris et al., 1984). D is the diameter (km, *diameter is from JPL SBN). Other diameters were derived from *H* and p_V values. The last column gives the a/b ratio, based on the amplitude, for an assumed triaxial ellipsoid viewed equatorially.

Number	Name	yyyy mm/dd	Phase	L_{PAB}	B_{PAB}	Period(h)	P.E.	Amp	A.E.	Grp
143487	2003 CR20	2009 09/21-09/28	46.1,22.7	23	-3	7.021	0.004	0.19	0.03	NEO
152664	1998 FW4	2009 09/21-09/23	15.8	350	0	17.19	0.0.11	0.23	0.01	NEO
159402	1999 AP10	2009 09/21-09/23	5.0	158	6	7.919	0.005	0.30	0.01	NEO
159402	1999 AP10	2009 12/18-12/20	14.5	170	8	7.922	0.004	0.41	0.01	NEO
159402	1999 AP10	2010 01/10	13.4	171	8	7.92	0.01	0.36	0.02	NEO
160092	2000 PL6	2011 10/09-10/11	29.2	26	33	3.0176	0.0009	0.17	0.02	NEO
163081	2002 AG29	2011 10/22-10/24	3.7	30	2	19.85	0.03	0.23	0.02	NEO
178783	2001 BY2	2011 01/28-01/30	5.8	122	-5	59.	1.	0.66	0.05	MC
181882	1999 RF14	2011 03/02-03/11	12.0	148	7					MC
188174	2002 JC	2011 05/13-05/21	78.5	227	52	2.4719	0.0002	0.33	0.02	NEO
218863	2006 WO127	2009 10/12-2010 01/10	8.9,66.4	25	-17	210.	5.	0.7	0.1	NEO
222073	1999 HY1	2009 10/22-10/23	13.0	40	4	5.18	0.04	0.16	0.03	NEO
241370	2008 LW8	2010 06/09-06/10	26.6	236	14	10.83	0.16	0.03	0.01	NEO
253841	2003 YG118	2011 02/14	62.0	185	8	3.43	0.04	0.16	0.02	NEO
274138	2008 FU6	2011 04/12	8.5	196	4	2.66	0.04	0.05	0.01	NEO
276741	2004 EM66	2011 04/13-04/15	13.1	214	6	4.573	0.004	0.13	0.02	MC
302831	2003 FH	2011 10/30-11/01	64.9	8	26	13.97	0.02	0.98	0.03	NEO
307190	2002 EK130	2011 08/05-08/07	6.8	317	7	8.25	0.04	0.11	0.02	MC
307544	2003 EJ16	2010 03/24	12.0	167	2	3.99	0.12	0.04	0.01	MC
326683	2002 WP	2009 11/12-11/26	34.0	51	-22	6.2632	0.0008	1.65	0.03	NEO
351545	2005 TE15	2009 09/21-09/26	19.1,9.7	8	-7	10.610	0.005	0.52	0.03	NEO
366833	2005 MC	2009 11/24-11/26	63.0	106	33	9.33	0.06	0.35	0.03	NEO
385343	2002 LV	2009 07/13-07/15	43.5	272	34	6.20	0.01	0.74	0.03	NEO
387632	2002 PD40	2010 04/26	30.6	198	30	2.815	0.009	0.16	0.01	MC
387632	2002 PD40	2010 07/03-07/10	46.0	236	41	2.8133	0.0002	0.23	0.01	MC
407656	2011 SL102	2011 12/25-12/27	31.0	84	19	25.	1.	1.4	0.1	NEO
420187	2011 GA55	2011 08/30-08/31	8.0	334	6	2.575	0.001	0.14	0.02	NEO
448972	2011 VY15	2012 03/11-03/12	11.3	180	2	2.851	0.004	0.09	0.01	NEO
451397	2011 EZ78	2011 05/27-06/07	44.0	255	33	3.115	0.001	0.42	0.05	NEO
483504	2002 XN14	2009 12/18-12/20	25.2	71	-2	18.02	0.13	0.24	0.02	NEO
523654	2011 SR5	2011 09/20-09/22	29.2	349	15	10.07	0.02	0.21	0.02	NEO
524196	2001 QP181	2011 04/25-04/30	15.0	205	2			0.4	0.1	NEO
530520	2011 LT17	2011 06/11	56.0	252	29	1.284	0.007	0.16	0.03	NEO
612050	1997 GL3	2010 09/05-09/06	25.3	357	10					NEO
	2000 CP101	2011 08/21	80.0	292	28	10.	2.	1.0	0.2	NEO
	2009 MC9	2009 09/21-09/26	27.8	340	10	4.789	0.002	0.93	0.03	NEO
	2009 NH	2009 07/30-07/31	16.0	318	5	3.024	0.005	0.17	0.03	NEO
	2009 WV25	2009 11/25	13.0	59	5	2.92	0.07	0.92	0.05	NEO
	2011 CG2	2011 02/06-02/09	8.5	137	-5	10.798	0.004	1.35	0.05	NEO
	2011 CY46	2011 03/09-03/11	52.0	168	30	5.5663	0.0008	0.57	0.03	NEO
	2011 GM62	2011 04/22	55.0	213	28	8.	2.			NEO
	2011 GP59	2011 04/11	33.0	213	12	0.12250	0.00001	1.97	0.15	NEO
	2011 HS	2011 04/26-04/27	50.0	216	29			2.	0.1	NEO
	2011 KE	2011 05/23-05/24	29.0	249	17	8.02	0.02	0.50	0.04	NEO
	2011 LJ19	2011 09/18	38.0	342	16	6.69	0.01	0.46	0.03	NEO
	2011 LJ19	2011 09/19	32.0	347	15	6.69	0.01	0.61	0.02	NEO
	2011 LJ19	2011 09/24	21.0	0	12	6.69	0.01	0.44	0.02	NEO
	2011 MD	2011 06/25	64.0	261	30	0.19372	0.00009	0.79	0.06	NEO
	2011 MD	2011 06/26	63.3	261	29	0.19372	0.00004	0.83	0.04	NEO
	2011 OQ5	2011 09/22	7.5	358	6	5.92	0.03	0.20	0.01	NEO
	2011 PT1	2011 09/29	28.5	16	15	8.3	0.2	0.08	0.03	NEO

Table I. Observing circumstances and results. The phase angle is given for the first and last date. If preceded by an asterisk, the phase angle reached an extrema during the period. L_{PAB} and B_{PAB} are the approximate phase angle bisector longitude/latitude at mid-date range (see Harris et al., 1984). D is the diameter (km, *diameter is from JPL SBN). Other diameters were derived from H and p_V values. The last column gives the a/b ratio, based on the amplitude, for an assumed triaxial ellipsoid viewed equatorially.

Harris, A.W.; Young, J.W.; Scaltriti, F.; Zappala, V. (1984). "Lightcurves and phase relations of the asteroids 82 Alkmene and 444 Gyptis." *Icarus* **57**, 251-258.

Hasegawa, S.; Kuroda, D.; Kitazato, K.; and 40 colleagues (2018). "Physical properties of near-Earth asteroids with a low delta-v: survey of target candidates for the Hayabusa2 mission." *Publ. Astron. Soc. Japan* **70**, 114-144.

Ivarsen, K.; Willis, S.; Ingleby, L.; Matthews, D.; Simet, M. (2004). "CCD observations and period determination of fifteen minor planets." *Minor Planet Bull*. **31**, 29.

Kamél, L. (1998). "Photometry of the asteroids (5682) 1990 TB and (7930) 1987 VD." *Minor Planet Bull*. **25**, 16.

Koehn, B.W.; Bowell, E.L.G. (2000). "Lowell Observatory Near-Earth-Object Search enhancements." *Bull. Amer. Astron. Soc.* DPS meeting 32, 14.03 (abstract).

Koff, R.A. (2005). "Lightcurve photometry of asteroids 212 Medea, 517 Edith, 3581 Alvarez 5682 Beresford, and 5817 Robertfrazer." *Minor Planet Bull*. **32**, 32-34.

Lazzaro, D.; Florczak, M.A.; Angeli, C.A.; Carvano, J.M.; Betzler, A.S.; Casati, A.A.; Baarucci, M.A.; Doressoundiram, A.; Lazzarin, M. (1997). "Photometric monitoring of 2060 Chiron's brightness at perihelion." *Plan. & Sp. Sci.* **45**, 1607-1614.

Linder, T.R.; Sampson, R.; Holmes, R. (2013). "Astronomical Research Institute photometric results." *Minor Planet Bull.* **40**, 4-6.

Magnier, E.A.; Schlafly, E.F.; Finkbeiner, D.P.; Tonry, J.L.; and 17 colleagues (2016). "Pan-STARRS Photometric and Astrometric Calibration."
https://arxiv.org/abs/1612.05242; *Ap. J.*; submitted.

Maleszewski, C.; Clark, M. (2004). "Bucknell University Observatory lightcurve results for 2003-2004." *Minor Planet Bull.* **31**, 93.

Marsden, B.G. (1992). "(4015) 1979 VA = Comet Wilson-Harrington (1949 III)." IAU *Circ*. 5585.
http://www.cbat.eps.harvard.edu/iauc/05500/05585.html

Melton, E.; Carver, S.; Harris, A.; Karnemaat, R.; Klaasse, M.; Ditteon, R. (2012). "Asteroid lightcurve analysis at the Oakley Southern Sky Observatory: 2011 November-December." *Minor Planet Bull.* **39**, 131-133.

Mommert, M.; Farnocchia, D.; Hora, J.L.; Chesley, S.R.; Trilling, D.E.; Chodas, P.W.; Mueller, M.; Harris, A.W.; Fazio, G.G. (2014). "Physical Properties of Near-Earth Asteroid 2011 MD." *Astrophys. J.* **789**, L22.

Oey, J.; Kušnirák, P.; Pravec, P.; Hornoch, K.; Pray, D.; Benishek, V.; Montaigut, R.; Leroy, A.; Vilagi, J. (2018). "(4666) Dietz." *CBET* 4536.
http://mail.spaceobs.com/pipermail/iaude_spaceobs.com/2018-July/013334.html

Owings, L.E. (2012). "Lightcurves for 2567 Elba, 2573 Hannu Olavi, 2731 Cucula, 4930 Rephiltim 6952 Niccolo, and 7750 McEwen." *Minor Planet Bull.* **39**, 22-23.

Owings, L.E. (2021). "Lightcurve analysis of ten asteroids." *Minor Planet Bull.* **48**, 236-238.

Pál, A.; Szakáts, R.; Kiss, C.; Bódi, A.; Bognár, Z.; Kalup, C.; Kiss, L.L.; Marton, G.; Molnár, L.; Plachy, E.; Sárneczky, K.; Szabó, G.M.; Szabó, R. (2020). "Solar System Objects Observed with TESS - First Data Release: Bright Main-belt and Trojan Asteroids from the Southern Survey." *Ap. J.* **247**, A26.

Polakis, T. (2021). "Period determinations for seventeen minor planets." *Minor Planet Bull.* **48**, 158-163.

Polishook, D.; Brosch, N. (2008). "Photometry of Aten asteroids - more than a handful of binaries." *Icarus* **184**, 111-124.

Pravec, P. (2002web, 2011web, 2019web).
http://www.asu.cas.cz/~ppravec/neo.htm

Pravec, P, Wolf, M.; Šarounová, L. (1998). "Lightcurves of 26 near-Earth asteroids." *Icarus* **136**, 124-153.

Pravec, P.; Hergenrother, C.; Whiteley, R.; Šarounová, L.; Kušnirák, P.; Wolf, M. (2000). "Fast rotating asteroids 1999 TY2, 1999 SF10, and 1998 WB2." *Icarus* **147**, 477-486.

Skiff, B.A. (2011web). Postings on CALL web site.
https://www.minorplanet.info/php/call.php

Skiff, B.A.; McLelland, K.P.; Sanborn, J.J.; Pravec, P.; Koehn, B.W.; (2019a). "Lowell Observatory Near-Earth Asteroid Photometric Survey (NEAPS): Paper 3." *Minor Planet Bull.* **46**, 238-265.

Skiff, B.A.; McLelland, K.P.; Sanborn, J.J.; Pravec, P.; Koehn, B.W. (2019b). "Lowell Observatory Near-Earth Asteroid Photometric Survey (NEAPS): Paper 4." *Minor Planet Bull.* **46**, 458-503.

Stephens, R.D. (2014). "Asteroids observed from CS3: 2014 January - March." *Minor Planet Bull.* **41**, 171-175.

Stephens, R.D.; Warner, B.D. (2020). "Main-belt asteroids observed from CS3: 2019 July to September." *Minor Planet Bull.* **47**, 50-60.

Urakawa, S.; Okumura, S.; Nishiyama, K.; and 14 colleagues (2011). "Photometric observations of 107P/Wilson-Harrington." *Icarus* **215**, 17-26.

Vaduvescu, O.; Aznar Macías, A.; Tudor, V.; Predatu, M.; and 16 colleagues (2017). "The EURONEAR lightcurve survey of near-Earth asteroids." *Earth, Moon, & Planets* **120**, 41-100.

Warner, B.D. (2005). "Lightcurve analysis for asteroids 242, 893, 921, 1373, 1853, 2120, 2448 3022, 6490, 6517, 7187, 7757, and 18108." *Minor Planet Bull.* **32**, 4-7.

Warner, B.D.; Harris, A.W.; Pravec, P. (2009). "The Asteroid Lightcurve Database." *Icarus* **202**, 134-146. Updated 2019 Jul. *http://www.minorplanet.info/lightcurvedatabase.html*

Warner, B.D. (2010). "Asteroid lightcurve analysis at the Palmer Divide Observatory: 2009 September - December." *Minor Planet Bull.* **37**, 57-64.

Warner, B.D. (2011). "Asteroid lightcurve analysis at the Palmer Divide Observatory: 2011 March - July." *Minor Planet Bull.* **38**, 190-195.

Warner, B.D.; Megna, R.; Skiff, B.A.; Wasserman, L.H.; Harris, A.W. (2011). "Lightcurve analysis of 27810 Daveturner: A long period Hungaria." *Minor Planet Bull.* **38**, 150-151.

Warner, B.D. (2012a). "Asteroid lightcurve analysis at the Palmer Divide Observatory: 2011 September - December." *Minor Planet Bull.* **39**, 69-80.

Warner, B.D. (2012b). "Asteroid lightcurve analysis at the Palmer Divide Observatory: 2011 December - 2012 March." *Minor Planet Bull.* **39**, 158-167.

Warner, B.D.; Klinglesmith, D.A.; Skiff, B.A. (2012a). "Lightcurve inversion of 47035 (1998 WS)." *Minor Planet Bull.* **39**, 216-220.

Warner, B.D.; Pravec, P.; Kusnirak, P.; Harris, A.W. (2012b). "A trio of tumbling Hungaria asteroids." *Minor Planet Bull.* **39**, 89-92.

Warner, B.D. (2014a). "Near-Earth asteroid lightcurve analysis at CS3-Palmer Divide Station: 2013 June-September." *Minor Planet Bull.* **41**, 41-47.

Warner, B.D. (2014b). "Near-Earth asteroid lightcurve analysis at CS3-Palmer Divide Station: 2014 March-June." *Minor Planet Bull.* **41**, 213-224.

Warner, B.D. (2014c). "Asteroid lightcurve analysis at CS3-Palmer Divide Station: 2014 March-June." *Minor Planet Bull.* **41**, 235-241.

Warner, B.D. (2015). "Near-Earth asteroid lightcurve analysis at CS3-Palmer Divide Station: 2015 January - March." *Minor Planet Bull.* **42**, 172-183.

Warner, B.D. (2016a). "Near-Earth asteroid lightcurve analysis at CS3-Palmer Divide Station: 2015 June-September." *Minor Planet Bull.* **43**, 66-79.

Warner, B.D. (2016b). "Near-Earth asteroid lightcurve analysis at CS3-Palmer Divide Station: 2016 January-April." *Minor Planet Bull.* **43**, 240-250.

Warner, B.D. (2017). "Near-Earth asteroid lightcurve at CS3-Palmer Divide Station: 2017 April thru June." *Minor Planet Bull.* **44**, 335-344.

Warner, B.D.; Stephens, R.D. (2019). "7002 Bronshten: a new Mars-crossing binary." *Minor Planet Bull.* **46**, 53-54.

Warner, B.D.; Stephens, R.D. (2020). "Near-Earth asteroid lightcurve analysis at the Center for Solar System Studies: 2019 December - 2020 April." *Minor Planet Bull.* **47**, 200.

Warner, B.D.; Stephens, R.D. (2022a). "Near-Earth asteroid lightcurve analysis at the Center for Solar System Studies: 2021 August-October." *Minor Planet Bull.* **49**, 16-22.

Warner B.D.; Stephens R.D. (2022b). "Near-Earth asteroid lightcurve analysis at the Center for Solar System Studies: 2021 October-December." *Minor Planet Bull.;* **49**, 83-89.

Waszczak, A.; Chang, C.-K.; Ofek, E.O.; Laher, R.; Masci, F.; Levitan, D.; Surace, J.; Cheng, Y.-C.; Ip, W.-H.; Kinoshita, D.; Helou, G.; Prince, T.A.; Kulkarni, S. (2015). "Asteroid Light Curves from the Palomar Transient Factory Survey: Rotation Periods and Phase Functions from Sparse Photometry." *Astron. J.* **150**, A75.

Wisniewski, W.Z.; Michałowski, T.M.; Harris, A.W.; McMillan, R.S. (1997). "Photometric observations of 125 asteroids." *Icarus* **126**, 395-449.

LIGHTCURVE ANALYSIS FOR THREE MAIN BELT ASTEROIDS

Giovanni Battista Casalnuovo
Filzi School Observatory D12
Laives, ITALY
gb.minorplanet@gmail.com

(Received: 2022 August 29)

Photometric observations of three main-belt asteroids 4494 Marimo, 5516 Jawilliamson, and (57754) 2001 VW12, were made at the Filzi School Observatory (School in country Laives - Italy) MPC Station D12.

CCD photometric observations, were made at the Filzi School Observatory, all are without filter (clear). All images were obtained with a 0.35-m reflector telescope reduced to *f*/8.0, a QHY9 CCD camera, and calibrated with dark and flat-field frames. The pixel scale was 1.56 arcsec when binned at 4×4 pixels. All exposures were 120 seconds. The computer clock was synchronized with an Internet time server before each session. Differential photometry and period analysis were done using *MPO Canopus* version 10.7.12.9 (Warner, 2018). Solar type stars from CMC15 catalog in R band were used as comparison stars.

4494 Marimo. This main-belt asteroid was reported as a lightcurve photometry opportunity for 2022 January on the MinorPlanet.info web site (*https://www.minorplanet.info/php/callopplcdbquery.php*; hereafter referenced as MPI). It was discovered in 1988-10-13 by Ueda and Kaneda at Kushiro. It is a main-belt asteroid with a semi-major axis of 2.34 AU, eccentricity 0.12, inclination 2.47 deg, and orbital period of 3.58 yr. Its absolute magnitude is H= 13.68 mag. It was observed for seven nights (January-February 2022), the derived synodic period is P = 8.24 ± 0.01 h with an amplitude of A = 0.22 ± 0.05 mag. The lightcurve is asymmetric multimodal. There were no entries in the LCDB (Warner et al., 2009) for this asteroid.

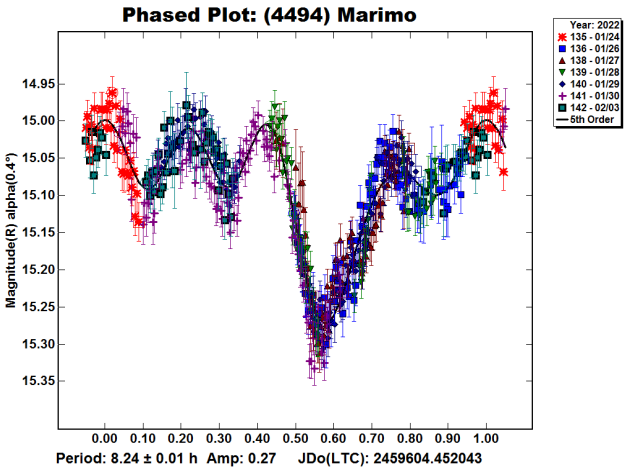

Number	Name	yyyy mm/dd	Phase	L_{PAB}	B_{PAB}	Period(h)	P.E.	Amp	A.E.	Grp
4494	Marimo	2022 01/24-02/03	0.5 5.5	124.6	-0.7	8.24	0.01	0.22	0.05	MB
5516	Jawilliamson	2022 03/22-03/27	5.5 4.9	185.9	7.0	5.153	0.002	0.17	0.04	MB
57754	2001 VW12	2022 08/03-08/24	13.8 10.2	326.9	13.2	9.772	0.001	0.77	0.04	MB

Table I. Observing circumstances and results. The phase angle is given for the first and last date. If preceded by an asterisk, the phase angle reached an extrema during the period. L_{PAB} and B_{PAB} are the approximate phase angle bisector longitude/latitude at mid-date range (see Harris et al., 1984). Grp is the asteroid family/group (Warner et al., 2009).

5516 Jawilliamson. This main-belt asteroid was reported as a lightcurve photometry opportunity for 2022 March on the MPI. It was discovered in 1989-05-02 by E.F. Helin at Palomar. It is a main-belt asteroid with a semi-major axis of 2.58 AU, eccentricity 0.17, inclination 12.98 deg, and orbital period of 4.16 yr. Its absolute magnitude is H = 13.39 mag. It was observed for five nights (2022 March). The derived synodic period is P = 5.153 ± 0.002 h with an amplitude of A = 0.17 ± 0.04 mag. There were no entries in the LCDB (Warner et al., 2009) for this asteroid.

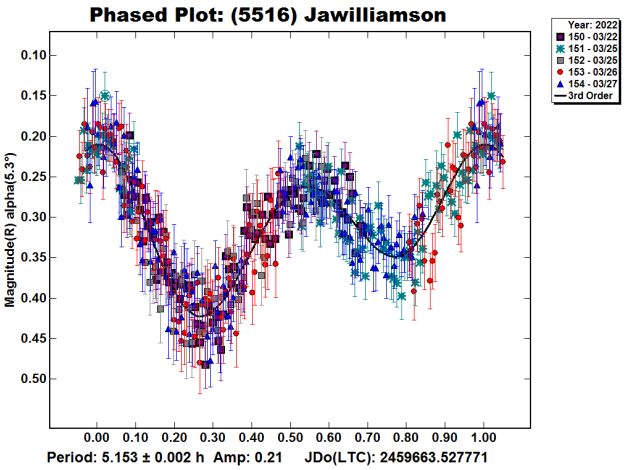

(57754) 2001 VW12. This main-belt asteroid was reported as a lightcurve photometry opportunity for 2022 August on the MinorPlanet.info. It was discovered in 2001-11-10 by LINEAR at Socorro. It is a main-belt asteroid with a semi-major axis of 2.35 AU, eccentricity 0.21, inclination 12.15 deg, and orbital period of 3.59 yr. Its absolute magnitude is H = 14.36 mag. It was observed for seven nights (2022 August). The derived synodic period was P = 9.722 ± 0.001 h with a large amplitude of A = 0.77 ± 0.04 mag. There were no entries in the LCDB (Warner et al., 2009) for this asteroid.

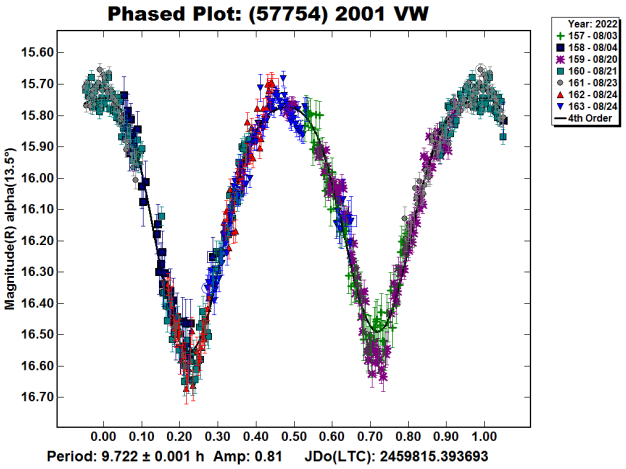

References

Harris, A.W.; Young, J.W.; Scaltriti, F.; Zappala, V. (1984). "Lightcurves and phase relations of the asteroids 82 Alkmene and 444 Gyptis." *Icarus* **57**, 251-258.

Warner, B.D.; Harris, A.W.; Pravec, P. (2009). "The Asteroid Lightcurve Database." *Icarus* **202**, 134-146. Updated 2018 June. *http://www.minorplanet.info/lightcurvedatabase.html*

Warner, B.D. (2018). *MPO Software, MPO Canopus* version 10.7.12.9. *Bdw Publishing. http://minorplanetobserver.com*

MINOR PLANETS AT UNUSUALLY FAVORABLE ELONGATIONS IN 2023

Frederick Pilcher
4438 Organ Mesa Loop
Las Cruces, NM 88011 USA
pilcher@ic.edu

(Received: 2022 September 26)

A list is presented of minor planets which are much brighter than usual at their 2023 apparitions.

The minor planets in the lists which follow will be much brighter at their 2023 apparitions than at their average distances at maximum elongation. Many years may pass before these objects will be again as bright as in 2023. Observers are encouraged to give special attention to those objects reaching peak brightness near the limit of their equipment.

These lists have been prepared by an examination of the maximum elongation circumstances of minor planets computed by the author for all years through 2060 with a full perturbation program written by Dr. John Reed, and to whom he expresses his thanks. Elements are from EMP 1992, or for more recently discovered minor planets from the MPC in which they were also assigned permanent numbers. Planetary positions are from the JPL DE-200 ephemeris, courtesy of Dr. E. Myles Standish.

Any minor planets whose brightest magnitudes near the time of maximum elongation vary by at least 2.0 in this interval and in 2023 will be within 0.3 of the brightest occurring, or vary by at least 3.0 and in 2023 will be within 0.5 of the brightest occurring; and which are visual magnitude 14.5 or brighter, are included. For planets brighter than visual magnitude 13.5, which are within the range of a large number of observers, these standards have been relaxed somewhat to include a larger number of planets. Magnitudes have been computed from the updated magnitude parameters published in MPC28104-28116, on 1996 Nov. 25, or more recently in the Minor Planet Circulars.

Oppositions may be in right ascension or in celestial longitude. Here we use still a third representation, maximum elongation from the Sun, instead of opposition. Though unconventional, it has the advantage that many close approaches do not involve actual opposition to the Sun near the time of minimum distance and greatest brightness and are missed by an opposition-based program. Other data are also provided according to the following tabular listings: Minor planet number, date of maximum elongation from the Sun in format yyyy/mm/dd, maximum elongation in degrees, right ascension on date of maximum elongation, declination on date of maximum elongation, both in J2000 coordinates, date of brightest magnitude in format yyyy/mm/dd, brightest magnitude, date of minimum distance in format yyyy/mm/dd, and minimum distance in AU.

Users should note that when the maximum elongation is about 177° or greater, the brightest magnitude is sharply peaked due to enhanced brightening near zero phase angle. Even as near as 10 days before or after predicted greatest brightest, the appearance is generally about 0.4 magnitudes brighter. This effect takes place in greater time interval for smaller maximum elongations. There is some interest in very small minimum phase angles. For maximum elongations E near 180° at Earth distance Δ, an approximate formula for the minimum phase angle ϕ is

$$\phi=(180°-E)/(\Delta+1)$$

A special list of asteroids approaching the Earth more closely than 0.3 AU is provided following the list of temporal sequence of favorable elongations.

Table I. Numerical Sequence of Favorable Elongations

Planet	Max Elon D	Max E	RA	Dec	Br Mag D	Br Mag	Min Dist D	Min Dist
9	2023/12/22	176.1°	6h 2m	+27°	2023/12/22	8.4	2023/12/21	1.119
18	2023/11/05	159.2°	3h 7m	- 4°	2023/11/03	8.1	2023/10/30	0.859
32	2023/05/04	179.4°	14h43m	-15°	2023/05/04	10.2	2023/05/03	1.384
37	2023/12/18	174.5°	5h42m	+28°	2023/12/18	9.7	2023/12/16	1.211
47	2023/08/25	175.7°	22h22m	-14°	2023/08/25	10.9	2023/08/23	1.504
53	2023/02/02	178.3°	9h 1m	+15°	2023/02/02	11.0	2023/01/29	1.169
54	2023/07/21	174.1°	20h 4m	-26°	2023/07/21	10.0	2023/07/21	1.164
55	2023/09/21	177.3°	23h57m	- 3°	2023/09/21	10.5	2023/09/22	1.372
64	2023/01/03	179.0°	6h55m	+23°	2023/01/03	10.3	2023/01/05	1.389
95	2023/11/30	178.3°	4h24m	+19°	2023/11/30	11.2	2023/11/27	1.661
96	2023/03/20	163.9°	11h33m	-14°	2023/03/19	11.3	2023/03/20	1.653
103	2023/07/22	177.4°	20h 3m	-17°	2023/07/22	10.7	2023/07/23	1.491
114	2023/03/29	176.5°	12h35m	+ 0°	2023/03/29	11.0	2023/03/27	1.351
144	2023/11/16	176.6°	3h28m	+15°	2023/11/16	10.1	2023/11/09	1.142
146	2023/06/17	179.2°	17h42m	-24°	2023/06/17	11.3	2023/06/16	1.554
162	2023/04/21	179.0°	13h53m	-10°	2023/04/20	12.1	2023/04/16	1.660
182	2023/11/21	177.0°	3h49m	+16°	2023/11/21	10.7	2023/11/20	0.977
234	2023/07/29	168.1°	20h11m	- 8°	2023/07/30	10.5	2023/08/04	0.850
288	2023/03/07	174.5°	11h17m	+10°	2023/03/07	12.4	2023/03/13	1.282
343	2023/10/30	179.7°	2h17m	+13°	2023/10/30	12.7	2023/10/31	0.871
353	2023/12/27	178.5°	6h24m	+21°	2023/12/27	12.4	2023/12/19	0.919
368	2023/09/27	171.3°	23h57m	+ 9°	2023/09/26	13.3	2023/09/21	1.560
380	2023/07/09	177.8°	19h14m	-24°	2023/07/09	12.3	2023/07/13	1.442
393	2023/07/06	150.1°	18h57m	+ 7°	2023/07/10	10.5	2023/07/12	0.930
413	2023/07/10	176.7°	19h23m	-25°	2023/07/11	11.9	2023/07/25	0.982
428	2023/10/04	178.3°	0h39m	+ 2°	2023/10/04	12.9	2023/10/06	0.918
429	2023/09/27	170.0°	23h57m	+10°	2023/09/28	12.6	2023/09/29	1.315
449	2023/01/04	178.1°	7h 2m	+24°	2023/01/05	11.6	2023/01/08	1.168
453	2023/05/03	174.0°	14h35m	-21°	2023/05/03	12.2	2023/05/05	0.941
459	2023/10/14	176.9°	1h20m	+ 5°	2023/10/14	12.5	2023/10/17	1.112
481	2023/11/21	177.6°	3h47m	+17°	2023/11/21	11.2	2023/11/20	1.321
485	2023/12/05	159.0°	5h 0m	+ 1°	2023/12/07	11.3	2023/12/09	1.332
492	2023/10/01	178.3°	0h32m	+ 1°	2023/10/01	13.0	2023/09/27	1.587
503	2023/11/24	178.9°	3h58m	+19°	2023/11/24	11.8	2023/11/28	1.382
505	2023/01/13	173.2°	7h44m	+28°	2023/01/12	11.0	2023/01/06	1.174
512	2023/07/20	176.4°	20h 1m	-24°	2023/07/21	11.7	2023/08/01	0.780
538	2023/11/01	169.9°	2h35m	+ 4°	2023/10/31	12.9	2023/10/28	1.683
542	2023/09/28	169.1°	0h38m	- 7°	2023/09/28	12.6	2023/09/27	1.500
545	2023/09/12	175.3°	23h11m	- 0°	2023/09/11	12.5	2023/09/06	1.762
598	2023/11/14	165.0°	3h27m	+ 3°	2023/11/13	12.0	2023/11/08	1.137
601	2023/08/29	173.7°	22h19m	- 3°	2023/08/29	13.4	2023/08/28	1.800
602	2023/09/23	166.6°	23h45m	+12°	2023/09/24	11.2	2023/09/25	1.335
629	2023/01/05	175.2°	7h 8m	+27°	2023/01/05	13.3	2023/01/07	1.668
648	2023/02/01	174.2°	8h50m	+11°	2023/01/31	13.0	2023/01/30	1.592
678	2023/10/02	168.2°	0h11m	+14°	2023/10/03	11.2	2023/10/06	1.076
704	2023/12/18	173.0°	5h37m	+30°	2023/12/17	9.9	2023/12/13	1.850
709	2023/09/18	165.8°	23h25m	+11°	2023/09/18	12.6	2023/09/16	1.604
717	2023/10/20	178.0°	1h33m	+11°	2023/10/20	13.7	2023/10/15	1.334
756	2023/03/31	169.3°	12h15m	-13°	2023/03/31	13.4	2023/04/03	1.767
758	2023/11/30	174.6°	4h28m	+16°	2023/11/30	11.8	2023/11/29	1.737
759	2023/07/24	167.2°	20h15m	-32°	2023/07/25	12.8	2023/07/27	1.100
760	2023/03/04	175.6°	10h51m	+ 2°	2023/03/04	10.9	2023/03/06	1.427
765	2023/12/04	168.9°	4h33m	+33°	2023/12/03	14.0	2023/11/26	0.903
767	2023/08/24	176.2°	22h18m	-14°	2023/08/24	13.2	2023/08/26	1.557
773	2023/08/16	179.6°	21h40m	-13°	2023/08/16	12.3	2023/08/14	1.642
774	2023/06/07	178.9°	16h58m	-21°	2023/06/07	11.7	2023/06/10	1.555
776	2023/12/20	175.6°	5h51m	+27°	2023/12/19	11.1	2023/12/15	1.661
800	2023/09/14	175.8°	23h20m	+ 0°	2023/09/13	12.7	2023/09/06	0.805
817	2023/11/13	159.7°	3h32m	- 1°	2023/11/13	13.4	2023/11/12	1.165
882	2023/11/17	176.0°	3h22m	+22°	2023/11/16	13.3	2023/11/11	1.367
899	2023/12/18	175.1°	5h43m	+18°	2023/12/17	13.4	2023/12/11	1.593
900	2023/08/11	164.1°	20h57m	- 0°	2023/08/10	14.1	2023/08/08	1.085
937	2023/05/29	179.5°	16h23m	-21°	2023/05/29	13.3	2023/06/09	0.943
985	2023/08/22	173.7°	21h54m	- 5°	2023/08/22	13.3	2023/08/27	0.675
988	2023/11/24	179.1°	3h56m	+21°	2023/11/24	14.2	2023/11/17	1.532
1066	2023/10/26	172.7°	1h52m	+19°	2023/10/25	14.2	2023/10/20	0.953
1133	2023/11/24	179.3°	3h57m	+21°	2023/11/24	13.5	2023/11/16	0.916
1150	2023/08/29	175.5°	22h20m	- 5°	2023/08/29	13.5	2023/08/30	0.740
1178	2023/02/08	173.5°	9h15m	+ 9°	2023/02/08	13.9	2023/02/12	1.239
1187	2023/09/16	171.2°	23h21m	+ 5°	2023/09/17	13.7	2023/09/22	1.179
1196	2023/11/27	161.5°	4h18m	+ 2°	2023/11/25	13.4	2023/11/20	1.387
1227	2023/09/25	179.2°	0h 7m	+ 1°	2023/09/25	13.7	2023/09/19	1.804
1270	2023/09/03	167.8°	23h 7m	-18°	2023/09/03	13.7	2023/09/05	0.783
1283	2023/11/28	165.6°	4h22m	+ 6°	2023/11/26	13.8	2023/11/22	1.580
1362	2023/11/10	137.0°	3h32m	-25°	2023/11/03	14.1	2023/10/31	1.203

Planet	Max Elon D	Max E	RA	Dec	Br Mag D	Br Mag	Min Dist D	Min Dist
1369	2023/09/30	177.5°	0h27m	+ 0°	2023/09/29	14.1	2023/09/22	1.670
1407	2023/09/11	168.7°	23h 1m	+ 5°	2023/09/13	12.7	2023/09/17	1.041
1419	2023/11/17	175.9°	3h33m	+14°	2023/11/17	13.0	2023/11/20	1.004
1429	2023/11/10	179.8°	2h59m	+16°	2023/11/10	13.9	2023/10/26	0.943
1456	2023/07/08	179.0°	19h 8m	-21°	2023/07/08	14.4	2023/07/15	1.735
1525	2023/09/16	168.6°	23h18m	+ 7°	2023/09/16	14.3	2023/09/13	0.996
1590	2023/07/31	170.9°	20h29m	- 9°	2023/07/30	13.3	2023/07/26	0.901
1655	2023/01/04	177.5°	6h55m	+20°	2023/01/04	13.3	2022/12/30	1.204
1659	2023/09/23	167.5°	23h44m	+11°	2023/09/23	12.3	2023/09/24	1.078
1662	2023/09/30	175.6°	0h18m	+ 6°	2023/09/30	13.9	2023/10/02	1.303
1694	2023/09/18	171.7°	23h51m	- 9°	2023/09/19	12.6	2023/09/21	0.791
1699	2023/07/19	178.3°	19h52m	-19°	2023/07/19	13.7	2023/07/23	0.861
1817	2023/06/15	174.7°	17h30m	-18°	2023/06/15	13.5	2023/06/11	0.956
1914	2023/07/14	178.2°	19h31m	-19°	2023/07/14	14.2	2023/07/12	1.042
2036	2023/06/21	171.5°	17h58m	-31°	2023/06/22	14.1	2023/06/25	0.840
2081	2023/08/02	173.2°	20h57m	-24°	2023/08/02	14.2	2023/07/30	1.060
2259	2023/06/30	179.3°	18h32m	-23°	2023/06/30	13.7	2023/07/02	0.862
2374	2023/09/28	172.0°	0h 6m	+ 9°	2023/09/28	14.5	2023/09/26	1.424
2382	2023/06/12	156.8°	17h56m	- 1°	2023/06/17	13.6	2023/06/23	1.010
2397	2023/12/16	165.3°	5h34m	+ 8°	2023/12/16	14.4	2023/12/16	1.584
2433	2023/03/30	179.4°	12h32m	- 3°	2023/03/30	14.3	2023/04/08	1.299
2536	2023/08/05	173.7°	20h52m	-11°	2023/08/06	14.5	2023/08/14	0.903
2569	2023/09/27	160.3°	0h44m	-16°	2023/09/28	14.0	2023/09/29	1.261
2699	2023/11/16	174.4°	3h26m	+13°	2023/11/15	14.4	2023/11/10	1.336
2763	2023/08/21	177.5°	21h55m	- 9°	2023/08/21	13.9	2023/08/23	0.879
2831	2023/10/01	170.8°	0h41m	- 5°	2023/09/30	13.8	2023/09/27	0.795
2873	2023/07/17	177.1°	19h47m	-24°	2023/07/17	14.4	2023/07/13	0.903
2880	2023/06/27	169.4°	18h27m	-33°	2023/06/27	14.0	2023/06/29	0.830
3099	2023/03/18	164.3°	12h 9m	+15°	2023/03/18	14.3	2023/03/20	1.326
3127	2023/09/11	172.5°	23h 3m	+ 2°	2023/09/10	14.4	2023/09/06	1.108
3173	2023/07/17	169.0°	19h59m	-31°	2023/07/17	14.2	2023/07/18	0.733
3184	2023/08/20	167.0°	22h21m	-24°	2023/08/21	14.0	2023/08/21	0.972
3563	2023/06/21	179.6°	17h58m	-23°	2023/06/21	14.3	2023/06/19	1.288
3662	2023/08/26	172.1°	22h28m	-18°	2023/08/26	14.4	2023/08/25	1.193
3738	2023/06/03	177.3°	16h44m	-24°	2023/06/04	13.9	2023/06/06	0.843
3855	2023/09/03	167.1°	23h 9m	-19°	2023/09/02	14.3	2023/09/01	0.771
3921	2023/10/03	165.1°	1h 5m	- 8°	2023/10/03	14.4	2023/10/02	0.907
3958	2023/11/19	173.1°	3h29m	+26°	2023/11/18	14.0	2023/11/15	0.976
4222	2023/11/28	174.2°	4h21m	+15°	2023/11/28	13.0	2023/11/27	0.680
4226	2023/09/07	172.4°	22h48m	+ 0°	2023/09/07	13.5	2023/09/06	1.127
4265	2023/09/30	172.3°	0h36m	- 4°	2023/09/30	14.5	2023/09/29	0.946
4288	2023/09/27	162.4°	0h34m	-15°	2023/09/27	14.4	2023/09/27	1.189
4340	2023/06/07	173.9°	16h55m	-16°	2023/06/07	14.4	2023/06/08	0.830
4349	2023/12/10	175.8°	5h 8m	+18°	2023/12/10	14.2	2023/12/01	1.248
4486	2023/02/17	171.0°	10h20m	+19°	2023/03/20	14.5	2023/04/11	0.163
4608	2023/10/28	176.8°	2h13m	+10°	2023/10/28	14.1	2023/10/29	0.858
4729	2023/09/21	175.2°	23h43m	+ 3°	2023/09/21	14.3	2023/09/23	0.850
4770	2023/08/05	176.9°	21h 4m	-19°	2023/08/05	14.0	2023/08/08	1.013
4797	2023/12/13	177.0°	5h18m	+26°	2023/12/13	14.4	2023/12/07	1.060
4860	2023/09/28	167.9°	0h 1m	+13°	2023/09/27	14.5	2023/09/25	1.264
5090	2023/12/12	163.4°	5h19m	+ 6°	2023/12/09	14.5	2023/11/29	1.065
5199	2023/07/11	177.0°	19h21m	-25°	2023/07/11	14.2	2023/07/10	1.136
5445	2023/05/31	177.8°	16h31m	-24°	2023/05/31	14.0	2023/05/29	0.993
5747	2023/12/29	173.5°	6h21m	+29°	2023/12/28	13.8	2023/12/28	0.839
6016	2023/08/30	172.8°	22h18m	- 2°	2023/08/30	14.2	2023/09/01	0.841
6037	2023/08/05	157.8°	21h13m	+ 4°	2023/08/19	14.3	2023/08/23	0.041
6193	2023/05/13	162.5°	14h56m	-35°	2023/05/15	14.3	2023/05/18	0.909
6265	2023/08/07	170.3°	21h22m	-25°	2023/08/08	14.5	2023/08/09	0.747
6325	2023/05/05	178.5°	14h46m	-17°	2023/05/05	14.5	2023/05/03	1.211
6572	2023/09/13	177.2°	23h29m	- 6°	2023/09/13	13.7	2023/09/08	0.880
6649	2023/07/12	171.0°	19h28m	-30°	2023/07/13	14.5	2023/07/18	0.912
7965	2023/04/05	130.5°	11h57m	-54°	2023/04/18	14.3	2023/04/22	0.945
8356	2023/09/14	175.9°	23h27m	- 7°	2023/09/14	14.1	2023/09/23	0.854
14870	2023/08/09	178.8°	21h11m	-15°	2023/08/09	14.5	2023/08/11	0.850
15127	2023/10/13	167.1°	0h57m	+20°	2023/10/12	14.5	2023/10/09	1.197
26853	2023/10/29	170.8°	2h16m	+ 4°	2023/10/28	14.2	2023/10/24	0.978
30105	2023/07/02	166.7°	19h 2m	-35°	2023/07/06	14.0	2023/07/16	0.549
37638	2023/03/15	157.4°	11h13m	+24°	2023/02/25	14.6	2023/02/21	0.044
88264	2023/07/07	177.1°	18h51m	-22°	2023/07/08	14.3	2023/07/19	0.175
97034	2023/03/02	165.2°	11h 8m	- 6°	2023/03/03	13.9	2023/03/06	0.381
139622	2024/02/10	141.4°	9h56m	+52°	2023/12/10	14.1	2023/12/06	0.037
154244	2023/05/21	174.2°	16h01m	-14°	2023/08/06	13.8	2023/08/05	0.064
154244	2023/10/12	176.7°	1h01m	+10°	2023/08/06	13.8	2023/08/05	0.064
164121	2023/10/31	129.2°	1h20m	-34°	2023/11/02	12.1	2023/11/03	0.059
199145	2023/02/06	155.6°	10h29m	- 1°	2023/02/14	13.2	2023/02/16	0.031

Table II. Temporal Sequence of Favorable Elongations

Planet	Max Elon D	Max E	RA	Dec	Br Mag D	Br Mag	Min Dist D	Min Dist
64	2023/01/03	179.0°	6h55m	+23°	2023/01/03	10.3	2023/01/05	1.389
449	2023/01/04	178.1°	7h 2m	+24°	2023/01/05	11.6	2023/01/08	1.168
1655	2023/01/04	177.5°	6h55m	+20°	2023/01/04	13.3	2022/12/30	1.204
629	2023/01/05	175.2°	7h 8m	+27°	2023/01/05	13.3	2023/01/07	1.668
505	2023/01/13	173.2°	7h44m	+28°	2023/01/12	11.0	2023/01/06	1.174
648	2023/02/01	174.2°	8h50m	+11°	2023/01/31	13.0	2023/01/30	1.592
53	2023/02/02	178.3°	9h 1m	+15°	2023/02/02	11.0	2023/01/29	1.169
199145	2023/02/06	155.6°	10h29m	- 1°	2023/02/14	13.2	2023/02/16	0.031
1178	2023/02/08	173.5°	9h15m	+ 9°	2023/02/08	13.9	2023/02/12	1.239
4486	2023/02/17	171.0°	10h20m	+19°	2023/03/20	14.5	2023/04/11	0.163
97034	2023/03/02	165.2°	11h 8m	- 6°	2023/03/03	13.9	2023/03/06	0.381
760	2023/03/04	175.6°	10h51m	+ 2°	2023/03/04	10.9	2023/03/06	1.427
288	2023/03/07	174.5°	11h17m	+10°	2023/03/07	12.4	2023/03/13	1.282
37638	2023/03/15	157.4°	11h13m	+24°	2023/02/25	14.6	2023/02/21	0.044
3099	2023/03/18	164.3°	12h 9m	+15°	2023/03/18	14.3	2023/03/20	1.326
96	2023/03/20	163.9°	11h33m	-14°	2023/03/19	11.3	2023/03/20	1.653
114	2023/03/29	176.5°	12h35m	+ 0°	2023/03/29	11.0	2023/03/27	1.351
2433	2023/03/30	179.4°	12h32m	- 3°	2023/03/30	14.3	2023/04/08	1.299
756	2023/03/31	169.3°	12h15m	-13°	2023/03/31	13.4	2023/04/03	1.767
7965	2023/04/05	130.5°	11h57m	-54°	2023/04/18	14.3	2023/04/22	0.945
162	2023/04/21	179.0°	13h53m	-10°	2023/04/20	12.1	2023/04/16	1.660
453	2023/05/03	174.0°	14h35m	-21°	2023/05/03	12.2	2023/05/05	0.941
32	2023/05/04	179.4°	14h43m	-15°	2023/05/04	10.2	2023/05/03	1.384
6325	2023/05/05	178.5°	14h46m	-17°	2023/05/05	14.5	2023/05/03	1.211
6193	2023/05/13	162.5°	14h56m	-35°	2023/05/15	14.3	2023/05/18	0.909
154244	2023/05/21	174.2°	16h01m	-14°	2023/08/06	13.8	2023/08/05	0.064
937	2023/05/29	179.5°	16h23m	-21°	2023/05/29	13.3	2023/06/09	0.943
5445	2023/05/31	177.8°	16h31m	-24°	2023/05/31	14.0	2023/05/29	0.993
3738	2023/06/03	177.3°	16h44m	-24°	2023/06/04	13.9	2023/06/06	0.843
774	2023/06/07	178.9°	16h58m	-21°	2023/06/07	11.7	2023/06/10	1.555
4340	2023/06/07	173.9°	16h55m	-16°	2023/06/07	14.4	2023/06/08	0.830
2382	2023/06/12	156.8°	17h56m	- 1°	2023/06/17	13.6	2023/06/23	1.010
1817	2023/06/15	174.7°	17h30m	-18°	2023/06/15	13.5	2023/06/11	0.956
146	2023/06/17	179.2°	17h42m	-24°	2023/06/17	11.3	2023/06/16	1.554
2036	2023/06/21	171.5°	17h58m	-31°	2023/06/22	14.1	2023/06/25	0.840
3563	2023/06/21	179.6°	17h58m	-23°	2023/06/21	14.3	2023/06/19	1.288
2880	2023/06/27	169.4°	18h27m	-33°	2023/06/27	14.0	2023/06/29	0.830
2259	2023/06/30	179.3°	18h32m	-23°	2023/06/30	13.7	2023/07/02	0.862
30105	2023/07/02	166.7°	19h 2m	-35°	2023/07/06	14.0	2023/07/16	0.549
393	2023/07/06	150.1°	18h57m	+ 7°	2023/07/10	10.5	2023/07/12	0.930
88264	2023/07/07	177.1°	18h51m	-22°	2023/07/08	14.3	2023/07/19	0.175
1456	2023/07/08	179.0°	19h 8m	-21°	2023/07/08	14.4	2023/07/15	1.735
380	2023/07/09	177.8°	19h14m	-24°	2023/07/09	12.3	2023/07/13	1.442
413	2023/07/10	176.7°	19h23m	-25°	2023/07/11	11.9	2023/07/25	0.982
5199	2023/07/11	177.0°	19h21m	-25°	2023/07/11	14.2	2023/07/10	1.136
6649	2023/07/12	171.0°	19h28m	-30°	2023/07/13	14.5	2023/07/18	0.912
1914	2023/07/14	178.2°	19h31m	-19°	2023/07/14	14.2	2023/07/12	1.042
2873	2023/07/17	177.1°	19h47m	-24°	2023/07/17	14.4	2023/07/13	0.903
3173	2023/07/17	169.0°	19h59m	-31°	2023/07/17	14.2	2023/07/18	0.733
1699	2023/07/19	178.3°	19h52m	-19°	2023/07/19	13.7	2023/07/23	0.861
512	2023/07/20	176.4°	20h 1m	-24°	2023/07/21	11.7	2023/08/01	0.780
54	2023/07/21	174.1°	20h 4m	-26°	2023/07/21	10.0	2023/07/21	1.164
103	2023/07/22	177.4°	20h 3m	-17°	2023/07/22	10.7	2023/07/23	1.491
759	2023/07/24	167.2°	20h15m	-32°	2023/07/25	12.8	2023/07/27	1.100
234	2023/07/29	168.1°	20h11m	- 8°	2023/07/30	10.5	2023/08/04	0.850
1590	2023/07/31	170.9°	20h29m	- 9°	2023/07/30	13.3	2023/07/26	0.901
2081	2023/08/02	173.2°	20h57m	-24°	2023/08/02	14.2	2023/07/30	1.060
2536	2023/08/05	173.7°	20h52m	-11°	2023/08/06	14.5	2023/08/14	0.903
4770	2023/08/05	176.9°	21h 4m	-19°	2023/08/05	14.0	2023/08/08	1.013
6037	2023/08/05	157.8°	21h13m	+ 4°	2023/08/19	14.3	2023/08/23	0.041
6265	2023/08/07	170.3°	21h22m	-25°	2023/08/08	14.5	2023/08/09	0.747
14870	2023/08/09	178.8°	21h11m	-15°	2023/08/09	14.5	2023/08/11	0.850
900	2023/08/11	164.1°	20h57m	- 0°	2023/08/10	14.1	2023/08/08	1.085
773	2023/08/16	179.6°	21h40m	-13°	2023/08/16	12.3	2023/08/14	1.642
3184	2023/08/20	167.0°	22h21m	-24°	2023/08/21	14.0	2023/08/21	0.972
2763	2023/08/21	177.5°	21h55m	- 9°	2023/08/21	13.9	2023/08/23	0.879
985	2023/08/22	173.7°	21h54m	- 5°	2023/08/22	13.3	2023/08/27	0.675
767	2023/08/24	176.2°	22h18m	-14°	2023/08/24	13.2	2023/08/26	1.557
47	2023/08/25	175.7°	22h22m	-14°	2023/08/25	10.9	2023/08/23	1.504
3662	2023/08/26	172.1°	22h28m	-18°	2023/08/26	14.4	2023/08/25	1.193
601	2023/08/29	173.7°	22h19m	- 3°	2023/08/29	13.4	2023/08/28	1.800
1150	2023/08/29	175.5°	22h20m	- 5°	2023/08/29	13.5	2023/08/30	0.740
6016	2023/08/30	172.8°	22h18m	- 2°	2023/08/30	14.2	2023/09/01	0.841
1270	2023/09/03	167.8°	23h 7m	-18°	2023/09/03	13.7	2023/09/05	0.783
3855	2023/09/03	167.1°	23h 9m	-19°	2023/09/02	14.3	2023/09/01	0.771

Planet	Max Elon D	Max E	RA	Dec	Br Mag D	Br Mag	Min Dist D	Min Dist
4226	2023/09/07	172.4°	22h48m	+ 0°	2023/09/07	13.5	2023/09/06	1.127
1407	2023/09/11	168.7°	23h 1m	+ 5°	2023/09/13	12.7	2023/09/17	1.041
3127	2023/09/11	172.5°	23h 3m	+ 2°	2023/09/10	14.4	2023/09/06	1.108
545	2023/09/12	175.3°	23h11m	- 0°	2023/09/11	12.5	2023/09/06	1.762
6572	2023/09/13	177.2°	23h29m	- 6°	2023/09/13	13.7	2023/09/08	0.880
800	2023/09/14	175.8°	23h20m	+ 0°	2023/09/13	12.7	2023/09/06	0.805
8356	2023/09/14	175.9°	23h27m	- 7°	2023/09/14	14.1	2023/09/23	0.854
1187	2023/09/16	171.2°	23h21m	+ 5°	2023/09/17	13.7	2023/09/22	1.179
1525	2023/09/16	168.6°	23h18m	+ 7°	2023/09/16	14.3	2023/09/13	0.996
709	2023/09/18	165.8°	23h25m	+11°	2023/09/18	12.6	2023/09/16	1.604
1694	2023/09/18	171.7°	23h51m	- 9°	2023/09/19	12.6	2023/09/21	0.791
55	2023/09/21	177.3°	23h57m	- 3°	2023/09/21	10.5	2023/09/22	1.372
4729	2023/09/21	175.2°	23h43m	+ 3°	2023/09/21	14.3	2023/09/23	0.850
602	2023/09/23	166.6°	23h45m	+12°	2023/09/24	11.2	2023/09/25	1.335
1659	2023/09/23	167.5°	23h44m	+11°	2023/09/23	12.3	2023/09/24	1.078
1227	2023/09/25	179.2°	0h 7m	+ 1°	2023/09/25	13.7	2023/09/19	1.804
368	2023/09/27	171.3°	23h57m	+ 9°	2023/09/26	13.3	2023/09/21	1.560
429	2023/09/27	170.0°	23h57m	+10°	2023/09/28	12.6	2023/09/29	1.315
2569	2023/09/27	160.3°	0h44m	-16°	2023/09/28	14.0	2023/09/29	1.261
4288	2023/09/27	162.4°	0h34m	-15°	2023/09/27	14.4	2023/09/27	1.189
542	2023/09/28	169.1°	0h38m	- 7°	2023/09/28	12.6	2023/09/27	1.500
2374	2023/09/28	172.0°	0h 6m	+ 9°	2023/09/28	14.5	2023/09/26	1.424
4860	2023/09/28	167.9°	0h 1m	+13°	2023/09/27	14.5	2023/09/25	1.264
1369	2023/09/30	177.5°	0h27m	+ 0°	2023/09/29	14.1	2023/09/22	1.670
1662	2023/09/30	175.6°	0h18m	+ 6°	2023/09/30	13.9	2023/10/02	1.303
4265	2023/09/30	172.3°	0h36m	- 4°	2023/09/30	14.5	2023/09/29	0.946
492	2023/10/01	178.3°	0h32m	+ 1°	2023/10/01	13.0	2023/09/27	1.587
2831	2023/10/01	170.8°	0h41m	- 5°	2023/09/30	13.8	2023/09/27	0.795
678	2023/10/02	168.2°	0h11m	+14°	2023/10/03	11.2	2023/10/06	1.076
3921	2023/10/03	165.1°	1h 5m	- 8°	2023/10/03	14.4	2023/10/02	0.907
428	2023/10/04	178.3°	0h39m	+ 2°	2023/10/04	12.9	2023/10/06	0.918
154244	2023/10/12	176.7°	1h01m	+10°	2023/08/06	13.8	2023/08/05	0.064
15127	2023/10/13	167.1°	0h57m	+20°	2023/10/12	14.5	2023/10/09	1.197
459	2023/10/14	176.9°	1h20m	+ 5°	2023/10/14	12.5	2023/10/17	1.112
717	2023/10/20	178.0°	1h33m	+11°	2023/10/20	13.7	2023/10/15	1.334
1066	2023/10/26	172.7°	1h52m	+19°	2023/10/25	14.2	2023/10/20	0.953
4608	2023/10/28	176.8°	2h13m	+10°	2023/10/28	14.1	2023/10/29	0.858
26853	2023/10/29	170.8°	2h16m	+ 4°	2023/10/28	14.2	2023/10/24	0.978
343	2023/10/30	179.7°	2h17m	+13°	2023/10/30	12.7	2023/10/31	0.871
164121	2023/10/31	129.2°	1h20m	-34°	2023/11/02	12.1	2023/11/03	0.059
538	2023/11/01	169.9°	2h35m	+ 4°	2023/10/31	12.9	2023/10/28	1.683
18	2023/11/05	159.2°	3h 7m	- 4°	2023/11/03	8.1	2023/10/30	0.859
1362	2023/11/10	137.0°	3h32m	-25°	2023/11/03	14.1	2023/10/31	1.203
1429	2023/11/10	179.8°	2h59m	+16°	2023/11/10	13.9	2023/10/26	0.943
817	2023/11/13	159.7°	3h32m	- 1°	2023/11/13	13.4	2023/11/12	1.165
598	2023/11/14	165.0°	3h27m	+ 3°	2023/11/13	12.0	2023/11/08	1.137
144	2023/11/16	176.6°	3h28m	+15°	2023/11/16	10.1	2023/11/09	1.142
2699	2023/11/16	174.4°	3h26m	+13°	2023/11/15	14.4	2023/11/10	1.336
882	2023/11/17	176.0°	3h22m	+22°	2023/11/16	13.3	2023/11/11	1.367
1419	2023/11/17	175.9°	3h33m	+14°	2023/11/17	13.0	2023/11/20	1.004
3958	2023/11/19	173.1°	3h29m	+26°	2023/11/18	14.0	2023/11/15	0.976
182	2023/11/21	177.0°	3h49m	+16°	2023/11/21	10.7	2023/11/20	0.977
481	2023/11/21	177.6°	3h47m	+17°	2023/11/21	11.2	2023/11/20	1.321
503	2023/11/24	178.9°	3h58m	+19°	2023/11/24	11.8	2023/11/28	1.382
988	2023/11/24	179.1°	3h56m	+21°	2023/11/24	14.2	2023/11/17	1.532
1133	2023/11/24	179.3°	3h57m	+21°	2023/11/24	13.5	2023/11/16	0.916
1196	2023/11/27	161.5°	4h18m	+ 2°	2023/11/25	13.4	2023/11/20	1.387
1283	2023/11/28	165.6°	4h22m	+ 6°	2023/11/26	13.8	2023/11/22	1.580
4222	2023/11/28	174.2°	4h21m	+15°	2023/11/28	13.0	2023/11/27	0.680
95	2023/11/30	178.3°	4h24m	+19°	2023/11/30	11.2	2023/11/27	1.661
758	2023/11/30	174.6°	4h28m	+16°	2023/11/30	11.8	2023/11/29	1.737
765	2023/12/04	168.9°	4h33m	+33°	2023/12/03	14.0	2023/11/26	0.903
485	2023/12/05	159.0°	5h 0m	+ 1°	2023/12/07	11.3	2023/12/09	1.332
4349	2023/12/10	175.8°	5h 8m	+18°	2023/12/10	14.2	2023/12/01	1.248
5090	2023/12/12	163.4°	5h19m	+ 6°	2023/12/09	14.5	2023/11/29	1.065
4797	2023/12/13	177.0°	5h18m	+26°	2023/12/13	14.4	2023/12/07	1.060
2397	2023/12/16	165.3°	5h34m	+ 8°	2023/12/16	14.4	2023/12/16	1.584
37	2023/12/18	174.5°	5h42m	+28°	2023/12/18	9.7	2023/12/16	1.211
704	2023/12/18	173.0°	5h37m	+30°	2023/12/17	9.9	2023/12/13	1.850
899	2023/12/18	175.1°	5h43m	+18°	2023/12/17	13.4	2023/12/11	1.593
776	2023/12/20	175.6°	5h51m	+27°	2023/12/19	11.1	2023/12/15	1.661
9	2023/12/22	176.1°	6h 2m	+27°	2023/12/22	8.4	2023/12/21	1.119
353	2023/12/27	178.5°	6h24m	+21°	2023/12/27	12.4	2023/12/19	0.919
5747	2023/12/29	173.5°	6h21m	+29°	2023/12/28	13.8	2023/12/28	0.839
139622	2024/02/10	141.4°	9h56m	+52°	2023/12/10	14.1	2023/12/06	0.037

Table III. Numerical list of approaches closer than 0.3 AU

Planet	Max Elon D	Max E	RA	Dec	Br Mag D	Br Mag	Min Dist D	Min Dist
4486	2023/02/17	171.0°	10h20m	+19°	2023/03/20	14.5	2023/04/11	0.163
6037	2023/08/05	157.8°	21h13m	+ 4°	2023/08/19	14.3	2023/08/23	0.041
37638	2023/03/15	157.4°	11h13m	+24°	2023/02/25	14.6	2023/02/21	0.044
88264	2023/07/07	177.1°	18h51m	-22°	2023/07/08	14.3	2023/07/19	0.175
139622	2024/02/10	141.4°	9h56m	+52°	2023/12/10	14.1	2023/12/06	0.037
154244	2023/05/21	174.2°	16h01m	-14°	2023/08/06	13.8	2023/08/05	0.064
154244	2023/10/12	176.7°	1h01m	+10°	2023/08/06	13.8	2023/08/05	0.064
164121	2023/10/31	129.2°	1h20m	-34°	2023/11/02	12.1	2023/11/03	0.059
199145	2023/02/06	155.6°	10h29m	- 1°	2023/02/14	13.2	2023/02/16	0.031

ASTEROID-DEEPSKY APPULSES IN 2023

Brian D. Warner
Center for Solar System Studies
446 Sycamore Ave.
Eaton, CO 80615
brian@MinorPlanetObserver.com

(Received: 2022 October 7)

The following list is a *very small* subset of the results of a search for asteroid-deepsky appulses for 2023, presenting only the highlights for the year based on close approaches of brighter asteroids to brighter DSOs. For the complete set visit

https://www.minorplanet.info/php/dsoappulses.php

For any event not covered, the Minor Planet Center's web site at *https://www.minorplanetcenter.net/cgi-bin/checkmp.cgi* allows you to enter the location of a suspected asteroid or supernova and check if there are any known targets in the area.

The table gives the following data:

Date/Time	Universal Date (MM DD) and Time of closest approach.
#/Name	The number and name of the asteroid.
RA/Dec	The J2000 position of the asteroid.
AM	The approximate visual magnitude of the asteroid.
Sep/PA	The separation in arcseconds and the position angle from the DSO to the asteroid.
DSO	The DSO name or catalog designation.
DM	The approximate total magnitude of the DSO.
DT	DSO Type: OC = Open Cluster; GC = Globular Cluster; G = Galaxy.
SE/ME	The elongation in degrees from the sun and moon, respectively.
MP	The phase of the moon: 0 = New, 1.0 = Full. Positive = waxing; Negative = waning.

Date	UT	#	Name	RA	Dec	AM	Sep	PA	DSO	DM	DT	SE	ME	MP
02	15 09:32	631	Philippina	09:11.41	-14 50.7	12.5	179	207	NGC 2781	11.6	G	151	108	-0.31
02	**23 11:37**	**68**	**Leto**	**12:58.10**	**+01 34.9**	**12.3**	**4**	**208**	**NGC 4845**	**11.2**	**G**	**141**	**172**	**0.14**
02	25 04:08	96	Aegle	11:54.78	-14 01.3	11.7	212	161	NGC 3962	10.7	G	149	142	0.29
02	26 01:49	410	Chloris	12:42.76	+13 13.1	12.4	277	231	NGC 4639	11.5	G	148	129	0.38
02	26 14:58	1	Ceres	12:43.93	+13 07.0	7.2	90	226	NGC 4654	10.5	G	148	123	0.43
03	19 00:32	753	Tiflis	12:22.48	+15 27.9	12.9	322	199	NGC 4312	11.7	G	164	141	-0.10
03	22 05:19	1	Ceres	12:27.17	+15 30.7	6.9	170	20	NGC 4421	11.6	G	163	163	0.00
03	23 04:31	410	Chloris	12:25.60	+16 31.8	11.9	186	27	NGC 4383	12.1	G	162	152	0.03
03	23 14:13	1	Ceres	12:25.99	+15 36.9	6.9	262	201	NGC 4396	12.6	G	163	148	0.05
03	24 07:13	1	Ceres	12:25.37	+15 40.1	6.9	194	19	NGC 4379	11.7	G	163	139	0.09
03	24 22:13	179	Klytaemnestra	11:39.27	-09 18.1	12.9	131	27	NGC 3771	12.6	G	168	133	0.13
03	24 23:19	410	Chloris	12:24.05	+16 43.4	11.9	97	26	NGC 4350	11.0	G	162	130	0.13
03	25 07:13	410	Chloris	12:23.75	+16 45.5	11.9	101	26	NGC 4340	11.2	G	162	125	0.16
03	**26 13:42**	**1**	**Ceres**	**12:23.41**	**+15 49.4**	**6.9**	**23**	**19**	**NGC 4328**	**13.0**	**G**	**162**	**110**	**0.26**
03	***27 00:18***	***1***	***Ceres***	***12:23.02***	***+15 51.1***	***6.9***	***68***	***16***	***M100***	***9.4***	***G***	***162***	***105***	***0.30***
04	13 09:33	68	Leto	12:22.54	+04 36.7	11.9	166	13	NGC 4303A	13.0	G	159	110	-0.50
04	***13 14:53***	***194***	***Prokne***	***12:37.90***	***+11 52.1***	***12.3***	***155***	***36***	***M58***	***9.7***	***G***	***156***	***113***	***-0.47***
04	14 10:41	6	Hebe	08:14.23	+21 16.1	10.6	292	175	NGC 2545	12.4	G	97	172	-0.38
04	14 15:08	138	Tolosa	12:47.87	-01 39.2	12.4	73	199	NGC 4690	12.9	G	167	120	-0.36
04	14 22:36	68	Leto	12:21.36	+04 40.6	11.9	280	12	NGC 4292	12.2	G	158	133	-0.32
04	15 10:31	270	Anahita	13:04.29	-10 21.2	11.8	16	207	NGC 4939	11.3	G	173	123	-0.27
04	16 15:10	194	Prokne	12:35.65	+12 15.1	12.3	78	35	NGC 4550	11.7	G	153	155	-0.15
04	**18 03:31**	**68**	**Leto**	**12:19.00**	**+04 47.7**	**12.0**	**16**	**190**	**NGC 4255**	**12.8**	**G**	**154**	**176**	**-0.05**
04	**21 17:57**	**579**	**Sidonia**	**13:53.00**	**+02 49.9**	**12.4**	**4**	**195**	**NGC 5335**	**12.8**	**G**	**165**	**150**	**0.03**
04	26 04:26	194	Prokne	12:29.21	+13 14.8	12.5	191	30	NGC 4461	11.2	G	143	74	0.34
04	26 11:04	194	Prokne	12:29.05	+13 16.2	12.5	81	31	NGC 4458	12.1	G	143	70	0.37
05	19 14:32	268	Adorea	15:13.78	-14 17.4	12.3	87	192	NGC 5878	11.5	G	171	171	0.00
06	12 23:50	1	Ceres	12:08.42	+10 26.1	8.3	267	46	NGC 4124	11.4	G	96	156	-0.26
06	18 10:44	393	Lampetia	19:08.52	+04 39.6	10.7	184	243	NGC 6756	10.6	OC	145	144	0.00
07	12 14:28	94	Aurora	17:59.02	-34 34.1	12.8	114	7	NGC 6453	9.9	GC	157	140	-0.24
07	16 22:33	247	Eukrate	20:58.01	-51 55.7	12.9	229	164	NGC 6984	12.7	G	146	148	-0.01
07	***23 14:06***	***739***	***Mandeville***	***20:53.35***	***-12 29.3***	***12.9***	***208***	***321***	***M72***	***9.4***	***GC***	***167***	***128***	***0.28***
07	23 20:22	148	Gallia	01:59.60	-06 03.0	12.2	312	197	NGC 779	11.2	G	95	156	0.30
08	13 09:51	47	Aglaja	22:32.47	-14 10.9	11.6	244	165	NGC 7302	12.3	G	165	133	-0.08
08	22 02:38	148	Gallia	02:32.79	-10 46.9	11.7	254	227	NGC 977	13.0	G	114	155	0.28
09	07 10:56	148	Gallia	02:43.77	-14 44.6	11.4	65	66	NGC 1076	13.0	G	125	56	-0.44
09	**10 08:12**	**140**	**Siwa**	**01:50.52**	**+06 07.5**	**12.3**	**37**	**145**	**NGC 693**	**12.4**	**G**	**139**	**88**	**-0.19**
09	10 15:09	148	Gallia	02:45.09	-15 35.6	11.4	99	250	NGC 1081	13.0	G	127	89	-0.17
09	12 22:28	326	Tamara	20:07.22	-56 24.7	12.7	212	102	NGC 6855	12.8	G	115	135	-0.04
09	14 10:45	140	Siwa	01:48.97	+05 52.5	12.2	109	147	NGC 676	10.5	G	143	137	0.00
09	17 04:58	304	Olga	03:04.08	-01 04.1	12.9	259	78	NGC 1194	12.9	G	128	150	0.04
10	**13 14:16**	**678**	**Fredegundis**	**00:02.40**	**+12 56.9**	**11.7**	**7**	**147**	**NGC 7810**	**13.0**	**G**	**162**	**167**	**-0.01**
10	18 08:38	459	Signe	01:16.01	+05 12.1	12.6	64	5	NGC 455	12.6	G	175	132	0.13
10	20 03:50	537	Pauly	02:30.52	-01 02.6	13.0	220	340	NGC 955	12.0	G	163	121	0.29
10	21 04:44	18	Melpomene	03:18.96	-01 59.9	8.4	78	132	NGC 1289	12.6	G	153	117	0.40
10	21 11:07	345	Tercidina	00:38.20	+08 35.2	11.8	247	133	NGC 180	12.9	G	164	84	0.43
11	**06 12:43**	**416**	**Vaticana**	**01:26.00**	**-01 19.0**	**12.5**	**58**	**1**	**NGC 545**	**12.2**	**G**	**154**	**127**	**-0.39**
12	**15 17:56**	**451**	**Patientia**	**10:02.25**	**+24 43.4**	**11.9**	**48**	**303**	**NGC 3098**	**12.0**	**G**	**119**	**155**	**0.10**

`

LIGHTCURVE PHOTOMETRY OPPORTUNITIES: 2023 JANUARY-MARCH

Brian D. Warner
Center for Solar System Studies (CS3)
446 Sycamore Ave.
Eaton, CO 80615 USA
brian@MinorPlanetObserver.com

Alan W. Harris
Center for Solar System Studies (CS3)
La Cañada, CA 91011-3364 USA

Josef Ďurech
Astronomical Institute
Charles University
18000 Prague, CZECH REPUBLIC
durech@sirrah.troja.mff.cuni.cz

Lance A.M. Benner
Jet Propulsion Laboratory
Pasadena, CA 91109-8099 USA
lance.benner@jpl.nasa.gov

We present lists of asteroid photometry opportunities for objects reaching a favorable apparition and have no or poorly-defined lightcurve parameters. Additional data on these objects will help with shape and spin axis modeling using lightcurve inversion. The "Radar-Optical Opportunities" section includes a list of potential radar targets as well as some that might be in critical need of astrometric data.

We present several lists of asteroids that are prime targets for photometry and/or astrometry during the period 2023 January through March. The "Radar-Optical Opportunities" section provides an expanded list of potential NEA targets, many of which are planned or good candidates for radar observations.

In the first three sets of tables, "Dec" is the declination and "U" is the quality code of the lightcurve. See the latest asteroid lightcurve data base (LCDB from here on; Warner et al., 2009) documentation for an explanation of the U code:

http://www.minorplanet.info/lightcurvedatabase.html

The ephemeris generator on the MinorPlanet.info web site allows creating custom lists for objects reaching V ≤ 18.0 during any month in the current year and up to five years in the future, e.g., limiting the results by magnitude and declination, family, and more.

https://www.minorplanet.info/php/callopplcdbquery.php

We refer you to past articles, e.g., Warner et al. (2021a; 2021b) for more detailed discussions about the individual lists and points of advice regarding observations for objects in each list.

Once you've obtained and analyzed your data, it's important to publish your results. Papers appearing in the *Minor Planet Bulletin* are indexed in the Astrophysical Data System (ADS) and so can be referenced by others in subsequent papers. It's also important to make the data available at least on a personal website or upon request. We urge you to consider submitting your raw data to the ALCDEF database, accessible for uploading and downloading at *http://www.alcdef.org*.

The database contains almost 10.2 million observations for 24,075 objects (as of 2022 October 5), making it one of the more useful sources for raw data of *dense* time-series asteroid photometry.

Lightcurve/Photometry Opportunities

Objects with U = 3– or 3 are excluded from this list since they will likely appear in the list for shape and spin axis modeling. Those asteroids rated U = 1 or have only a lower limit on the period, should be given higher priority over those rated U = 2 or 2+. On the other hand, do not overlook asteroids with U = 2/2+ on the assumption that the period is sufficiently established. Regardless, do not let the existing period influence your analysis since even highly-rated result have been proven wrong at times. Note that the lightcurve amplitude in the tables could be more or less than what's given. Use the listing only as a guide.

		Brightest			LCDB Data		
Number	Name	Date	Mag	Dec	Period	Amp	U
33697	1999 KJ11	01 03.6	16.4	+24	4.888	0.28	2
54906	2001 OT80	01 04.6	15.6	+27	9.93	0.10	1
11254	Konkohekisui	01 05.1	16.3	+16	8.794	0.24	2
20602	1999 RC198	01 05.4	15.7	+40	7.306	0.37	2
17663	1996 VK30	01 05.7	16.2	+19	34.062	0.17	2
4439	Muroto	01 05.9	16.0	+26 S	8.314		2
58625	1997 VE2	01 06.8	16.4	+13	124.572	0.61	2
4739	Tomahrens	01 07.4	16.3	+20	5.104	0.20-0.26	2
19668	1999 RB145	01 07.5	16.5	+43	170.497	0.55	2
2378	Pannekoek	01 11.1	14.6	+0	11.874	0.08-0.19	2
6287	Lenham	01 11.2	16.4	+24	5.623	0.34-0.45	2
2212	Hephaistos	01 11.9	12.9	+43	48	0.08-0.35	2
1478	Vihuri	01 14.0	14.9	+27	19.5	0.23	1
3809	Amici	01 14.6	15.6	+19	5.71	0.39	2+
21486	1998 HA148	01 16.2	16.1	+15	12.3	1.0	2-
15853	Benedettafoglia	01 17.1	16.5	+20	75.183	0.56	2
17847	1998 HQ115	01 18.5	16.5	+17	289.84	0.64	2
11303	1993 CA1	01 19.0	16.0	+30	5.618	0.31	2
27026	1998 QG86	01 19.0	16.1	+16	25.488	0.14	2
15781	1993 OJ7	01 19.1	16.3	+20	3.863		2-
9833	Rilke	01 19.9	16.4	+19	7.819	0.16	2
3299	Hall	01 20.9	15.7	+13	10.45	0.08-0.71	2
131774	2002 AZ18	01 20.9	16.4	+21	187.273	0.75	2
3210	Lupishko	01 21.6	15.0	+18	14.255	0.67-0.74	2+
162385	2000 BM19	01 24.1	16.4	+69	9.463	1.34-1.38	2+
10893	1997 SB10	01 26.3	16.5	+11	2.924	0.20	2
13338	1998 SK119	01 27.8	16.1	+33 S	4.129		2
33634	Strickler	01 29.1	16.2	+24	2.939	0.30	2
1956	Artek	01 29.2	15.9	+17	9.4	0.07	1+
37586	1991 BP2	02 01.6	15.1	+9	887	0.92-0.96	2+
3201	Sijthoff	02 03.2	15.7	+19	4.607	0.29	2
16993	1999 CC10	02 04.0	15.3	+17	94.762	0.32	2
5478	Wartburg	02 06.4	15.4	+2	8.552	0.38	2
1903	Adzhimushkaj	02 06.8	14.3	+16	4.622	0.04	2
2560	Siegma	02 07.2	15.5	+14	10.309	0.07-0.10	2
11928	Akimotohiro	02 07.7	15.5	+17	2.957	0.12	2
9769	Nautilus	02 08.4	16.4	+17	6.184	0.63	2
1178	Irmela	02 08.5	14.6	+9	11.989	0.25-0.40	2
2846	Ylppo	02 08.8	15.7	+14	18.894	0.17-0.25	2
1911	Schubart	02 10.0	14.7	+13	11.915	0.11-0.22	2
6393	1990 HM1	02 12.0	16.0	+28	32.7	0.24-0.41	2
16858	1997 YG10	02 12.9	16.4	+19	5.232	0.24	2
6302	Tengukogen	02 13.9	16.2	+20	3.092	0.46	1+
15692	1984 RA	02 14.2	16.4	+15	37.44	0.66	2
6652	1991 SJ1	02 15.7	15.4	+4	85.56	0.75	2
19246	1994 EL7	02 15.7	16.1	+18	4.05	0.44	2
1483	Hakoila	02 16.9	14.5	+20	239.1	0.62	2
8548	Sumizihara	02 16.9	14.8	+14	3.192	0.10	2
12552	1998 QQ45	02 17.5	16.1	+10	4.8	0.33	2
56071	1998 YF6	02 18.8	16.2	+10	13.36	0.16	2
1907	Rudneva	02 21.7	15.0	+11	44	0.1	1+
8788	Labeyrie	02 21.7	16.2	+8	12.571	0.50	2
39510	1982 DU	02 25.0	15.7	+13 S	15.582		2
7895	Kaseda	02 25.2	15.1	+17	5.11	0.10	2+
36057	1999 RC33	02 25.2	16.3	+10	5.424	0.35	2
6793	Palazzolo	02 25.7	16.3	+15	6.231	0.14-0.16	2
6529	Rhoads	02 27.2	16.0	+0	9.729	0.43	2
4113	Rascana	03 01.0	15.5	+14	4.416	0.25-0.46	2
2396	Kochi	03 01.7	15.0	+8	26.17	0.14-0.26	2
52005	Maik	03 02.6	16.2	+6	10.655	0.34	2
2796	Kron	03 02.9	15.1	+8	22.99	0.07- 0.6	2
3286	Anatoliya	03 04.0	15.9	+24 S	5.81		2
19125	1987 CH	03 07.6	16.4	+9	76	0.66-0.86	2
3142	Kilopi	03 09.1	15.2	-6	15.128	0.04-0.29	2

Number	Name	Brightest Date	Mag	Dec	LCDB Data Period	Amp	U
45156	1999 XV114	03 09.5	16.4	-4	18.929	0.05	2
33131	1998 CW3	03 12.9	16.5	+9 S	8.35		2
7896	Svejk	03 13.9	16.1	+5 S	16.206		2
8404	1995 AN	03 14.2	15.5	-4	3.202	0.06-0.16	2+
9123	Yoshiko	03 14.9	15.7	-5	3.359	0.21	2
9192	1992 AR1	03 15.2	15.8	-8	43.297	0.24	2
11736	Viktorfischl	03 18.1	15.9	+7	9.783		2-
9325	Stonehenge	03 19.7	16.3	-5	4.607	0.16-0.22	2
4219	Nakamura	03 19.8	15.9	+4	115.492	0.20	2
21037	1990 EB	03 19.8	16.1	+11	17.923	0.12	2
86666	2000 FL10	03 19.8	15.7	-23	206	0.85	2
4486	Mithra	03 20.6	14.4	+35	67.5	1.	2
218863	2006 WO127	03 20.9	16.1	+21 S	3.275		2
21976	1999 XV2	03 21.5	15.5	-14	3.848	0.11	2
3527	McCord	03 22.8	14.8	-6	321	0.44	2
9324	1989 CH4	03 23.1	15.9	-3	6.558	0.16	2
16091	Malchiodi	03 26.4	16.3	-1	20.362	0.30-0.31	2
20771	2000 QY150	03 28.4	16.5	-10 S	8.3		2
5274	Degewij	03 28.7	15.5	-6	7.58	0.19-0.20	2
6767	Shirvindt	03 30.9	16.3	+0	10.787	0.48	2
22298	1990 EJ	03 31.2	16.0	-10 S	2.986		2
6667	Sannaimura	03 31.3	15.6	-1	2.893	0.05	2

Low Phase Angle Opportunities

The Low Phase Angle list includes asteroids that reach very low phase angles ($\alpha < 1°$). The "α" column is the minimum solar phase angle for the asteroid. Getting accurate, calibrated measurements (usually V band) at or very near the day of opposition can provide important information for those studying the "opposition effect." Use the on-line query form for the LCDB to get more details about a specific asteroid.

https://www.minorplanet.info/php/callopplcdbquery.php

The best chance of success comes with covering at least half a cycle a night, meaning periods generally < 16 h, when working objects with low amplitude. Objects with large amplitudes and/or long periods are much more difficult for phase angle studies since, for proper analysis, the data must be reduced to the average magnitude of the asteroid for each night. Refer to Harris et al. (1989) for the details of the analysis procedure.

As an aside, it is arguably better for physical interpretation (e.g., *G* value versus albedo) to use the maximum light rather than mean level to find the phase slope parameter (*G*), which better models the behavior of a spherical object of the same albedo, but it can produce significantly different values for both *H* and *G* versus using average light, which is the method used for values listed by the Minor Planet Center. Using and reporting the results of both methods can provide additional insights into the physical properties of an asteroid.

The International Astronomical Union (IAU) has adopted a new system, H-G_{12}, introduced by Muinonen et al. (2010). It will be some years before H-G_{12} becomes widely used, and hopefully not until a discontinuity flaw in the G_{12} function has been fixed. This discontinuity results in false "clusters" or "holes" in the solution density and makes it impossible to draw accurate conclusions.

We strongly encourage obtaining data as close to 0° as possible, then every 1-2° out to 7°, below which the curve tends to be non-linear due to the opposition effect. From 7° out to about 30°, observations at 3-6° intervals should be sufficient. Coverage beyond 50° or so is not generally helpful since the H-G system is best defined with data from 0-30°.

It's important to emphasize that all observations should (must) be made using high-quality catalogs to set the comparison star magnitudes. These include ATLAS, Pan-STARRS, SkyMapper, and Gaia2/3. Catalogs such as CMC-15, APASS, or the MPOSC from *MPO Canopus* have too high of significant systematic errors.

Also important is that that there are sufficient data from each observing run such that their location can be found on a combined, phased lightcurve derived from two or more nights obtained *near the same phase angle.* If necessary, the magnitudes for a given run should be adjusted so that they correspond to mid-light of the combined lightcurve. This goes back to the H-G system being based on average, not maximum or minimum light.

The asteroid magnitudes are brighter than in others lists because higher precision is required and the asteroid may be a full magnitude or fainter when it reaches phase angles out to 20-30°.

Num	Name	Date	α	V	Dec	Period	Amp	U
64	Angelina	01 03.7	0.43	10.4	+24	8.752	0.04-0.42	3
449	Hamburga	01 04.9	0.81	12.0	+24	36.516	0.06-0.17	3
43	Ariadne	01 05.3	0.72	11.2	+21	5.762	0.06-0.73	3
891	Gunhild	01 08.2	0.22	13.7	+23	11.892	0.18-0.37	3-
165	Loreley	01 16.3	0.57	12.5	+23	7.226	0.06-0.17	3
544	Jetta	01 20.1	0.10	13.9	+20	7.745	0.44-0.52	3
295	Theresia	01 26.7	0.87	13.1	+17	10.702	0.11-0.22	3
551	Ortrud	01 28.1	0.20	13.2	+19	17.416	0.14-0.19	3
53	Kalypso	02 02.8	0.77	11.0	+15	9.036	0.09-0.14	3
221	Eos	02 04.6	0.55	12.3	+15	10.443	0.05-0.12	3
461	Saskia	02 11.5	0.25	14.0	+14	7.348	0.25-0.36	3
1639	Bower	02 19.0	0.57	14.0	+10	22.181	0.15-0.38	3-
335	Roberta	02 24.6	0.37	12.6	+11	12.054	0.05-0.78	3
50	Virginia	02 25.0	0.40	13.6	+8	14.315	0.07-0.20	3
185	Eunike	02 26.5	0.78	11.7	+11	21.797	0.08-0.22	3
489	Comacina	03 05.9	0.23	12.5	+5	9.02	0.12-0.33	3
308	Polyxo	03 06.2	0.68	11.9	+4	12.029	0.08-0.15	3-
573	Recha	03 08.3	0.35	14.0	+4	7.166	0.16-1.05	3
570	Kythera	03 09.9	0.54	14.0	+3	8.117	0.09-0.20	3
693	Zerbinetta	03 10.4	0.34	13.5	+5	11.475	0.14-0.29	3-
586	Thekla	03 13.1	0.70	13.3	+1	13.670	0.24-0.30	3
737	Arequipa	03 17.8	0.87	13.1	-1	7.026	0.08-0.26	3
257	Silesia	03 18.8	0.97	13.9	+4	15.709	0.29-0.30	3
190	Ismene	03 22.7	0.23	13.1	+0	6.521	0.10-0.16	3
73	Klytia	03 24.9	0.09	12.4	-1	8.297	0.26-0.35	3
787	Moskva	03 28.9	0.61	13.1	-2	6.056	0.27-0.68	3
62	Erato	03 29.7	0.79	13.7	-1	9.221	0.12-0.28	3
373	Melusina	03 30.0	0.55	14.0	-5	12.987	0.20-0.31	3

Shape/Spin Modeling Opportunities

Those doing work for modeling should contact Josef Ďurech at the email address above. If looking to add lightcurves for objects with existing models, visit the Database of Asteroid Models from Inversion Techniques (DAMIT) web site.

https://astro.troja.mff.cuni.cz/projects/damit/

Additional lightcurves could lead to the asteroid being added to or improving one in DAMIT, thus increasing the total number of asteroids with spin axis and shape models.

Included in the list below are objects that:

1. Are rated U = 3– or 3 in the LCDB.
2. Do not have reported pole in the LCDB Summary table.
3. Have at least three entries in the Details table of the LCDB where the lightcurve is rated U ≥ 2.

The caveat for condition #3 is that no check was made to see if the lightcurves are from the same apparition or if the phase angle bisector longitudes differ significantly from the upcoming apparition. The last check is often not possible because the LCDB does not list the approximate date of observations for all details records. Including that information is an on-going project.

With the wide use of sparse data from the surveys for modeling that produces hundreds of statistically valid poles and shapes, the need

for data for main-belt objects is not what it used to be. The best use of observing time might be to concentrate on near-Earth asteroids, or on asteroids where the only period was derived from sparse data, which can help eliminate alias periods. The latter targets are usually flagged with an 'S' on the LCDB summary line. Regardless, it's a good idea to visit the DAMIT site and see what it has, if anything, on the target(s) you've picked for observations.

Objects in **bold** text are at a favorable apparition.

		Brightest			LCDB Data		
Num	Name	Date	Mag	Dec	Period	Amp	U
701	Oriola	01 02.1	13.4	+17	9.09	0.20-0.37	3
468	Lina	01 03.6	14.1	+23	16.33	0.13-0.18	3
2491	**Tvashtri**	**01 07.4**	**15.0**	**+4**	**4.085**	**0.06-0.24**	**3**
891	**Gunhild**	**01 08.2**	**13.6**	**+23**	**11.892**	**0.18-0.37**	**3-**
4497	Taguchi	01 09.0	14.7	+27	3.563	0.07-0.21	3
764	Gedania	01 11.2	13.9	+14	24.968	0.01-0.35	3-
577	Rhea	01 11.4	14.4	+26	12.249	0.19-0.24	3-
477	Italia	01 12.2	14.0	+30	19.413	0.15-0.32	3
1093	Freda	01 14.7	15.0	+49	19.67	0.06-0.21	3
191	Kolga	01 15.8	13.1	+9	17.604	0.24-0.50	3
392	Wilhelmina	01 15.9	14.0	-1	13.058	0.06-0.70	3
464	Megaira	01 18.5	13.8	+25	12.879	0.08-0.12	3
359	Georgia	01 19.8	13.5	+29	5.537	0.14-0.54	3
2209	Tianjin	01 21.2	14.8	+18	9.47	0.41-0.42	3
1078	**Mentha**	**01 22.5**	**13.3**	**+26**	**85**	**0.31-0.87**	**3**
1224	Fantasia	01 22.9	14.3	+10	4.995	0.06-0.47	3
530	Turandot	01 24.7	14.5	+18	19.96	0.10-0.17	3-
2965	**Surikov**	**01 25.4**	**14.7**	**+17**	**9.061**	**0.23-0.29**	**3**
295	Theresia	01 26.6	13.1	+17	10.702	0.11-0.22	3
551	Ortrud	01 28.1	13.1	+19	17.416	0.14-0.19	3
261	**Prymno**	**01 30.7**	**11.7**	**+21**	**8.002**	**0.08-0.37**	**3**
1544	Vinterhansenia	01 31.9	14.6	+23	13.536	0.11-0.18	3-
1823	Gliese	02 06.9	15.0	+15	4.486	0.13-0.27	3
654	**Zelinda**	**02 07.2**	**10.4**	**-12**	**31.735**	**0.08- 0.3**	**3**
868	Lova	02 11.2	13.9	+18	41.118	0.28-0.40	3
197	Arete	02 17.4	14.1	+23	6.608	0.10-0.16	3
5080	Oja	02 18.8	14.8	+14	7.222	0.31-0.39	3
1639	Bower	02 18.9	14.0	+10	22.181	0.15-0.38	3-
169	Zelia	02 20.2	12.9	+14	14.537	0.13-0.17	3
1523	**Pieksamaki**	**02 20.5**	**14.1**	**+10**	**5.32**	**0.28- 0.5**	**3**
613	Ginevra	02 20.6	13.7	+15	12.906	0.12-0.20	3
1189	Terentia	02 23.1	14.6	-2	19.308	0.32-0.38	3
514	Armida	02 25.2	13.5	+4	21.851	0.16-0.27	3
111	Ate	02 25.4	11.0	+5	22.072	0.08-0.18	3
796	Sarita	02 26.9	14.2	+28	8.175	0.27-0.33	3
2196	Ellicott	03 06.1	14.9	-4	9.071	0.10-0.23	3-
308	**Polyxo**	**03 06.2**	**11.8**	**+4**	**12.029**	**0.08-0.15**	**3-**
1516	Henry	03 11.2	14.8	+14	17.599	0.35-0.54	3-
2323	Zverev	03 11.6	15.0	+5	3.921	0.28-0.39	3
586	Thekla	03 13.1	13.3	+1	13.67	0.24-0.30	3
626	Notburga	03 14.6	13.5	-6	19.353	0.10-0.21	3
535	Montague	03 15.5	12.7	+12	10.248	0.18-0.25	3
737	Arequipa	03 18.0	13.1	-1	7.026	0.08-0.26	3
3099	**Hergenrother**	**03 18.8**	**14.5**	**+16**	**25.58**	**0.28-0.35**	**3-**
841	**Arabella**	**03 19.2**	**14.9**	**+0**	**3.142**	**0.22-0.32**	**3**
1250	Galanthus	03 20.4	14.7	-29	3.92	0.22-0.28	3
410	Chloris	03 23.9	11.9	+17	32.5	0.19-0.33	3
379	Huenna	03 24.3	14.0	-1	14.141	0.07-0.22	3
1394	Algoa	03 25.2	14.5	-1	2.768	0.20-0.21	3
1830	Pogson	03 27.5	14.8	+2	2.57	0.07-0.18	3
605	Juvisia	03 28.0	15.0	-14	15.851	0.18-0.26	3
907	Rhoda	03 29.3	13.1	+14	22.44	0.06-0.16	3-
194	Prokne	03 29.9	12.1	+10	15.679	0.08-0.27	3
301	Bavaria	03 31.2	13.9	+1	12.253	0.25-0.31	3
522	Helga	03 31.2	14.6	+1	8.129	0.13-0.31	3

Radar-Optical Opportunities

Table I below gives a list of near-Earth asteroids reaching maximum brightness for the current quarter-year based on calculations by Warner. We switched to this presentation in lieu of ephemerides for reasons outlined in the 2021 October-December opportunities paper (Warner et al., 2021b), which centered on the potential problems with ephemerides generated several months before publication.

The initial list of targets started using the planning tool at:

https://www.minorplanet.info/php/callopplcdbquery.php

where the search was limited to near-Earth asteroids only that were V ≤ 18 for at least part of the quarter.

The list was then filtered to include objects that might be targets for the Goldstone radar facility or, if it were still operational, the Arecibo radar. This was based on the calculated radar SNR using

http://www.naic.edu/~eriverav/scripts/index.php

and assuming a rotation period of 4 hours (2 hours if $D \leq 200$ m) if a period was not given in the asteroid lightcurve database (LCDB; Warner et al., 2009). The SNR values are estimates only and assume that the radar is fully functional.

If an asteroid was on the list but failed the SNR test, we checked if it might be a suitable target for radar and/or photometry sometime through 2050. If so, it was kept on the list to encourage physical and astrometric observations during the current apparition. In most of those cases, the SNR values in the "A" and "G" columns are not for the current quarter but the year given in the Notes column. If a better apparition is forthcoming through 2050, the Notes column in Table I contains SNR values for that time.

The final step was to cross-reference our list with that found on the Goldstone planned targets schedule at

http://echo.jpl.nasa.gov/asteroids/goldstone_asteroid_schedule.html

In Table I, objects in bold text are on the Goldstone proposed observing list as of early 2022 October.

It's important to note that the final list in Table I is based on *known* targets and orbital elements when it was prepared. It is common for newly discovered objects to move in or out of the list. We recommend that you keep up with the latest discoveries by using the Minor Planet Center observing tools.

In particular, monitor NEAs and be flexible with your observing program. In some cases, you may have only 1-3 days when the asteroid is within reach of your equipment. Be sure to keep in touch with the radar team (through Benner's email or their Facebook or Twitter accounts) if you get data. The team may not always be observing the target but your initial results may change their plans. In all cases, your efforts are greatly appreciated.

For observation planning, use these two sites

MPC: *http://www.minorplanetcenter.net/iau/MPEph/MPEph.html*
JPL: *http://ssd.jpl.nasa.gov/?horizons*

Cross-check the ephemerides from the two sites just in case there is discrepancy that might have you imaging an empty sky.

About YORP Acceleration

Near-Earth asteroids are particularly sensitive to YORP acceleration. YORP (Yarkovsky-O'Keefe-Radzievskii-Paddack; Rubincam, 2000) is the asymmetric thermal re-radiation of sunlight that can cause an asteroid's rotation period to increase or decrease. High precision lightcurves at multiple apparitions can be used to model the asteroid's *sidereal* rotation period and see if it's changing.

Num	Name	H	Diam	BDate	BMag	BDec	Period	AMn	AMx	U	A	G	Notes
	2020 DG4	28.20	0.007	02 19.4	17.8	-29							
	2009 QH6	22.50	0.094	02 16.0	17.0	-77					10	–	
367789	**2011 AG5**	**21.88**	**0.125**	**02 01.9**	**14.3**	**-9**					**7200**	**2000**	**PHA, NHATS**
199145	**2005 YY128**	**18.36**	**0.632**	**02 15.0**	**13.3**	**-80**					**3800**	**1100**	**PHA N Obs: Jan 23-Feb11**
	2006 BE55	**21.90**	**0.124**	**02 26.7**	**16.1**	**50**					**625**	**180**	**PHA**
	2017 BM123	**23.8**	**0.052**	**02 27.0**	**18.2**	**39**	**2.150**	**0.37**	**0.55**	**3**	**65**	**20**	**NHATS Warner (2017) Pravec (2020web)**
535844	**2015 BY310**	**21.87**	**0.126**	**03 03.5**	**16.3**	**-17**	**0.09267**	**0.67**	**0.7**	**3**	**90**	**25**	**NHATS Pravec (2019web)**
	2018 UQ1	**21.98**	**0.119**	**03 20.6**	**16.5**	**-49**	**3.9291**	**0.65**	**0.88**	**3**	**530**	**150**	
	2007 ED125	**21.00**	**0.187**	**03 07.3**	**16.2**	**-28**	**5.62**		**0.55**	**3-**	**830**	**235**	**Warner (2015)**
	2012 BV13	22.20	0.108	01 14.3	17.0	43					190	55	
199145	2005 YY128	18.36	0.632	02 14.5	13.1	-53					3800	1100	
37638	**1993 VB**	**19.26**	**0.418**	**02 25.3**	**14.5**	**38**					**525**	**150**	**PHA**
	2017 WO28	22.50	0.094	02 26.0	17.6	19					10	–	
226554	2003 WR21	19.64	0.351	01 02.3	15.6	55					40	10	
	2019 BC1	20.34	0.254	01 16.2	17.9	-2					30	–	
162385	2000 BM19	18.58	0.571	01 24.1	16.4	69	9.463	1.34	1.38	2+	100	25	Skiff (2019)
	2009 CT5	18.80	0.516	02 01.9	16.6	-29					20	–	
137175	1999 JA11	18.36	0.632	02 20.7	17.4	65					20	5	
140039	2001 SO73	18.22	0.675	02 19.2	16.1	-37					20	5	
98943	2001 CC21	18.80	0.516	02 01.9	15.9	49	5.017		0.81	3	10		Pravec (2002web)
4486	Mithra	15.68	2.170	03 20.6	14.4	35	67.5		1	2	145	40	Brozovic (2010) Goldstone: April
2212	Hephaistos	13.53	5.850	01 11.9	12.9	43	48	0.08	0.35	2	130	35	Warner (2021)

Table I. A list of near-Earth asteroids reaching brightest in 2023 January-March. PHA: potentially hazardous asteroid. NHATS: Near-Earth Object Human Space Flight Accessible Targets Study. Diameters are based on p_V = 0.20. The Date, V, and Dec columns are the mm/dd.d, approximate magnitude, and declination when at brightest. Amp is the single or range of amplitudes. The A and G columns are the approximate SNRs for an assumed full-power Arecibo (not operational) and Goldstone radars. The references in the Notes column are those for the reported periods and amplitudes. `

It usually takes four apparitions to have sufficient data to determine if the asteroid rotation rate is changing under the influence of YORP. This is why observing an asteroid that already has a well-known period remains a valuable use of telescope time. It is even more so when considering the BYORP (binary-YORP) effect among binary asteroids that has stabilized the spin so that acceleration of the primary body is not the same as if it would be if there were no satellite.

The Quarterly Target List Table

The Table I columns are

Num	Asteroid number, if any.
Name	Name assigned by the MPC.
H	Absolute magnitude from MPCOrb.
Dkm	Diameter (km) assuming $p_V = 0.2$.
Date	Date (mm dd.d) of brightest magnitude.
V	Approximate V magnitude at brightest.
Dec	Approximate declination at brightest.
Period	Synodic rotation period from summary line in the LCDB summary table.
Amp	Amplitude range (or single value) of reported lightcurves.
U	LCDB U (solution quality) from 1 (probably wrong) to 3 (secure).
A	Approximate SNR for Arecibo (if operational and at full power).
G	Approximate SNR for Goldstone radar at full power.
Notes	Comments about the object.

"PHA" is a potentially hazardous asteroid. NHATS is for "Near-Earth Object Human Space Flight Accessible Targets Study." Presume that that astrometry and photometry have been requested to support Goldstone observations. The sources for the rotation period are given in the Notes column. If none are qualified with a specific period, then the periods from multiple sources were in general agreement. Higher priority should be given to those where the current apparition is the last one V ≤ 18 through 2050 or several years to come.

References

Brozovic, M.; Benner, L.A.M.; Magri, C.; Ostro, S.J.; Scheeres, D.J.; Giorgini, J.D.; Nolan, M.C.; Margot, J.-L.; Jurgens, R.F.; Rose, R. (2010). "Radar observations and a physical model of contact binary Asteroid 4486 Mithra." *Icarus* **208**, 207-220.

Harris, A.W.; Young, J.W.; Bowell, E.; Martin, L.J.; Millis, R.L.; Poutanen, M.; Scaltriti, F.; Zappala, V.; Schober, H.J.; Debehogne, H.; Zeigler, K.W. (1989). "Photoelectric Observations of Asteroids 3, 24, 60, 261, and 863." *Icarus* **77**, 171-186.

Muinonen, K.; Belskaya, I.N.; Cellino, A.; Delbò, M.; Levasseur-Regourd, A.-C.; Penttilä, A.; Tedesco, E.F. (2010). "A three-parameter magnitude phase function for asteroids." *Icarus* **209**, 542-555.

Pravec, P.; Wolf, M.; Sarounova, L. (2002web; 2019web; 2020web). *http://www.asu.cas.cz/~ppravec/neo.htm*

Rubincam, D.P. (2000). "Radiative Spin-up and Spin-down of Small Asteroids." *Icarus* **148**, 2-11.

Skiff, B.A.; McLelland, K.P.; Sanborn, J.; Pravec, P.; Koehn, B.W. (2019). "Lowell Observatory Near-Earth Asteroid Photometric Survey (NEAPS): Paper 4." *Minor Planet Bull.* **46**, 458-503.

Warner, B.D. (2015). "Near-Earth Asteroid Lightcurve Analysis at CS3-Palmer Divide Station: 2015 January - March." *Minor Planet Bull.* **42**, 172-183.

Warner, B.D. (2017). "Near-Earth Asteroid Lightcurve Analysis at CS3-Palmer Divide Station: 2016 December thru 2017 April." *Minor Planet Bull.* **44**, 223-237.

Warner, B.D.; Stephens, R.D. (2021). "Near-Earth Asteroid Lightcurve Analysis at the Center for Solar System Studies: 2020 September to 2021 January." *Minor Planet Bull.* **48**, 170-179.

Warner, B.D.; Harris, A.W.; Pravec, P. (2009). "The Asteroid Lightcurve Database." *Icarus* **202**, 134-146. Updated 2021 Dec. *http://www.minorplanet.info/lightcurvedatabase.html*

Warner, B.D.; Harris, A.W.; Durech, J.; Benner, L.A.M. (2021a). "Lightcurve Photometry Opportunities" 2021 January-March." *Minor Planet Bull.* **48**, 89-97.

Warner, B.D.; Harris, A.W.; Durech, J.; Benner, L.A.M. (2021b). "Lightcurve Photometry Opportunities" 2021 October-December." *Minor Planet Bull.* **48**, 406-410.

IN THIS ISSUE

This list gives those asteroids in this issue for which physical observations (excluding astrometric only) were made. This includes lightcurves, color index, and H-G determinations, etc. In some cases, no specific results are reported due to a lack of or poor-quality data. The page number is for the first page of the paper mentioning the asteroid. EP is the "go to page" value in the electronic version.

Number	Name	EP	Page
78	Diana	47	47
175	Andromache	43	43
198	Ampella	47	47
282	Clorinde	65	65
414	Liriope	65	65
599	Luisa	74	74
786	Bredichina	51	51
795	Fini	51	51
866	Fatme	65	65
892	Seeligeria	51	51
895	Helio	47	47
993	Moultona	6	6
1051	Merope	65	65
1060	Magnolia	47	47
1151	Ithaka	74	74
1180	Rita	33	33
1237	Genevieve	65	65
1252	Celestia	62	62
1255	Schilowa	65	65
1261	Legia	65	65
1300	Marcelle	65	65
1343	Nicole	51	51
1355	Magoeba	74	74
1374	Isora	74	74
1389	Onnie	7	7
1389	Onnie	8	8
1461	Jean-Jacques	54	54
1501	Baade	74	74
1543	Bourgeois	47	47
1582	Martir	65	65
1585	Union	65	65
1605	Milankovitch	65	65
1724	Vladimir	65	65
1806	Derice	47	47
1904	Massevitch	65	65
2030	Belyaev	54	54
2060	Chiron	74	74
2088	Sahlia	65	65
2100	Ra-Shalom	21	21
2149	Schwambraniya	54	54
2454	Olaus Magnus	62	62
2685	Masursky	11	11
2714	Matti	74	74
2717	Tellervo	51	51
2764	Moeller	12	12
2802	Weisell	65	65
3114	Ercilla	54	54
3153	Lincoln	58	58
3224	Irkutsk	51	51
3431	Nakano	65	65
3512	Eriepa	74	74
3533	Toyota	37	37
3893	DeLaeter	58	58
3977	Maxine	62	62
3988	Huma	74	74
4015	Wilson-Harrington	74	74
4103	Chahine	74	74
4132	Bartok	74	74
4133	Heureka	41	41
4287	Trisov	74	74
4429	Chinmoy	58	58
4429	Chinmoy	65	65
4494	Marimo	101	101
4666	Dietz	74	74
4901	O Briain	65	65
5131	1990 BG	74	74
5147	Maruyama	15	15
5209	Oloosson	74	74
5496	1973 NA	74	74
5516	Jawilliamson	101	101
5621	Erb	74	74
5626	Melissabrucker	74	74
5682	Beresford	74	74
5736	Sanford	62	62
5736	Sanford	74	74
6569	Ondaatje	43	43
7002	Bronshten	74	74
7189	Kuniko	62	62
7334	Sciurus	58	58
7335	1989 JA	16	16
7353	Kazuya	40	40
7357	1995 UJ7	54	54
7365	Sejong	62	62
7750	McEwen	74	74
7757	Kameya	74	74
7784	Watterson	74	74
9661	Hohmann	33	33
10548	1992 PJ2	58	58
10590	1996 OP2	40	40
11739	Baton Rouge	33	33
12225	Yanfernandez	74	74
12896	geoffroy	33	33
12919	Tomjohnson	17	17
12919	Tomjohnson	54	54
12919	Tomjohnson	65	65
12920	1998 VM15	33	33
13520	Felicienrops	62	62
13819	1999 SX5	74	74
14335	Alexosipov	74	74
14569	1998 QB32	33	33
14764	Kilauea	74	74
15673	Chetaev	74	74
16452	Goldfinger	41	41
16556	1991 VQ1	62	62
17511	1992 QN	21	21
17744	Jodiefoster	74	74
18081	2000 GB126	74	74
18882	1999 YN4	74	74
19379	Labrecque	74	74
20895	2000 WU106	54	54
21930	1999 VP61	33	33
23183	2000 OY21	74	74
23552	1994 NB	74	74
24475	2000 VN2	74	74
25332	1999 KK6	62	62
27810	Daveturner	74	74
29168	1990 KJ	74	74
29798	1999 CP79	62	62
30019	2000 DD	74	74
30722	Biblioran	74	74
31425	1999 BF3	74	74
32802	1990 SK	74	74
32906	1994 RH	74	74
34759	2001 QL151	74	74
36284	2000 DM8	74	74
41365	2000 AO98	33	33
41434	2000 GB82	74	74
43750	1981 QG3	74	74
44262	1998 QR51	74	74
47035	1998 WS	74	74
49483	1999 BP13	41	41
54660	2000 UJ1	74	74
54789	2002 MZ7	21	21
55854	Stoppani	74	74
57754	2001 VW12	101	101
66008	1998 QH2	74	74
75079	1999 VN24	74	74
77645	2001 KX66	74	74
81298	2000 GW1	74	74
85804	1998 WQ5	37	37
85953	1999 FK21	74	74
89486	2001 XL31	58	58
101465	1998 WL12	58	58
103067	1999 XA143	74	74
136617	1994 CC	74	74
138524	2000 OJ8	74	74
141018	2001 WC47	74	74
143487	2003 CR20	74	74
152664	1998 FW4	74	74
159402	1999 AP10	74	74
160092	2000 PL6	74	74
163081	2002 AG29	74	74
178783	2001 BY2	74	74
181882	1999 RF14	74	74
188174	2002 JC	74	74
218863	2006 WO127	74	74
222073	1999 HY1	74	74
241370	2008 LW8	74	74
253841	2003 YG118	74	74
274138	2008 FU6	74	74
276741	2004 EM66	74	74
285263	1998 QE2	19	19
302831	2003 FH	74	74
307190	2002 EK130	74	74
307544	2003 EJ16	74	74
326683	2002 WP	74	74
351545	2005 TE15	74	74
366833	2005 MC	74	74
385343	2002 LV	74	74
387632	2002 PD40	74	74
398188	Agni	21	21
407656	2011 SL102	74	74
420187	2011 GA55	74	74
448972	2011 VY15	74	74
451397	2011 EZ78	74	74
483504	2002 XN14	74	74
523654	2011 SR5	74	74
524196	2001 QP181	74	74
530520	2011 LT17	74	74
612050	1997 GL3	74	74
	2000 CP101	74	74
	2002 SG3	26	26
	2006 NL	43	43
	2009 MC9	74	74
	2009 NH	74	74
	2009 WV25	74	74
	2011 CG2	74	74
	2011 CY46	74	74
	2011 GM62	74	74
	2011 GP59	74	74
	2011 HS	74	74
	2011 KE	74	74
	2011 LJ19	74	74
	2011 MD	74	74
	2011 OQ5	74	74
	2011 PT1	74	74
	2011 TG2	21	21
	2012 PG6	21	21
	2022 NE	26	26
	2022 NR	26	26
	2022 QC	26	26
	2022 QT7	26	26
	2022 QV	26	26
	2022 QX4	26	26
	2022 SW3	26	26

THE MINOR PLANET BULLETIN (ISSN 1052-8091) is the quarterly journal of the Minor Planets Section of the Association of Lunar and Planetary Observers (ALPO, http://www.alpo-astronomy.org). Current and most recent issues of the *MPB* are available on line, free of charge from:

https://mpbulletin.org/

The Minor Planets Section is directed by its Coordinator, Prof. Frederick Pilcher, 4438 Organ Mesa Loop, Las Cruces, NM 88011 USA (fpilcher35@gmail.com). Robert Stephens (rstephens@foxandstephens.com) serves as Associate Coordinator. Dr. Alan W. Harris (MoreData! Inc.; harrisaw@colorado.edu), and Dr. Petr Pravec (Ondrejov Observatory; ppravec@asu.cas.cz) serve as Scientific Advisors. The Asteroid Photometry Coordinator is Brian D. Warner (Center for Solar System Studies), Palmer Divide Observatory, 446 Sycamore Ave., Eaton, CO 80615 USA (brian@MinorPlanetObserver.com).

The Minor Planet Bulletin is edited by Professor Richard P. Binzel, MIT 54-410, 77 Massachusetts Ave, Cambridge, MA 02139 USA (rpb@mit.edu). Brian D. Warner (address above) is Associate Editor. Assistant Editors are Dr. David Polishook, Department of Earth and Planetary Sciences, Weizmann Institute of Science (david.polishook@weizmann.ac.il) and Dr. Melissa Hayes-Gehrke, Department of Astronomy, University of Maryland (mhayesge@umd.edu). The *MPB* is produced by Dr. Pedro A. Valdés Sada (psada2@ix.netcom.com).

Effective with Volume 50, the *Minor Planet Bulletin* is an electronic-only journal; print subscriptions are no longer available. In addition to the free electronic download of the *MPB* as noted above, electronic retrieval of all *Minor Planet Bulletin* articles (back to Volume 1, Issue Number 1) is available through the Astrophysical Data System:

http://www.adsabs.harvard.edu/

Authors should submit their manuscripts by electronic mail (rpb@mit.edu). Author instructions and a Microsoft Word template document are available at the web page given above. All materials must arrive by the deadline for each issue. Visual photometry observations, positional observations, any type of observation not covered above, and general information requests should be sent to the Coordinator.

* * * * *

The deadline for the next issue (50-2) is January 15, 2023. The deadline for issue 50-3 is April 15, 2023.